

DEVELOPMENT OF CHEMICAL PROBES TO DEFINE BIOSYNTHETIC
PATHWAYS, STRUCTURES, AND FUNCTIONS OF PROTEOGLYCANS

by

Vy My Tran

A dissertation submitted to the faculty of
The University of Utah
in partial fulfillment of the requirements for the degree of

Doctor of Philosophy

Department of Bioengineering

The University of Utah

August 2012

Copyright © Vy My Tran 2012

All Rights Reserved

The University of Utah Graduate School

STATEMENT OF DISSERTATION APPROVAL

The dissertation of _____ Vy My Tran _____
has been approved by the following supervisory committee members:

_____ Kuberan Balagurunathan _____	, Chair	_____ 08-May-2012 _____ <small>Date Approved</small>
_____ Vladimir Hlady _____	, Member	_____ 08-May-2012 _____ <small>Date Approved</small>
_____ Jindrich Kopecek _____	, Member	_____ 08-May-2012 _____ <small>Date Approved</small>
_____ Yan-Ting Shiu _____	, Member	_____ 08-May-2012 _____ <small>Date Approved</small>
_____ Janis Louie _____	, Member	_____ 08-May-2012 _____

and by _____ Vladimir Hlady _____, Chair of
the Department of _____ Bioengineering _____

and by Charles A. Wight, Dean of The Graduate School.

ABSTRACT

Proteoglycans (PGs), a special class of glycoconjugates, which decorate the outer surface of mammalian cells, consist of a core protein and several glycosaminoglycan (GAG) side chains. PGs regulate many important biological processes, such as fertilization, cell-cell communication, immune defense, anticoagulation, angiogenesis, axon guidance, and many more. Controlling the fine structures of endogenous GAG chains or modulating expression levels of GAG chains can significantly impact many biological processes. However, very little is known about the factors that regulate PG biosynthesis. In this thesis work, chemical probes were designed and synthesized to understand biosynthetic pathways, structures, and functions of PGs. A library of xylosides with different aglycone groups was synthesized using “click chemistry” to stimulate and inhibit GAG production *in vitro*. These molecular probes serve as excellent tools to unravel the biological significance of PGs and GAG multivalency in many biological systems and lead to the discovery of drugs to treat human disorders/diseases that are associated with aberrant PG structures.

TABLE OF CONTENTS

ABSTRACT.....	iii
LIST OF FIGURES.....	vi
LIST OF TABLES.....	x
LIST OF SCHEMES.....	xi
LIST OF ABBREVIATIONS.....	xii
ACKNOWLEDGEMENTS.....	xiv
Chapters	
1 INTRODUCTION.....	1
1.1 Literature Review.....	2
1.2 Research Objectives.....	15
1.3 References.....	19
2 MODULATION OF GAG BIOSYNTHESIS BY CLICK-XYLOSIDES.....	25
2.1 Synthesis of Click-xylosides That Initiate GAG Biosynthesis.....	26
2.2 Inhibition of GAG Biosynthesis by Fluoro-xylosides.....	33
2.3 Conclusions.....	41
2.4 Experimental Methods.....	42
2.5 Supporting Information.....	45
2.6 References.....	56
3 DESIGN OF FLUORESCENT XYLOSIDES TO PROFILE CELL-SPECIFIC GAG CHAINS.....	58
3.1 Introduction.....	59
3.2 Results and Discussion.....	60
3.3 Conclusions.....	71
3.4 Experimental Methods.....	72

3.5 Supporting Information.....	78
3.6 References.....	90
4 RGD-XYLOSIDE CONJUGATES PRIME GAG CHAINS.....	95
5 SYNTHESIS AND BIOLOGICAL EVALUATION OF CLUSTER-XYLOSIDES AS POTENTIAL PROTEOGLYCAN MIMETICS.....	105
5.1 Introduction.....	106
5.2 Results.....	108
5.3 Discussion.....	118
5.4 Conclusions.....	119
5.5 Experimental Methods.....	121
5.6 Supporting Information.....	135
5.7 References.....	167
6 CONCLUSIONS	170
APPENDIX.....	182
CURRICULUM VITAE.....	183

LIST OF FIGURES

1.1	Structure of proteoglycans.....	3
1.2	Functions of proteoglycans in cell physiology.....	4
1.3	Biosynthesis of glycosaminoglycans.....	10
1.4	Xylosides prime GAG chains.....	14
2.1	Stability of click-xylosides.....	31
2.2	Priming activity of click-xylosides.....	32
2.3	Effect of various hydrophobic moieties on the DEAE elution profiles of GAG chains.....	34
2.4	Inhibition of PG biosynthesis by xyloside derivatives.....	39
2.5	Dose-dependent decrease of GAG biosynthesis by 4-deoxy-4-fluoroxylsides in CHO cells.....	40
2.6	Cytotoxicity of 4-deoxy-4-fluoroxylsides.....	41
S2.1	NMR spectra of click-xyloside 1.....	46
S2.2	Mass spectra of click-xyloside 1.....	47
S2.3	NMR spectra of click-xyloside 2.....	48
S2.4	Mass spectra of click-xyloside 2.....	49
S2.5	NMR spectra of click-xyloside 3.....	50
S2.6	NMR spectra of click-xyloside 4.....	51
S2.7	Mass spectra of click-xyloside 4.....	52

S2.8	NMR spectra of click-xyloside 5.....	53
S2.9	Mass spectra of click-xyloside 5.....	54
S2.10	NMR spectra of click-xyloside 6.....	55
3.1	Priming activity of fluorescent xylosides (12c and 8) in pgsA-745 cell line.....	67
3.2	Priming activity of UMB-click-xylosides (16a, 16b) and UMB- <i>O</i> -xylosides (control) in pgsA-745 cell line.....	68
3.3	Sulfate density profile of fluorescent xyloside 12c primed GAG chains...	69
3.4	Size exclusion profiles of GAG chains primed by fluorescent xyloside 12c.....	70
3.5	Size exclusion profiles of GAG chains primed by fluorescent xylosides (UMB- <i>O</i> -xyloside, 16a and 16b).....	71
S3.1	NMR spectra of fluorescent xylosides 6.....	79
S3.2	NMR spectra of fluorescent xylosides 7.....	80
S3.3	NMR spectra of fluorescent xylosides 8.....	81
S3.4	NMR spectra of fluorescent xylosides 12a.....	82
S3.5	Mass spectra of fluorescent xylosides 12a.....	83
S3.6	NMR spectra of fluorescent xylosides 12b.....	84
S3.7	NMR spectra of fluorescent xylosides 12c.....	85
S3.8	NMR spectra of fluorescent xylosides 16a.....	86
S3.9	Mass spectra of fluorescent xylosides 16a.....	87
S3.10	NMR spectra of fluorescent xylosides 16b.....	88
S3.11	Mass spectra of fluorescent xylosides 16b.....	89
5.1	Schematic representation of various cell surface & ECM-bound PGs.....	106
5.2	Priming activity of cluster-xylosides.....	112

5.3	Molecular weight profiles of GAG chains primed by cluster-xylosides.....	113
5.4	Structural analysis of primed GAG chains.....	114
5.5	Disaccharide profiles of bis-xyloside primed CS chains.....	116
5.6	Periodate oxidation-alkaline elimination of GAG chains.....	117
5.7	Structural analysis of GAG chains primed by bis-xyloside.....	120
S5.1	Comparison of priming activity of mono-xylosides and bis-xylosides.....	136
S5.2	HS and CS compositions of GAG chains primed by bis-xylosides.....	137
S5.3	GAG priming activity was determined at 100 μ M concentration by bis-xylosides.....	138
S5.4	Ozonolysis of GAG chains.....	139
S5.5	NMR spectra of cluster-xylosides 1.....	140
S5.6	Mass spectra of cluster-xylosides 1.....	141
S5.7	NMR spectra of cluster-xylosides 2.....	142
S5.8	Mass spectra of cluster-xylosides 2.....	143
S5.9	NMR spectra of cluster-xylosides 3.....	144
S5.10	Mass spectra of cluster-xylosides 3.....	145
S5.11	NMR spectra of cluster-xylosides 4.....	146
S5.12	Mass spectra of cluster-xylosides 4.....	147
S5.13	NMR spectra of cluster-xylosides 5.....	148
S5.14	Mass spectra of cluster-xylosides 5.....	149
S5.15	NMR spectra of cluster-xylosides 6.....	150
S5.16	Mass spectra of cluster-xylosides 6.....	151
S5.17	NMR spectra of cluster-xylosides 7.....	152

S5.18	Mass spectra of cluster-xylosides 7.....	153
S5.19	NMR spectra of cluster-xylosides 8.....	154
S5.20	Mass spectra of cluster-xylosides 8.....	155
S5.21	NMR spectra of cluster-xylosides 9.....	156
S5.22	NMR spectra of cluster-xylosides 12.....	157
S5.23	Mass spectra of cluster-xylosides 12.....	158
S5.24	NMR spectra of cluster-xylosides 13.....	159
S5.25	NMR spectra of cluster-xylosides 14.....	160
S5.26	Mass spectra of cluster-xylosides 14.....	161
S5.27	NMR spectra of cluster-xylosides 15.....	162
S5.28	Mass spectra of cluster-xylosides 15.....	163
S5.29	NMR spectra of cluster-xylosides 16.....	164
S5.30	Mass spectra of cluster-xylosides 17.....	165
S5.31	NMR spectra of cluster-xylosides 18.....	166

LIST OF TABLES

2.1	Click-xylosides with various aglycone groups.....	27
2.2	Structures of 4-deoxy-4-fluoro-xylosides.....	36
5.1	Structures of cluster-xylosides.....	109
5.2	Structures of bis-xylosides carrying an aryl group in the aglycone.....	115
S5.1	Yield of reactions.....	123
S5.2	Yield of reactions.....	124
S5.3	Yield of reactions.....	126

LIST OF SCHEMES

2.1	Synthesis of click-xylosides.....	28
2.2	4-deoxy-4-fluoro-click xylosides inhibit GAG biosynthesis.....	37
3.1	Synthesis of amino- <i>N</i> -(2, 3, 4-trihydroxyl- β -xylopyranosyl) acetamide.....	61
3.2	Synthesis of fluorogenic xylosides with amide linkages.....	62
3.3	Synthesis of fluorogenic xylosides with triazole linkages.....	62
3.4	Synthesis of UMB-click-xylosides with triazole-linkages.....	63
5.1	Synthesis of cluster-xylosides.....	110
S5.1	Preparation of precursors carrying alkyne group of click-chemistry.....	123
S5.2	Preparation of propargylated precursors for the synthesis of bis- and tris-xylosides.....	124
S5.3	Preparation of additional propargylated precursors.....	125
S5.4	Preparation of the precursor for the synthesis of tris-xyloside 9.....	127
S5.5	Synthesis of mono-xylosides using click chemistry.....	127
S5.6	Synthesis of cluster-xylosides using click chemistry.....	128

LIST OF ABBREVIATIONS

ATIII	Antithrombin III
CS	Chondroitin sulfate
DS	Dermatan sulfate
ECM	Extracellular matrix
EXT	Exostoses
FGF	Fibroblast growth factor
GAG	Glycosaminoglycan
Gal	Galactose
GalNAc	<i>N</i> -acetyl galactosamine
GlcA	Glucuronic acid
GlcNAc	<i>N</i> -acetyl glucosamine
GP	Glycoprotein
HS	Heparan sulfate
IdoA	Iduronic acid
KS	Keratan sulfate
LC	Liquid chromatography
MS	Mass spectrometry
NA	<i>N</i> -acetyl

NS	<i>N</i> -sulfo
NSEpi	<i>N</i> -sulfated, epimerized
NDST	<i>N</i> -deacetylase <i>N</i> -sulfotranferase
OST	<i>O</i> -sulfotransferase
PAPS	3'-phosphoadenosine-5'-phosphosulfate
PgsA-745	Mutant Chinese hamster ovary cell type
PG	Proteoglycans
RGD	Arginine-glycine-aspartic acid
UMB	Umbelliferyl
Xyl	Xylose

ACKNOWLEDGEMENTS

I have been extremely fortunate over the last few years to have the support of my mentors, colleagues, and family as I have worked towards my doctorate degree.

Professor Kuberan Balagurunathan has been an excellent mentor and has guided and supported me throughout my undergraduate and PhD studies. He is not only my PhD mentor but is also the person that introduced me to the sciences. He opened many doors by helping me during my undergraduate research and giving me the chance to work in the field of Glycoscience.

Dr. Mani Ethirajan's knowledge of organic chemistry and Dr. Xylophone Victor's knowledge of cell biology were instrumental for helping me solve the many problems I encountered during the first few years of my graduate study.

I have been very fortunate to get a knowledgeable and supportive PhD committee. Professor Vladimir Hlady, Professor Jindrich Kopecek, Professor Yan-Ting Shiu, and Professor Janis Louis dedicated a lot of time and have always been a source of inspiration and support for me during the dissertation process.

I would also like to thank Professor Durraikanu Loganathan for providing me with tetrakis-xylosides, Dr. Dinesh R. Garud for synthesizing the 4-F-xyloside, Professor James Yockman for his advice in the RGD-xyloside project, and Professor Christopher Reilly for allowing me to use the mass spectrometer in his laboratory. Their

help and support were invaluable in helping me gather the materials and know-how that I needed to complete my PhD project.

My labmates, Dr. Manivannan Ethirajan, Dr. Xylophone Victor, Thao Nguyen, Karthik Raman, Dr. Sorna Venkataswamy, Dr. Sailaja Arungundram, Dr. Babu Ponnusamy, Vimal Swarup, Spencer Brown, and Caitlin Mencio, have been a constant source of inspiration and guidance for both research and personal matters. They have offered me a lot of help, advice, and provided a sounding board for discussing my research and for my life in Utah.

On a personal note, I would like to thank my parents, my brothers, and my sisters for their unconditional support. Without their love and support, it would have been impossible for me to get through graduate study.

CHAPTER 1

INTRODUCTION

1.1. Literature Review

1.1.1. Structures of Proteoglycans

Proteoglycans (PGs) are the most ubiquitous glycoconjugates found on cell surfaces and in the extracellular matrix (ECM) (1-8). PG consists of a core protein and two or more glycosaminoglycan (GAG) chains with the exception of decorin (1-8). Four major classes of sulfated GAG chains are heparan sulfate (HS), chondroitin sulfate (CS), dermatan sulfate (DS), and keratan sulfate (KS) (1-8). GAG chains, with the exception of KS, are linked to a serine residue of the core proteins by *O*-glycosylation via a specific tetrasaccharide linker, “Xyl-Gal-Gal-GlcA” (1-8). The differences among HS, CS, and DS are in their constituent repeating disaccharide units. HS consists of glucosamine and glucuronic (GlcA)/iduronic (IdoA) acid, CS consists of galactosamine and GlcA, and DS is composed of galactosamine and GlcA/IdoA (Figure 1.1) (1-8). In addition to having differing disaccharide compositions and chain length, GAGs display structural variation through sulfation of hydroxyl groups (8). Since GAGs have a large number of potential sulfate sites and different combinations of sulfated disaccharides, the sulfate patterns of GAG are diverse (8). For example, HS disaccharide units can be sulfated at C-2 of hexuronic acid or at C-3 and C-6 positions of glucosamine. C-2 amine of glucosamine can be acetylated, sulfated, or unmodified. CS disaccharides units can be sulfated at the C-4 and C-6 of galactosamine as well as C-2 of uronic acid (8). Moreover, the structural diversity is also obtained by conformational flexibility of the pyranose ring of IdoA, which exists in equilibrium between the chair and skew-boat conformations (9). In conclusion, the combination of different sequences, charge

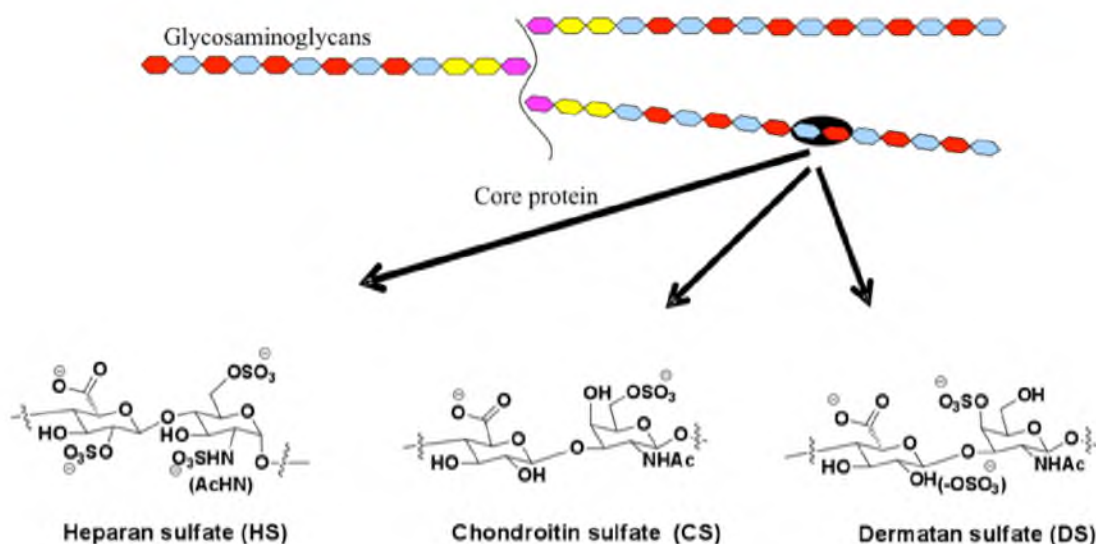


Figure 1.1. Structure of proteoglycans

distribution, and conformations give structural diversity within GAG chains that regulate many important and specific biological functions.

1.1.2. Functions of Proteoglycans

PGs regulate many biological/pathological processes by binding to various proteins, such as growth factors, morphogens, antithrombin, and viral proteins. The list of normal and pathological processes is as follows: development, cell-cell communication, immune defense, viral and parasitic infections, anticoagulation, angiogenesis, tumor metastasis, organogenesis, morphogenesis, axon guidance, growth, and many more (Figure 1.2) (1, 2, 8, 10-15).

Recombinant heparinase I and heparinase III from *Pedobacter heparinus* depolymerize HS in a mouse model into HS fragments, which either promote or inhibit tumor (16). Chondroitinase ABC, which degrades CS, promotes functional recovery following central nervous system injury in adult rats (17). The biological functions of

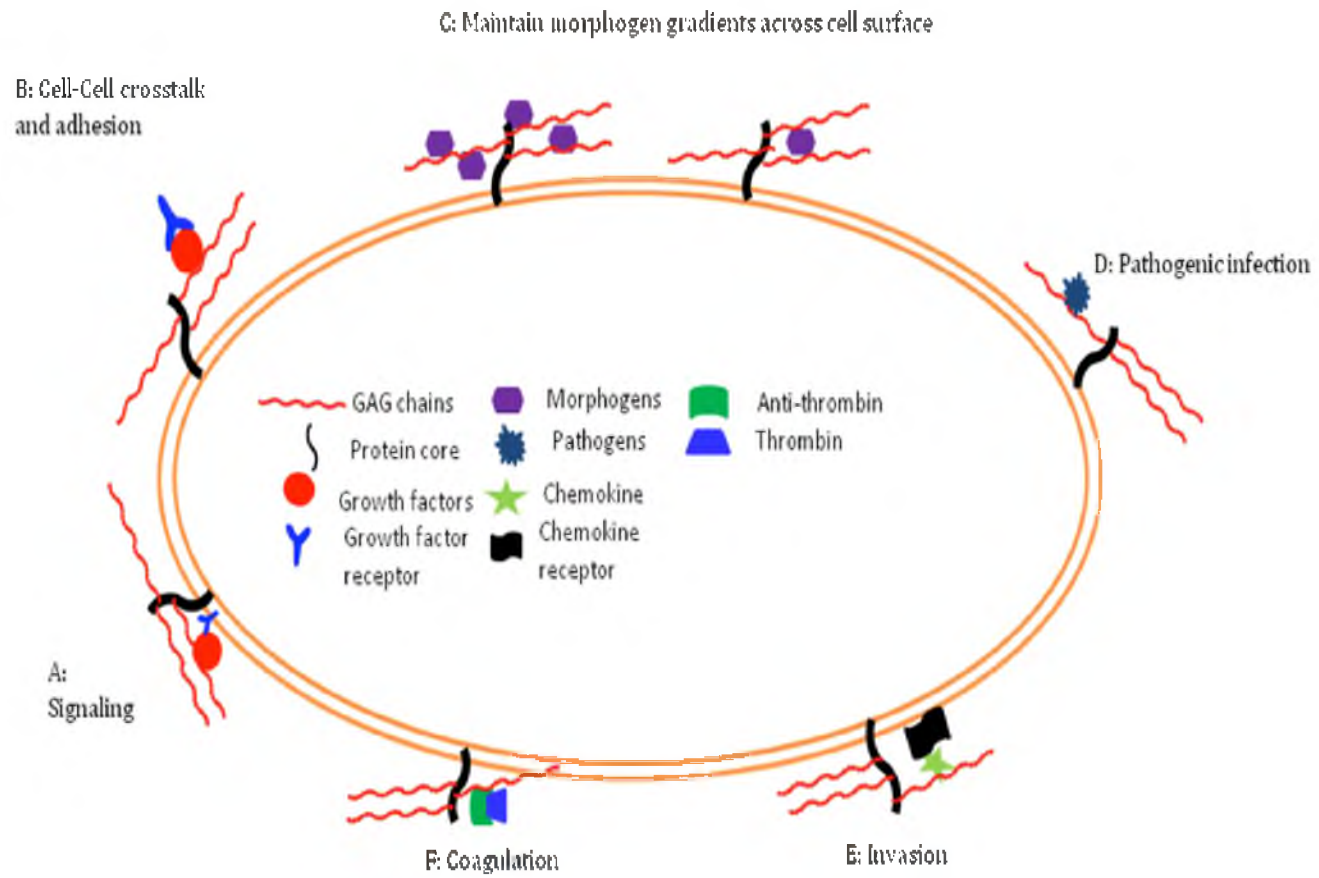


Figure 1.2. Functions of proteoglycans in cell physiology

PGs depend on the interactions between specific sulfate groups and cationic amino acids of protein ligands (1, 2, 10-14, 18, 19). For example, 2-*O*-sulfate groups are important for the kidney development, whereas 6-*O*-sulfate groups of HS are necessary for the fibroblast growth-driven formation of the tracheal system in *Drosophila* (20). The pentasaccharide subunit of heparin with 3-*O*-sulfate groups is required for binding to antithrombin III and producing a 1000-fold increase in antithrombin III's ability to neutralize thrombin. The heparin-antithrombin III complex also inhibits thrombin production by inactivating factor Xa (18, 20, 21).

Another prominent example of the importance of GAG chains in pathology is that of HS in cancers (1-3, 19). Dramatic changes in the expression of biosynthetic and catabolic enzymes are attributed to alterations in HS structures, which are suggested to affect tumor cell growth, invasion, and metastasis (1-3). For example, heparanase, a β -endoglucuronidase, which is over-expressed in malignant tumors, cleaves HS chains into smaller biologically active oligosaccharides that promote cancer growth, angiogenesis, tumor-cell invasion, and migration (22-24).

Even though PGs play a fundamental role in many biological processes, a molecular level understanding of the roles of specific number of chains, average molecular weight, and sulfate patterns in mediating their functions is largely unknown (8). PGs purified from natural sources are mixtures of chains that contain different sulfate patterns and chain lengths (8). Current clinical data and *in vitro* studies suggest that several GAG chains and their derivatives can be used as therapeutics in antithrombolysis (21, 25-27). However, direct administration of these animal-derived GAG chains faces the problem of molecular heterogeneity, possible contamination with

pathogens, or intentional chemical adulteration (28). Therefore, the synthesis of PGs containing defined number of chains, average molecular weight, sulfate patterns, and HS/CS compositions has the potential to advance our understanding of the structure-activity relationships of PGs and the use of PG inducers as therapeutic agents. In this thesis, a chemical approach using xylosides was designed and induced GAG chain biosynthesis without a core protein. The xyloside technology can control the molecular weight, sulfate pattern, and GAG composition by introducing and changing the hydrophobic aglycone group next to the xylose unit. Therefore, these xylosides can decipher the roles of PGs in biological process accurately. Moreover, the xyloside technology will have potential to be used as therapeutics to ameliorate a variety of disease states.

1.1.3. The Roles of RGD Peptides in Targeting Specific Cells and Antiplatelet Aggregation Therapy

The thrombotic process involves the aggregation of platelets, which is mediated by fibrinogen binding to the glycoprotein (GP) IIb/IIIa receptor on the surface of activated platelets (29). Inhibition of fibrinogen binding to the GP IIb/IIIa has been demonstrated to inhibit platelet aggregation (29). Several GP IIb/IIIa inhibitors have a tripeptide sequence, RGD, which is responsible for the recognition of fibrinogen by the GPIIb/IIIa (29). Therefore, RGD derivative can bind to GP IIb/IIIa receptor instead of fibrinogen in order to inhibit platelet aggregation (29). Moreover, RGD selectively binds to $\alpha_v\beta_3$ integrins that are abundantly expressed on the surface of activated endothelial cells and cancers (30).

Linear and cyclic RGD peptides have been employed as targeting vehicles for selective delivery of therapeutic and diagnostic agents (30). Therefore, conjugating RGD peptides to xylose residues leads to the development of anticoagulant or anticancer drugs because they can selectively target activated endothelial cells, which can induce therapeutic GAGs at a local site, and can bind to GP IIb/IIIa receptor to inhibit the platelet aggregation.

1.1.4. Biosynthesis of GAG Chains

The biosynthesis of GAG chains involves many enzymes with many isoforms as well as sugar activators (31, 32). The specific structures of GAG chains are synthesized in specific compartments that contain a specific enzyme in the Golgi apparatus called GAGOSOMES (18, 33). The biosynthesis of GAG chains involves three stages: tetrasaccharide linkage region assembly, GAG chain elongation, and GAG chain modification (18, 31, 32). The tetrasaccharide linkage is assembled to initiate the GAG chains, followed by GAG chain elongation. When the chain polymerizes, it undergoes a series of modifications (18, 31, 32). However, the expression level of enzymes affects both polymerization and type/extent of modifications (34). For example, exostosin proteins (EXT1 and EXT2) affect the action of *N*-deacetylase *N*-sulfotransferase 1 (NDST 1), which influences further modification (34).

1.1.4.1. Assembly of GAG linkage region

The biosynthesis of GAG chains is initiated by the transfer of xylose (Xyl) residue from the UDP-Xyl to certain serine amino acids in the core proteins by

xylosyltransferase in the endoplasmic reticulum (18, 31, 32, 35). Next, two galactose (Gal) residues are transferred by galactosyltransferases I and II (18, 31, 32). Subcellular fractionation of chick cartilage demonstrated that two Gal transferases reside in different parts of the cis/medial Golgi (18, 31, 32). The attachment of one GlcA residue by glucuronosyltransferase completes the formation of the tetrasaccharide linkage region (18, 31, 32). The linkage region undergoes a series of additional modifications such as sulfation/sulfonation and phosphorylation (18). 2-*O*-Phosphorylation of Xyl and 6-*O*-sulfation of Gal affect the activity of glucuronyltransferase-I in order to complete the tetrasaccharide linkage (36). The linkage region in a variety of CS and DS contains 4-*O* or 6-*O*-sulfated Gal residues, but the linkage region of HS does not (18, 31). No specific Gal sulfotransferases have been found for the linkage region, which suggests that sulfate of both Gal residues are catalyzed by the same sulfotransferases that add sulfate groups to the disaccharides of CS (31). A sequence of core protein amino acids contributes to the specification of CS/DS or HS (31, 37). In general, Ser-Gly sites are necessary to facilitate the xylose transfer. Amino acid sequences of CS attachment sites have the following consensus sequence: a-a-a-a-Gly-Ser-Gly-a-b-a (where a = Glu or Asp and b = Gly, Glu or Asp) (31).

1.1.4.2. GAG elongation and modification

The pathways of HS and CS/DS synthesis are different after the formation of the linkage region. The addition of α -4-*N*-acetyl glucosamine (GlcNAc) to the linkage region is required for the assembly of HS, whereas the addition of β -4-*N*-acetyl galactosamine (GalNAc) is necessary for CS/DS chains (31, 32, 38). The GlcNAc

transferase has a domain that interacts with the acidic residues either near the core protein or one or more hydrophobic residues of exogenous xylosides; this then facilitates selective addition of α -4-GlcNAc to trigger HS assemblies (32, 38). After the attachment of the first α -GlcNAc residue, HS chains are formed by repetitive addition of GlcA and GlcNAc units by enzymes EXT1 and EXT2 (18, 32). For CS biosynthesis, upon completion of the linkage region and the addition of the first GalNAc, the polymerization of CS chains continues with the repetitive addition of GlcA and GalNAc residues using CS synthase (31). Density gradient subfractionation have indicated that the polymer formation in CS happens in medial/trans Golgi (31).

While elongation is in progress, parts of the GAG chains are modified via highly coordinated multiple sulfation/epimerization steps (18). For HS biosynthesis, one of the important modifications is *N*-deacetylation and *N*-sulfation of GlcNAc residues (32). The *N*-acetyl groups from GlcNAc units are removed to generate positively charged free amino groups, which are then substituted with sulfate groups using 3'-phosphoadenosine 5'-phosphosulfate (PAPS) as sulfate donor by a bifunctional enzyme (NDST) (18, 32). *L*-IdoA residues are formed by epimerization of *D*-GlcA next to the reducing side of GlcNS units using C5-epimerase (18, 32). The latter modifications are facilitated by a variety of *O*-sulfotransferases (OST), which transfer the sulfate groups from PAPS to the HS chains at specific locations such as the C-2 position of IdoA (2-OST), and to the C-3 and C-6 position of Glc residues (3-OST and 6-OST) (Figure 1.3) (18, 32). For CS sulfate, 4-OST and 6-OST enzymes transfer sulfate groups from PAPS to C-4 and C-6 of GalNAc residues, and 2-OST enzymes add sulfate groups to C-2 of GlcA residues (31). In the

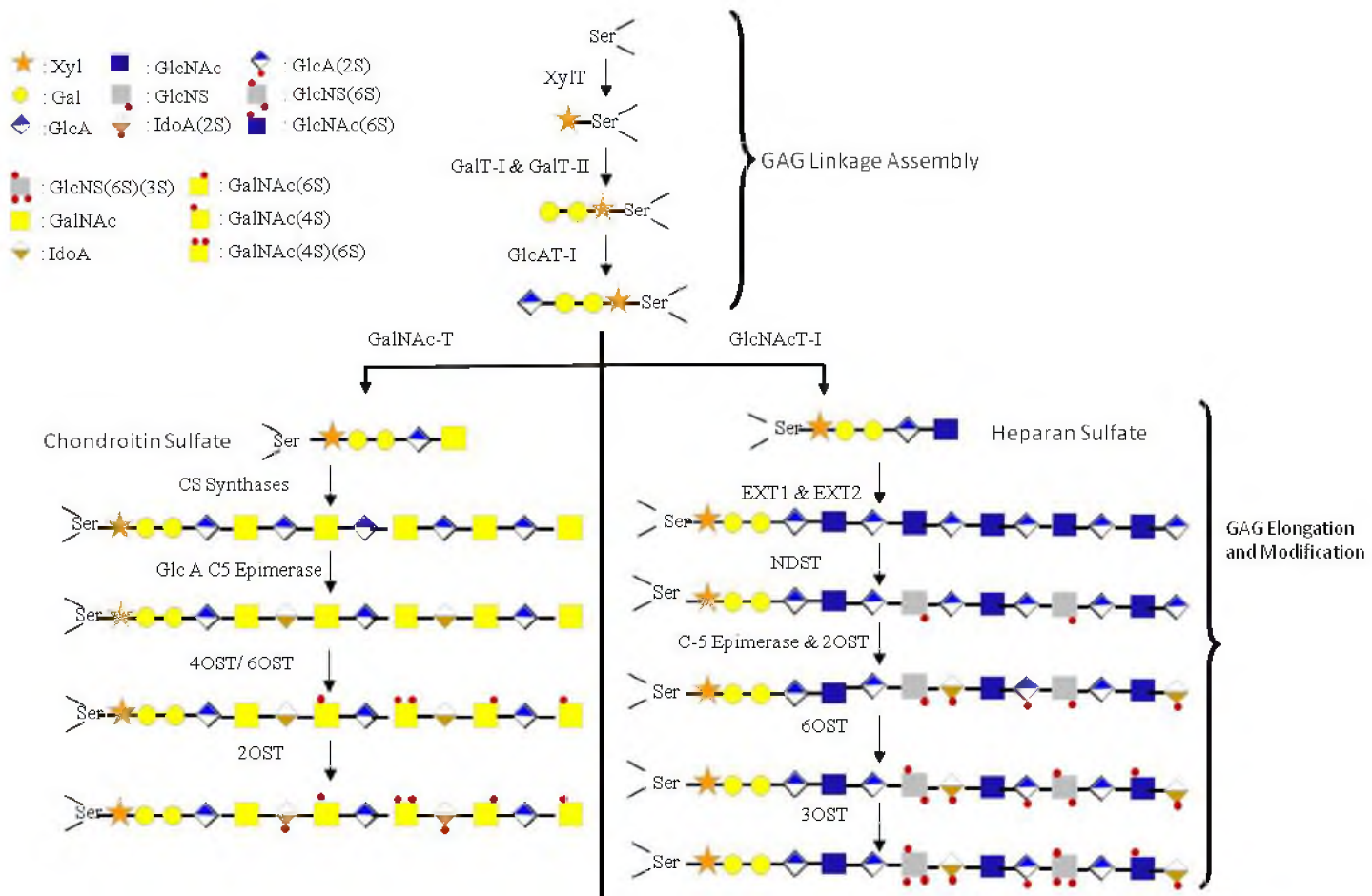


Figure 1.3. Biosynthesis of glycosaminoglycans

case of DS, 4-OST and 6-OST transfer sulfate groups from PAPS to C-4 and C-6 of GalNAc residues and 2-OST transfers sulfate groups to C-2 of IdoA residues (31).

1.1.5. Chemical Approaches to Modulate Cellular GAG Biosynthesis

1.1.5.1. Stimulation of GAG chains

Exogenous xylosides have been used both *in vitro* and *in vivo* to probe the functional significance of GAG chains in various dynamic systems under different conditions (39-51). The story began with *D*-xylose, which acted as an initiator of CS biosynthesis in progeny of brd U-treated limb bud cells at high concentrations (52). Several studies observed that β -*D*-xylosides, such as *p*-nitro-phenyl- β -*D*-xylopyranoside and 4-methyl-umbellifery- β -*D*-xylopyranoside, can stimulate protein-free CS chains more effectively than *D*-xylose in various cell types at much lower concentrations (50). An interesting observation is that the nature of the aglycone group and glycosidic linkages of β -*D*-xylosides influenced the extent of stimulation of CS biosynthesis (47). These molecules containing a hydrophobic aglycone can compete with endogenous core protein receptor sites for the assembly of GAG chains in the Golgi apparatus (39-43, 45) (46). In addition, the hydrophobic aglycone could help xylosides pass through the membrane and therefore increase priming activity/production of GAG chains. The glycosidic linkage of β -*D*-xylosides also affects GAG priming activity (45). A library of aryl and alkyl-*O*- β -*D*-xylosides and their analogues with S, NH, or CH₂ in the glycosidic linkage was synthesized and tested for their priming activities (53). *S*-xylosides were more effective primers than the corresponding *N*-xylosides and *C*-xylosides (53). In addition, the relationship of the structure of the sugars to their priming

activity was evaluated by synthesizing β -*D*-xyloside analogs in which the hydroxyls were substituted with -hydrogen, -fluorine, -*O*-methyl, -amino, -*O*-isopropyl, -*O*-benzyl groups, and epimers at the 2-, 3-, and 4-position of xylose units (44). The substitution of 2-OH and 3-OH with -OCH₃ of xylose units primed better at a higher concentration (1mM) (44). The fluorine derivative at C-3 primed more efficiently than the 3-OH group (44). However, methylated and deoxy analogs at C-4 did not prime due to the loss of the acceptor hydroxyl group (44).

In most cases, priming of CS dominates and synthesis of core-protein free HS chains is low or undetectable (53, 54). Several studies suggested that increased yields of HS can be obtained when the aglycones of the xylosides comprise aromatic, polycyclic structures such as naphthyl derivatives. 2-(6-hydroxynaphthyl)- β -*D*-xylopyranoside is the first molecules that primed a small amount of HS, which selectively inhibited growth of transformed or tumor-derived cells (55, 56). Moreover, the composition of GAG chains also depends on the chemical structures of the aglycone groups (56). For example, ortho-nitro-phenyl-*D*-xyloside produced the composition of HS and CS (20- and 100-fold) (56). However, para-nitro-phenyl-xyloside produced only 37 and 3-fold of CS and HS, respectively (56). Estradiol- β -*D*-xyloside was also an efficient primer for HS biosynthesis and the proportion of HS was raised with increasing concentration of this xylosides (57). Earlier studies led to a conclusion that β -*D*-xyloside carrying two aromatic rings efficiently primed HS, and replacing an oxygen atom with a sulfur atom also increased the efficiency of HS priming (39). However, these synthetic xylosides are very labile. Therefore, it is important to synthesize stable, small molecular xylosides that prime both HS and CS at lower dosages to study biological roles.

Several studies describe an additional approach to stimulate the GAG biosynthesis by using disaccharides as primers (58). However, Chinese hamster ovary cells did not take up these disaccharides efficiently, and the priming activity of disaccharides was improved by protecting the hydroxyl groups with acetyl groups (58).

Multiple GAG attachment sites are found in various PGs (5). This implied that multiple GAG chains are required for optimal biological functionality of PG in various species. Single GAG chains can perhaps not provide the same functionality that multiple GAG chains can. Several earlier studies have rigorously utilized synthetic mono-xylosides to further our understanding of the role of endogenous PGs in model organisms and also to elucidate the elusive biosynthetic mechanism (39-51). Only one study has examined synthetic bis-xylosides, which carry two xylose residues per molecular scaffold, for their priming activity (48). However, these synthetic bis-xylosides carry labile *O*-glycosidic linkage. Therefore, it is important to synthesize stable, small molecular scaffolds carrying a variable number of xylose residues to study the importance of multivalency of GAG.

The priming activity of xylosides is often tested using a mutant Chinese hamster ovary cell line (pgsA-745) (59). This cell line lacks active xylosyltransferases enzyme; therefore, the process requires an exogenous supply of xylosides to produce GAG chains (59). These xylosides pass through membranes of cells, stimulate GAG in the Golgi apparatus, then secret outside of the membranes (Figure 1.4).

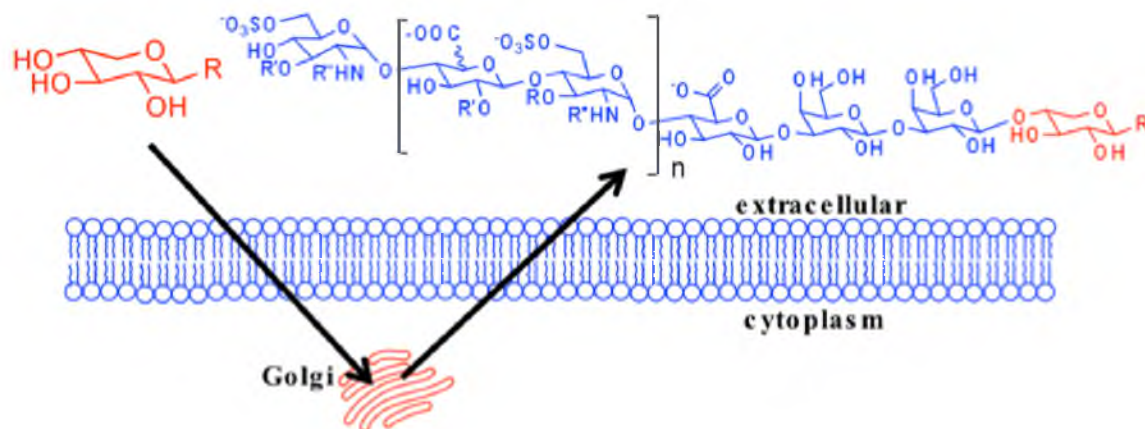


Figure 1.4. Xylosides prime GAG chains

1.1.5.2. Inhibition of GAG biosynthesis

No group has developed a selective or effective inhibitor of endogenous GAG production. The majority of inhibitors developed lack specificity and cannot be used for *in vivo* studies (60-65). Rhodamine B inhibited GAG production by an unknown mechanism, which effectively reduced GAG storage in somatic tissues and brain (60). However, the use of rhodamine B in clinical practice is unlikely due to its possible toxic effects (61). Brefeldin A (BFA), a fungal isoprenoid metabolite, inhibits the secretory transport of Golgi vesicles, an important step in HS and CS biosynthesis (62). However, BFA affects the biosynthesis of other glycoconjugates as well (63). Therefore, BFA is not an effective inhibitor of endogenous GAG production because it is difficult to use BFA to pinpoint the biological actions of GAG chains without affecting other glycosylation events (63). To elucidate the biological significance of sulfated groups of GAG chains, several approaches have been employed (64, 65). For example, sodium chlorate can inhibit the formation of PAPS by competitively binding to PAPS synthase and thereby affect GAG sulfation (64, 65). However, since a high concentration of

chlorate is required for it to be effective, chlorate is not suitable for *in vivo* experiments (65). In addition, sodium chlorate unselectively affects all the sulfation patterns (65). In another approach, a series of 4-deoxyglucosamine analogs were examined for their ability to inhibit GAG biosynthesis in hepatocytes (66). GAG chains isolated from analog-treated hepatocytes were shown to be smaller in size than those isolated from control cells (66). Unfortunately, these analogs are not selective inhibitors of GAG biosynthesis and affect the biosynthesis of other glycoconjugates as well. Therefore, it is important to synthesize a library that can selectively inhibit GAG biosynthesis without having any toxic effects on cells to identify the biological functions of GAG chains.

1.2. Research Objectives

Overall, my goals are to study structure-function relationship and biosynthesis of PGs *in vitro* by synthesizing carbohydrate-based cellular probes. Controlling the fine structures of endogenous and exogenous GAG chains significantly regulates many important biological processes. In addition, targeting the exogenous GAG chains to activated endothelial cells and cancer cells impacts the growth, invasion, and metastatic properties of tumor cells. Therefore, a library of xylosides was synthesized to understand biosynthetic pathways, structure, and functions of PGs.

1.2.1. Specific Aim I

A number of xylosides were studied to understand the mechanism of GAG biosynthesis. In the first part, the importance of the chemical structures of aglycone groups was demonstrated in priming activity and fine structures of primed GAG chains.

Most of the xylosides that were studied make mostly CS and a very little HS. For example, a library of β -*O*-xylosides was examined to stimulate different amounts of CS and DS chains at specific concentrations. However, *O*-xylosides are considered to be hydrolytically unstable in cells. A library of xylosides with different aglycone groups was designed using fast reactions “click chemistry” because of its high efficiency, regioselectivity, biological compatibility, and chemical stability in aqueous/organic solvents. These xylosides were tested in a Chinese hamster ovary cell line (pgsA-745), which lacks active xylosyltransferases enzyme. The results show that these xylosides are stable for at least five days, and demonstrate the importance of aglycone groups in priming activity and induce specific structures of GAGs. In the second part of this study, GAG biosynthesis was inhibited using 4-F-xylosides. From the first part, xylosides containing a specific hydrophobic aglycone are efficient acceptors for the elongation of GAG chains; therefore, the 4-OH group of these xylosides was blocked to prevent the galactosyltransferase from transferring galactose to the xylosides and inhibits GAG biosynthesis without toxicity to cells at various concentrations.

1.2.2. Specific Aim II

GAGs play decisive roles in various cancer-associated processes. Changes in the expression of GAG fine structures, attributed to deregulation of their biosynthetic and catabolic enzymes, are hallmarks of tumor progression and pathogenicity. The widespread role of GAG chains in tumor biology, tumor-associated angiogenesis, and metastasis has led to the development of therapeutic agents including enzyme inhibitors, modified GAG chains, and GAG binding peptides. Xylosides carrying hydrophobic

aglycone have been known to induce GAG biosynthesis whose composition depends on the nature of aglycone. Given the important roles of GAG chains in tumor biology, RGD-conjugated xylosides were synthesized to target cells expressing $\alpha_v\beta_3$ integrin, including cancer cells and the endothelium surrounding cancer cells, and thereby modulate the tumor behavior through induction of GAG chains. Our results demonstrate that RGD-conjugated xylosides are able to prime GAG chains in various cell types and future studies are aimed toward evaluating potential utility of such xylosides in treating myocardial infarction as well as cancer-associated thrombotic complications.

1.2.3. Specific Aim III

Deciphering dynamic changes in GAG structures will provide new avenues to diagnose disease states and better understand their dynamic spatio-temporal role in developing embryos. Radioactive chemicals are used to label GAG chains in most cellular studies; however, they are usually toxic in animal models. Fluorescent xylosides may serve as excellent chemical probes to profile cell-specific GAG structures and to define the role of GAG chains in various patho-physiological processes. 4-methyl-umbellifery- β -D-xyloside is the only known fluorescent molecule that can prime GAG chains. However, it makes mostly CS chains of low average molecular weight (< 3000 Da). Therefore, fluorescent xylosides were synthesized and tested for their priming activities of HS and CS *in vitro*. Our result showed that neither dansyl-xylosides nor fluorescein-xylosides primed any detectable GAG chains and pyrene- and umbelliferyl-click-xylosides were able to prime GAG with higher average MW than commercial umbelliferyl-O-xylosides.

1.2.4. Specific Aim IV

Most PGs have multiple polysaccharide chains that regulate numerous cell signaling events in many biological systems. One distinct structural feature of all PG, except decorin, is the covalent linkage of two or more GAG side chains to a core protein. The biological significance of GAG multivalency is largely unknown. Previous studies have shown that the synergistic biological activity of multivalent GAG chains is not accomplished by the sum of the activities of individual chains. Furthermore, it is still unclear how multiple GAG chains are assembled onto a given PG. To delineate the biological significance of GAG valency and to probe their potential assembly mechanism, a library of cluster xylosides carrying two, three, or four xylose residues on the same scaffold was designed to induce multiple GAG chains and mimic naturally occurring PGs. These results show bis-xylosides primed higher molecular weight GAG chains compared to tris- and tetrakis-xylosides. Cluster xylosides prime significant CS/DS and less HS on a given scaffold in CHO cells and the distance between xylose units affects the priming activity. Multivalent GAG chains, induced by cluster-xylosides, can better mimic PGs and therefore can be used as molecular probes to examine the biological significance of GAG multivalency in model organisms.

1.3. References

1. Sasisekharan, R., Shriver, Z., Venkataraman, G., and Narayanasami, U. (2002) Roles of heparan-sulphate glycosaminoglycans in cancer, *Nat Rev Cancer* 2, 521-528.
2. Powell, A. K., Yates, E. A., Fernig, D. G., and Turnbull, J. E. (2004) Interactions of heparin/heparan sulfate with proteins: appraisal of structural factors and experimental approaches, *Glycobiology* 14, 17R-30R.
3. Murrey, H. E., and Hsieh-Wilson, L. C. (2008) The chemical neurobiology of carbohydrates, *Chem Rev* 108, 1708-1731.
4. Hacker, U., Nybakken, K., and Perrimon, N. (2005) Heparan sulphate proteoglycans: the sweet side of development, *Nat Rev Mol Cell Biol* 6, 530-541.
5. Kjellen, L., and Lindahl, U. (1991) Proteoglycans: structures and interactions, *Annu Rev Biochem* 60, 443-475.
6. Bernfield, M., Gotte, M., Park, P. W., Reizes, O., Fitzgerald, M. L., Lincecum, J., and Zako, M. (1999) Functions of cell surface heparan sulfate proteoglycans, *Annu Rev Biochem* 68, 729-777.
7. Iozzo, R. V. (1998) Matrix proteoglycans: from molecular design to cellular function, *Annu Rev Biochem* 67, 609-652.
8. Sasisekharan, R., Raman, R., and Prabhakar, V. (2006) Glycomics approach to structure-function relationships of glycosaminoglycans, *Annu Rev Biomed Eng* 8, 181-231.
9. Mulloy, B., and Forster, M. J. (2000) Conformation and dynamics of heparin and heparan sulfate, *Glycobiology* 10, 1147-1156.
10. Lander, A. D. (1993) Proteoglycans in the nervous system, *Curr Opin Neurobiol* 3, 716-723.
11. Capila, I., and Linhardt, R. J. (2002) Heparin-protein interactions, *Angew Chem Int Ed Engl* 41, 391-412.
12. Salmivirta, M., Lidholt, K., and Lindahl, U. (1996) Heparan sulfate: a piece of information, *FASEB J* 10, 1270-1279.
13. Maeda, N., Ishii, M., Nishimura, K., and Kamimura, K. (2011) Functions of chondroitin sulfate and heparan sulfate in the developing brain, *Neurochem Res* 36, 1228-1240.

14. Carney, S. L., and Muir, H. (1988) The structure and function of cartilage proteoglycans, *Physiol Rev* 68, 858-910.
15. Bishop, J. R., Schuksz, M., and Esko, J. D. (2007) Heparan sulphate proteoglycans fine-tune mammalian physiology, *Nature* 446, 1030-1037.
16. Liu, D., Shriver, Z., Venkataraman, G., El Shabrawi, Y., and Sasisekharan, R. (2002) Tumor cell surface heparan sulfate as cryptic promoters or inhibitors of tumor growth and metastasis, *Proc Natl Acad Sci U S A* 99, 568-573.
17. Bradbury, E. J., Moon, L. D., Popat, R. J., King, V. R., Bennett, G. S., Patel, P. N., Fawcett, J. W., and McMahon, S. B. (2002) Chondroitinase ABC promotes functional recovery after spinal cord injury, *Nature* 416, 636-640.
18. Esko, J. D., and Selleck, S. B. (2002) Order out of chaos: assembly of ligand binding sites in heparan sulfate, *Annu Rev Biochem* 71, 435-471.
19. Fuster, M. M., and Esko, J. D. (2005) The sweet and sour of cancer: glycans as novel therapeutic targets, *Nat Rev Cancer* 5, 526-542.
20. Gorski, B., and Stringer, S. E. (2007) Tinkering with heparan sulfate sulfation to steer development, *Trends Cell Biol* 17, 173-177.
21. Petitou, M., Herault, J. P., Bernat, A., Driguez, P. A., Duchaussoy, P., Lormeau, J. C., and Herbert, J. M. (1999) Synthesis of thrombin-inhibiting heparin mimetics without side effects, *Nature* 398, 417-422.
22. Nasser, N. J. (2008) Heparanase involvement in physiology and disease, *Cell Mol Life Sci* 65, 1706-1715.
23. Vlodaysky, I., Ilan, N., Nadir, Y., Brenner, B., Katz, B. Z., Naggi, A., Torri, G., Casu, B., and Sasisekharan, R. (2007) Heparanase, heparin and the coagulation system in cancer progression, *Thromb Res* 120 Suppl 2, S112-120.
24. Lever, R., and Page, C. P. (2002) Novel drug development opportunities for heparin, *Nat Rev Drug Discov* 1, 140-148.
25. Li, W., Johnson, D. J., Esmon, C. T., and Huntington, J. A. (2004) Structure of the antithrombin-thrombin-heparin ternary complex reveals the antithrombotic mechanism of heparin, *Nat Struct Mol Biol* 11, 857-862.
26. Nenci, G. G. (2002) Dermatan sulphate as an antithrombotic drug, *Pathophysiol Haemost Thromb* 32, 303-307.

27. Maimone, M. M., and Tollefsen, D. M. (1990) Structure of a dermatan sulfate hexasaccharide that binds to heparin cofactor II with high affinity, *J Biol Chem* 265, 18263-18271.
28. Simasathien, S., Thomas, S. J., Watanaveeradej, V., Nisalak, A., Barberousse, C., Innis, B. L., Sun, W., Putnak, J. R., Eckels, K. H., Hutagalung, Y., Gibbons, R. V., Zhang, C., De La Barrera, R., Jarman, R. G., Chawachalasai, W., and Mammen, M. P., Jr. (2008) Safety and immunogenicity of a tetravalent live-attenuated dengue vaccine in flavivirus naive children, *Am J Trop Med Hyg* 78, 426-433.
29. Wang, W., Borchardt, R. T., and Wang, B. (2000) Orally active peptidomimetic RGD analogs that are glycoprotein IIb/IIIa antagonists, *Curr Med Chem* 7, 437-453.
30. Temming, K., Schiffelers, R. M., Molema, G., and Kok, R. J. (2005) RGD-based strategies for selective delivery of therapeutics and imaging agents to the tumour vasculature, *Drug Resist Updat* 8, 381-402.
31. Silbert, J. E., and Sugumaran, G. (2002) Biosynthesis of chondroitin/dermatan sulfate, *IUBMB Life* 54, 177-186.
32. Sugahara, K., and Kitagawa, H. (2002) Heparin and heparan sulfate biosynthesis, *IUBMB Life* 54, 163-175.
33. Victor, X. V., Nguyen, T. K., Ethirajan, M., Tran, V. M., Nguyen, K. V., and Kuberan, B. (2009) Investigating the elusive mechanism of glycosaminoglycan biosynthesis, *J Biol Chem* 284, 25842-25853.
34. Presto, J., Thuveson, M., Carlsson, P., Busse, M., Wilen, M., Eriksson, I., Kusche-Gullberg, M., and Kjellen, L. (2008) Heparan sulfate biosynthesis enzymes EXT1 and EXT2 affect NDST1 expression and heparan sulfate sulfation, *Proc Natl Acad Sci U S A* 105, 4751-4756.
35. Vertel, B. M., Walters, L. M., Flay, N., Kearns, A. E., and Schwartz, N. B. (1993) Xylosylation is an endoplasmic reticulum to Golgi event, *J Biol Chem* 268, 11105-11112.
36. Tone, Y., Pedersen, L. C., Yamamoto, T., Izumikawa, T., Kitagawa, H., Nishihara, J., Tamura, J., Negishi, M., and Sugahara, K. (2008) 2-O-phosphorylation of xylose and 6-O-sulfation of galactose in the protein linkage region of glycosaminoglycans influence the glucuronyltransferase-I activity involved in the linkage region synthesis, *J Biol Chem* 283, 16801-16807.
37. Longas, M. O., and Meyer, K. (1982) Evidence that a reducible xylosyl-lysine is the protein linkage of dermatan sulfate, *Proc Natl Acad Sci U S A* 79, 6225-6228.

38. Esko, J. D., and Zhang, L. (1996) Influence of core protein sequence on glycosaminoglycan assembly, *Curr Opin Struct Biol* 6, 663-670.
39. Mani, K., Belting, M., Ellervik, U., Falk, N., Svensson, G., Sandgren, S., Cheng, F., and Fransson, L. A. (2004) Tumor attenuation by 2(6-hydroxynaphthyl)-beta-D-xylopyranoside requires priming of heparan sulfate and nuclear targeting of the products, *Glycobiology* 14, 387-397.
40. Okayama, M., Kimata, K., and Suzuki, S. (1973) The influence of p-nitrophenyl beta-d-xyloside on the synthesis of proteochondroitin sulfate by slices of embryonic chick cartilage, *J Biochem (Tokyo)* 74, 1069-1073.
41. Robinson, H. C., Brett, M. J., Tralaggan, P. J., Lowther, D. A., and Okayama, M. (1975) The effect of D-xylose, beta-D-xylosides and beta-D-galactosides on chondroitin sulphate biosynthesis in embryonic chicken cartilage, *Biochem J* 148, 25-34.
42. Fritz, T. A., Lugemwa, F. N., Sarkar, A. K., and Esko, J. D. (1994) Biosynthesis of heparan sulfate on beta-D-xylosides depends on aglycone structure, *J Biol Chem* 269, 300-307.
43. Kuberan, B., Ethirajan, M., Victor, X. V., Tran, V., Nguyen, K., and Do, A. (2008) "Click" xylosides initiate glycosaminoglycan biosynthesis in a mammalian cell line, *Chembiochem* 9, 198-200.
44. Lugemwa, F. N., Sarkar, A. K., and Esko, J. D. (1996) Unusual beta-D-xylosides that prime glycosaminoglycans in animal cells, *J Biol Chem* 271, 19159-19165.
45. Jacobsson, M., Mani, K., and Ellervik, U. (2007) Effects of oxygen-sulfur substitution on glycosaminoglycan-priming naphthoxylosides, *Bioorg Med Chem* 15, 5283-5299.
46. Jacobsson, M., Winander, C., Mani, K., and Ellervik, U. (2008) Xylose as a carrier for boron containing compounds, *Bioorg Med Chem Lett* 18, 2451-2454.
47. Malmberg, J., Mani, K., Sawen, E., Wiren, A., and Ellervik, U. (2006) Synthesis of aromatic C-xylosides by position inversion of glucose, *Bioorg Med Chem* 14, 6659-6665.
48. Johnsson, R., Mani, K., and Ellervik, U. (2007) Synthesis and biology of bis-xylosylated dihydroxynaphthalenes, *Bioorg Med Chem* 15, 2868-2877.
49. Tran, V. M., Victor, X. V., Yockman, J. W., and Kuberan, B. (2010) RGD-xyloside conjugates prime glycosaminoglycans, *Glycoconj J* 27, 625-633.

50. Okayama, M., Kimata, K., and Suzuki, S. (1973) The influence of p-nitrophenyl beta-d-xyloside on the synthesis of proteochondroitin sulfate by slices of embryonic chick cartilage, *J Biochem* 74, 1069-1073.
51. Galligani, L., Hopwood, J., Schwartz, N. B., and Dorfman, A. (1975) Stimulation of synthesis of free chondroitin sulfate chains by beta-D-xylosides in cultured cells, *J Biol Chem* 250, 5400-5406.
52. Levitt, D., and Dorfman, A. (1973) Control of chondrogenesis in limb-bud cell cultures by bromodeoxyuridine, *Proc Natl Acad Sci U S A* 70, 2201-2205.
53. Sobue, M., Habuchi, H., Ito, K., Yonekura, H., Oguri, K., Sakurai, K., Kamohara, S., Ueno, Y., Noyori, R., and Suzuki, S. (1987) beta-D-xylosides and their analogues as artificial initiators of glycosaminoglycan chain synthesis. Aglycone-related variation in their effectiveness *in vitro* and *in vivo*, *Biochem J* 241, 591-601.
54. Schwartz, N. B., Galligani, L., Ho, P. L., and Dorfman, A. (1974) Stimulation of synthesis of free chondroitin sulfate chains by beta-D-xylosides in cultured cells, *Proc Natl Acad Sci U S A* 71, 4047-4051.
55. Belting, M., Borsig, L., Fuster, M. M., Brown, J. R., Persson, L., Fransson, L. A., and Esko, J. D. (2002) Tumor attenuation by combined heparan sulfate and polyamine depletion, *Proc Natl Acad Sci U S A* 99, 371-376.
56. Moreira, C. R., Lopes, C. C., Cuccovia, I. M., Porcionatto, M. A., Dietrich, C. P., and Nader, H. B. (2004) Heparan sulfate and control of endothelial cell proliferation: increased synthesis during the S phase of the cell cycle and inhibition of thymidine incorporation induced by ortho-nitrophenyl-beta-D-xylose, *Biochim Biophys Acta* 1673, 178-185.
57. Lagemwa, F. N., and Esko, J. D. (1991) Estradiol beta-D-xyloside, an efficient primer for heparan sulfate biosynthesis, *J Biol Chem* 266, 6674-6677.
58. Sarkar, A. K., Fritz, T. A., Taylor, W. H., and Esko, J. D. (1995) Disaccharide uptake and priming in animal cells: inhibition of sialyl Lewis X by acetylated Gal beta 1-->4GlcNAc beta-O-naphthalenemethanol, *Proc Natl Acad Sci U S A* 92, 3323-3327.
59. Esko, J. D., Stewart, T. E., and Taylor, W. H. (1985) Animal cell mutants defective in glycosaminoglycan biosynthesis, *Proc Natl Acad Sci U S A* 82, 3197-3201.
60. Roberts, A. L., Thomas, B. J., Wilkinson, A. S., Fletcher, J. M., and Byers, S. (2006) Inhibition of glycosaminoglycan synthesis using rhodamine B in a mouse model of mucopolysaccharidosis type IIIA, *Pediatr Res* 60, 309-314.

61. Roberts, A. L., Rees, M. H., Klebe, S., Fletcher, J. M., and Byers, S. (2007) Improvement in behaviour after substrate deprivation therapy with rhodamine B in a mouse model of MPS IIIA, *Mol Genet Metab* 92, 115-121.
62. Calabro, A., and Hascall, V. C. (1994) Effects of brefeldin A on aggrecan core protein synthesis and maturation in rat chondrosarcoma cells, *J Biol Chem* 269, 22771-22778.
63. Sherwood, A. L., and Holmes, E. H. (1992) Brefeldin A induced inhibition of de novo globo- and neolacto-series glycolipid core chain biosynthesis in human cells. Evidence for an effect on beta 1-->4galactosyltransferase activity, *J Biol Chem* 267, 25328-25336.
64. Greve, H., Cully, Z., Blumberg, P., and Kresse, H. (1988) Influence of chlorate on proteoglycan biosynthesis by cultured human fibroblasts, *J Biol Chem* 263, 12886-12892.
65. Safaiyan, F., Kolset, S. O., Prydz, K., Gottfridsson, E., Lindahl, U., and Salmivirta, M. (1999) Selective effects of sodium chlorate treatment on the sulfation of heparan sulfate, *J Biol Chem* 274, 36267-36273.
66. Berkin, A., Szarek, W. A., and Kisilevsky, R. (2005) Biological evaluation of a series of 2-acetamido-2-deoxy-D-glucose analogs towards cellular glycosaminoglycan and protein synthesis *in vitro*, *Glycoconj J* 22, 443-451.

CHAPTER 2

MODULATION OF GAG BIOSYNTHESIS BY CLICK-XYLOSIDES

2.1. Synthesis of Click-xylosides That Initiate GAG Biosynthesis

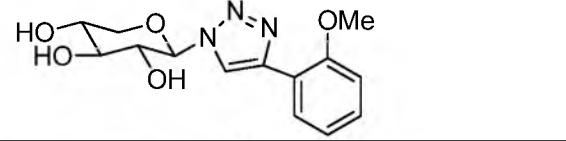
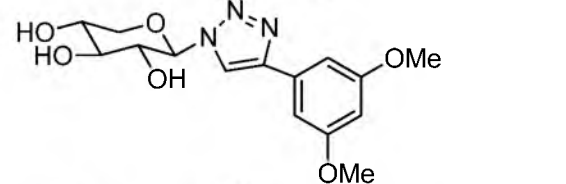
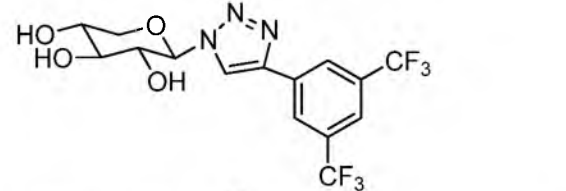
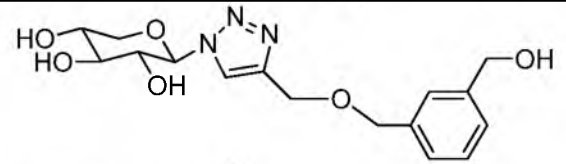
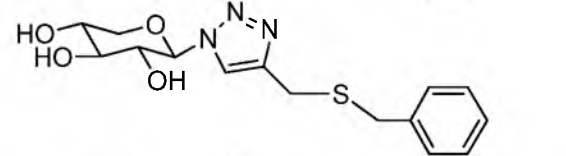
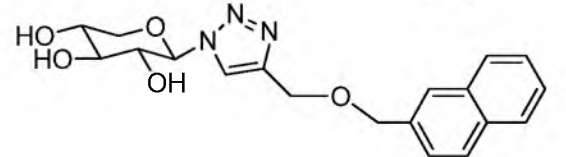
2.1.1. Introduction

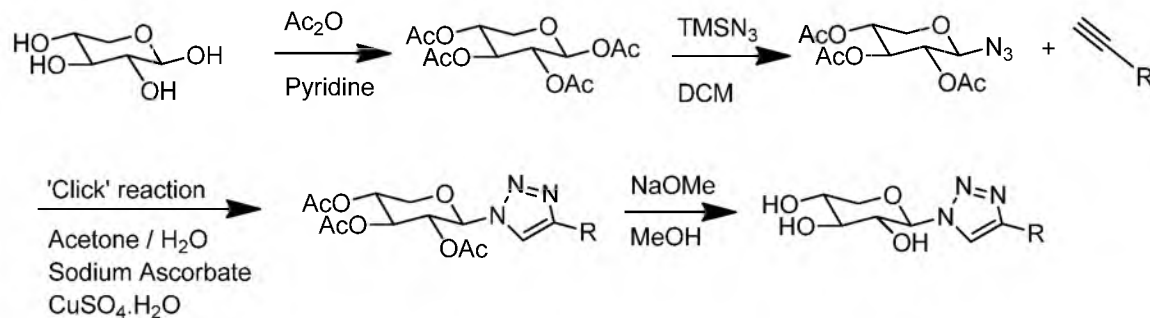
A number of xylosides were studied to further understand the mechanism of GAG biosynthesis (1-5). It is observed that the priming activity and composition of GAG chains depends on the structure of the aglycone moiety (1-5). However, most of the xylosides that were studied made mostly CS and fewer HS. For example, a library of β -*O*-xylosides was examined to stimulate different amounts of CS and DS chains at specific concentrations (1-5). However, *O*-xylosides are considered to be hydrolytically unstable in cells. In addition, *S*- and *C*-xylosides which are more stable than *O*-xylosides are also shown to prime GAG chains, but only a select few of these xylosides were examined in detail (6). A library of xylosides with different aglycone groups was designed using “click chemistry” because of its high efficiency, regioselectivity, biological compatibility, and chemical metabolic/ stability in aqueous/ organic solvents (7). Click-xylosides offer two advantages: (1) the 1, 2, 3-triazole ring, generated during “click chemistry,” is a metabolically stable linker between xylose residues and aglycones and (2) the triazole ring can facilitate hydrogen-bonding interactions, resulting in favorable and productive biological effects.

2.1.2. Synthesis of Click-xylosides

To define the importance of aglycone structures in GAG priming activity, a library of click-xylosides carrying different aglycones (Table 2.1) was synthesized using click-chemistry as depicted in Scheme 2.1.

Table 2.1 Click-xylosides with various aglycone groups

Entry	Structure
1	 <p>Chemical structure 1: A xylofuranose ring (a five-membered ring with an oxygen atom at the top and hydroxyl groups at the 2, 3, and 4 positions) is linked via its C1 position to the 4-position of a 1,2,3-triazole ring. The 5-position of the triazole ring is substituted with a 4-methoxyphenyl group (a benzene ring with a methoxy group, -OMe, at the para position).</p>
2	 <p>Chemical structure 2: A xylofuranose ring is linked via its C1 position to the 4-position of a 1,2,3-triazole ring. The 5-position of the triazole ring is substituted with a 3,5-dimethoxyphenyl group (a benzene ring with methoxy groups, -OMe, at the meta positions).</p>
3	 <p>Chemical structure 3: A xylofuranose ring is linked via its C1 position to the 4-position of a 1,2,3-triazole ring. The 5-position of the triazole ring is substituted with a 3,5-bis(trifluoromethyl)phenyl group (a benzene ring with trifluoromethyl groups, -CF₃, at the meta positions).</p>
4	 <p>Chemical structure 4: A xylofuranose ring is linked via its C1 position to the 4-position of a 1,2,3-triazole ring. The 5-position of the triazole ring is substituted with a 4-(hydroxymethyl)benzyloxy group (a benzene ring with a hydroxymethyl group, -CH₂OH, at the para position, connected to the triazole via a -CH₂-O-CH₂- linker).</p>
5	 <p>Chemical structure 5: A xylofuranose ring is linked via its C1 position to the 4-position of a 1,2,3-triazole ring. The 5-position of the triazole ring is substituted with a benzylsulfanyl group (a benzene ring connected to the triazole via a -CH₂-S-CH₂- linker).</p>
6	 <p>Chemical structure 6: A xylofuranose ring is linked via its C1 position to the 4-position of a 1,2,3-triazole ring. The 5-position of the triazole ring is substituted with a naphthalen-1-ylmethyl group (a naphthalene ring system connected to the triazole via a -CH₂-O-CH₂- linker).</p>



Scheme 2.1. Synthesis of click-xylosides

This conjugation approach relies on the Cu(I)-catalyzed orthogonal reaction of azide-containing xylosyl scaffold with a terminal alkyne containing aglycone. This approach introduces a diverse set of aglycones very quickly and allows one to systematically examine the effect of aglycone moieties on the stimulation of GAGs in a variety of cellular systems.

Click-xyloside 1: ^1H NMR (CD_3OD): δ 8.45 (1H, s, triazolyl H), 8.11 (1H, d, $J = 7.8$, Ar-H), 7.35 (1H, dd, $J = 7.0, 8.6$ Hz, Ar-H), 7.11 (1H, d, $J = 8.2$ Hz, Ar-H), 7.06 (1H, dd, $J = 7.4, 8.6$ Hz, Ar-H), 5.56 (1H, d, $J = 9.4$ Hz, H-1), 4.06-4.00 (2H, m, H-2, H-5a), 3.96 (3H, s), 3.75-3.68 (1H, m, H-4), 3.54-3.47 (2H, m, H-3, H-5b); Mass (ESI): calculated for $\text{C}_{14}\text{H}_{18}\text{N}_3\text{O}_5$ 308.125, found 307.933

Click-xyloside 2: ^1H NMR (CD_3OD): δ 8.54 (1H, s, triazolyl H), 7.02 (2H, d, $J = 2.3$ Hz, Ar-H), 6.48 (1H, t, $J = 2.3$ Hz, Ar-H), 5.54 (1H, d, $J = 9.4$ Hz, H-1), 4.03 (1H, dd, $J = 5.5, 11.3$ Hz, H-5a), 3.94 (1H, d, $J = 9.4$ Hz, H-2), 3.82 (6H, s), 3.71-3.67 (1H, m, H-4), 3.54-3.47 (2H, m, H-3, H-5b); Mass (ESI): calculated for $\text{C}_{15}\text{H}_{20}\text{N}_3\text{O}_6$ 338.135, found 338.000

Click-xyloside **3**: ^1H NMR (CD_3OD): δ 8.87 (1H, s, triazolyl H), 8.47 (2H, s, Ar-H), 7.95 (1H, s, Ar-H), 5.59 (1H, d, $J = 9.4$ Hz, H-1), 4.05 (1H, dd, $J = 5.5, 11.3$ Hz, H-5a), 3.94 (1H, d, $J = 9.4$ Hz, H-2), 3.74-3.68 (1H, m, H-4), 3.55-3.48 (2H, m, H-3, H-5b); Mass (ESI): calculated for $\text{C}_{15}\text{H}_{14}\text{F}_6\text{N}_3\text{O}_4$ 414.089, found 413.933

Click-xyloside **4**: ^1H NMR (CD_3OD): δ 8.15 (1H, s, triazolyl H), 7.36 (1H, s, Ar-H), 7.25-7.34 (3H, m, Ar-H), 5.51 (1H, d, $J = 9.4$ Hz, H-1), 4.76 (2H, s), 4.59 (2H, s), 4.01 (1H, dd, $J = 5.5, 11.5$ Hz, H-5a), 3.89 (1H, t, $J = 9.4$ Hz, H-2), 3.64-3.70 (1H, m, H-4), 3.44-3.51 (2H, m, H-3, H-5b); Mass (ESI): calculated for $\text{C}_{16}\text{H}_{21}\text{N}_3\text{O}_5\text{Na}$ 374.130, found 374.300

Click-xyloside **5**: ^1H NMR (CD_3OD): δ 7.90 (1H, s, triazolyl H), 7.35 (2H, d, $J = 7.42$ Hz, Ar-H), 7.27 (2H, t, $J = 7.44$, Ar-H), 7.20 (1H, t, $J = 7.42$ Hz, Ar-H), 5.43 (1H, d, $J = 9.0$ Hz, H-1), 4.22 (2H, s), 3.97 (1H, dd, $J = 5.4, 11.3$ Hz, H-5a), 3.82 (1H, t, $J = 9.0$ Hz, H-2), 3.61-3.67 (1H, m, H-4), 3.40-3.51 (2H, m, H-3, H-5b); Mass (ESI): calculated for $\text{C}_{14}\text{H}_{18}\text{N}_3\text{O}_4\text{S}$ 324.100, found 324.000

Click-xyloside **6**: ^1H NMR (400 MHz, CD_3OD): δ 8.17 (1H, s, triazolyl H), 7.82-7.84 (4H, m, Ar-H), 7.43-7.48 (3H, m, Ar-H), 5.52 (1H, d, $J = 9.0$ Hz, H-1), 4.73 (2H, s), 4.69 (2H, s), 4.01 (1H, dd, $J = 5.47, 11.3$ Hz, H-5a), 3.90 (1H, t, $J = 8.98$ Hz, H-2), 3.65-3.71 (1H, m, H-4), 3.44-3.52 (2H, m, H-3, H-5b); Mass (ESI): calculated for $\text{C}_{19}\text{H}_{21}\text{N}_3\text{O}_5\text{Na}$ 394.130, found 394.070

2.1.3. Priming Activity of Click-xylosides

Most of the previous investigations used *O*-xylosides and a few *S*-xylosides, which are metabolically unstable, with the exception of two studies that have examined

stable *C*-xylosides (1-5). We have synthesized metabolically stable click-xylosides. A mutant pgsA-745 cell line, which lacks active xylosyltransferase enzyme, was used to test the priming activity of click-xylosides. Since the mutant pgsA-745 cell line does not make GAG chains, it requires an exogenous supply of β -xylosides to produce GAG chains and thus makes it a convenient cellular system to determine the priming ability of exogenously supplied click-xylosides and elucidate the role of aglycone groups (8). These click-xylosides have been determined to continuously prime GAG chains for at least five days. Moreover, migration time of these primed GAG chains for at least five days that were analyzed by size exclusion chromatography remained the same. Therefore, click-xylosides are metabolically stable (Figure 2.1).

We have examined whether the concentration of xylosides would affect the priming activity and determined the optimal primer concentration of each xyloside for the maximal production of GAG chains. The priming activity of the xylosides was determined as described in the “Experimental Methods” section [2.4] utilizing the mutant CHO cell line (pgsA-745) at the following five concentrations: 0.1 μ M, 1 μ M, 10 μ M, 100 μ M and 1 mM (Figure 2.2).

From the screening experiments with the above concentrations, we were able to determine the optimal concentration range for each xyloside for its maximal priming activity. The results indicate that the priming is concentration-dependant and significant priming for many click-xylosides was observed at a concentration of 100 μ M. For the same xylosides, the concentration that was required to observe optimal priming activity was higher. The priming activity of the xylosides in this study shows that most of the primers generate a significant quantity of GAG chains, although a few

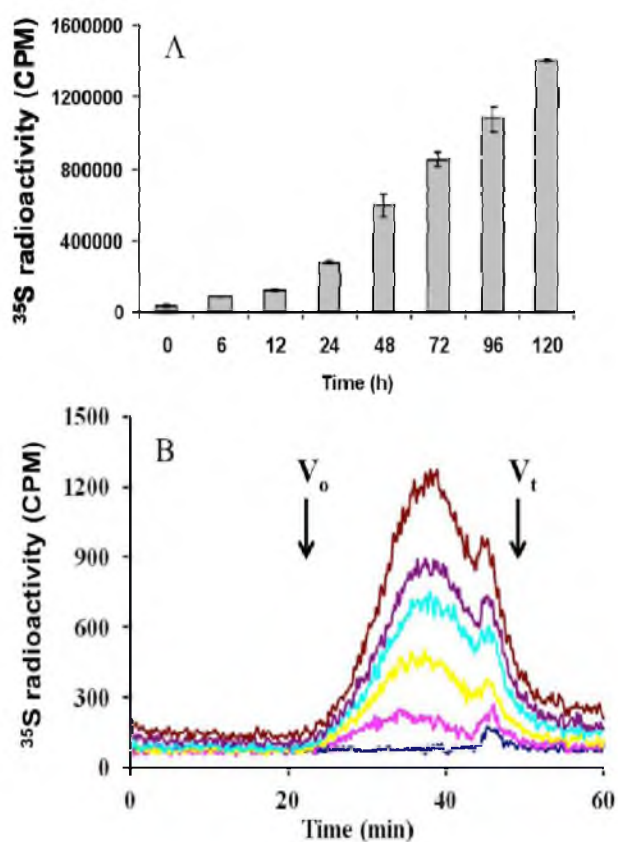


Figure 2.1. Stability of click-Xylosides. The click-xylosides were examined using xylosyl transferase deficient CHO cells (pgsA-745). A. Long-term priming ability of GAG chains by click-xylosides at 24, 48, 96, and 120 h. The primed GAG chains were quantitated using a liquid scintillation counter. B. Size exclusion profiles of GAG chains primed by click-xylosides at 100 μM concentration in the presence of 50 μM $\text{Na}_2^{35}\text{SO}_4$. The GAG chains were then purified and quantified as described under “Experimental Methods” [2.4]. The results were the average of two independent experiments.

are not effective primers. One possible explanation is that the diffusion rates of the primers depend on the aglycones that led to differential biosynthesis of the GAG chains. However, the click-xylosides **1**, **3**, **5** and **6** primed more effectively at 100 μM than they did at 1 mM. If diffusion was the only factor that governs priming activity, the priming activity would be predicted to be higher at 1mM. However, inhibition of GAG priming observed at a higher concentration of xylosides might possibly be due to substrate level

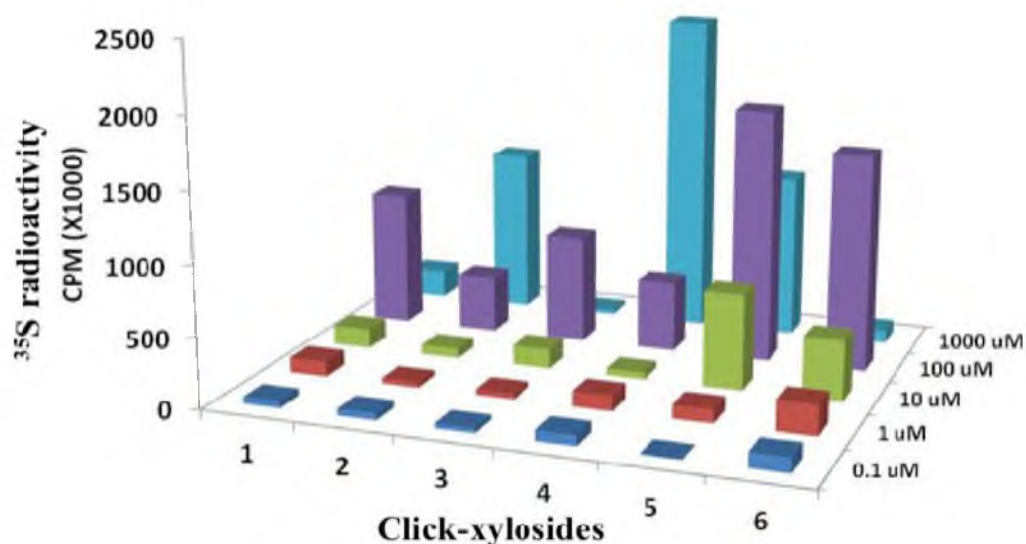


Figure 2.2. Priming activity of click-xylosides. The novel xylosides were examined for their priming ability using xylosyl transferase deficient CHO cells (pgsA-745). 100,000 cells were seeded per well of 24-well plates and treated with various xylosides at 0.1, 1, 10, 100 μM and 1 mM concentrations for 24 h in the presence of 50 μCi $^{35}\text{S}\text{-SO}_4^{2-}$ or $D\text{-}[6\text{-}^3\text{H}]\text{-glucosamine}$. The GAG chains were then purified and quantified as described under “Experimental Methods” [2.4].

inhibition of enzymes involved in the assembly of linkage region that would lead to reduction in the amount of GAG chains primed. These data clearly suggest that differential priming activity among various xylosides does not solely depend on the diffusion but also on various factors that are influenced by the aglycones.

2.1.4. Sulfation Patterns of GAG chains Induced by Click-xylosides

DEAE anion exchange chromatography was utilized to compare the extent of sulfation of primed GAG chains. GAG chains were recovered from the conditioned media by DEAE-sepharose chromatography, followed by isolation of [^{35}S]-GAG chains as described under “Experimental Methods.” The GAG chains were quantitatively

retained by the column, but they required different concentrations of NaCl for their elution. These findings served as a basis to attribute the differences in the elution profiles/migration time of various GAG chains on the HPLC anion-exchange column to the extent of sulfation of GAG chains primed by various xylosides as described. GAG chains that have less sulfate elute at lower ionic strength, whereas heavily sulfated GAG chains elute at higher ionic strength. The differences in the elution profiles of the primed GAG chains indicate differences in the extent of sulfation among these GAG chains. We focused our investigation on HPLC analysis of the GAG chains primed by the click-xylosides at the optimal concentration (100 μ M). The sulfate profile of the xyloside **1** with a single substituent of -OMe is heterogeneous; however, the sulfate profile of the xyloside **2** with a double substituent of -OMe is homogeneous. The highly electron withdrawing substituents, -OCF₃, also resulted in broad GAG chains (Figure 2.3). In this study, we observed a wide variation in the sulfation patterns of GAG chains primed by various click-xylosides. This variation in the sulfation patterns should be attributed to the presence of discrete enzyme complexes in different Golgi subcompartments.

2.2. Inhibition of GAG Biosynthesis by Fluoro-xylosides

2.2.1. Introduction

To elucidate the biological significance of GAG chains, several chemical approaches have been employed to inhibit their biosynthesis (9-12). The most important ones are sodium chlorate, brefeldin A, and 4-deoxy-glucosamine analogs (10, 12). Unfortunately, these analogs are not selective inhibitors of GAG biosynthesis

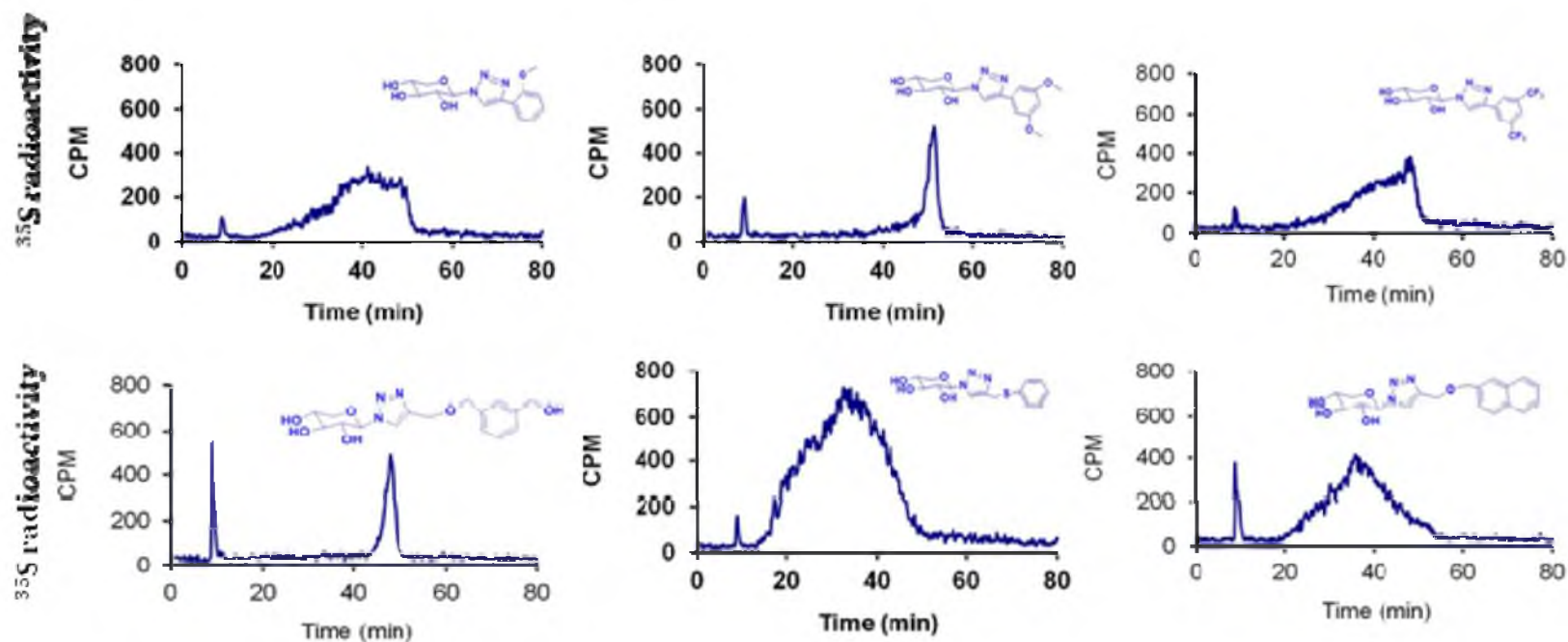


Figure 2.3. Effect of various hydrophobic moieties on the DEAE elution profiles of GAG chains. GAG chains primed by various click-xylosides eluted from analytical anion-exchange column (7.5 mm x 7.5 cm) using linear gradient of 1 M NaCl solution. GAG samplers were diluted five-fold prior to analysis by DEAE-HPLC, as described under “Experimental Methods” [2.4]. The variations in the elution profiles and migration times indicate differences in both sulfation pattern and extent of sulfation of the primed GAG chains. The elution profiles are representative of at least two independent experiments.

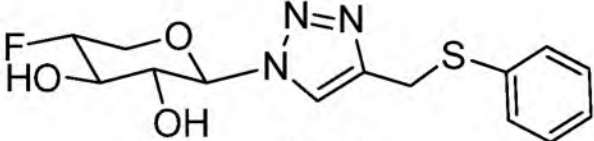
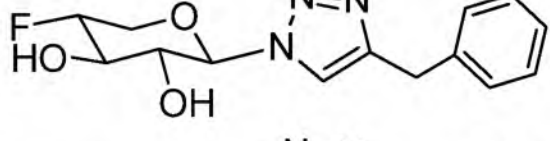
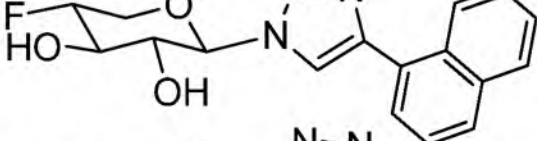
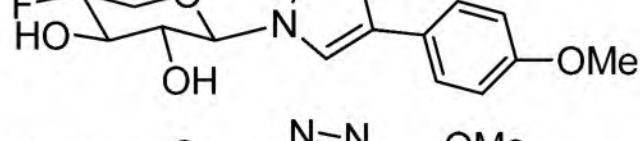
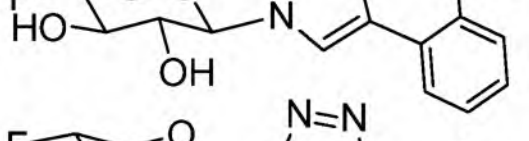
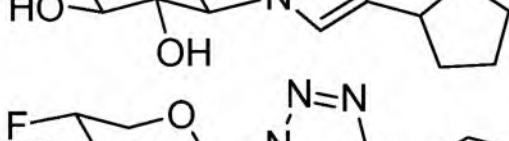
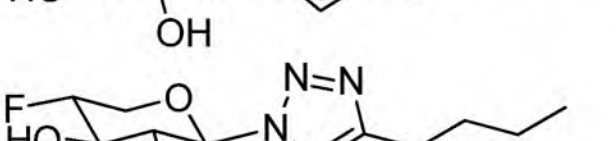
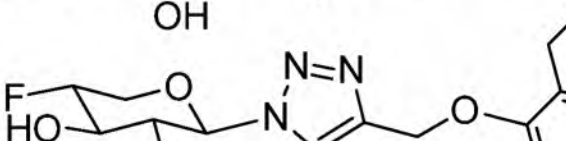
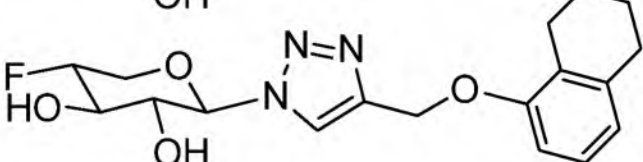
and affect biosynthesis of other glycoconjugates as well. Many xylosides containing hydrophobic aglycones act as acceptors for the elongation of GAG chains, as described in the previous section.

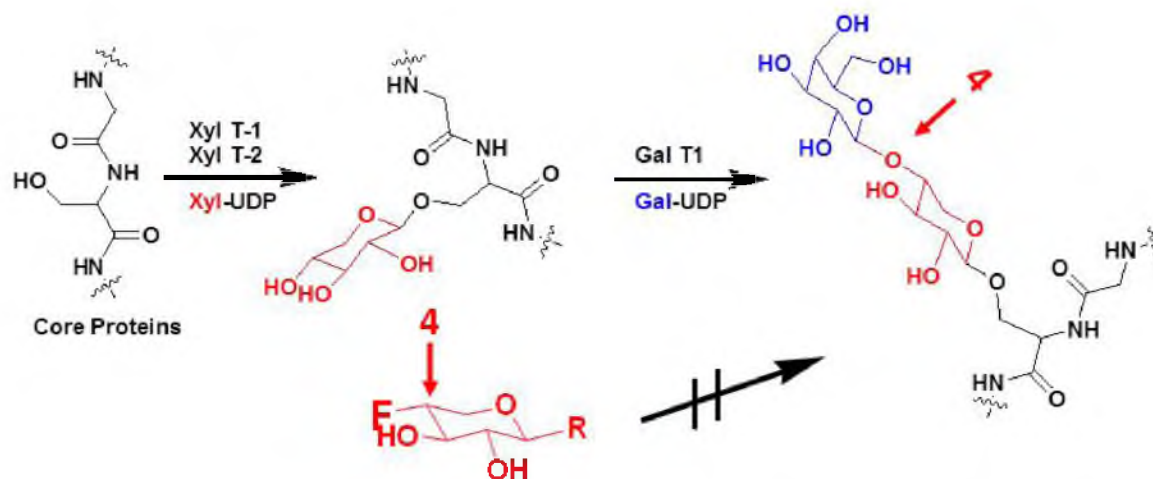
As an approach to perturb GAG biosynthesis, we propose that 4-deoxy-4-fluoro-xylosides (Table 2.2) cannot prime GAG chains as they do not have the acceptor hydroxyl group at C-4 position for subsequent sugar attachment and elongation. Furthermore, these modified xylosides could affect galactosyl transferase I, an enzyme involved in the assembly of linkage region and thereby inhibit the PG biosynthesis (Scheme 2.2). Therefore, a library of 4-deoxy-4-fluoro-xyloside was screened to determine which scaffolds can selectively and efficiently inhibit the PG biosynthesis in a selective manner. We expect that these novel xyloside derivatives will become powerful chemical biology tools to define the developmental and physiological actions of PG in model organisms by inhibiting or perturbing their biosynthesis in a spatiotemporal manner.

2.2.2. Screening of Potential Inhibitor of PG Biosynthesis

We have examined various 4-deoxy-4-fluoro-xylosides, **7-15**, for their ability to inhibit the PG biosynthesis using wild-type CHO cells as a model cellular system. The CHO cells produce both HS and CS chains and therefore, the extent of selective inhibition of either HS or CS chains can also be determined. HS and CS chains could be resolved and identified using an anion exchange DEAE high-pressure liquid chromatography column. Furthermore, elution profiles of GAG chains indicate both the extent of sulfate and the sulfation pattern. Thus, GAG chains that have less sulfate elute

Table 2.2. Structures of 4-deoxy-4-fluoro-xylosides

Entry	Structures
7	
8	
9	
10	
11	
12	
13	
14	
15	



Xyl T1 and *Xyl T2*: xylosyltransferase-1 and xylosyltransferase-2;
Gal T1 and *Gal T2*: galactosyltransferase-1 and galactosyltransferase-2

Scheme 2.2. 4-deoxy-4-fluoro-click xylosides inhibit GAG biosynthesis

at lower ionic strength, whereas heavily sulfated GAG chains elute at higher ionic strength. Therefore, we utilized the anion exchange HPLC to deduce whether 4-deoxy-4-fluoro-xylosides inhibit PG biosynthesis and the extent of inhibition.

Wild-type CHO cells were grown under conditional media containing radioactive $\text{Na}_2^{35}\text{SO}_4$ in the absence (control) or presence of various potential inhibitors at various concentrations for about 24 h. CHO cells were then subjected to pronase treatment and subsequently passed through small disposable DEAE-sepharose columns to enrich and elute the radioactive GAG chains. The resulting extract was then analyzed using HPLC coupled to an inline radiodetector, as described in the “Experimental Methods” [2.4]. GAG chains, composed of both HS and CS chains, extracted from cells that are not treated with the inhibitor, migrated between 20-50 minutes as two peaks. The earlier peak is attributed to HS chains, whereas the later one is attributed to CS chains (13). We also observed two very sharp peaks eluting around 5

and 17 minutes. Structural identities of those peaks are unknown. This chromatogram served as a control and was utilized to deduce the extent of inhibition of biosynthesis by 4-deoxy-4-fluoro-xylosides. We then analyzed the extracts from CHO cells that were grown in the presence of various inhibitors and compared them against the elution profile of GAG chains extracted from control CHO cells. GAG chains from xyloside 7-treated cells were shown to have an elution profile that was very identical to that of wild-type cells and eluted between 20-50 minutes, suggesting that xyloside 7 is a poor inhibitor of PG biosynthesis. On the other hand, xylosides **8**, **9**, and **10** were able to reduce the amount of GAG chains up to 20 %, suggesting that they are weak inhibitors of PG biosynthesis. Xylosides **11**, **14**, and **15** were able to inhibit approximately 50% of total GAG production. Xylosides **12** and **13** were found to be the best inhibitors as they reduced about 90% of total GAG chains produced (Figure 2.4).

Dose-response experiments were done to investigate the extent of inhibition of biosynthesis by various xyloside derivatives. Cells were treated with inhibitors at various concentrations in the presence of ^3H -GlcN for 24 h. As shown in Figure 2.5, amounts of isolated GAG chains decreased with the increasing concentration of xyloside derivatives, **11** and **13**. Moreover, it is interesting to note that we did not observe any differential effect of these scaffolds on the biosynthesis of HS and CS.

2.2.3. Cytotoxicity of Potential Inhibitor of PG Biosynthesis

Assessment of cell viability is critical before utilizing these novel molecular scaffolds in animal models to deduce the biological roles of GAG chains. Therefore,

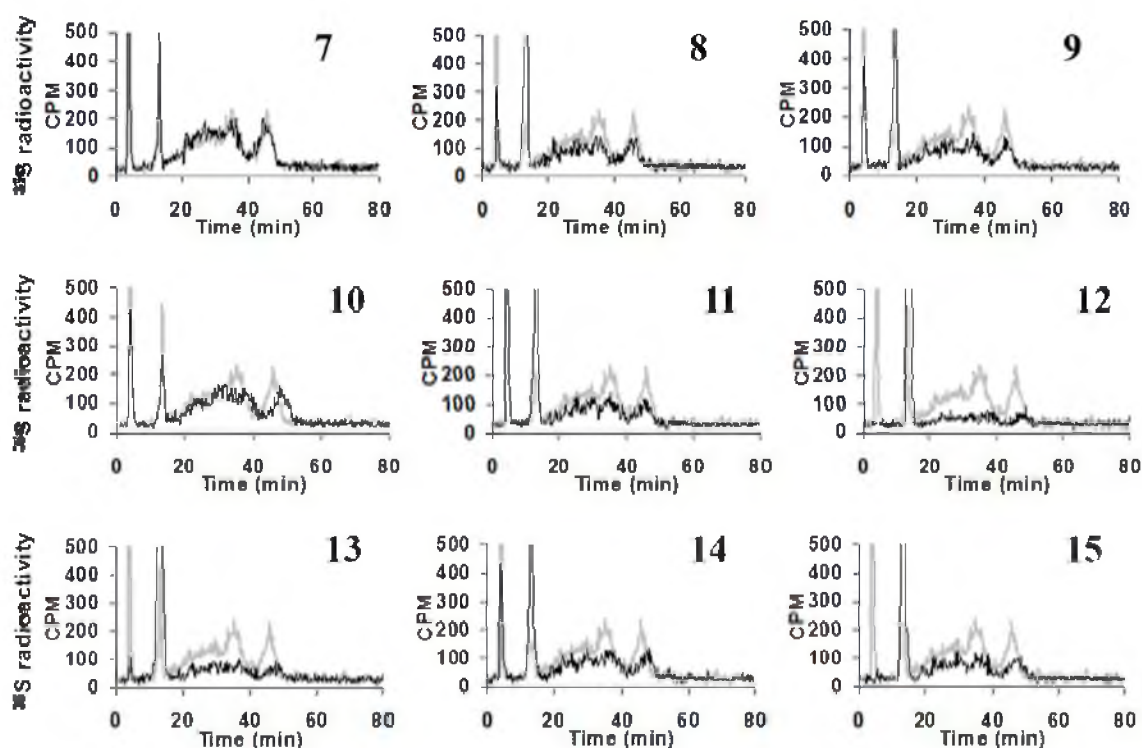


Figure 2.4. Inhibition of PG biosynthesis by xyloside derivatives. ^{35}S -Labeled GAG chains were isolated from control and 4-deoxy-4-fluoro-xylosides-treated cells as described under “Experimental Methods” [2.4]. Radiolabeled GAG chains were then fractionated on a DEAE HPLC column and analyzed for radioactivity with the aid of an in-line radiometric detector. The bound GAG chains were eluted with a linear gradient of 1 M NaCl. The elution profiles of GAG chains isolated from cells that were untreated (*gray trace*) or treated (*black trace*) with PG biosynthetic inhibitors (compounds 7-15) are shown above.

after screening xyloside derivatives for their ability to inhibit PG biosynthesis, we investigated whether these derivatives are toxic to the cells. Though several methods are available, we chose a fluorescent assay, Alamar Blue assay, which is convenient for the measurement measurement of cell viability in a reliable and rapid manner. The fluorescent dye, used in this assay, is easily soluble in growth media, stable in solution, and the least toxic to cells. Cell viability assay confirmed that these xyloside

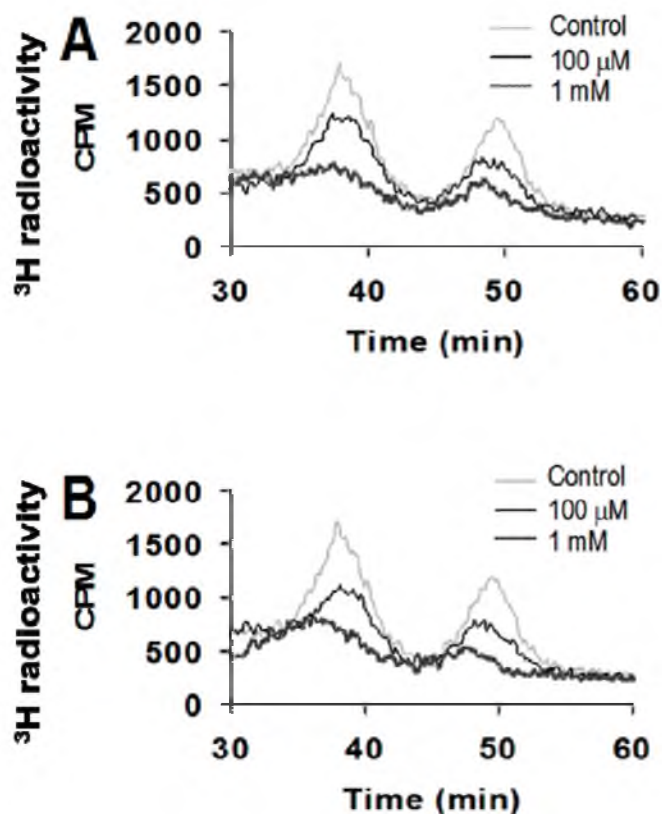


Figure 2.5. Dose-dependent decrease of GAG biosynthesis by 4-deoxy-4-fluoroxylosides in CHO cells. Samples of ^3H -labeled GAG chains from control and 4-deoxy-4-fluoroxyloside-treated (compounds **11** (panel A) and **13** (panel B)) CHO cells were applied to a DEAE HPLC column, eluted with a linear NaCl gradient starting with 0.2 M NaCl, as described under “Experimental Methods” [2.4], and analyzed for radioactivity with an in-line radiodetector

derivatives are not toxic to cells at various concentrations. However, we observed that xylosides **9** and **15** are toxic at 1 mM and higher concentrations to CHO cells (Figure 2.6).

2.2.4. 4-deoxy-4-fluoro-xylosides Do Not Affect Biosynthesis of Glycolipids/ Glycopeptides

These fluorinated xylosides were examined for whether they affect the biosynthesis of other glycoconjugates such as glycolipids and glycopeptides. (14) Cells

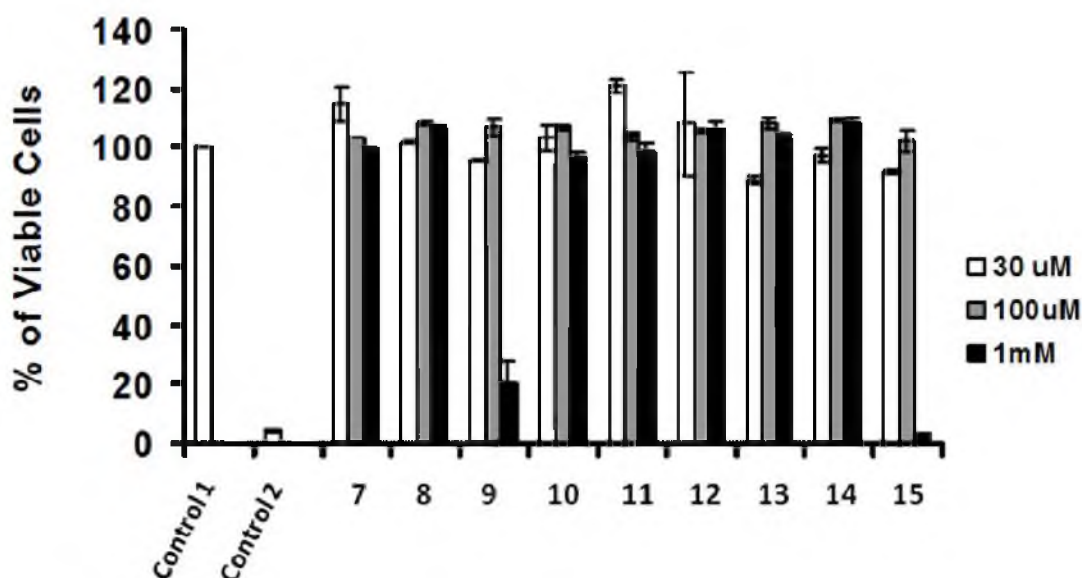


Figure 2.6. Cytotoxicity of 4-deoxy-4-fluoroxylsides. CHO cells were treated with different concentrations of xylosides (compounds 7–15) for 24 h and then incubated with CellTiter-Blue reagent for 2 h, as described under “Experimental Methods” section, [2.4] to estimate the percent of viable cells. CHO cells were grown in the absence of inhibitors (vehicle alone) as a control (Control 1), and the values of treated cells were compared with Control 1. Cells were also grown in the presence of 3% H₂O₂ as an additional control (Control 2), under which cells were subjected to oxidative stress.

were labeled with [³H] glucosamine in the presence of xyloside derivatives to determine whether these scaffolds affect other glycosyltransferases involved in biosynthesis.⁽¹⁴⁾ Quantitation of [³H]glucosamine-labeled glycolipids extracted from both treated and untreated cells suggested that these scaffolds did not affect glycoprotein/glycolipid biosynthesis.⁽¹⁴⁾ Thus, we can conclude that these scaffolds selectively inhibit GAG biosynthesis without affecting other glycol-conjugates.

2.3. Conclusions

Aglycone groups of xylosides are important in priming activity and induce specific structures of GAG chains. This demonstrates that different combinations of GAG biosynthetic enzymes in the GAGOSOME may generate cell-specific-combinatorial GAG structures with differential sulfation patterns. We also found that many of the best stimulatory aglycones of click-xylosides, examined in our earlier studies, seem to be essential in the design and construction of potential PG biosynthetic inhibitors. Thus, our observation clearly suggests that the hydrophobic nature of aglycones is as important as the fluoro atom replacing acceptor the hydroxyl group at the C-4 position. It is interesting that these modified xylosides inhibit PG biosynthesis to different extents, thus providing novel approaches to fine tune the extent of inhibition of PG biosynthesis in the quest to determine the biological consequences of variable inhibition *in vivo*.

2.4. Experimental Methods

2.4.1. General Procedure for the Synthesis of Click-xylosides

Sodium ascorbate (0.1 mmol), followed by $\text{Cu}_2\text{SO}_4 \cdot 5\text{H}_2\text{O}$ (0.01 mmol) were added to a solution of alkyne (1 mmol) and azide (1 mmol) in acetone/ water (1:1) at room temperature, and the mixture was stirred for 12 h (specific time or disappearance of one of the starting materials as indicated by TLC). At the end of the reaction, as determined by TLC analysis, the mixture was evaporated at reduced pressure to give the crude product, which was purified on silica gel column by eluting with ethylacetate/ hexane to obtain the desired xyloside derivative.

2.4.2. Deprotection Procedure

A freshly prepared solution of CH_3ONa (0.5 M, 0.1 ml) in dry methanol was added to a given fully protected xyloside (0.1 mmol) in dry methanol (3 ml), and the reaction mixture was stirred at room temperature for about 3 h. Neutralization with H^+ resin, followed by concentration at reduced pressure gave a syrupy liquid, which was then purified on silica gel column to obtain the deprotected xylosides for biological evaluation.

2.4.3. General Procedures for Screening Xylosides

To determine whether the xylosides are able to prime the synthesis of GAGs in cells *in vitro*, experiments were performed using CHO pgsA-745. The cells were treated with appropriate primers in the presence of $^{35}\text{S}\text{-Na}_2\text{SO}_4$; GAGs were purified and analyzed as described below. 1×10^4 cells were plated per well in Ham's F12 complete growth medium in a 24-well plate. The cells were incubated at 37 °C in a humidified incubator for 24 h to a confluency of about 50%. The cells were washed with sterile PBS and replaced with 450 μL Ham's F12 containing 10% dialyzed FBS. Solutions containing a specific primer at 100X the final concentration were prepared. 5 μL of appropriate 100X primer were added to various wells to yield a final concentration of 100 μM . 50 μCi of $^{35}\text{S}\text{-Na}_2\text{SO}_4$ was also added to each well as tracer. The 24-well plates were placed back in the 37 °C incubator for 24 h before the addition of 100 μl 6X pronase solution, followed by incubation at 37 °C overnight.

2.4.4. Purification and Quantification of GAG Chains

The entire contents of the wells were transferred to a microcentrifuge tube and subjected to centrifugation at 16,000xg for 5 minutes. The supernatant was transferred to a fresh tube and half-a-volume of 0.016% Triton X-100 was added. The diluted supernatant was loaded on 0.2 mL DEAE-sepharose column pre-equilibrated with 2 mL of 20 mM NaOAc buffer pH 6.0 containing 0.1 M NaCl and 0.01% Triton X-100 and the column was washed with 4 mL of buffer described above. The bound HS/CS was eluted using 1.2 mL elution buffer, 20 mM NaOAc, pH 6.0 containing 1 M NaCl. The extent of priming by the various xyloside primers was evaluated by quantifying the ³⁵S-radioactivity incorporated into the purified HS/CS elute by liquid scintillation. 50 µL of the various elutes were added to 5 mL of scintillation cocktail and the vials were counted in a scintillation counter in triplicate. The amount of radioactivity corresponds to the total GAG synthesized by the primer.

2.4.5. HPLC Analysis of GAGs

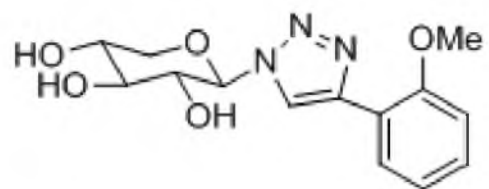
The purified GAGs were analyzed by HPLC with an inline radiodetector. 50 µl of elute was diluted five times with the HPLC solvent A (10 mM KH₂PO₄, pH 6.0, 0.2 % CHAPS) and loaded on to a weak anion exchange column, DEAE-3SW (TosoHaas Inc.), and analyzed with the following elution profile. The sample was eluted from the column with a linear gradient of 0.2 M NaCl at 0 minute to 1 M NaCl at 80 minutes at a flowrate of 1 ml per minute. The radioactive GAGs were detected by a Radiomatic flow one A505A radio-chromatography detector. The HPLC effluent was mixed with

Ultima-Flo AP scintillation cocktail in a 2:1 ratio and detected in the flow scintillation detector.

2.4.6. Cell Viability Assay

CHO-K1 cells were examined for viability in the presence of 4-deoxy-4-fluoroxylsides derivatives using CellTiter-Blue reagent (Promega). Cells were seeded into duplicate wells of a 96-well plate at a density of 2.5×10^4 viable cells/well in 125 μ l of Ham's F-12 complete growth medium supplemented with 10% fetal bovine serum and grown for 24 h with vehicle alone or xyloside derivatives. Cells were also treated with 3% H_2O_2 as an additional control for the cell viability assay. After 24 h of treatment with vehicle, H_2O_2 , or xyloside derivative, 25 μ l of CellTiter-Blue reagent was added to each well according to the manufacturer's protocol. After incubation in the humidified incubator for 2 h, the fluorescence generated in the assay was then stopped and stabilized by addition of 50 μ l of 3% SDS solution. The fluorescence was immediately measured using a Spectra-Max M5 microplate reader (Molecular Devices, Sunnyvale, CA) at an excitation wavelength of 560 nm and an emission wavelength of 590 nm.

2.5. Supporting Information



1

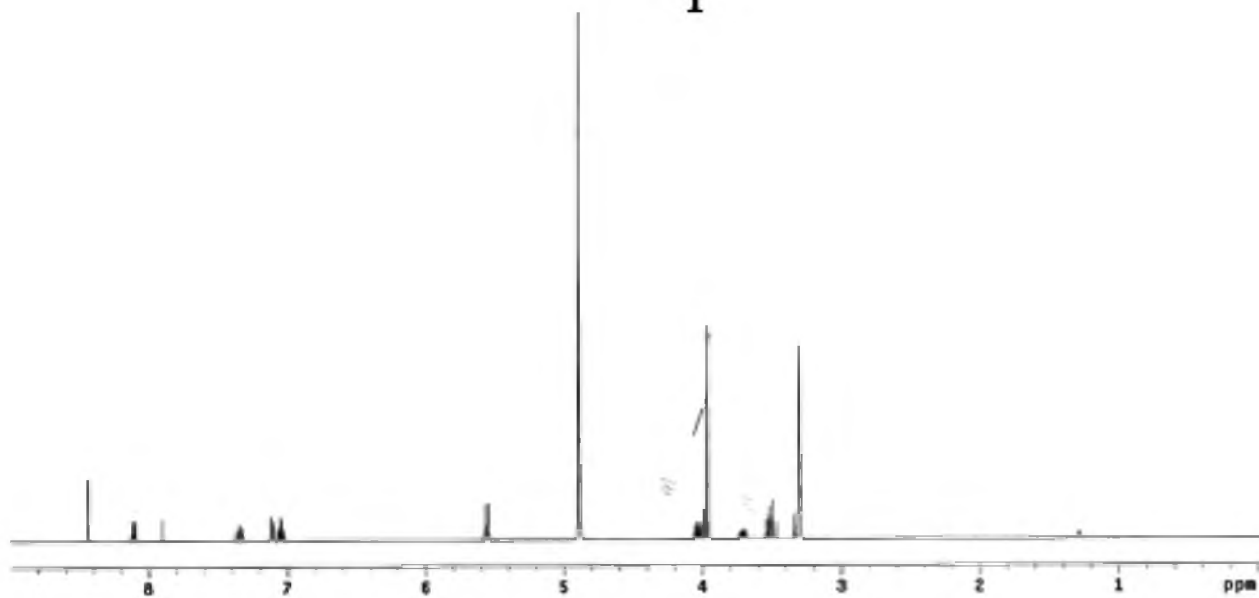


Figure S2.1. NMR spectra of click-xyloside 1

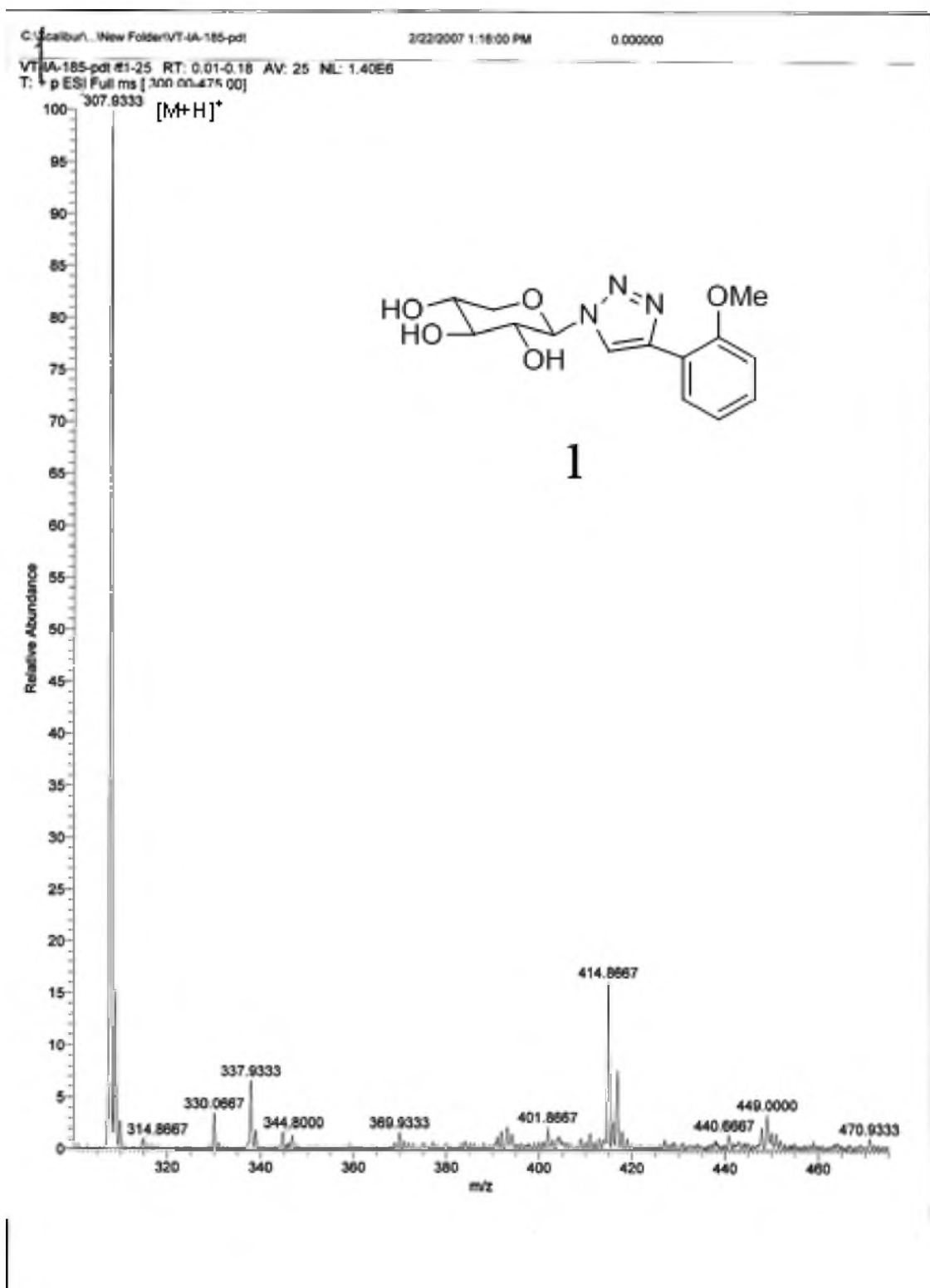


Figure S2.2. Mass spectra of click-xyloside 1

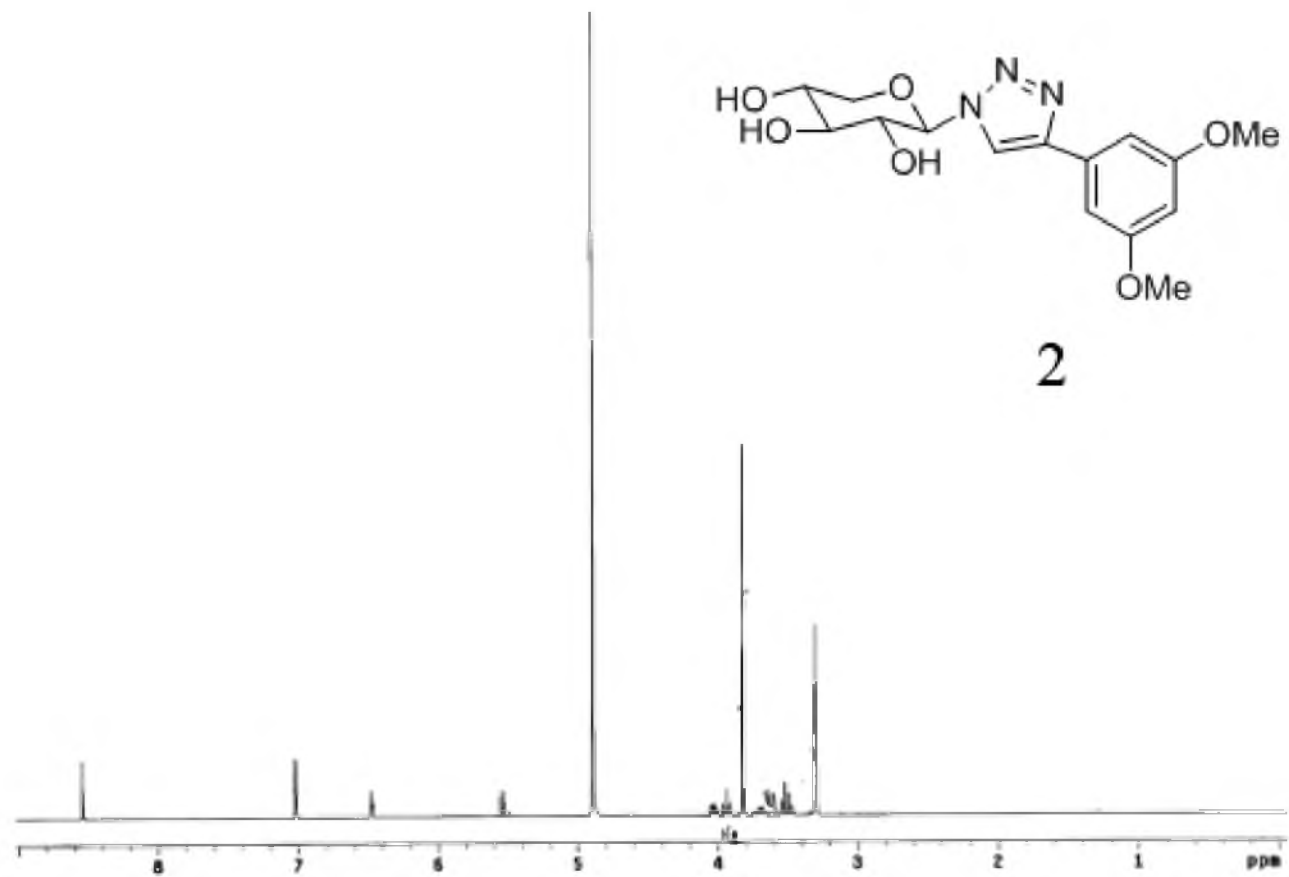


Figure S2.3. NMR spectra of click-xyloside 2

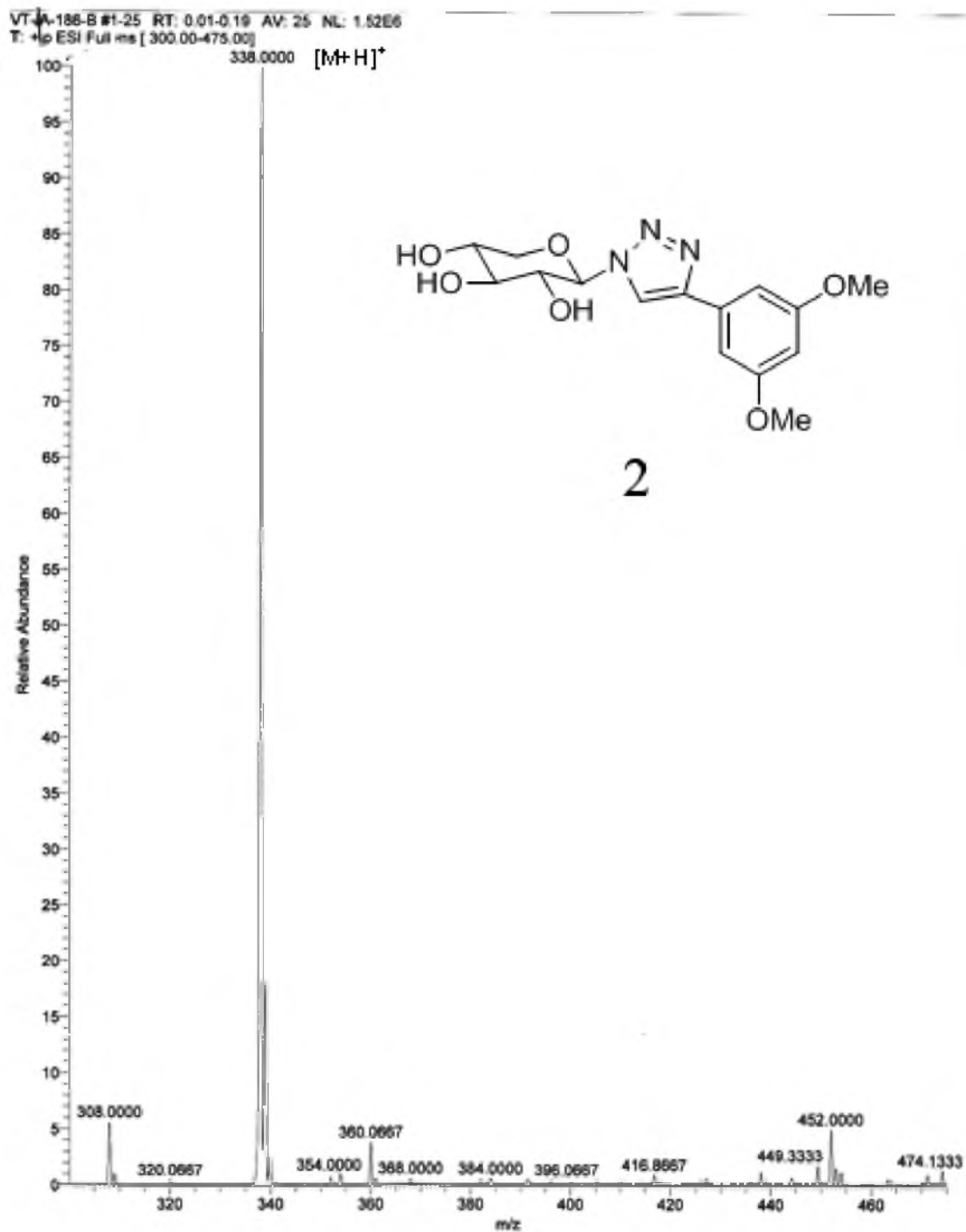
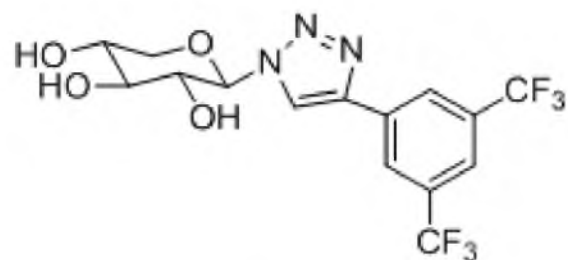


Figure S2.4. Mass spectra of click-xyloside 2



3

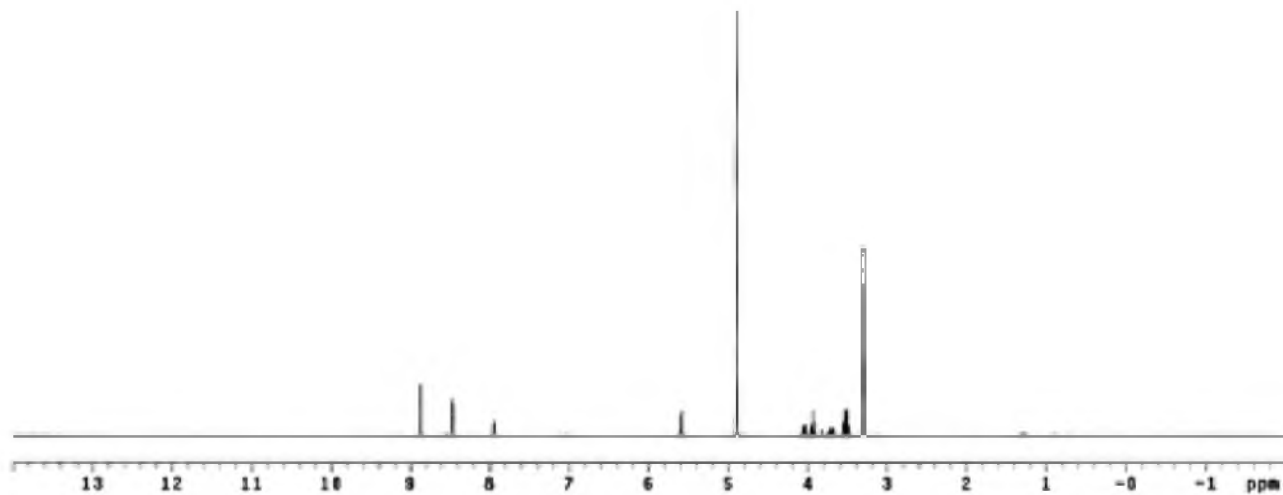


Figure S2.5. NMR spectra of click-xyloside 3

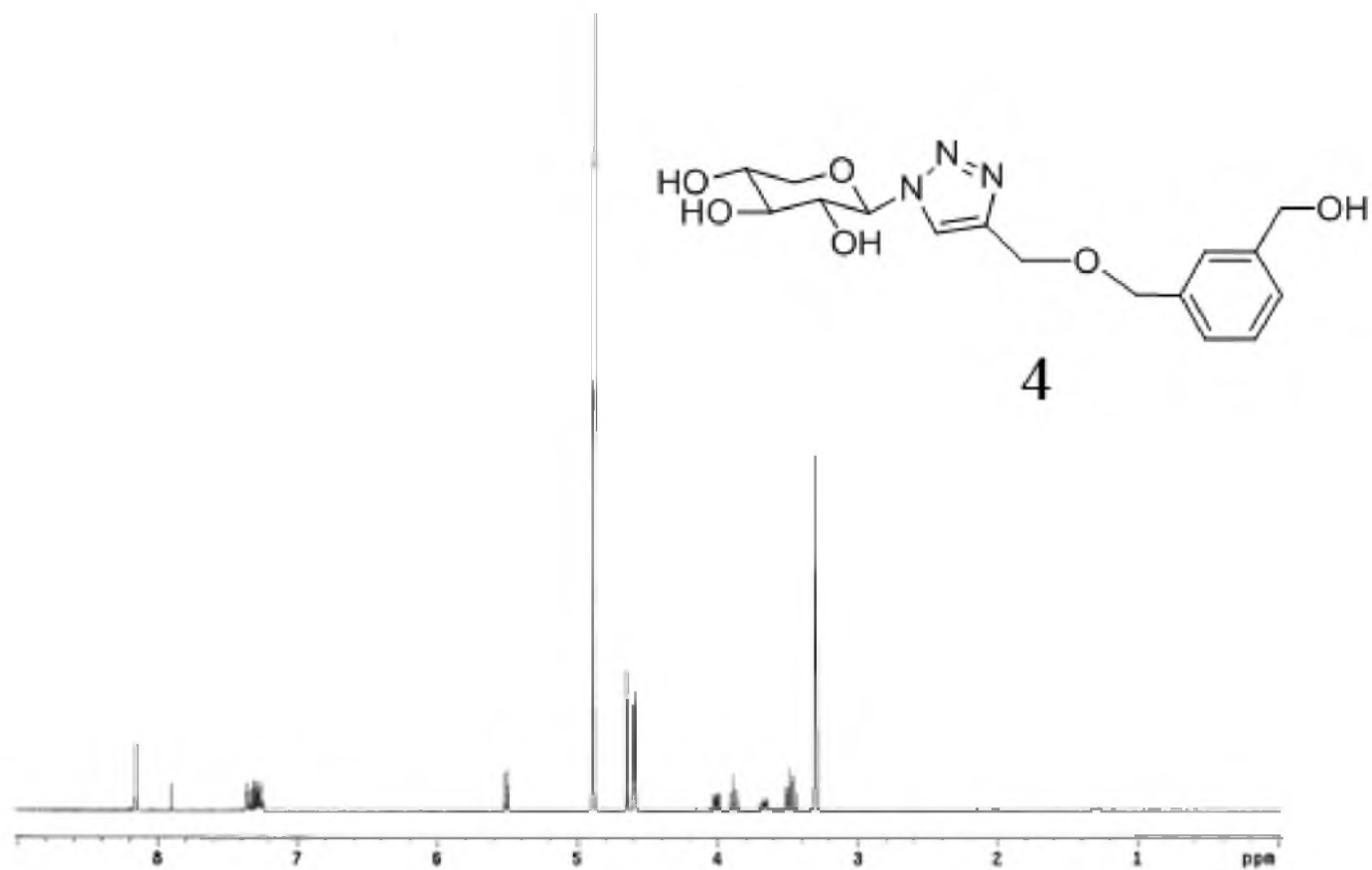


Figure S2.6. NMR spectra of click-xyloside 4

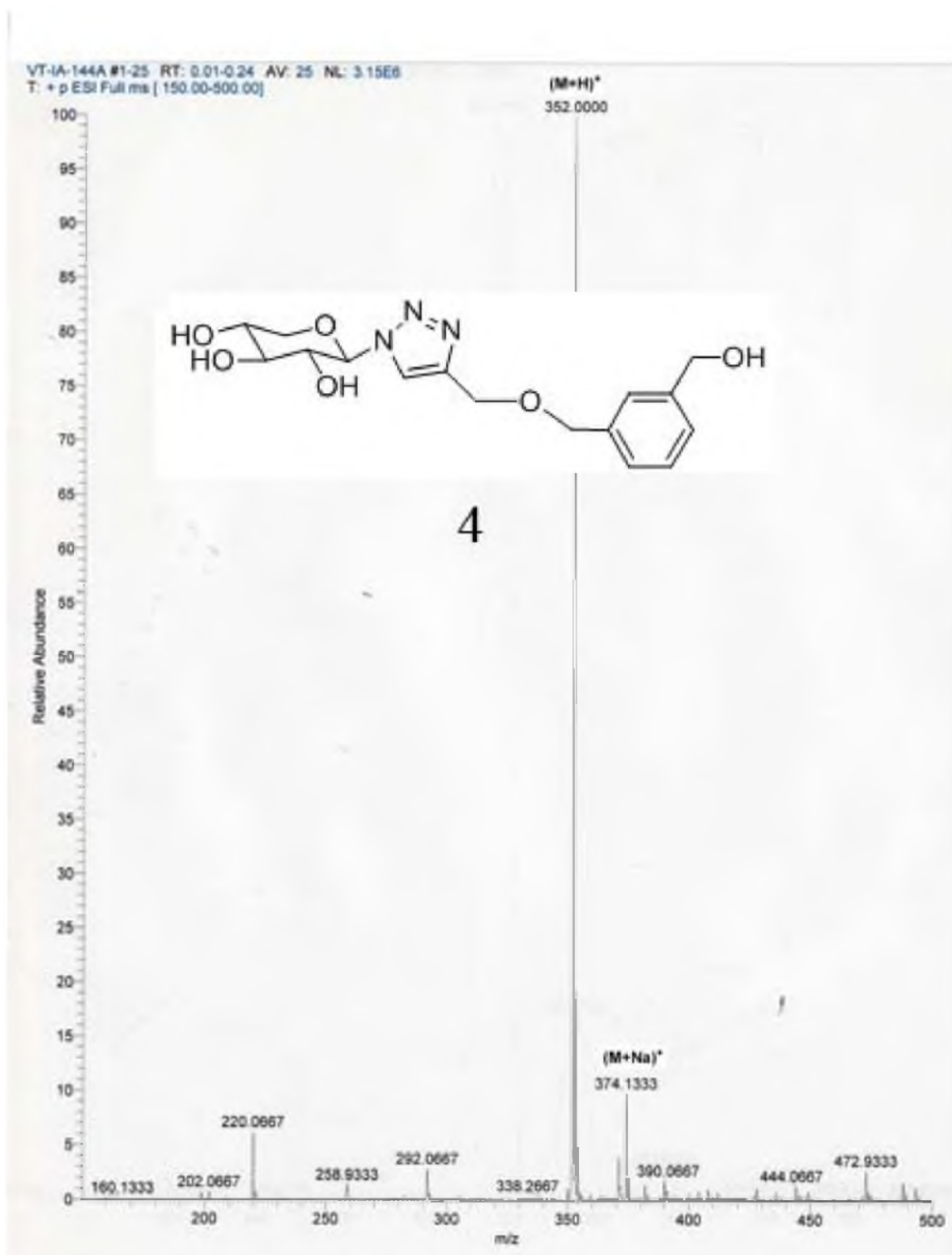


Figure S2.7. Mass spectra of click-xyloside 4

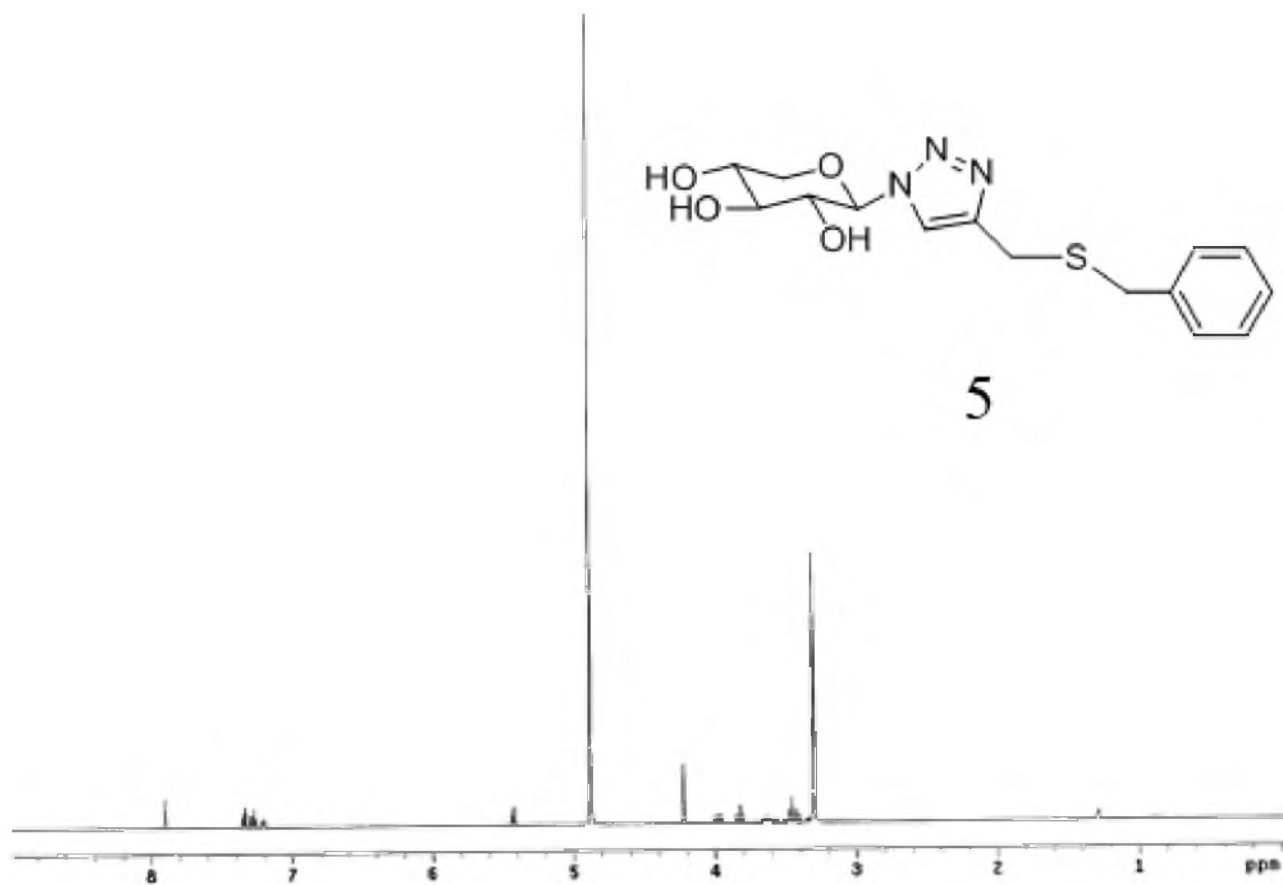


Figure S2.8. NMR spectra of click-xyloside 5

VT-1A-184-B #15-16 RT: 0.16-0.17 AV: 2 NL: 2.76E5
T: +p ESI Full ms [200.00-475.00]

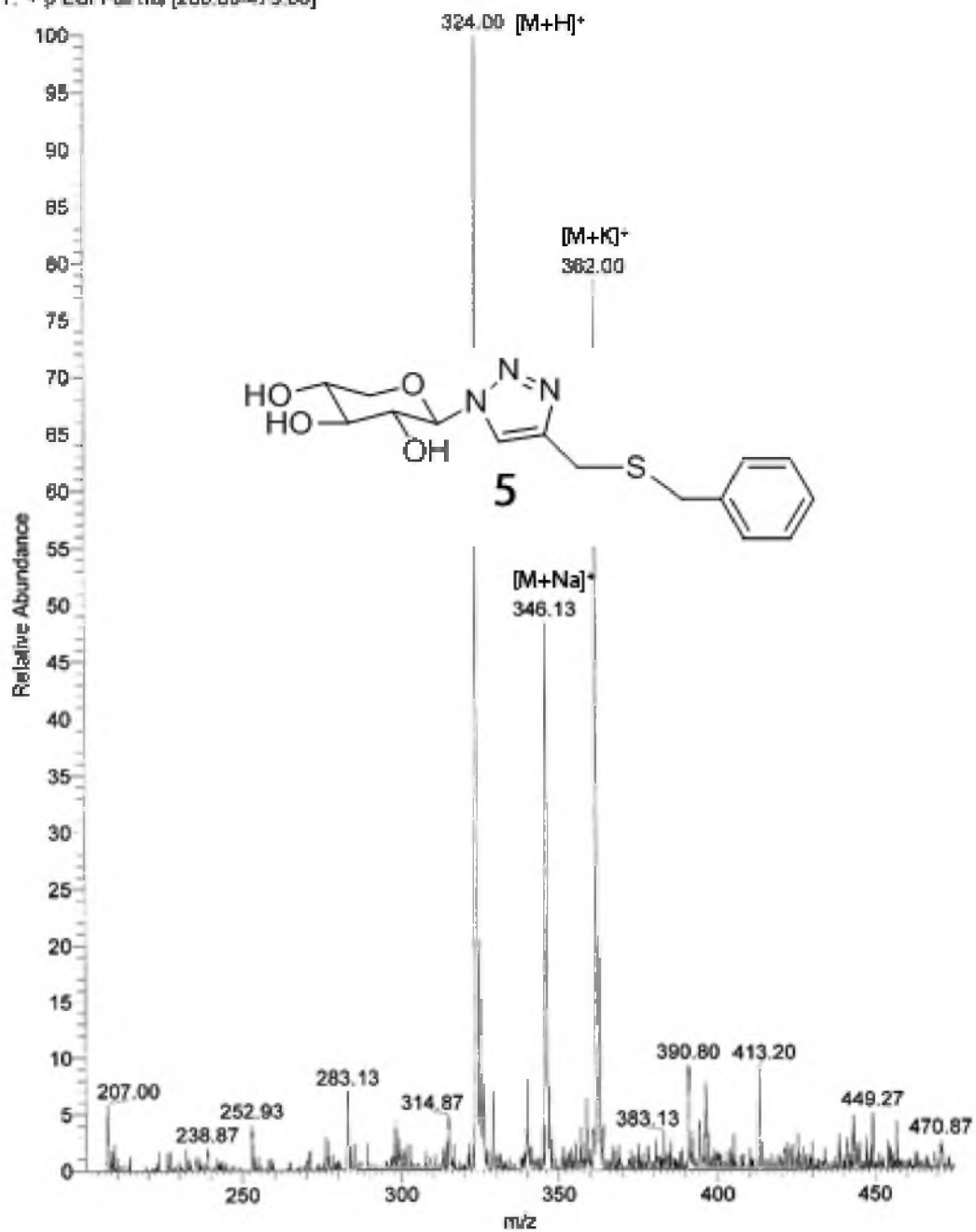


Figure S2.9. Mass spectra of click-xyloside 5

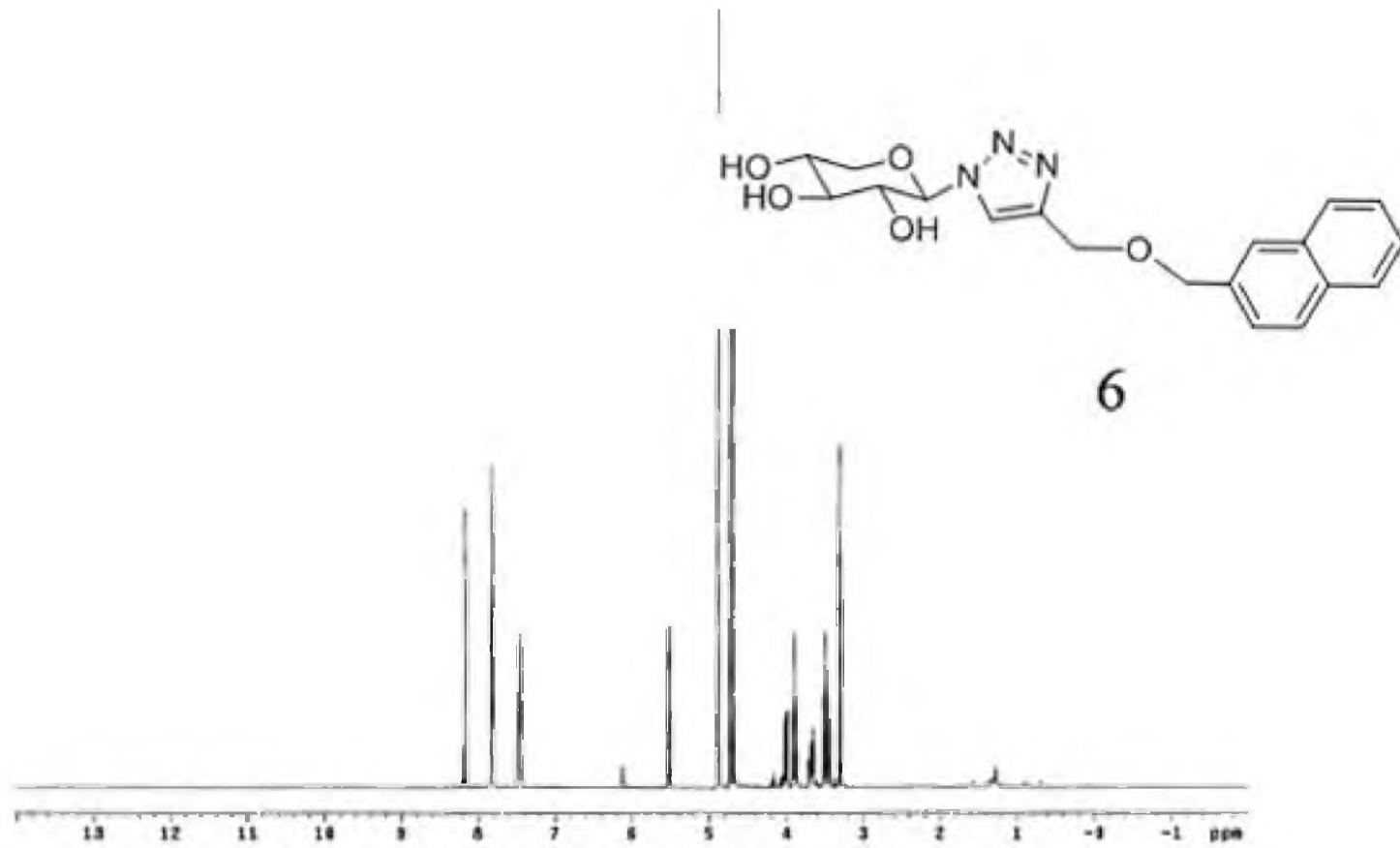


Figure S2.10. Mass spectra of click-xyloside 6

2.6. References

1. Mani, K., Belting, M., Ellervik, U., Falk, N., Svensson, G., Sandgren, S., Cheng, F., and Fransson, L. A. (2004) Tumor attenuation by 2(6-hydroxynaphthyl)-beta-D-xylopyranoside requires priming of heparan sulfate and nuclear targeting of the products, *Glycobiology* 14, 387-397.
2. Okayama, M., Kimata, K., and Suzuki, S. (1973) The influence of p-nitrophenyl beta-d-xyloside on the synthesis of proteochondroitin sulfate by slices of embryonic chick cartilage, *J Biochem* 74, 1069-1073.
3. Robinson, H. C., Brett, M. J., Tralaggan, P. J., Lowther, D. A., and Okayama, M. (1975) The effect of D-xylose, beta-D-xylosides and beta-D-galactosides on chondroitin sulphate biosynthesis in embryonic chicken cartilage, *Biochem J* 148, 25-34.
4. Fritz, T. A., Lugemwa, F. N., Sarkar, A. K., and Esko, J. D. (1994) Biosynthesis of heparan sulfate on beta-D-xylosides depends on aglycone structure, *J Biol Chem* 269, 300-307.
5. Lugemwa, F. N., Sarkar, A. K., and Esko, J. D. (1996) Unusual beta-D-xylosides that prime glycosaminoglycans in animal cells, *J Biol Chem* 271, 19159-19165.
6. Sobue, M., Habuchi, H., Ito, K., Yonekura, H., Oguri, K., Sakurai, K., Kamohara, S., Ueno, Y., Noyori, R., and Suzuki, S. (1987) beta-D-xylosides and their analogues as artificial initiators of glycosaminoglycan chain synthesis. Aglycone-related variation in their effectiveness in vitro and in ovo, *Biochem J* 241, 591-601.
7. Kolb, H., Finn, M., and Sharpless, K. (2001) Click chemistry: diverse chemical function from a few good reactions, *Angew Chem Int Edit* 40, 2004.
8. Esko, J. D., Stewart, T. E., and Taylor, W. H. (1985) Animal cell mutants defective in glycosaminoglycan biosynthesis, *Proc Natl Acad Sci U S A* 82, 3197-3201.
9. Roberts, A. L., Thomas, B. J., Wilkinson, A. S., Fletcher, J. M., and Byers, S. (2006) Inhibition of glycosaminoglycan synthesis using rhodamine B in a mouse model of mucopolysaccharidosis type IIIA, *Pediatr Res* 60, 309-314.
10. Calabro, A., and Hascall, V. C. (1994) Effects of brefeldin A on aggrecan core protein synthesis and maturation in rat chondrosarcoma cells, *J Biol Chem* 269, 22771-22778.
11. Greve, H., Cully, Z., Blumberg, P., and Kresse, H. (1988) Influence of chlorate on proteoglycan biosynthesis by cultured human fibroblasts, *J Biol Chem* 263, 12886-12892.

12. Berkin, A., Szarek, W. A., and Kisilevsky, R. (2005) Biological evaluation of a series of 2-acetamido-2-deoxy-D-glucose analogs towards cellular glycosaminoglycan and protein synthesis in vitro, *Glycoconj J* 22, 443-451.
13. Zhang, L., Beeler, D. L., Lawrence, R., Lech, M., Liu, J., Davis, J. C., Shriver, Z., Sasisekharan, R., and Rosenberg, R. D. (2001) 6-O-sulfotransferase-1 represents a critical enzyme in the anticoagulant heparan sulfate biosynthetic pathway, *J Biol Chem* 276, 42311-42321.
14. Garud, D. R., Tran, V. M., Victor, X. V., Koketsu, M., and Kuberan, B. (2008) Inhibition of heparan sulfate and chondroitin sulfate proteoglycan biosynthesis, *J Biol Chem* 283, 28881-28887.

CHAPTER 3

DESIGN OF FLUORESCENT XYLOSIDES TO PROFILE CELL-SPECIFIC GAG CHAINS

3.1. Introduction

PGs modulate numerous pathophysiological functions such as development (1-7), angiogenesis (8-12), axonal growth (13), anticoagulation (14-18), cancer progression (19, 20), microbial pathogenesis (21-25), etc. The quantity and quality of GAG structures, made by various cells, are dynamically regulated in a spatio-temporal manner during the development of an organism and during the normal aging of an organism, as well as during the progression of several pathological conditions. Profiling and deciphering dynamic changes in GAG structures will provide new avenues to diagnose disease states and may thwart those conditions with novel therapeutics (26). Most of these structural changes have been deduced using radiolabeled monosaccharides and sulfate as biosynthetic precursors in various cellular systems. However, these radiolabeled precursors cannot be used in organisms as they pose toxicity and other challenges. Several β -xyloside derivatives have been shown to act as acceptors and substitute for core proteins *in vivo* as well as *in vitro* in the production of core protein free GAG chains (27-36). Fluorogenic xylosides that are able to prime GAG chains will be an excellent tool to study the structure-function relationship *in vivo*. Commercial 4-methyl-umbelliferyl- β -D-xyloside (UMB-*O*-xyloside) has been shown until now to function as acceptor for the elongation of GAG chains; however, UMB-*O*-xylosides prime mostly CS chains or small oligosaccharides (37-39). Earlier studies examined several fluorescently labeled xylosides that were unable to prime GAG chains (40). Our efforts are, therefore, focused on the synthesis and screening of fluorescent tagged xylosides for their ability to prime GAG chains in a given cellular system and provides novel avenues to profile and elucidate cellular GAG

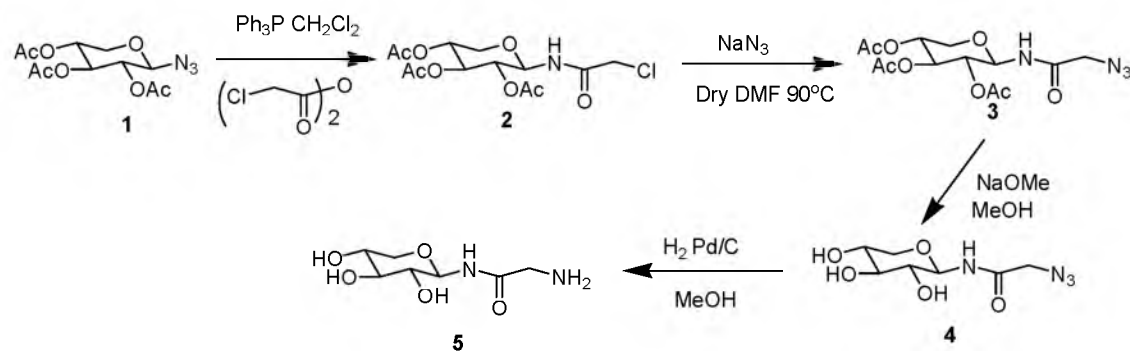
signatures in a robust manner, and assist in establishing cell-specific GAG-protein interactions.

3.2. Results and Discussion

Several fluorescent tagged xylosides were synthesized and are examined for whether these fluorescent tagged xylosides can elongate GAG chains. In the future, these fluorescent xylosides offer prospects to further our understanding of factors that regulate GAG biosynthesis as well as new knowledge on the role of GAG chains in various signaling events associated with pathophysiological processes.

3.2.1. Synthesis of Fluorescent Tagged Xylosides

Several studies proved that stimulation of GAG chains is not only affected by hydrophobic aglycones of xylosides but also by their glycosidic linkages (27-36). Therefore, several fluorescent xylosides with amide and triazole in the glycosidic linkage were synthesized in this study. *N*-(2, 3, 4-trihydroxyl- β -xylopyranosyl) acetamide **5** was synthesized from xyloside azide as outlined in Scheme 3.1. Xylose was converted to xyloside azide **1**, which was then coupled with chloroacetic anhydride to prepare the xyloside **2** (41). The chloro group in xyloside **2** was replaced with the azido group by treating xyloside **2** with NaN_3 to obtain the xyloside **3** (41). The azide group containing xyloside was then deprotected and reduced to obtain the xyloside **5** (42, 43). Fluorogenic xylosides (**6**, **7**, and **8**) were synthesized from corresponding commercially available activated fluorescent reagents (dansyl Chloride, FITC, and *N*-hydroxysuccinimidyl-1-pyrene butyrate) by reacting with the xyloside **5** that contains

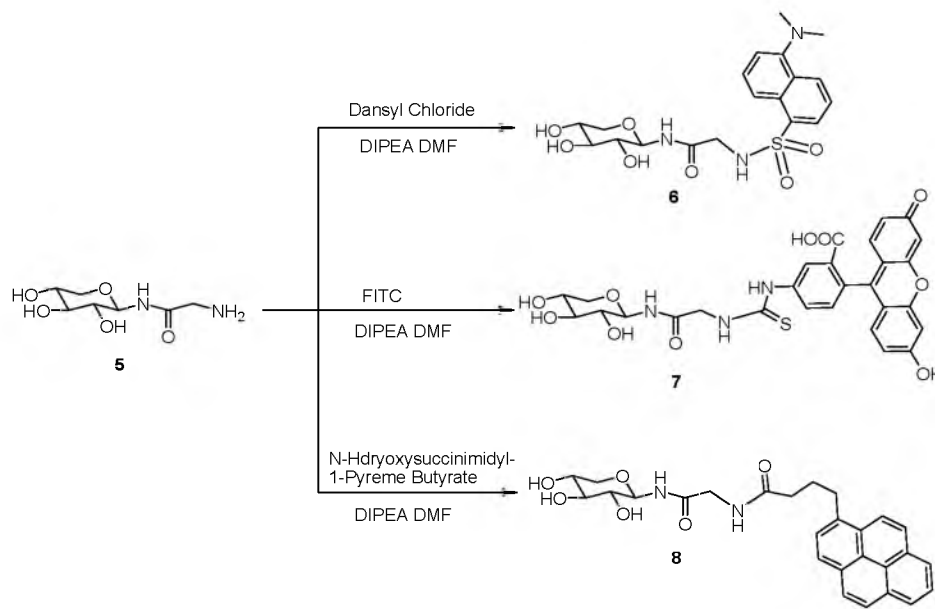


Scheme 3.1. Synthesis of amino-*N*-(2, 3, 4-trihydroxy- β -xylopyranosyl) acetamide

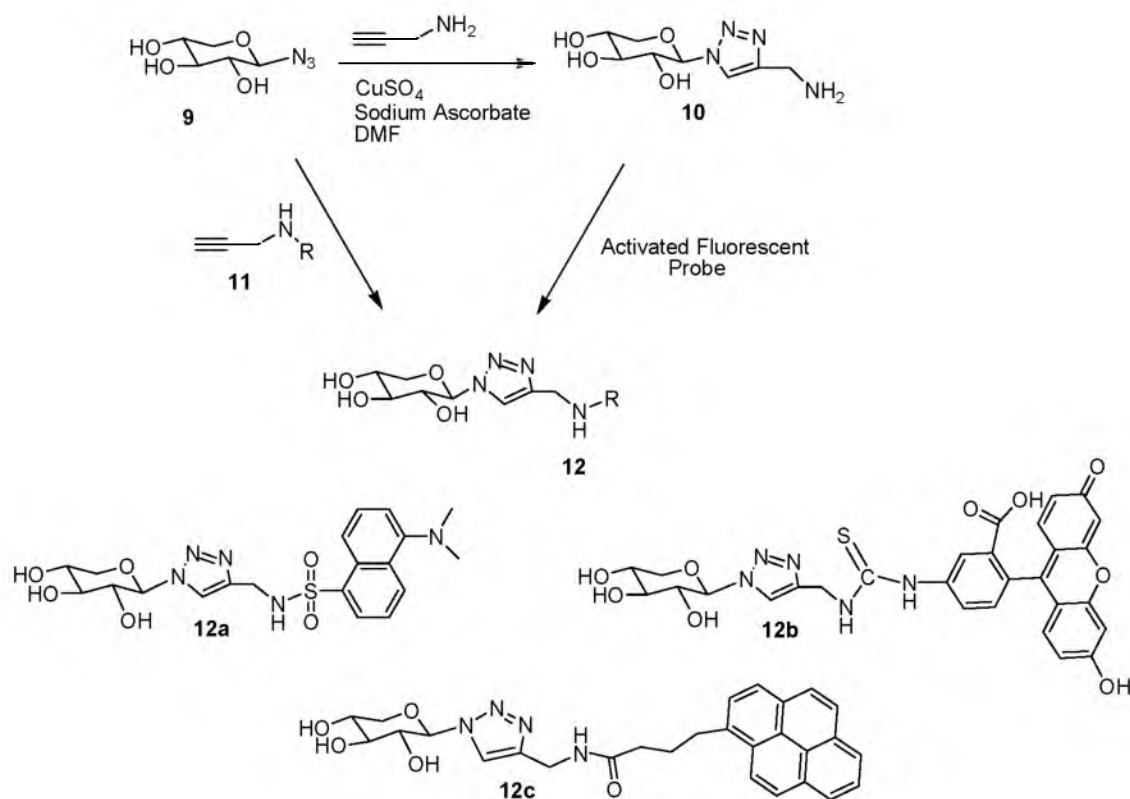
the reactive amine group (Scheme 3.2). Activated fluorescent probes are conjugated with xyloside amine to obtain the fluorescent conjugated xylosides in a rapid manner. Unfortunately, xyloside amine was unstable in our hands and therefore, the strategy outlined in Scheme 3.1 was chosen to introduce the reactive amine group.

It is known that the linker between xylose and the aglycone moiety (fluorogenic tag in this case) may dramatically influence the priming activity. Therefore, a second strategy was devised in which xylose was differentially attached to fluorescent tags by reacting xyloside azide **1** with triple bond containing fluorescent tags using click chemistry as shown in Scheme 3.3 (44). Xyloside **10** with a triozyl linkage is prepared, which contains the reactive amine group for conjugating with activated fluorescent reagents to obtain the fluorogenic xyloside **12**.

The commercial well-known UMB-*O*-xyloside primes mostly short chains of GAG chains or oligosaccharides in various cell types (37-39, 45). Click chemistry was used to conjugate fluorescent UMB derivatives **13a** and **13b** to the xylose unit. Fully acetylated xyloside was reacted with UMB derivatives containing triple bonds and



Scheme 3.2. Synthesis of fluorogenic xylosides with amide linkages



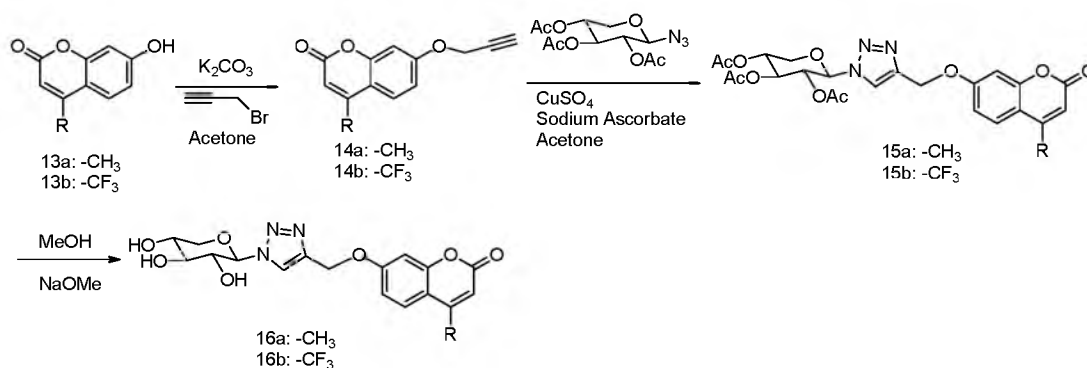
Scheme 3.3. Synthesis of fluorogenic xylosides with triazole linkages

these UMB-click-xylosides were deprotected under Zemplen condition to obtain the final products **16a** and **16b**, as outlined in Scheme 3.4. All final products were purified on a reverse phase C18 column using HPLC as described in the experimental section, followed by structural analysis using NMR spectrometer and mass spectrometry.

Compound **2**: $^1\text{H NMR}$ (CD_3Cl): δ 5.32 (t, $J = 9.4$ Hz, 1H), 5.12 (dd, $J = 9.0, 9.4$ Hz, 1H), 5.02-4.95(m, 1H), 4.94 (t, $J = 9.4$ Hz, 1H), 4.10 (dd, $J = 5.5, 11.5$ Hz, 1H), 4.03 (d, $J = 7.4$ Hz, 2H), 3.46 (t, $J = 11.14$ Hz, 1H), 2.07 (s, 3H), 2.06 (s, 3H), 2.05 (s, 3H).

Compound **3**: $^1\text{H NMR}$ (CD_3Cl): δ 5.31 (t, $J = 9.4$ Hz, 1H), 5.12 (t, $J = 9.4$ Hz, 1H), 4.98-4.95 (m, 1H), 4.90 (t, $J = 9.4$ Hz, 1H), 4.09 (dd, $J = 5.9, 11.5$ Hz, 1H), 4.00 (d, $J = 5.47$ Hz, 2H), 3.45 (t, $J = 11.7$ Hz, 1H), 2.07 (s, 3H), 2.05 (s, 3H), 2.03 (s, 3H).

Compound **4**: $^1\text{H NMR}$ (CD_3Cl): δ 4.84 (d, $J = 8.6$ Hz, 1H), 3.90 (d, $J = 5.9$ Hz, 2H), 3.83 (dd, $J = 5.1, 11.1$ Hz, 1H), 3.50-3.44 (m, 1H), 3.36-3.23 (m, 3H).



Scheme 3.4. Synthesis of UMB-click-xylosides with triazole-linkages

Compound **5**: ^1H NMR (CD_3Cl): δ 4.84 (d, $J = 8.98$ Hz, 1H), 3.82 (dd, $J = 5.1$, 11.33 Hz, 1H), 3.59 (s, 2H), 3.50-3.44 (m, 1H), 3.37-3.23 (m, 3H).

Compound **6**: ^1H NMR (CD_3OD): δ 8.57 (d, $J = 8.6$ Hz, 1H), 8.34 (d, $J = 9.0$ Hz, 1H), 8.20 (d, $J = 7.45$ Hz, 1H), 7.60 (t, $J = 8.0$ Hz, 1H), 7.57 (t, $J = 8.0$ Hz, 1H), 7.28 (d, $J = 7.8$ Hz, 1H), 4.70 (d, $J = 9.0$ Hz, 1H), 3.75 (dd, $J = 5.1$, 11.3 Hz, 1H), 3.56 (d, $J = 3.9$ Hz, 2H), 3.44-3.37 (m, 1H), 3.20-3.05 (m, 3H), 3.89 (s, 6H); Mass (**ESI**): calcd for $\text{C}_{19}\text{H}_{24}\text{N}_3\text{O}_7\text{S}$ $[\text{M}-\text{H}]^-$ 438.475, found 438.310.

Compound **7**: ^1H NMR (CD_3OD): δ 8.52 (s, 1H), 8.18 (d, $J = 2.0$ Hz, 1H), 7.81 (dd, $J = 2.0$, 8.2 Hz, 1H), 7.16 (d, $J = 8.2$ Hz, 1H), 6.83 (d, $J = 8.6$ Hz, 2H), 6.67 (d, $J = 2.4$ Hz, 1H), 6.57 (dd, $J = 2.3$, 8.6 Hz, 2H), 4.38 (d, $J = 11.3$ Hz, 1H), 3.85 (d, $J = 5.1$, 11.3 Hz, 1H), 3.50-3.46 (m, 1H), 3.39-3.24 (m, 3H), 3.89 (s, 6H); Mass (**ESI**): calcd for $\text{C}_{28}\text{H}_{26}\text{N}_3\text{O}_{10}\text{S}$ $[\text{M}+\text{H}]^+$ 596.134, found 596.139.

Compound **8**: ^1H NMR (CD_3OD): δ 8.37 (d, $J = 9.4$ Hz, 1H), 8.19-8.13 (m, 4H), 8.04-7.97 (m, 3H), 7.92 (d, $J = 7.8$ Hz, 1H), 3.91 (dd, m, 2H), 3.80 (dd, $J = 5.1$, 11.1 Hz, 1H), 3.48-3.21 (m, 7H), 2.44 (t, $J = 7.4$ Hz, 2H), 2.21-2.16 (m, 2H); Mass (**ESI**): calcd for $\text{C}_{27}\text{H}_{28}\text{N}_2\text{O}_6\text{Na}$ $[\text{M}+\text{Na}]^+$ 499.185, found 499.067.

Compound **12a**: ^1H NMR (CD_3OD): δ 8.55 (d, $J = 8.6$ Hz, 1H), 8.32 (d, $J = 8.6$ Hz, 1H), 8.20 (d, $J = 7.4$ Hz, 1H), 7.64 (s, 1H), 7.58 (dd, $J = 7.8$, 10.2 Hz, 1H), 7.56 (dd, $J = 7.4$, 8.6 Hz, 1H), 7.27 (d, $J = 7.42$ Hz, 1H), 5.34 (d, $J = 9.0$ Hz, 1H), 4.17 (s, 2H), 3.96 (dd, $J = 5.5$, 11.4 Hz, 1H), 3.68 (t, $J = 9.0$ Hz, 1H), 3.66-3.58 (m, 1H), 3.45-3.38 (m, 2H), 3.89 (s, 6H); Mass (**ESI**): calcd for $\text{C}_{20}\text{H}_{25}\text{N}_5\text{O}_6\text{SNa}$ $[\text{M}+\text{Na}]^+$ 486.142, found 486.200.

Compound **12b**: ^1H NMR (CD_3OD): δ 8.16 (2H, d, $J = 16.4$ Hz), 7.74 (1H, d, $J = 8.2$ Hz), 7.15 (1H, d, $J = 8.2$ Hz), 6.66 (3H, d, $J = 2.0$ Hz), 6.53 (2H, d, $J = 8.6$ Hz), 5.50 (1H, d, $J = 9.4$ Hz), 4.96 (2H, s), 3.90 (1H, dd, $J = 5.0, 11.1$ Hz), 3.88 (1H, t, $J = 8.6$ Hz), 3.70-3.63 (1H, m), 3.50-3.42 (2H, m); Mass (ESI): calcd for $\text{C}_{29}\text{H}_{24}\text{N}_5\text{O}_9\text{SNa}$ $[\text{M}-\text{H}+\text{Na}]^+$ 641.137, found 641.333

Compound **12c**: ^1H NMR (CD_3OD): δ 8.27-7.84 (m, 10H), 5.46 (d, $J = 9.4$ Hz, 1H), 4.45 (d, $J = 2.3$ Hz, 1H), 3.95 (dd, $J = 5.5, 11.3$ Hz, 1H), 3.86 (t, $J = 8.4$ Hz, 1H), 3.67-3.57 (m, 3H), 3.49-3.39 (m, 2H), 2.35 (round, 2H), 2.12 (round, 2H). Mass (ESI): calcd for $\text{C}_{28}\text{H}_{28}\text{N}_4\text{O}_5\text{Na}$ $[\text{M}+\text{Na}]^+$ 523.196, found 523.130.

Compound **14a**: ^1H NMR (CDCl_3): δ 7.53 (d, $J = 8.99$ Hz, 1H), 6.95 (s, 1H), 6.93 (d, $J = 2.7$ Hz, 1H), 6.17 (d, $J = 1.2$ Hz, 1H), 4.77 (d, $J = 2.3$ Hz, 2H), 2.58 (t, $J = 2.3$ Hz, 1H), 2.41 (s, 3H).

Compound **14b**: ^1H NMR (CDCl_3): δ 7.64 (d, $J = 8.2$ Hz, 1H), 6.99 (s, 1H), 6.97 (d, $J = 2.0$ Hz, 1H), 6.63 (s, 1H), 4.78 (d, $J = 2.3$ Hz, 2H), 2.59 (t, $J = 2.3$ Hz, 1H).

Compound **16a**: ^1H NMR (CD_3OD): δ 8.30 (s, 1H), 7.70 (d, $J = 9.6$ Hz, 1H), 7.05 (s, 1H), 7.03 (s, 1H), 6.17 (s, 1H), 5.53 (d, $J = 9.0$ Hz, 1H), 5.29 (2H, s), 4.00 (dd, $J = 5.5, 11.3$ Hz, 1H), 3.90 (t, $J = 9.0$ Hz, 1H), 3.70-3.64 (m, 1H), 3.52-3.44 (m, 2H), 2.44 (s, 3H), Mass (ESI): calcd for $\text{C}_{18}\text{H}_{19}\text{N}_3\text{O}_7\text{Na}$ $[\text{M}+\text{Na}]^+$ 412.122, found 412.200

Compound **16b**: ^1H NMR (CD_3OD): δ 8.32 (s, 1H), 7.69 (d, $J = 9.0$ Hz, 1H), 7.17 (d, $J = 2.3$ Hz, 1H), 7.10 (dd, $J = 2.3, 9.0$ Hz, 1H), 6.71 (s, 1H), 5.54 (d, $J = 9.0$ Hz, 1H), 5.33 (2H, s), 4.00 (dd, $J = 5.5, 11.3$ Hz, 1H), 3.90 (t, $J = 9.0$ Hz, 1H), 3.71-3.64 (m, 1H), 3.52-3.44 (m, 2H), Mass (ESI): calcd for $\text{C}_{18}\text{H}_{16}\text{F}_3\text{N}_3\text{O}_7\text{Na}$ $[\text{M}+\text{Na}]^+$ 466.094, found 466.098

3.2.2. Screening of Fluorogenic Xylosides

The priming activity of these novel xylosides may perhaps be attributed to the presence of a very hydrophobic fluorescent group, helping their transport across cell surface and Golgi membranes to GAGOSOMES. The priming ability of fluorescent-tagged xylosides are investigated using a mutant Chinese hamster ovary (CHO) cell line, pgsA-745, which lacks active xylosyltransferase enzyme (46). This cell line does not make GAG chains. It requires the exogenous supply of β -xylosides to produce GAG chains, and is thus a convenient cellular system to ascertain the quantity of the primed GAG chains by exogenously supplied fluorescent xylosides. Neither dansyl group attached xylosides (**6** and **12a**) nor fluorescein attached xylosides (**7** and **12b**) primed any detectable GAG chains. It may perhaps be due to the presence of charged amine (in dansyl moiety) and carboxyl (in fluorescein moiety) groups preventing the uptake of xylosides across the cell membrane. This is in accordance with Mani et al. who found out that the dansyl group attached xylosides were unable to prime any detectable amount of GAG chains. Fluorescent xylosides without a charged group are chosen to be synthesized. Fluorescent xylosides (**8**, **12c**, **16a** and **16b**), in which xylose residue is attached to 1-pyrene butyrate and UMB derivatives, were synthesized. Pyrene containing xyloside with amide linkages **8** were not able to prime GAG chains while the pyrene containing xyloside with triazolyl linkage **12c** were able to prime at 50 μ M and 100 μ M (Figure 3.1).

It is interesting to observe that the pyrene containing xyloside with triazole linkage **12c** can prime GAG chains but the pyrene containing xyloside with amide linkage **8** cannot prime GAG chains. Therefore, the triazole ring may increase

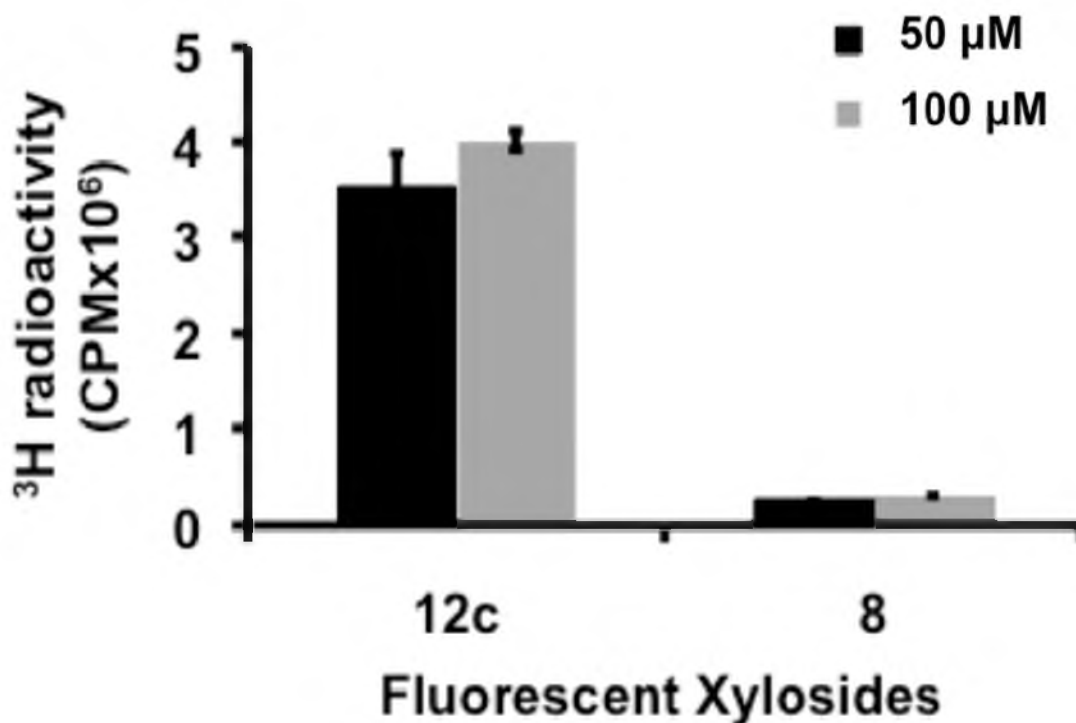


Figure 3.1. Priming activity of fluorescent xylosides (12c and 8) in pgsA-745 cell line. CHO cells were treated with fluorescent xylosides at 50 μM and 100 μM in the presence of ^3H (100 μCi) as described in “Experimental Methods” section [5.4]. The GAG chains were purified by anion exchange chromatography and quantitated using a liquid scintillation counter. The results were the average of two independent experiments

the diffusion rate and direct the primer to Golgi compartments. Next, UMB-click-xylosides **16a** and **16b** were designed and compared to the commercial UMB-*O*-xylosides that prime mostly GAG chains with a low chain length. The priming activities of the UMB-click-xylosides **16a** and **16b** and the commercial xyloside were compared at various concentration (50 μM , 100 μM , 300 μM , 600 μM , and 1 mM) (Figure 3.2). It is interesting to note that priming activity of the UMB-click-xylosides **16a** and **16b** was concentration-dependent but the UMB-*O*-xyloside was not.

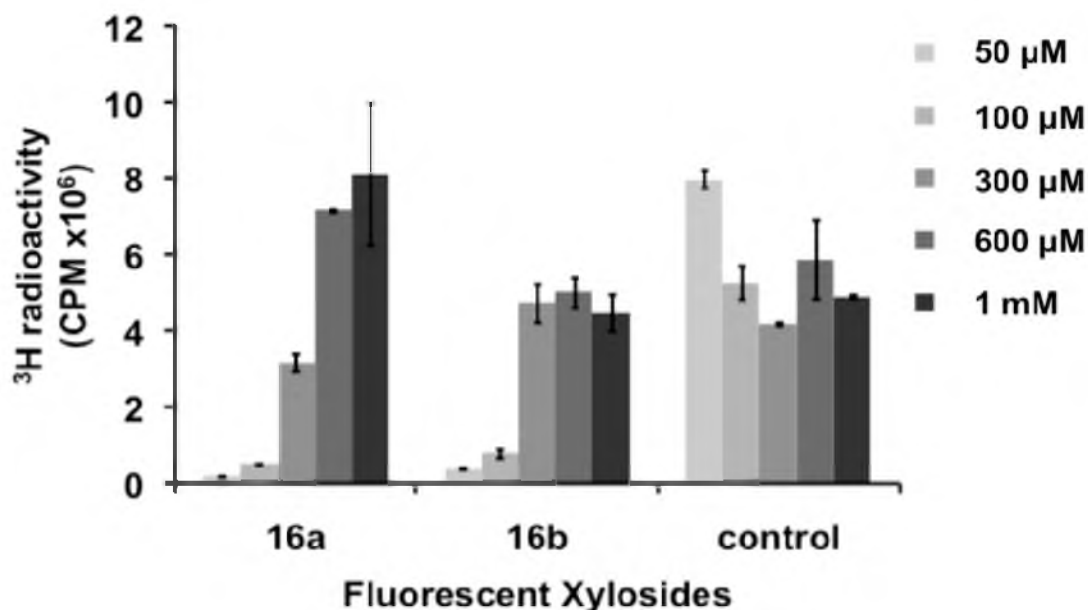


Figure 3.2. Priming activity of UMB-click-xylosides (**16a**, **16b**), and UMB-*O*-xylosides (control) in pgsA-745 cell line. CHO cells were treated with fluorescent xylosides at 50 μ M, 100 μ M, 300 μ M, 600 μ M, and 1 mM in the presence of ^3H (100 μ Ci) as described in the “Experimental Methods” section [5.4]. The GAG chains were purified by anion exchange chromatography and quantitated using a liquid scintillation counter. The results were the average of two independent experiments

3.2.3. Structural Analysis of Primed GAG Chains

The GAG chains primed by these fluorescent xylosides **12c**, **16a** and **16b** were further analyzed for their sulfation pattern by the DEAE-anion exchange HPLC column and for their molecular weights using size exclusion columns, as outlined in the “Experimental Methods” section [5.4]. GAG chains primed by xyloside **12c** at 50 μ M is more homogenous and has higher sulfate than at 100 μ M (Figure 3.3). The chain length of GAG chains primed by fluorescent xyloside **12c** in CHO cells was determined by measuring migration time of GAG chains in comparison to those of polystyrene sulfonate standards performed under similar conditions on the size exclusion column and suggests that GAG chains, primed by fluorescent xyloside **12c** in CHO cells, have

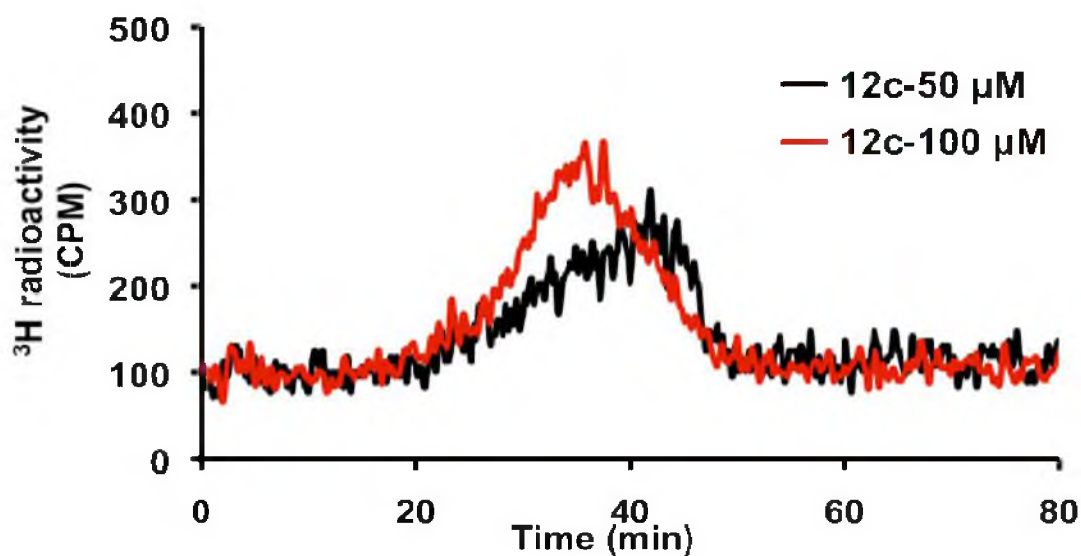


Figure 3.3. Sulfate density profile of fluorescent xyloside 12c primed GAG chains. GAG chains primed by fluorescent xyloside **12c** in *pgsA-745* cell lines at 50 μ M and 100 μ M were analyzed using anion exchange HPLC: the bound GAG chains were eluted with a linear gradient from 0.2 M to 1 M NaCl over 80 minutes at a flow rate of 1ml/ min. These elution profiles are representative of two independent experiments.

an 27 KDa at 50 μ M and 20 KDa at 100 μ M (Figure 3.4). We have estimated the percentage compositions of HS and CS chains in the total GAG pool. Unfortunately, fluorescent xyloside **12c** primed mostly CS (up to 95 %). Moreover, the fluorescent xyloside **12c** was not sensitive enough. Therefore, the structural analysis of GAG chains primed by the fluorescent xyloside **12c** could not be studied using fluorescent detectors.

The UMB-*O*-xyloside has been shown to function as acceptor for the elongation of GAG chains by several groups (37-39). However, this well-known fluorescent xyloside mostly prime CS with low MW chains. By changing the *O* linkage of the fluorescent xyloside to click linkage, the fluorescent click-xylosides were hoped to prime both HS and CS with higher MW chains. The results from priming activity

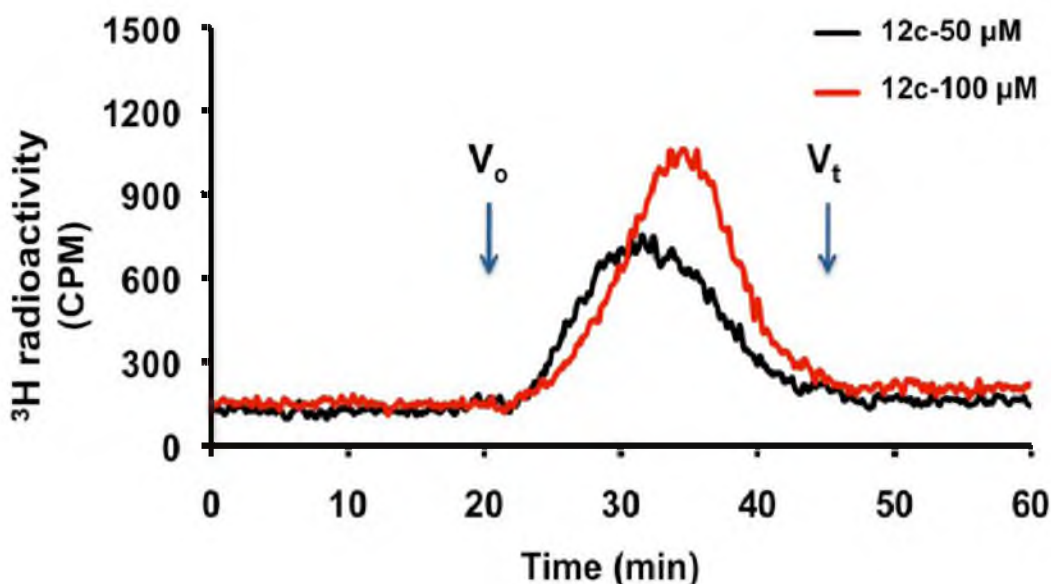


Figure 3.4. Size exclusion profiles of GAG chains primed by fluorescent xyloside 12c. GAG chains primed by fluorescent xyloside **12c** at 50 μM and 100 μM concentrations in pgs A-745 cells for 24 h. The purified GAG chains were analyzed by size exclusion chromatography, fractionated on two tandem 3000 SW_{XL} columns, and was eluted with an isocratic gradient of phosphate buffer for 90 minutes at a flow rate of 0.5 ml/ min.

analysis suggest that optimized priming concentration of UMB-click-xyloside **16a** and **16b** is 300 μM . Therefore, the GAG chains primed by these xylosides at 300 μM were further analyzed for their molecular weight using the size exclusion column and HS/ CS composition using heparin lyases I, II, and III (Figure 3.5). It notes that both fluorescent xylosides **16a** and **16b** primed GAG chains have an average molecular weight (42 KDa) is higher than those primed by commercial UMB-O-xyloside (4KDa). Moreover, it is surprising to note that fluorescent xylosides **16a** and **16b** primed about 30% HS chains, whereas commercial UMB-O-xylosides primed less than 5 % HS chains.

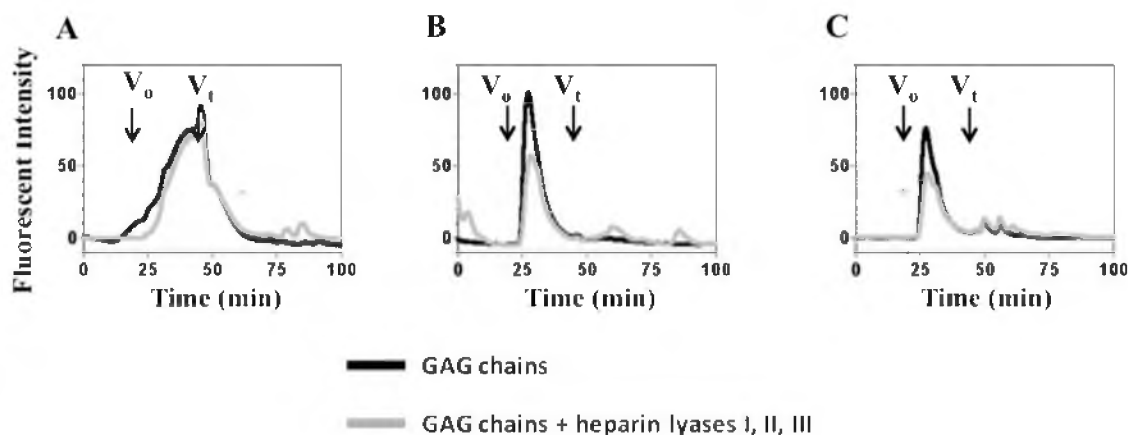


Figure 3.5. Size exclusion profiles of GAG chains primed by fluorescent xylosides (UMB-*O*-xyloside, 16a and 16b). GAG chains primed by fluorescent xylosides at 300 μ M concentration in pgsA-745 cells for 24 h. The HS/CS composition of the primed GAG chains was determined by digesting the GAG chains with heparin lyases I, II, III. The enzyme reaction and the purification of the primed GAG chains were described in the “Experimental Methods” section [5.4]. The purified GAG chains were analyzed by size exclusion chromatography, fractionated on two tandem 3000 SW_{XL} columns, and were eluted with an isocratic gradient of phosphate buffer for 90 minutes at a flow rate of 0.5 ml/ min. A: The elution profiles of GAG chains primed by UMB-*O*-xyloside. B: The elution profile of GAG chains primed by fluorescent xyloside **16a**. C: The elution profiles of GAG chains primed by fluorescent xyloside **16b**.

3.3. Conclusions

In conclusion, a small library of novel fluorescent xylosides was synthesized to evaluate their GAG-priming activity and structural analysis. Pyrene- and UMB-click-xylosides were able to participate in the stimulation of GAG biosynthesis. These fluorescent xylosides containing the triazol rings were more stable than commercially available xylosides and predictably have a longer *in vivo* half life. Moreover, these fluorescent xylosides were able to prime more HS and higher MW than commercial fluorescent xylosides. Therefore, these xylosides have potential to profile and elucidate cellular-specific heparanome to define various dynamic interactions in the complex systems and to offer prospects to further our understanding of factors that regulate GAG

biosynthesis as well as new knowledge on the role of GAG chains in various signaling events associated with pathophysiological processes.

3.4. Experimental Methods

3.4.1. General Synthetic Procedures

All chemical reactions were carried out under a nitrogen atmosphere in oven-dried glassware using standard techniques. ^1H and ^{13}C NMR spectra were obtained on a Bruker 400-MHz spectrometer. Chemical shifts are relative to the deuterated solvent peak or the tetramethylsilane (TMS) peak at (δ 0.00) and are in parts per million (ppm). High-resolution mass spectrometry (HRMS) was performed using a Finnigan LCQ mass spectrometer in either positive or negative ion mode. Thin layer chromatography (TLC) was done on 0.25 mm thick precoated silica gel aluminum sheets. Chromatograms were observed under short and long wavelength UV light, and were visualized by heating plates that were dipped in a solution of Von's reagent containing ammonium (VI) molybdate tetrahydrate (12.5 g) and cerium (IV) sulfate tetrahydrate (5.0 g) in 10% aqueous sulphuric acid (500 mL). Flash column chromatography was performed using silica gel 60 (230–400 mesh) and employed a stepwise solvent polarity gradient, correlated with TLC mobility, and were run under pressure of 5-7 psi. HPLC was used to purify final products using C18 column (VYDAC 2.2 cm x25cm) with solvent A (25mM formic acid) and solvent B (95% Acetonitrile) at a flow rate of 5 ml/minutes in a linear gradient over 120 minutes starting with 0% B.

2, 3, 4-Tri-*O*-acetyl-*D*-xylopyranosyl azide (**1**): Trimethylsilyl azide (1.5 mmol) and SnCl_4 (0.5 mmol) were added dropwise to a stirred solution of fully acetylate

xylose derivative (1mmol) in dry CH₂Cl₂, and stirring was continued at room temperature. The progress of the reaction was checked by TLC, and after the completion of the reaction, the reaction mixture was then evaporated under vacuum to give a residue that was further purified by low pressure flash silica column chromatography to yield the compound **1**.

N-(2,3,4-tri-*O*-acetyl- β -*D*-xylopyranosyl) chloroacetamide (**2**): 2,3,4-Tri-*O*-Acetyl- β -*D*-xylopyranosyl azide (**1**) (1 mmol) was dissolved in dry CH₂Cl₂ (20 ml). The mixture was cooled at 0°C. Chloroacetic anhydride (1 mmol) was added to the solution, followed by triphenyl phosphine (1 mmol), and the reaction was continued overnight. After the reaction was complete, the solvent was removed using rotary evaporator under reduced pressure. The reaction mixture was extracted using ethyl acetate and water. The organic layer was washed with saturated brine solution and evaporated under vacuum to give a residue, which was purified by silica column chromatography to give the title compound **2**.

N-(2,3,4-tri-*O*-acetyl- β -xylopyranosyl) azidoacetamide (**3**): *N*-(2,3,4-tri-*O*-acetyl- β -*D*-xylopyranosyl) chloroacetamide (**2**) (1 mmol) was taken in a 100 ml RB flask and dry DMF (20 ml) was added, followed by the addition of sodium azide (2 mmol). The reaction mixture was heated to 90°C under stirring. Progress of the reaction was monitored by TLC using ethyl acetate and hexane (1:1) as the eluant. After the reaction was complete, the reaction mixture was cooled and diluted with ethyl acetate. The organic layer was washed with water, dried over sodium sulfate, and concentrated to obtain a syrupy material that was further purified by silica flash column chromatography to give the title compound **3**.

N-(β -*D*-xylopyranosyl) azidoacetamide (**4**): *N*-(2,3,4-tri-*O*-acetyl- β -xylopyranosyl) azidoacetamide (**3**) (0.1 mmol) was taken in dry methanol and was treated with freshly prepared 0.5 M solution of CH₃ONa (0.1ml) in dry methanol at room temperature for 3 h. Neutralization with H⁺ resin followed by concentration at reduced pressure gave a syrupy liquid, which was purified by silica flash column chromatography to give the title compound **4**.

N-(β -*D*-xylopyranosyl) aminoacetamide (**5**): A solution of *N*-(β -*D*-xylopyranosyl) azidoacetamide (**4**) (0.1 mmol) in dry methanol (10 ml) was hydrogenated over Pd/C (0.1 mmol) for 1 h. After the starting material disappeared (TLC), the catalyst was removed by filtration through celite and washed with methanol (10 ml). The filtered solution was concentrated by rotovapor to get the final product **5** without purification steps.

Synthesis of fluorophore tagged xylosides with amide linkages (**6**, **7** and **8**): *N*-(β -*D*-xylopyranosyl) aminoacetamide **5** (0.1 mmol) was dissolved in dry DMF (10 ml). Dissopropylethylamine (0.1 mmol) was added. The whole mixture was stirred for 30 minutes before adding the commercially available activated fluorescent reagents (Dansyl chloride, FITC and N-hydroxysuccinimidyl-1-pyrene butyrate) (1 mmol). The reaction mixture was stirred for 4 h and purified by C18-HPLC column.

N-(β -*D*-xylopyranosyl) azide (**9**): 2, 3, 4-Tri-*O*-acetyl- β -*D*-xylopyranosyl azide **1** (0.1 mmol) was taken in dry methanol and was treated with freshly prepared 0.5 M solution of CH₃ONa (0.1ml) in dry methanol at room temperature for 3 h. Neutralization with H⁺ resin followed by concentration at reduced pressure gave a

syrupy liquid, which was purified by silica flash column chromatography to give the title compound **9**.

Propargyl UMB derivative (**14**): To the solution (10ml) of UMB derivative (**13a** and **13b**) (1 mmol) in acetone, was added potassium carbonate (3 mmol). The reaction mixture was stirred for 30 minutes at room temperature. Propargyl bromide (3 mmol) was then added and the mixture was stirred overnight. The reaction mixture was concentrated. The resulting crude material was dissolved in ethyl acetate, washed with water and saturated sodium chloride solution, dried over Na_2SO_4 and rotary evaporated under reduced pressure. The residue was purified by column chromatography to give the compound **14**.

Synthesis of fluorophore tagged xylosides with click linkages (**12a**, **12b**, **12c**, **15a** and **15b**): to a solution of alkyne (1mmol) and azide (1mmol) in DMF and water (4:1.3) solvent mixture were added sodium ascorbate (0.8 mmol) followed by $\text{Cu}_2\text{SO}_4 \cdot 5\text{H}_2\text{O}$ (0.4 mmol) at room temperature, and the mixture was stirred for 12 h or until disappearance of one of the starting materials as indicated by TLC. At the end of the reaction as confirmed by TLC analysis, the solvent of the reaction mixture was evaporated using rotary-evaporator under reduced pressure. The reaction mixture was purified by flash chromatography columns as described above. The purified acetylated product (0.1 mmol) was taken in dry methanol and was treated with freshly prepared 0.5 M solution of CH_3ONa (0.1ml) in dry methanol at room temperature for 3 h. Neutralization with H^+ resin followed by concentration at reduced pressure gave a syrupy liquid, which was purified on HPLC using C18 column to give the desired deprotected xyloside derivatives.

3.4.2. Screening of Fluorescent Xylosides in Cell Culture

The priming of the xylosides in xylosyl transferase-deficient CHO cell line pgsA-745 was performed as described in our earlier communication. Briefly, 1×10^5 cells were plated per well, containing the appropriate complete growth medium, in a 24-well plate and incubated at 37 °C in a humidified incubator for 24 h to reach a confluency of about 50%. The cells were then washed with sterile PBS and replaced with 450 μ L appropriate medium containing 10% dialyzed FBS. A serial dilution of the primers at 100X the final concentration was prepared and 5 μ L of appropriate 100X primer was added to various wells to yield a final concentration of 0.1, 1, 10, 100, and 1000 μ M, respectively. 50 μ Ci $6\text{-}^3\text{H}$ -glucosamine was then added to each well for radiolabeling the GAG chains synthesized. The 24-well plates were placed in the incubator for 24 h before the addition of 6X pronase solution (100 μ L) followed by incubation at 37 °C overnight.

3.4.3. Purification and Quantification of GAGs

After treating each well with pronase solution overnight, the entire contents of the wells were transferred to a microcentrifuge tube and subjected to centrifugation at 16,000xg for 5 minutes. The supernatant was transferred to a fresh tube and half-a-volume of 0.016% Triton X-100 was added. The diluted supernatant was loaded on to a DEAE-sepharose column (0.2 mL) pre-equilibrated with 10 column volumes of wash buffer (20 mM NaOAc buffer (pH 6.0) containing 0.1 M NaCl and 0.01% Triton X-100) and the column was washed with 20 column volumes of wash buffer. The bound HS/CS was eluted using 6 column volumes elution buffer (20 mM NaOAc (pH 6.0))

containing 1 M NaCl). The amount of GAG primed by various “Click”-xylosides was determined by quantifying the ^3H -radioactivity incorporated in the purified HS/CS eluate. 50 μL of the various eluates was diluted with 5 mL of scintillation cocktail and triplicate samples were measured using a scintillation counter for total radioactivity.

3.4.4. Analysis of Primed GAG Chains

The homogeneity and extent of sulfation of the GAG chains synthesized on the various primers was determined by measuring migration time on the anion exchange column using high-pressure liquid chromatography (HPLC) with inline radiodetector. 25 μL of eluate was diluted 10-fold with 10 mM KH_2PO_4 (pH 6.0) containing 0.2 % CHAPS, and loaded onto a DEAE column and eluted with a linear NaCl gradient of 0.2 to 1 M over 80 minutes.

The chain length of the primed GAG was determined by measuring the migration time on two tandem G3000SW_{XL} (Tosoh, 7.8 mm x 30 cm) size exclusion columns using the HPLC Hitachi system with an inline radiodetector or fluorescent detector. The solvent containing phosphate (100 mM KH_2PO_4 , 100 mM NaCl, pH 6) was used as an eluent. The average molecular weight was determined by measuring the migration time of GAG chains in comparison to those of polystyrene sulfonate standards examined under similar conditions.

The HS/CS composition of the primed GAG chains was determined by digesting the GAG chains with heparitinase I/II/III or chondroitinase ABC enzymes. The solution containing GAGs was diluted to 0.2 M NaCl, followed by the addition of heparitinase or chondroitinase ABC buffer and 5 mU of heparitinase I/II/III or

chondroitinase ABC enzyme. The reaction mixture was incubated at 37 °C for 2 h, the solution was then loaded on to two tandem G3000 SWXL columns (7.8 mm x 30 cm) and analyzed with the aid of an inline radiometric detector using phosphate buffer (100 mM KH₂PO₄, 100 mM NaCl, pH 6) as an eluent. The percentage of HS/CS was determined based on the percentage area of undigested and digested GAG peaks.

3.5. Supporting Information

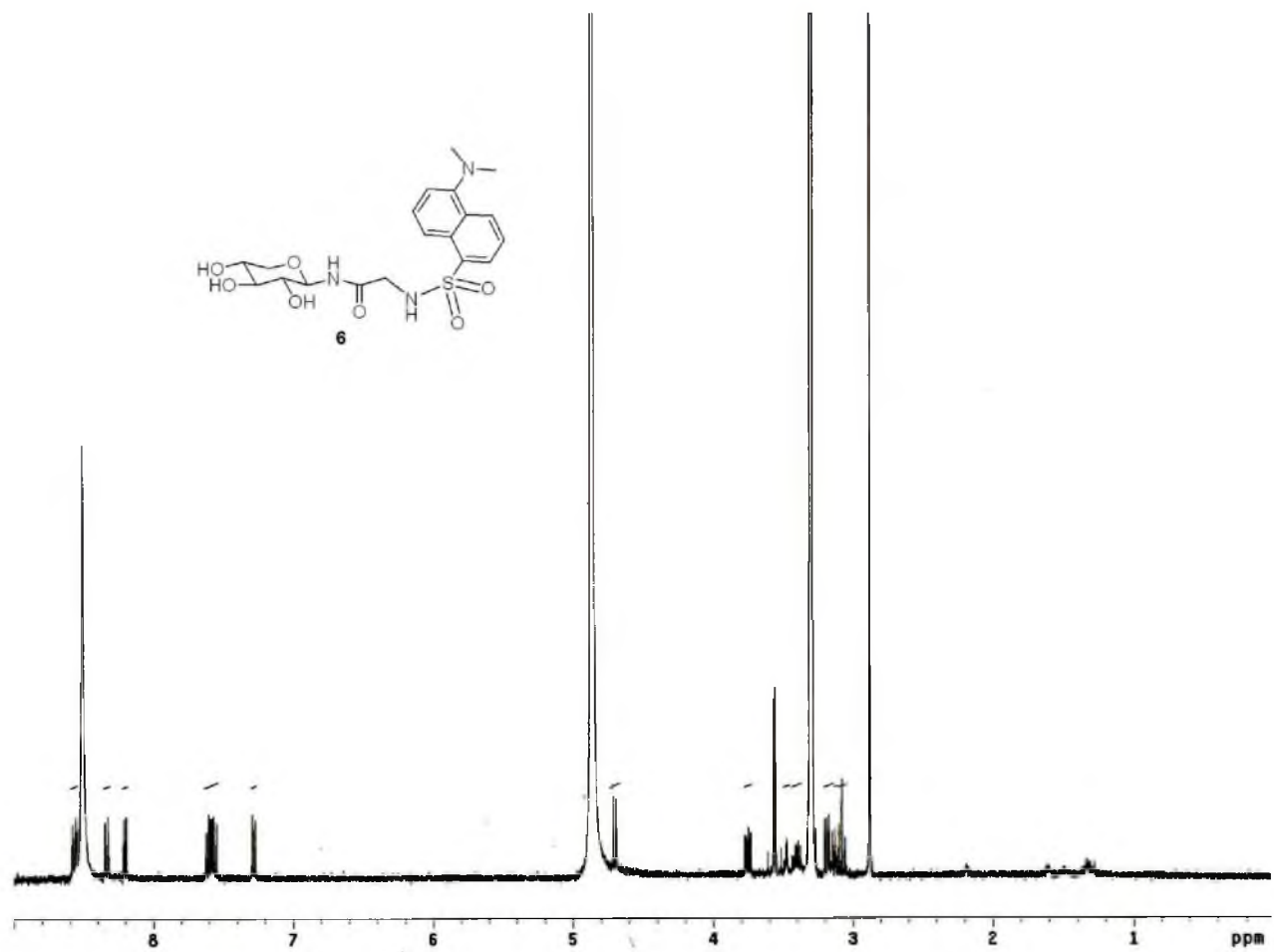


Figure S3.1. NMR spectra of fluorescent xyloside 6

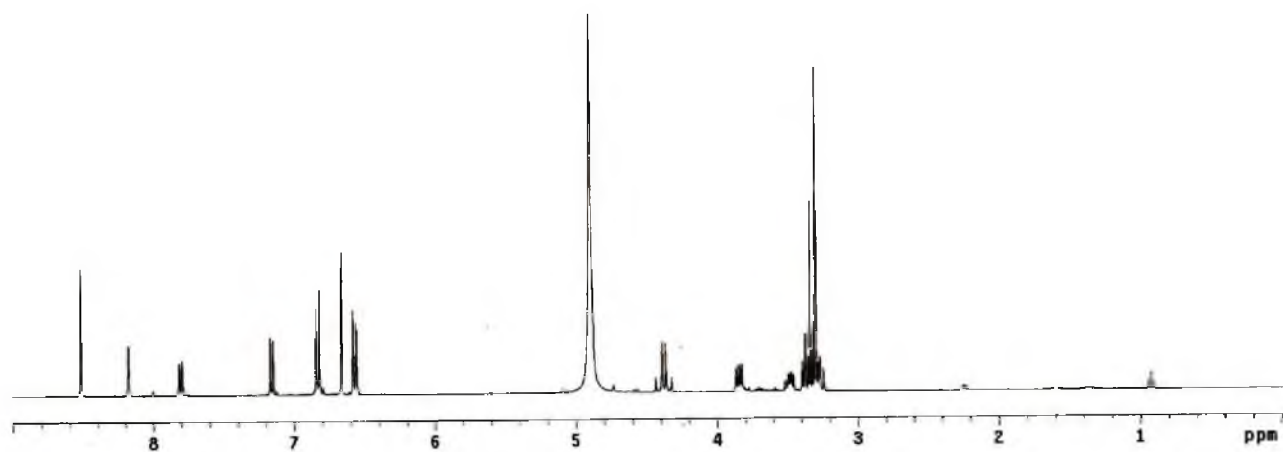
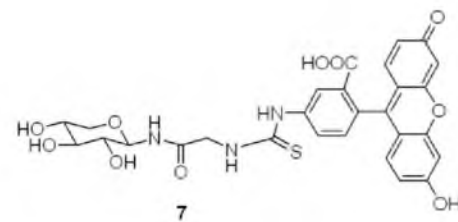


Figure S3.2. NMR spectra of fluorescent xyloside 7

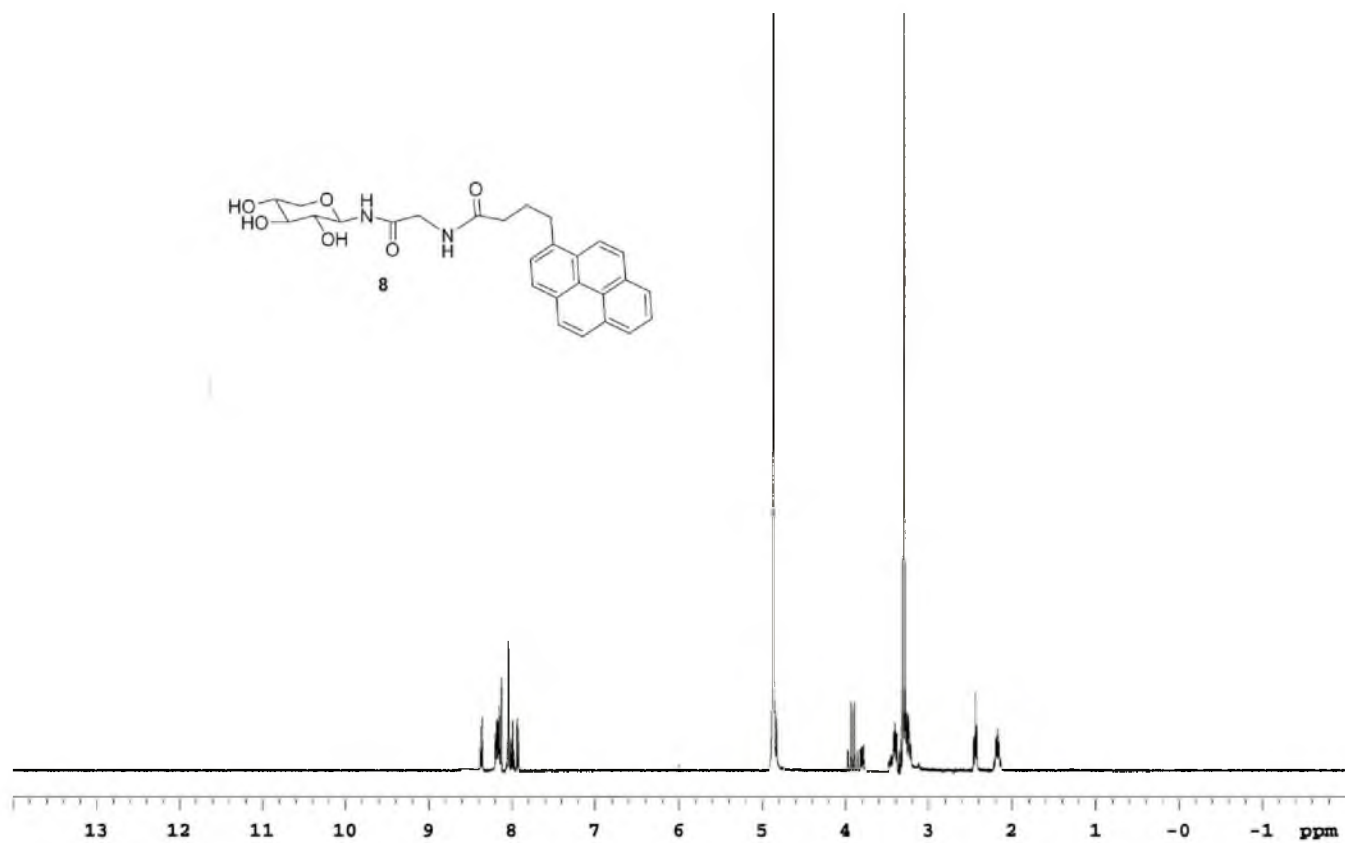


Figure S3.3. NMR spectra of fluorescent xyloside 8

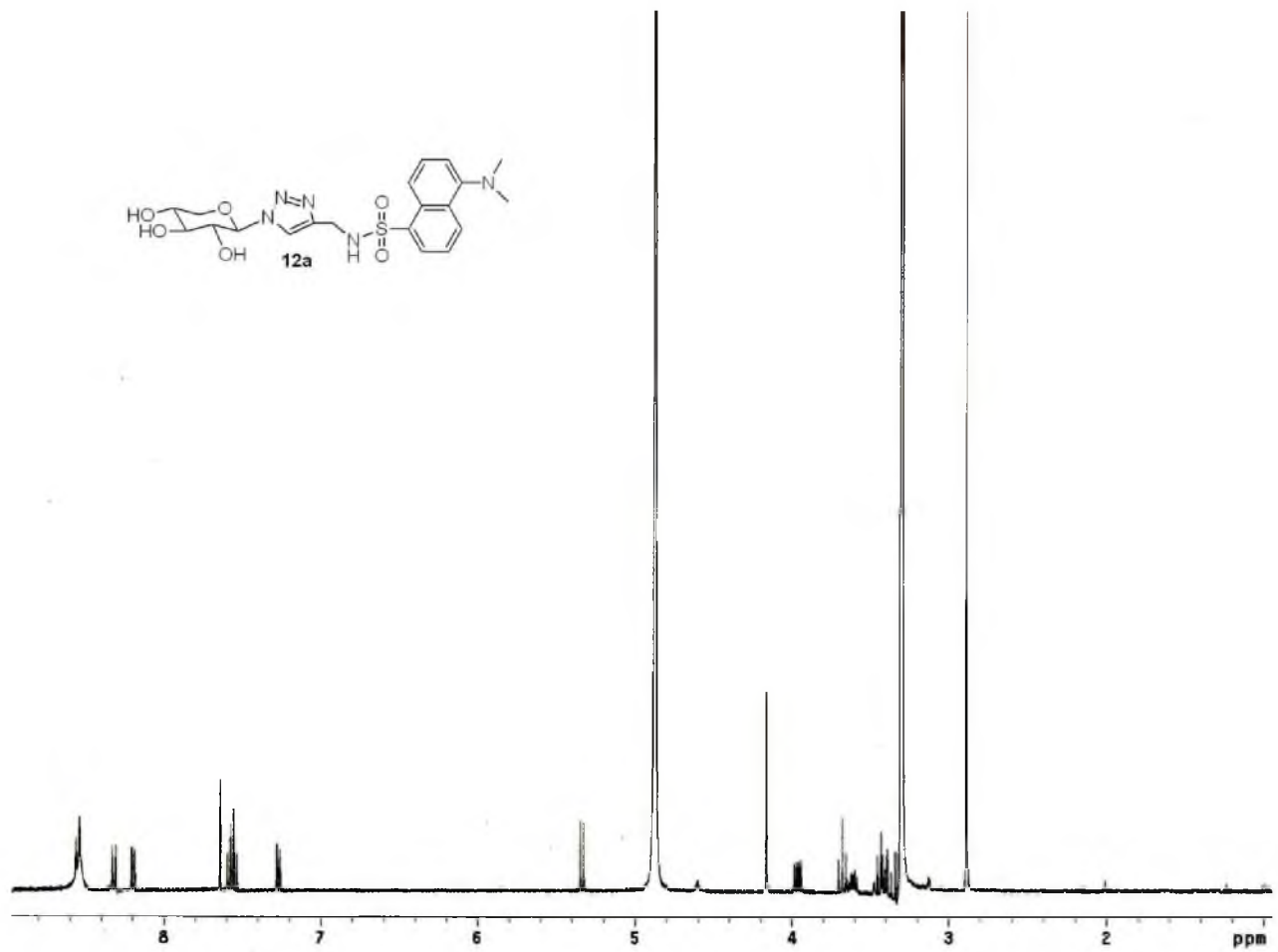


Figure S3.4. NMR spectra of fluorescent xyloside 12a

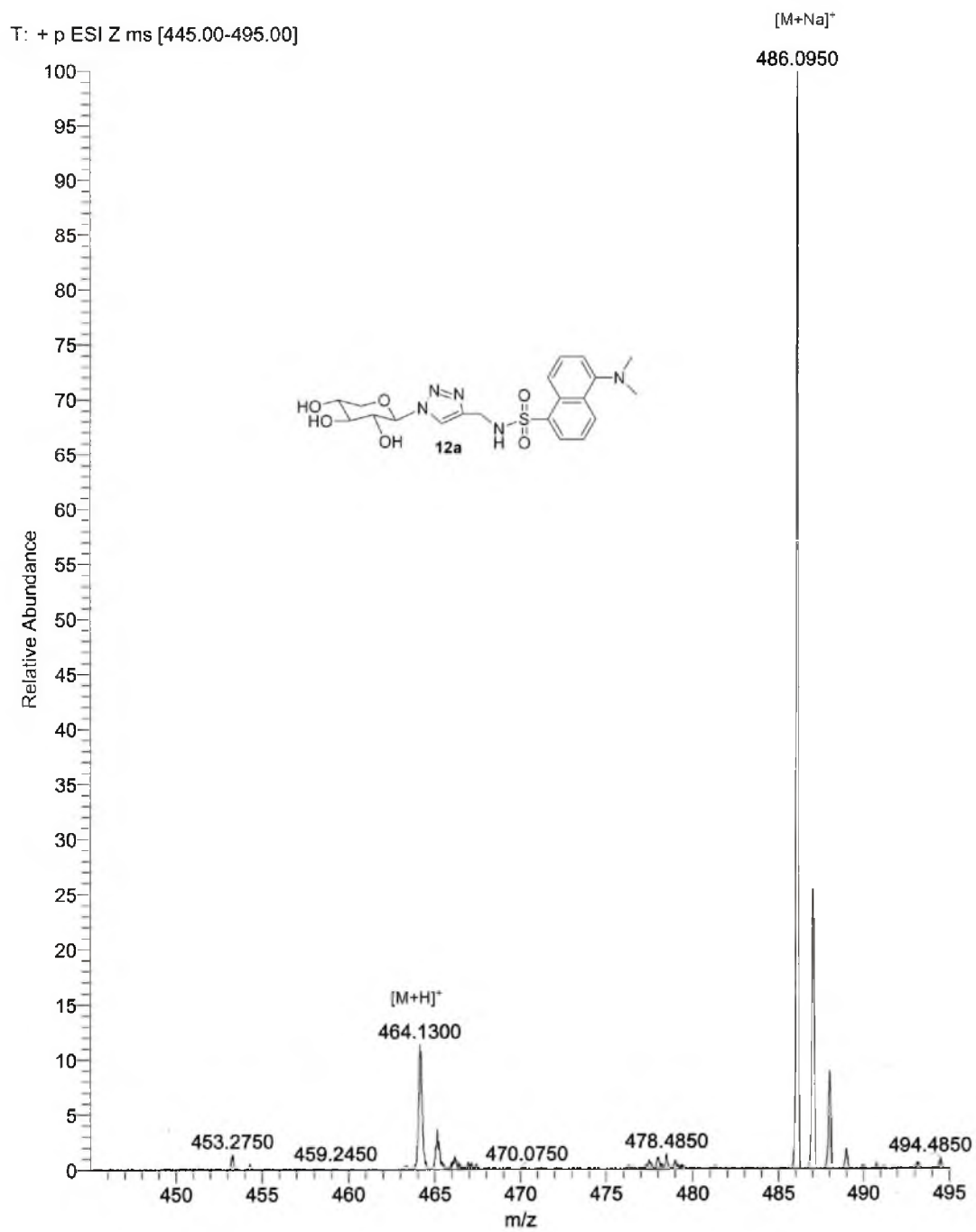


Figure S3.5 Mass spectra of fluorescent xyloside 12a

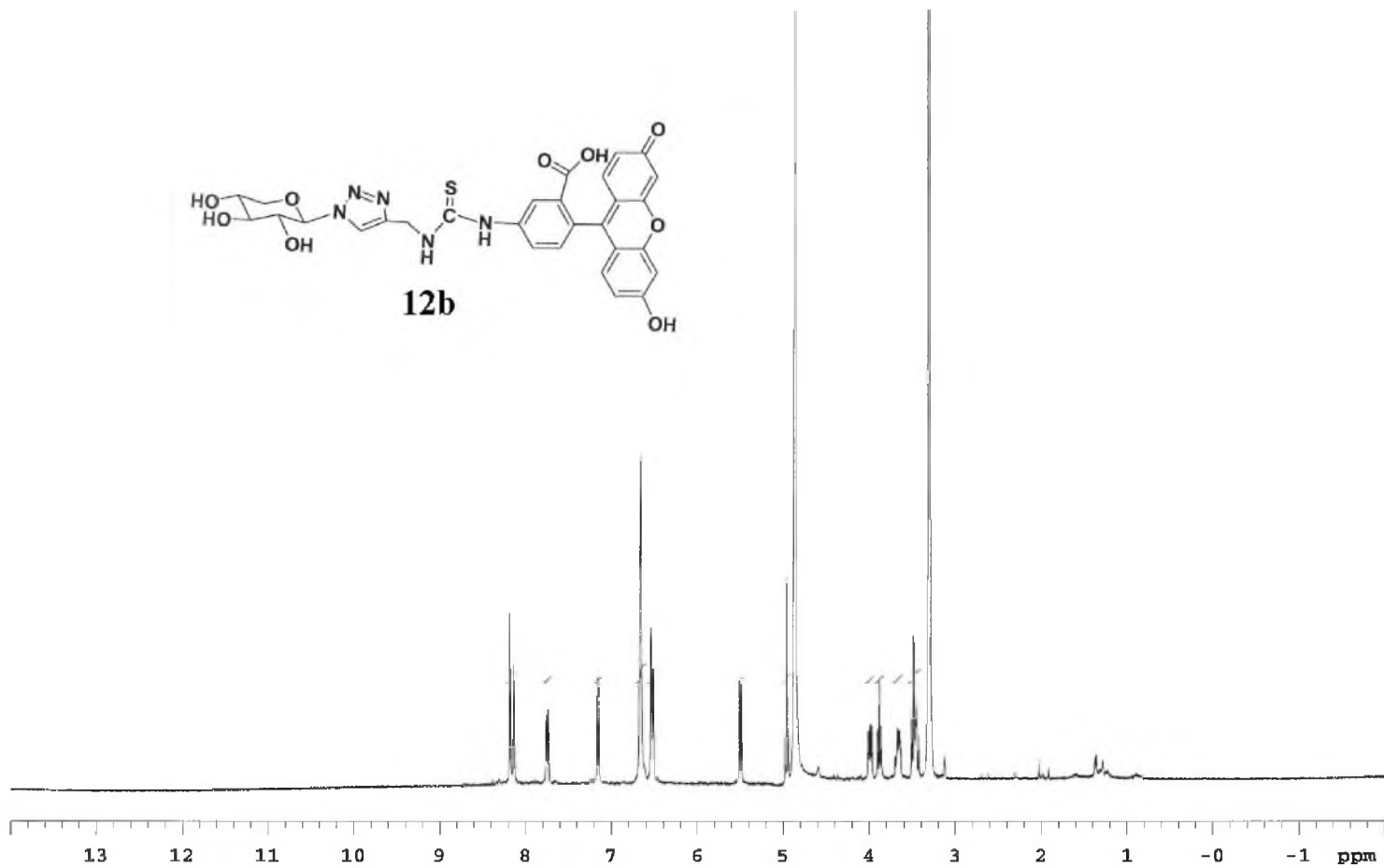


Figure S3.6. NMR spectra of fluorescent xyloside 12b

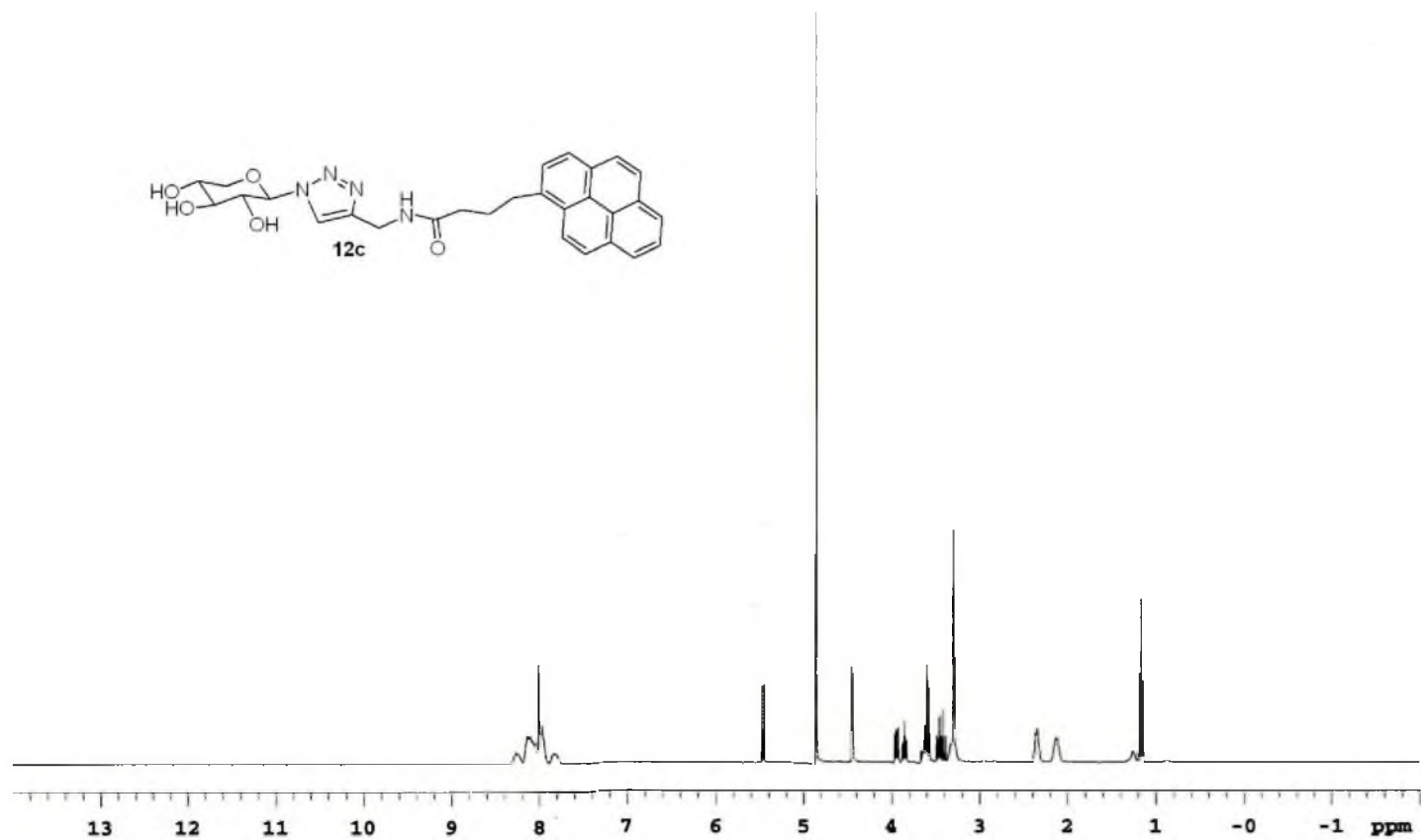


Figure S3.7. NMR spectra of fluorescent xyloside 12c

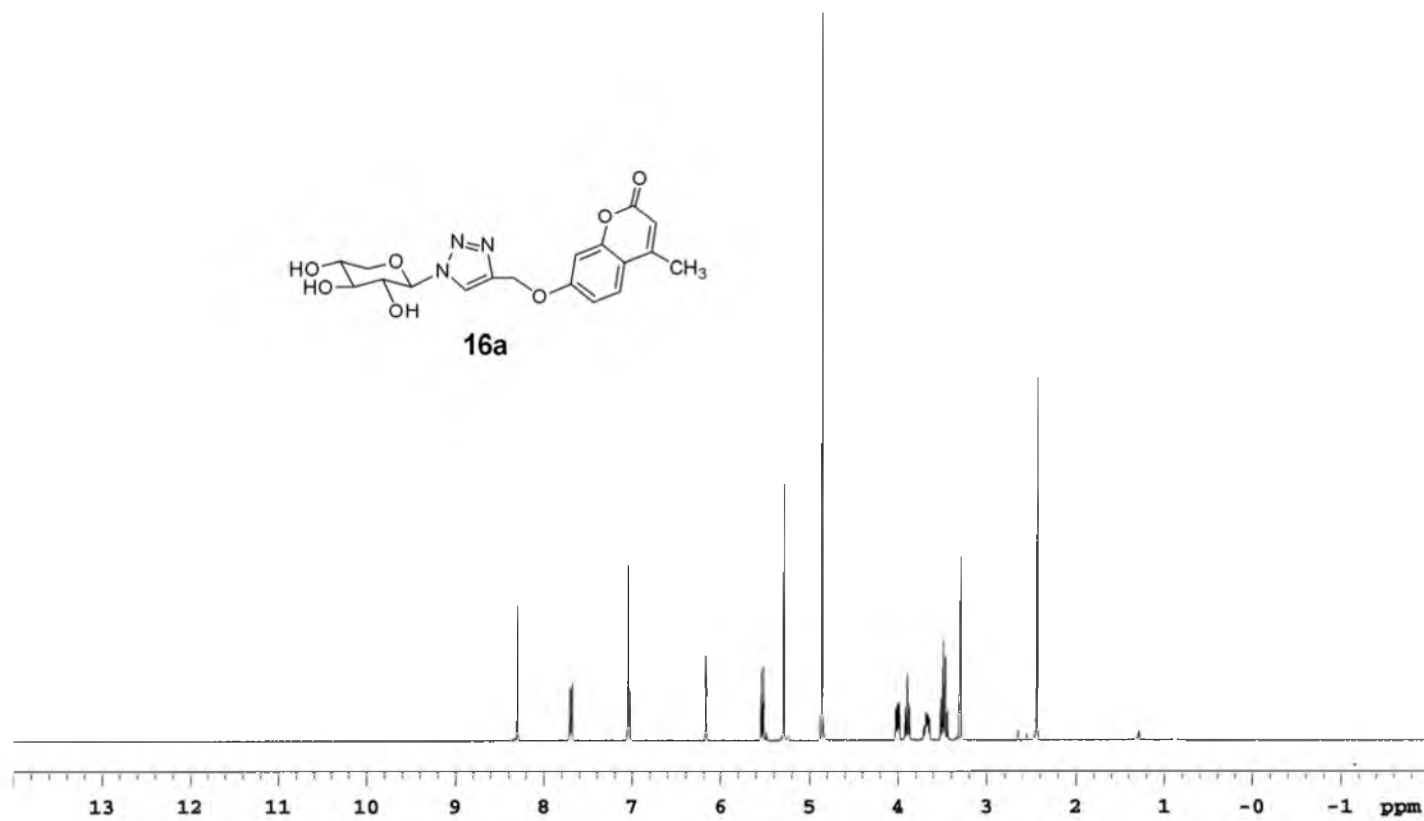


Figure S3.8. NMR spectra of fluorescent xyloside 16a

VT-IB-32pdt_101109111219 #466-479 RT: 8.08-8.31 AV: 14 NL: 2.26E5
T: + p ESI Full ms [150.00-1000.00]

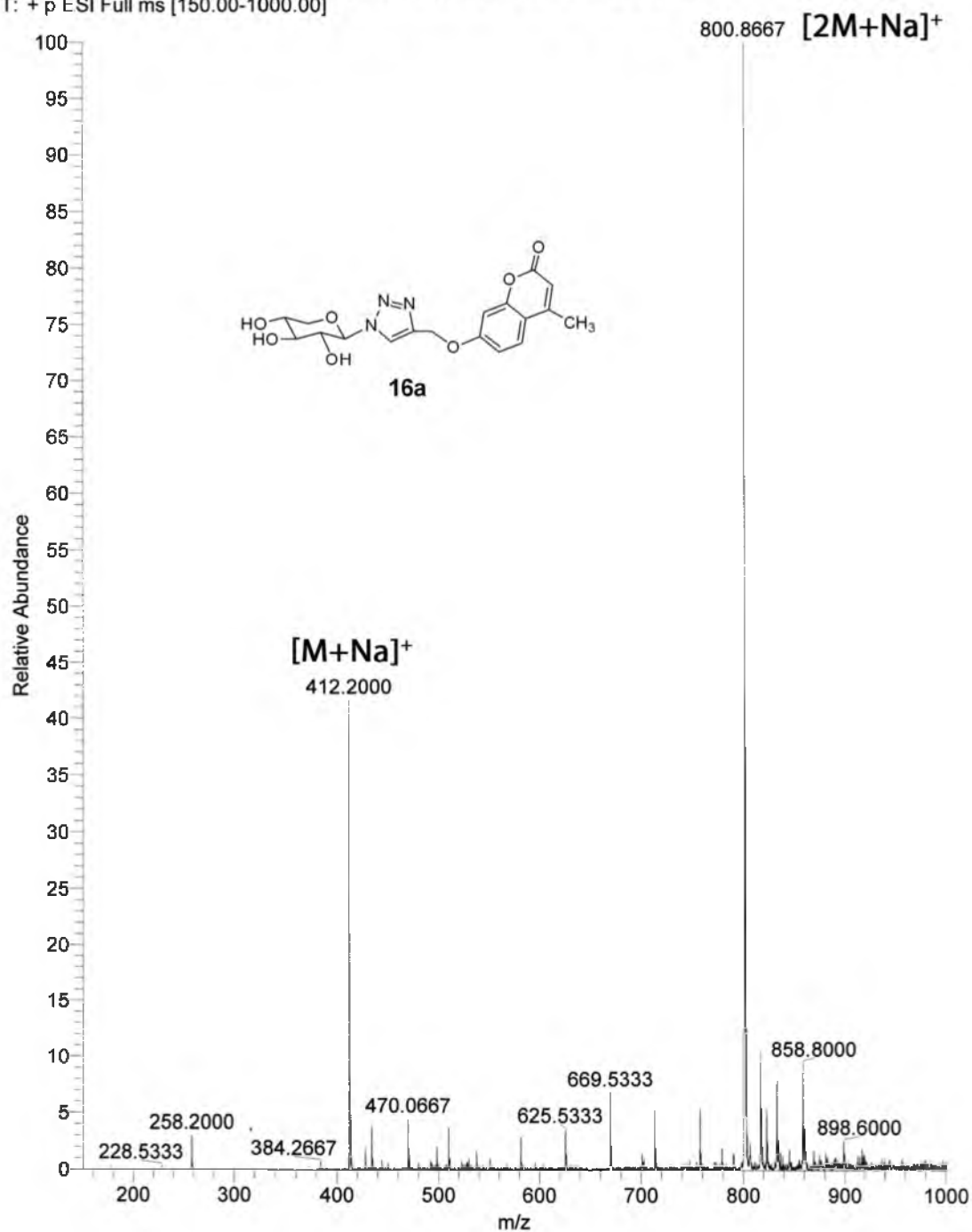


Figure S3.9. Mass spectra of fluorescent xyloside 16a

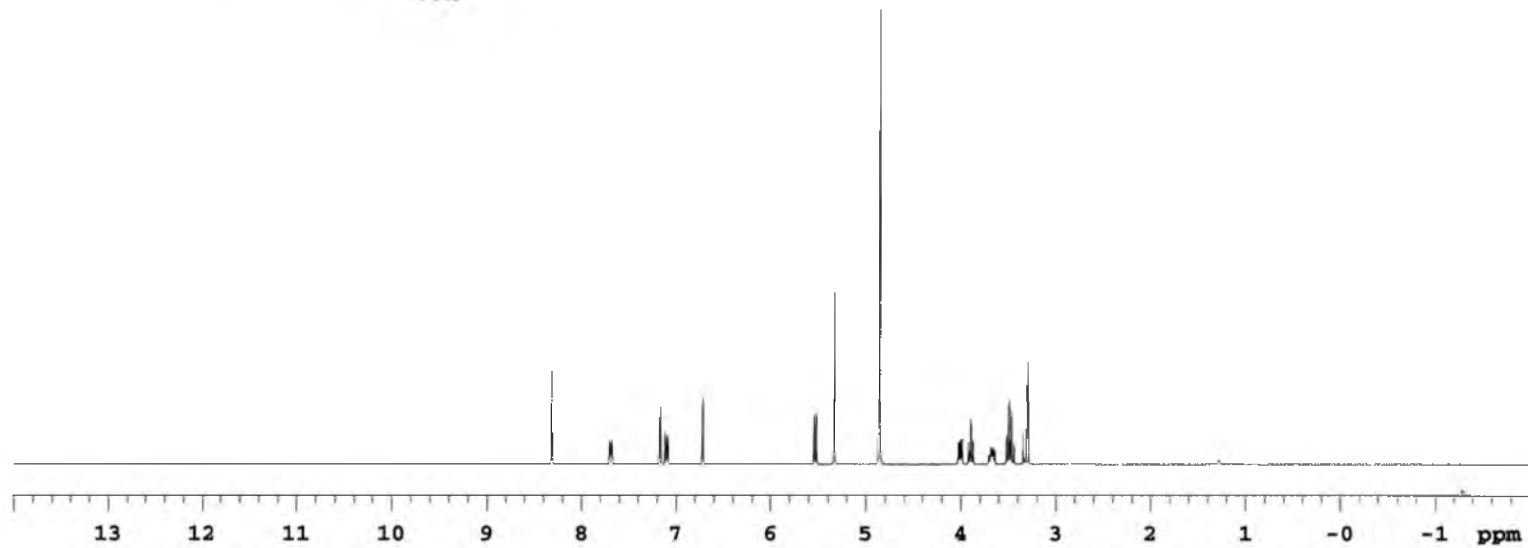
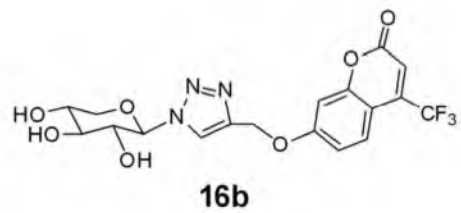


Figure S3.10. NMR spectra of fluorescent xyloside 16b

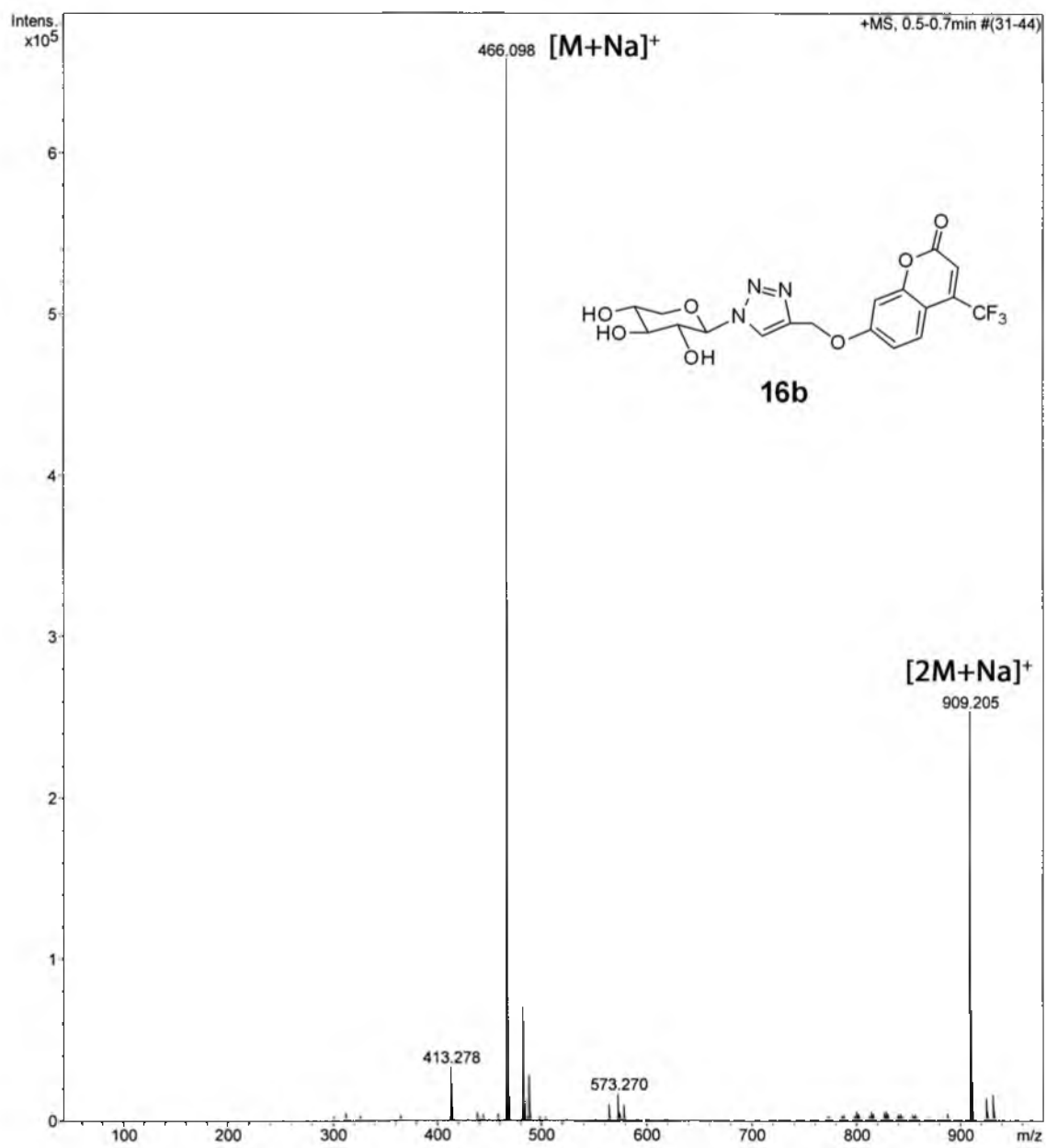


Figure S3.11. Mass spectra of fluorescent xyloside 16b

3.6. References

1. Dhoot, G. K., Gustafsson, M. K., Ai, X., Sun, W., Standiford, D. M., and Emerson, C. P., Jr. (2001) Regulation of Wnt signaling and embryo patterning by an extracellular sulfatase, *Science* 293, 1663-1666.
2. Hacker, U., Nybakken, K., and Perrimon, N. (2005) Heparan sulphate proteoglycans: the sweet side of development, *Nat Rev Mol Cell Biol* 6, 530-541.
3. Hwang, H. Y., Olson, S. K., Esko, J. D., and Horvitz, H. R. (2003) *Caenorhabditis elegans* early embryogenesis and vulval morphogenesis require chondroitin biosynthesis, *Nature* 423, 439-443.
4. Lin, X. (2004) Functions of heparan sulfate proteoglycans in cell signaling during development, *Development* 131, 6009-6021.
5. Mizuguchi, S., Uyama, T., Kitagawa, H., Nomura, K. H., Dejima, K., Gengyo-Ando, K., Mitani, S., Sugahara, K., and Nomura, K. (2003) Chondroitin proteoglycans are involved in cell division of *Caenorhabditis elegans*, *Nature* 423, 443-448.
6. Perrimon, N., and Bernfield, M. (2000) Specificities of heparan sulphate proteoglycans in developmental processes, *Nature* 404, 725-728.
7. Perrimon, N., and Hacker, U. (2004) Wingless, hedgehog and heparan sulfate proteoglycans, *Development* 131, 2509-2511; author reply 2511-2503.
8. Casu, B., Guerrini, M., Naggi, A., Perez, M., Torri, G., Ribatti, D., Carminati, P., Giannini, G., Penco, S., Pisano, C., Belleri, M., Rusnati, M., and Presta, M. (2002) Short heparin sequences spaced by glycol-split uronate residues are antagonists of fibroblast growth factor 2 and angiogenesis inhibitors, *Biochemistry* 41, 10519-10528.
9. Iozzo, R. V. (2005) Basement membrane proteoglycans: from cellar to ceiling, *Nat Rev Mol Cell Biol* 6, 646-656.
10. Iozzo, R. V., and San Antonio, J. D. (2001) Heparan sulfate proteoglycans: heavy hitters in the angiogenesis arena, *J Clin Invest* 108, 349-355.
11. Vlodavsky, I., Friedmann, Y., Elkin, M., Aingorn, H., Atzmon, R., Ishai-Michaeli, R., Bitan, M., Pappo, O., Peretz, T., Michal, I., Spector, L., and Pecker, I. (1999) Mammalian heparanase: gene cloning, expression and function in tumor progression and metastasis, *Nat Med* 5, 793-802.
12. Vlodavsky, I., Goldshmidt, O., Zcharia, E., Atzmon, R., Rangini-Guatta, Z., Elkin, M., Peretz, T., and Friedmann, Y. (2002) Mammalian heparanase:

- involvement in cancer metastasis, angiogenesis and normal development, *Semin Cancer Biol* 12, 121-129.
13. Benowitz, L. I., Goldberg, D. E., and Irwin, N. (2002) Inosine stimulates axon growth *in vitro* and in the adult CNS, *Prog Brain Res* 137, 389-399.
 14. Casu, B., Guerrini, M., and Torri, G. (2004) Structural and conformational aspects of the anticoagulant and anti-thrombotic activity of heparin and dermatan sulfate, *Curr Pharm Des* 10, 939-949.
 15. Fareed, J., Hoppensteadt, D. A., and Bick, R. L. (2000) An update on heparins at the beginning of the new millennium, *Semin Thromb Hemost* 26 Suppl 1, 5-21.
 16. Petitou, M., Casu, B., and Lindahl, U. (2003) 1976-1983, a critical period in the history of heparin: the discovery of the antithrombin binding site, *Biochimie* 85, 83-89.
 17. Petitou, M., and van Boeckel, C. A. (2004) A synthetic antithrombin III binding pentasaccharide is now a drug! What comes next?, *Angew Chem Int Ed Engl* 43, 3118-3133.
 18. Shriver, Z., Sundaram, M., Venkataraman, G., Fareed, J., Linhardt, R., Biemann, K., and Sasisekharan, R. (2000) Cleavage of the antithrombin III binding site in heparin by heparinases and its implication in the generation of low molecular weight heparin, *Proc Natl Acad Sci U S A* 97, 10365-10370.
 19. Sugahara, K., Mikami, T., Uyama, T., Mizuguchi, S., Nomura, K., and Kitagawa, H. (2003) Recent advances in the structural biology of chondroitin sulfate and dermatan sulfate, *Curr Opin Struct Biol* 13, 612-620.
 20. Eswarakumar, V. P., Lax, I., and Schlessinger, J. (2005) Cellular signaling by fibroblast growth factor receptors, *Cytokine Growth Factor Rev* 16, 139-149.
 21. Fry, E. E., Lea, S. M., Jackson, T., Newman, J. W., Ellard, F. M., Blakemore, W. E., Abu-Ghazaleh, R., Samuel, A., King, A. M., and Stuart, D. I. (1999) The structure and function of a foot-and-mouth disease virus-oligosaccharide receptor complex, *EMBO J* 18, 543-554.
 22. Ganesh, V. K., Smith, S. A., Kotwal, G. J., and Murthy, K. H. (2004) Structure of vaccinia complement protein in complex with heparin and potential implications for complement regulation, *Proc Natl Acad Sci U S A* 101, 8924-8929.
 23. Liu, J., Shriver, Z., Pope, R. M., Thorp, S. C., Duncan, M. B., Copeland, R. J., Raska, C. S., Yoshida, K., Eisenberg, R. J., Cohen, G., Linhardt, R. J., and Sasisekharan, R. (2002) Characterization of a heparan sulfate octasaccharide that

- binds to herpes simplex virus type 1 glycoprotein D, *J Biol Chem* 277, 33456-33467.
24. Mardberg, K., Trybala, E., Tufaro, F., and Bergstrom, T. (2002) Herpes simplex virus type 1 glycoprotein C is necessary for efficient infection of chondroitin sulfate-expressing gro2C cells, *J Gen Virol* 83, 291-300.
 25. Shukla, D., Liu, J., Blaiklock, P., Shworak, N. W., Bai, X., Esko, J. D., Cohen, G. H., Eisenberg, R. J., Rosenberg, R. D., and Spear, P. G. (1999) A novel role for 3-O-sulfated heparan sulfate in herpes simplex virus 1 entry, *Cell* 99, 13-22.
 26. Sasisekharan, R., Raman, R., and Prabhakar, V. (2006) Glycomics approach to structure-function relationships of glycosaminoglycans, *Annu Rev Biomed Eng* 8, 181-231.
 27. Okayama, M., Kimata, K., and Suzuki, S. (1973) The influence of p-nitrophenyl beta-d-xyloside on the synthesis of proteochondroitin sulfate by slices of embryonic chick cartilage, *J Biochem* 74, 1069-1073.
 28. Robinson, H. C., Brett, M. J., Tralaggan, P. J., Lowther, D. A., and Okayama, M. (1975) The effect of D-xylose, beta-D-xylosides and beta-D-galactosides on chondroitin sulphate biosynthesis in embryonic chicken cartilage, *Biochem J* 148, 25-34.
 29. Fukunaga, Y., Sobue, M., Suzuki, N., Kushida, H., and Suzuki, S. (1975) Synthesis of a fluorogenic mucopolysaccharide by chondrocytes in cell culture with 4-methylumbelliferyl beta-D-xyloside, *Biochim Biophys Acta* 381, 443-447.
 30. Lugemwa, F. N., and Esko, J. D. (1991) Estradiol beta-D-xyloside, an efficient primer for heparan sulfate biosynthesis, *J Biol Chem* 266, 6674-6677.
 31. Fritz, T. A., Lugemwa, F. N., Sarkar, A. K., and Esko, J. D. (1994) Biosynthesis of heparan sulfate on beta-D-xylosides depends on aglycone structure, *J Biol Chem* 269, 300-307.
 32. Sarkar, A. K., Fritz, T. A., Taylor, W. H., and Esko, J. D. (1995) Disaccharide uptake and priming in animal cells: inhibition of sialyl Lewis X by acetylated Gal beta 1-->4GlcNAc beta-O-naphthalenemethanol, *Proc Natl Acad Sci U S A* 92, 3323-3327.
 33. Mani, K., Belting, M., Ellervik, U., Falk, N., Svensson, G., Sandgren, S., Cheng, F., and Fransson, L. A. (2004) Tumor attenuation by 2(6-hydroxynaphthyl)-beta-D-xylopyranoside requires priming of heparan sulfate and nuclear targeting of the products, *Glycobiology* 14, 387-397.

34. Jacobsson, M., Ellervik, U., Belting, M., and Mani, K. (2006) Selective antiproliferative activity of hydroxynaphthyl-beta-D-xylosides, *J Med Chem* 49, 1932-1938.
35. Malmberg, J., Mani, K., Sawen, E., Wiren, A., and Ellervik, U. (2006) Synthesis of aromatic C-xylosides by position inversion of glucose, *Bioorg Med Chem* 14, 6659-6665.
36. Jacobsson, M., Mani, K., and Ellervik, U. (2007) Effects of oxygen-sulfur substitution on glycosaminoglycan-priming naphthoxylosides, *Bioorg Med Chem* 15, 5283-5299.
37. Salimath, P. V., Spiro, R. C., and Freeze, H. H. (1995) Identification of a novel glycosaminoglycan core-like molecule. II. Alpha-GalNAc-capped xylosides can be made by many cell types, *J Biol Chem* 270, 9164-9168.
38. Freeze, H. H., Sampath, D., and Varki, A. (1993) Alpha- and beta-xylosides alter glycolipid synthesis in human melanoma and Chinese hamster ovary cells, *J Biol Chem* 268, 1618-1627.
39. Shibata, S., Takagaki, K., Ishido, K., Konn, M., Sasaki, M., and Endo, M. (2003) HNK-1-Reactive oligosaccharide, sulfate-O-3GlcAbeta1-4Xylbeta1-MU, synthesized by cultured human colorectal cancer cells, *Tohoku J Exp Med* 199, 13-23.
40. Johnsson, R., Mani, K., and Ellervik, U. (2007) Evaluation of fluorescently labeled xylopyranosides as probes for proteoglycan biosynthesis, *Bioorg Med Chem Lett* 17, 2338-2341.
41. Aich, U., and Loganathan, D. (2005) Synthesis of N-(beta-Glycopyranosyl)azidoacetamides, *Journal of Carbohydrate Chemistry* 24, 1-12.
42. INAZU, T., and KOBAYASHI, K. (1993) A New Simple Method for the Synthesis of Nalpha-Fmoc-Nbeta- Glycosylated L-Asparagine Derivatives, *Synlett* 1993, 869-870.
43. Deng, W. P., Nam, G., Fan, J., and Kirk, K. L. (2003) Syntheses of beta,beta-difluorotryptamines, *J Org Chem* 68, 2798-2802.
44. Kolb, H. C., Finn, M. G., and Sharpless, K. B. (2001) Click Chemistry: Diverse Chemical Function from a Few Good Reactions, *Angew Chem Int Ed Engl* 40, 2004-2021.
45. Takagaki, K., Nakamura, T., Shibata, S., Higuchi, T., and Endo, M. (1996) Characterization and biological significance of sialyl alpha 2-3galactosyl beta 1-

4xylosyl beta 1-(4-methylumbelliferone) synthesized in cultured human skin fibroblasts, *J Biochem* 119, 697-702.

46. Esko, J. D., Stewart, T. E., and Taylor, W. H. (1985) Animal cell mutants defective in glycosaminoglycan biosynthesis, *Proc Natl Acad Sci U S A* 82, 3197-3201.

CHAPTER 4

RGD-XYLOSIDE CONJUGATES PRIME GLYCOSAMINOGLYCANS

Reprinted with permission from Springer

Tran VM, Victor XV, Yockman JW, Kuberan B. (2010) RGD-xyloside conjugates
prime glycosaminoglycans, *Glycoconj J.* 27, 625-633

RGD-xyloside conjugates prime glycosaminoglycans

Vy M. Tran · Xylophone V. Victor ·
 James W. Yockman · Balagurunathan Kuberan

Received: 25 May 2010 / Revised: 28 July 2010 / Accepted: 5 August 2010 / Published online: 18 August 2010
 © Springer Science+Business Media, LLC 2010

Abstract Glycosaminoglycans (GAG) play decisive roles in various cardio-vascular & cancer-associated processes. Changes in the expression of GAG fine structures, attributed to deregulation of their biosynthetic and catabolic enzymes, are hallmarks of vascular dysfunction and tumor progression. The wide spread role of GAG chains in blood clotting, wound healing and tumor biology has led to the development of modified GAG chains, GAG binding peptides and GAG based enzyme inhibitors as therapeutic agents. Xylosides, carrying hydrophobic aglycone, are known to induce GAG biosynthesis in various systems. Given the important roles of GAG chains in vascular and tumor biology, we envision that RGD-conjugated xylosides could be targeted to activated endothelial and cancer cells, which are known to express $\alpha_v\beta_3$ integrin, and thereby modulate the pathological processes. To accomplish this vision, xylose residue was conjugated to linear and cyclic

RGD containing peptides using click chemistry. Our results demonstrate that RGD-conjugated xylosides are able to prime GAG chains in various cell types, and future studies are aimed toward evaluating potential utility of such xylosides in treating myocardial infarction as well as cancer-associated thrombotic complications.

Keywords Proteoglycans · Glycosaminoglycans · Xylosides · RGD targeting · Biosynthesis · Heparan sulfate · Tumor · Cardiovascular · Chondroitin sulfate

Abbreviations

GAG	chains-Glycosaminoglycans
RGD	Arginine-Glycine-Aspartate
HS	Heparan Sulfate
CS	Chondroitin Sulfate
DS	Dermatan Sulfate
BLMVEC	Bovine Lung Endothelial vascular Cell
4T1	Mouse Breast Cancer Cell

V. M. Tran · B. Kuberan
 Department of Bioengineering,
 University of Utah,
 Salt Lake City, UT 84112, USA

X. V. Victor · B. Kuberan (✉)
 Department of Medicinal Chemistry,
 University of Utah,
 Skaggs Hall Rm#307, 30 South 2000 East,
 Salt Lake City, UT 84112, USA
 e-mail: KUBY@pharm.utah.edu

J. W. Yockman
 Department of Pharmaceutics & Pharmaceutical Chemistry,
 University of Utah,
 Salt Lake City, UT 84112, USA

B. Kuberan
 Graduate Program in Neuroscience,
 University of Utah,
 Salt Lake City, UT 84112, USA

Introduction

Proteoglycans (PG) consist of a core protein and one or more GAG chains. There are four major classes of sulfated GAG chains: heparan sulfate (HS), chondroitin sulfate (CS), dermatan sulfate (DS) and keratan sulfate. GAG side chains of PGs play an important role in various cardiovascular functions including haemostasis and thrombosis [1]. HS chains that contain a specific pentasaccharide sequence function as an endogenous anticoagulant through inhibition of factor Xa by activating anti-thrombin III (ATIII) [2–4]. One of the main causes of myocardial infarction (MI), a devastating disease that kills several million people world-

wide annually, is the formation of thrombi inside the coronary artery through platelet activation/aggregation. GAG side chains also play a major role in various cancer processes. Dramatic changes in the expression of biosynthetic and catabolic enzymes are attributed to alterations in GAG fine structures, which are suggested to affect tumor cell growth, invasion and metastasis [5, 6]. For example, heparanase, a β -endoglucuronidase which is over expressed in a variety of malignant tumors, cleaves HS chains into smaller biologically active oligosaccharides that promote cancer growth, angiogenesis, tumor-cell invasion and migration [7–9]. Melanoma associated CS and DS chains have been shown to stimulate tumor cell proliferation [10], while these GAG chains have been shown to surprisingly suppress angiogenesis [11].

Heparin, structurally similar to HS, has been in use as a major anticoagulant for seven decades because of its abundance, cost and potency. It is used as a blood thinner in surgical procedures and in tackling thrombotic complications associated with various cardiovascular and cerebrovascular dysfunctions. Heparin is also known to affect tumor biology in a variety of ways [11–13]. It decreases thrombin generation and fibrin formation, inhibits heparanase, modulates P-selectin-vascular wall interactions and adhesion. A chemically modified non-anticoagulant heparin-like molecule is shown to reduce metastasis by more than 50% [11]. In various clinical trials, low molecular weight heparin is shown to increase survival rate among patients with advanced malignancy.

Several animal derived GAGs and their derivatives have been in use as therapeutics to tackle thrombosis, MI and cancer. However, direct administration of these GAG chains faces the problem of molecular heterogeneity, possible contamination with pathogens or intentional chemical adulteration as evidenced in the latest tragic episode of heparin contamination [14, 15]. Furthermore, it is administered intravenously, which makes it less attractive for those who require prolonged prophylactic treatment. An alternative approach would be the use of xylosides to induce endogenous GAG chain biosynthesis without a core protein at specific sites. Xylosides containing a hydrophobic aglycone can compete with endogenous core protein acceptor sites for assembly of GAG chains in the Golgi apparatus [16–22]. The hydrophobic aglycone helps xylosides pass through the membrane and hence increases priming activity/production of GAG chains and its oral bioavailability. Interestingly, the composition of primed GAG chains depends on the structure of the aglycone moiety [23–25].

Arginine-glycine-aspartate (RGD) selectively binds to $\alpha_v\beta_3$ integrin, which is abundantly expressed on the surface of many tumor cell types and activated endothelial cells surrounding cancer and myocardial infarction. Linear and

cyclic peptide sequences containing RGD motifs have been employed as targeting vectors for selective delivery of therapeutic and diagnostic agents by conjugating them to RGD sequences [26–30]. Moreover, RGD derivatives are also shown to interact selectively with the GPIIb/IIIa receptor and therefore inhibit platelet aggregation [31]. Therefore, RGD-conjugated xylosides are predicted to have a dual use as anticoagulants as well as anti-platelet agents in tackling thrombotic complications associated with MI, cancer and other disease conditions. Here, we describe the synthesis of RGD-conjugated xylosides using click-chemistry and report on their GAG priming activity in a variety of cellular systems.

Experimental section

Materials

Chinese hamster ovary (CHO) cell line, pgsA-745, which is defective in xylosyl transferase, was obtained from American Type Culture Collection. The cell culture reagents for CHO cell line were obtained from HyClone. Bovine lung microvascular endothelial cell (BLMVEC) and Mouse breast cancer cells (4T1) were gifts from Dr Randall Dull and Dr David Bull, University of Utah, respectively. The cell culture reagents for BLMVEC and 4T1 (MCDB-131 complete) were obtained from Vec Technologies. $\text{Na}_2^{35}\text{SO}_4$ was purchased from MP Biochemicals and Ultima-FloAP scintillation cocktail for flow scintillation analysis was obtained from PerkinElmer Life Sciences. All other chemicals and biochemicals were obtained from Sigma. Linear RGD peptide **4** was synthesized using peptide synthesizer available through core facilities at the University of Utah, and cyclic RGD peptide **7** was purchased from Peptides International Inc. The DEAE-Sepharose gel was purchased from Amersham Biosciences. The anion-exchange chromatography column TSK-GEL DEAE-3SW (7.4 mm \times 7.5 cm, 10 μm particle size) and the size exclusion chromatography columns G3000SWXL (7.8 mm \times 30 cm) were obtained from Tosoh Bioscience.

General synthetic procedures

Anhydrous solvents were purchased and used directly or dried over standard drying agents and freshly distilled prior to use. Reactions were monitored by TLC on silica gel 60 F₂₅₄ with detection by Von's reagent. Intermediate compounds were purified by flash chromatography columns using silica gel 60 (230–400 mesh) and were run under pressure at 5–7 psi. Final products were purified by high performance liquid chromatography (HPLC) on reverse

phase C18 column (VYDAC 2.2 cm×25 cm) with solvent A (25 mM formic acid in water) and solvent B (95% acetonitrile) at a flow rate of 5 ml/min in a linear gradient over 120 min starting with 0% B. All synthetic compounds were characterized by mercury 400 MHz spectrometry. The compounds were also confirmed for their final structures using a Finnigan LCQ mass spectrometry in either positive or negative ion mode.

2,3,4-Tri-*O*-Acetyl- β -*D*-xylopyranosyl azide (1): Trimethylsilyl azide (1.5 mmol) and SnCl₄ (0.5 mmol) were added dropwise to a stirred solution of fully acetylated xylose derivative (1 mmol) in dry CH₂Cl₂, and stirring was continued at room temperature. The progress of the reaction was checked by TLC, and after the completion of the reaction, the reaction mixture was then evaporated under vacuum to give a residue that was further purified by low pressure flash silica column chromatography to yield the compound **1** [32].

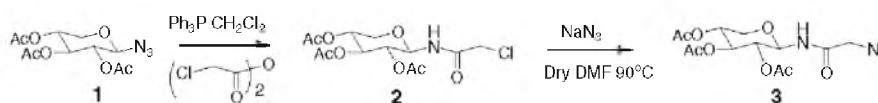
***N*-(2,3,4-tri-*O*-acetyl- β -*D*-xylopyranosyl) chloroacetamide (2):** 2,3,4-Tri-*O*-Acetyl- β -*D*-xylopyranosyl azide (**1**) (1 mmol) was dissolved in dry CH₂Cl₂ (20 ml). The mixture was cooled at 0°C. Chloroacetic anhydride (1 mmol) was added to the solution, followed by triphenyl phosphine (1 mmol), and the reaction was continued overnight. After the reaction was complete, the solvent was removed using rotary evaporator under reduced pressure. The reaction mixture was extracted using ethyl acetate and water. The organic layer was washed with saturated brine solution and evaporated under vacuum to give a residue, which was purified by silica column chromatography to give the title compound **2** [33].

***N*-(2,3,4-tri-*O*-acetyl- β -xylopyranosyl) azidoacetamide (3):** *N*-(2,3,4-tri-*O*-acetyl- β -*D*-xylopyranosyl) chloroacetamide (**2**) (1 mmol) was taken in a 100 ml RB flask and dry DMF (20 ml) was added, followed by the addition of sodium azide (2 mmol). The reaction mixture was heated to 90°C under stirring. Progress of the reaction was monitored by TLC using ethyl acetate and hexane (1:1) as the eluant. After the reaction was complete, the reaction mixture was cooled and diluted with ethyl acetate. The organic layer was washed with water, dried over sodium sulfate and concentrated to obtain a syrupy materials that was further purified by silica flash column chromatography to give the title compound **3** [34].

Propargylated cyclic RGD (8): Propionic acid (10 mmol) was taken in a RB flask and dry DMF (20 ml) was added,

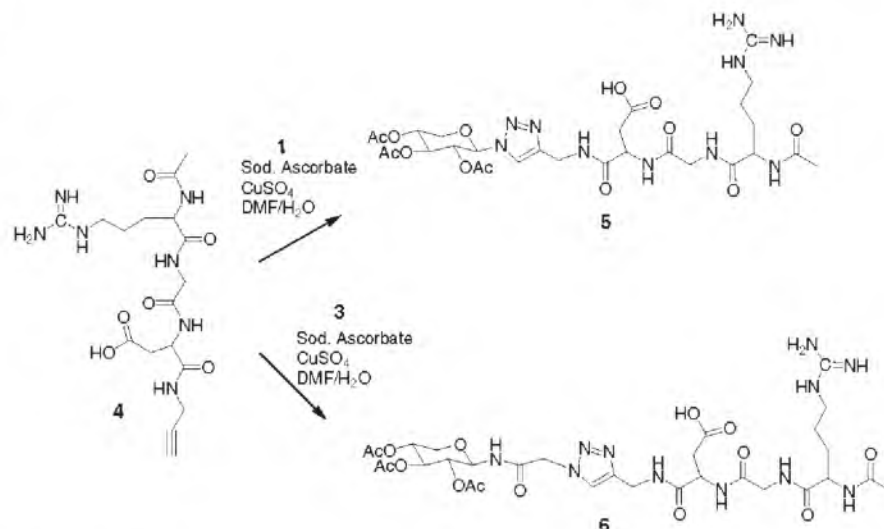
followed by addition of hydroxybenzotriazole (5 mmol) and 1, 3-dispropylcarbodiimide (5 mmol). The reaction mixture was stirred for 1 h before cyclic RGD (1 mmol) was added, and stirred for another hour. The reaction mixture was evaporated using a rotary evaporator under reduced pressure. The reaction mixture was purified by HPLC—reverse phase C18 column with solvent A (25 mM formic acid in water) and solvent B (95% acetonitrile) in a linear gradient starting with 0% B to give the pure compound **8**.

Preparation of RGD-conjugated xylosides (5, 6 and 9): To a solution of alkyne group containing linear or cyclic RGD derivative (1 mmol) and xylosyl azide derivative (1 mmol) in DMF (8 ml) / water (2.6 ml) mixture, sodium ascorbate (0.8 mmol) was added, followed by Cu₂SO₄·5 H₂O (0.4 mmol) at room temperature and the mixture was stirred until the disappearance of the starting materials as indicated by TLC. At the end of the reaction, the reaction mixture was concentrated using the rotary evaporator under reduced pressure. The reaction mixture was purified by HPLC—reverse phase C18 column with solvent A (25 mM formic acid in water) and solvent B (95% acetonitrile) to give the final compounds, **5**, **6** & **9**. Compound **5**: ¹H NMR (CD₃OD): δ 8.07 (s, 1H), 5.97 (d, J=8.98 Hz, 1H), 5.55–5.44 (m, 2H), 5.20–5.14 (m, 1H), 4.58 (t, J=4.68 Hz, 1H), 4.46 (dd, J=15.62 Hz, 24.80 Hz, 2H), 4.41–4.36 (m, 1H), 4.22 (dd, J=5.47 Hz, 11.33 Hz, 1H), 4.02 (d, J=17.18 Hz, 1H), 3.74 (t, J=10.54 Hz, 1H), 3.72 (d, J=16.79 Hz, 1H), 3.26–3.20 (m, 1H), 3.12–3.05 (m, 1H), 2.92 (dd, J=4.3 Hz, 16.60 Hz, 1H), 2.53 (dd, J=5.08 Hz, 16.40 Hz, 1H), 2.04 (s, 3H), 2.01 (s, 3H), 2.00 (s, 3H), 1.82 (s, 3H), 1.70–1.64 (m, 2H); MS (ESI): calcd for C₂₈H₄₃N₁₀O₁₃ [M+H]⁺ 727.2932; found 727.3333. Compound **6**: ¹H NMR (CD₃OD): δ 7.86 (s, 1H), 5.28 (t, J=9.37 Hz, 1H), 5.20 (d, J=8.98 Hz, 1H), 5.12 (d, J=1.95 Hz, 1H), 4.58–4.57 (m, 1H), 4.53 (s, 1H), 4.44 (s, 1H), 4.40–4.35 (m, 1H), 4.06–4.02 (m, 1H), 3.98 (s, 1H), 3.72 (d, J=16.79 Hz, 1H), 3.48 (t, J=11.13 Hz, 1H), 3.25–3.22 (m, 1H), 3.13–3.08 (m, 1H), 2.92 (dd, J=4.3 Hz, 16.4 Hz, 1H), 2.50 (dd, J=4.69 Hz, 16.60 Hz, 1H), 2.06–1.96 (m, 12 H), 1.68–1.63 (m, 2H); MS (ESI): calcd for C₃₀H₄₆N₁₁O₁₄ [M+H]⁺ 784.3226; found 784.3400. Compound **9**: ¹H NMR (CD₃OD): δ 8.65 (s, 1H), 8.60 (s, 1H), 8.34 (s, 1H), 7.86 (d, J=6.64 Hz, 1H), 7.54 (t, J=7.81 Hz, 1H), 7.25–7.16 (m, 3H), 6.09 (d, J=8.98 Hz, 1H), 5.62–5.56 (m, 1H), 5.50 (t, J=8.98 Hz, 1H), 5.24–5.18 (m, 1H), 4.66 (t, J=5.08 Hz, 1H), 4.54 (t, J=6.64 Hz, 1H), 4.41 (t, J=6.64 Hz, 1H), 4.30–4.24



Scheme 1 Synthesis of *N*-(2,3,4-tri-*O*-acetyl- β -xylopyranosyl) azidoacetamide: Ph₃P, triphenyl phosphine; CH₂Cl₂, dichloromethane; NaN₃, sodium azide; DMF, *N*, *N*-dimethylformamide

Scheme 2 Synthesis of linear RGD-conjugated xyloides using click chemistry: Sod. Ascorbate, sodium ascorbate; Cu_2SO_4 , copper (II) sulfate; DMF, *N,N*-dimethylformamide; H_2O , Deionized water

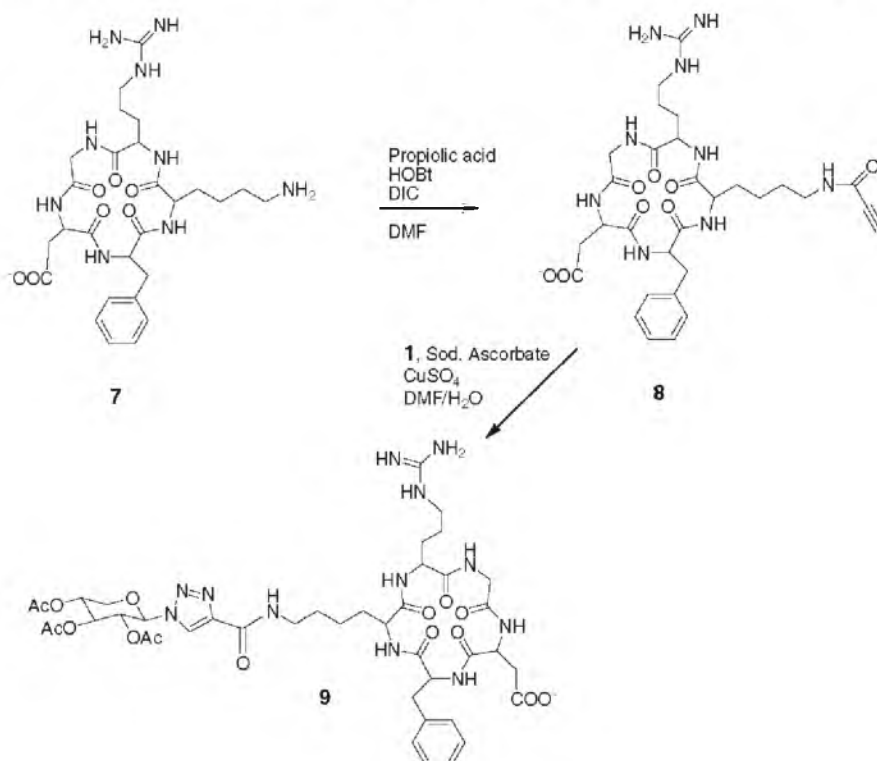


(m, 2H), 4.07–3.90 (m, 3H), 3.80–3.68 (m, 3H), 3.55–3.47 (m, 2H), 3.25–3.12 (m, 2H), 3.03 (t, $J=13.58$ Hz, 1H), 2.93 (dd, $J=6.65$ Hz, 13.28 Hz, 1H), 2.69–2.59 (m, 2H), 2.04 (s, 3H), 2.02 (s, 3H), 1.83 (s, 3H), 1.76–1.67 (m, 2H), 1.58–1.51 (m, 3H), 1.44–1.28 (m, 3H), 1.16–1.01 (m, 2H); MS (ESI): calcd for $\text{C}_{41}\text{H}_{57}\text{N}_{12}\text{O}_{15}$ [$\text{M}+\text{H}$] $^+$ 957.3988; found 957.2667.

Screening of RGD-xyloides in CHO cells, endothelial cells (BLMEC) and cancer cells (4T1): To determine

whether the RGD-xyloides were able to prime GAG chains, the cells were treated with RGD-conjugated xyloides at various concentrations in the presence of $\text{Na}_2^{35}\text{SO}_4$. GAG chains were purified and analyzed as described below. 1×10^5 cells were plated per well in complete growth medium in a 24 well plate. The cells were incubated at 37°C in a humidified incubator for 24 h to a confluence of about 50%. The cells were washed with sterile PBS and replaced with

Scheme 3 Synthesis of cyclic RGD conjugated xyloide: HOBt, *N*-Hydroxybenzotriazole; DIC, 1,3-Diisopropylcarbodiimide; DMF, *N,N*-dimethylformamide; Sod. Ascorbate, sodium ascorbate; Cu_2SO_4 , copper (II) sulfate; H_2O , Deionized water



495 μL Ham's/F12 containing 10% dialyzed FBS. A solution containing a specific primer at 100X the final concentration was prepared. 5 μL of appropriate 100X primer was added to various wells to yield the appropriate concentration and 50 μCi of $\text{Na}_2^{35}\text{SO}_4$ was also added to each well as tracer. The 24-well plates were incubated at 37°C in a humidified incubator (5% CO_2) for 24 h.

Purification and quantitation of GAG chains: The entire contents of the wells were transferred to a microcentrifuge tube and subjected to centrifugation at 16000 \times g for 5 min. The supernatant was transferred to a fresh tube and 0.016% Triton X-100 (1.5 volumes) was added. The diluted supernatant was loaded on a 0.2 ml DEAE-sepharose column pre-equilibrated with 2 ml of wash buffer (20 mM NaOAc, 0.1 M NaCl and 0.01% Triton X-100, pH 6.0) and the column was washed with 6 ml of wash buffer. The bound HS/CS was eluted using 1.2 ml of elution buffer (20 mM NaOAc and 1 M NaCl, pH 6.0). The priming activities of xylosides 5, 6 & 9 were evaluated by quantitating the ^{35}S -radioactivity incorporated in to the purified HS/CS chains by liquid scintillation counter.

Sulfate density analysis of GAG chains: The purified GAG chains were analyzed by HPLC coupled to an inline radiometric detector. Xyloside primed GAG chains of equal quantity were diluted five-fold with HPLC solvent A (10 mM KH_2PO_4 , pH 6.0, 0.2% CHAPS) for anion exchange chromatography analysis. The sample was loaded on a HPLC-DEAE column and eluted from the column with a linear gradient of 0.2 M to 1 M NaCl over 80 min at a flow rate of 1 ml/min. The radioactive GAG chains were detected by radiometric flow-one A505A detector. The HPLC effluent was mixed with Ultima-Flo AP scintillation cocktail in a 2:1 ratio and detected in the flow scintillation analyzer.

Chain length analysis of GAG chains primed by RGD-xylosides: The chain length of the GAG chains synthesized

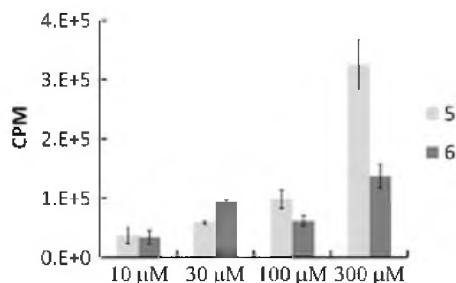


Fig. 1 Priming activity of two linear RGD-xylosides using pgs A-745 cell lines at various concentrations. CHO cells were treated with linear RGD xylosides 5 and 6 at 10, 30, 100 and 300 μM in the presence of $\text{Na}_2^{35}\text{SO}_4$ (50 μCi) as described in the experimental section. The GAG chains were purified by anion exchange chromatography and quantitated using liquid scintillation counter. The data shown is average of two independent experiments

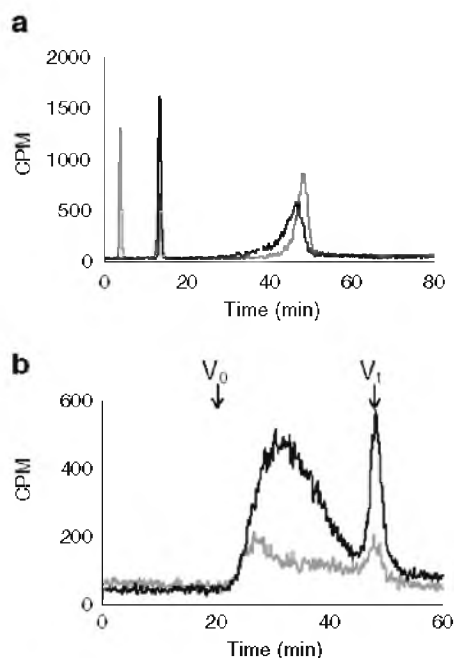


Fig. 2 a GAG chains primed by xyloside 5 in pgsA-745 cell lines were analyzed using anion exchange HPLC. The bound GAG chains were eluted with a linear gradient of 0.2 M to 1 M NaCl over 80 min at a flow rate of 1 ml/min. The elution profiles of GAG chains, primed at 100 μM (grey) and 300 μM (black), are shown. b The sizes of GAG chains primed by xyloside 5 in pgsA-745 cells were analyzed by size exclusion HPLC: the GAG chains, fractionated on two tandem 3000 $\text{SW}_{\text{L}}^{\text{X}}$ columns, were eluted with an isocratic gradient of phosphate buffer for 90 min at a flow rate of 0.5 ml/min as described in the experimental section. The elution profiles of the GAG chains primed at 100 μM (grey trace) and 300 μM (black trace) are shown. V_0 and V_t represent void and total volume, respectively. These elution profiles are representative of two independent experiments

by various RGD-xyloside conjugates was determined by measuring migration time on a size exclusion column using a HPLC with inline radiodetector. The GAG chains were loaded on to two tandem G3000 $\text{SW}_{\text{L}}^{\text{X}}$ columns (Tosoh, 7.8 mm \times 30 cm) and analyzed with the aid of an inline radiodetector using phosphate buffer (100 mM KH_2PO_4 , 100 mM NaCl, pH 6) as eluant. The average molecular weight was determined by measuring the migration time of the GAG chains in comparison to those of polystyrene sulfonate standards performed under similar conditions.

Results and discussion

Synthesis of RGD-xylosides

In recent years, there has been great interest in assembling a number of biologically active carbohydrate conjugates using click chemistry because of its mild reaction con-

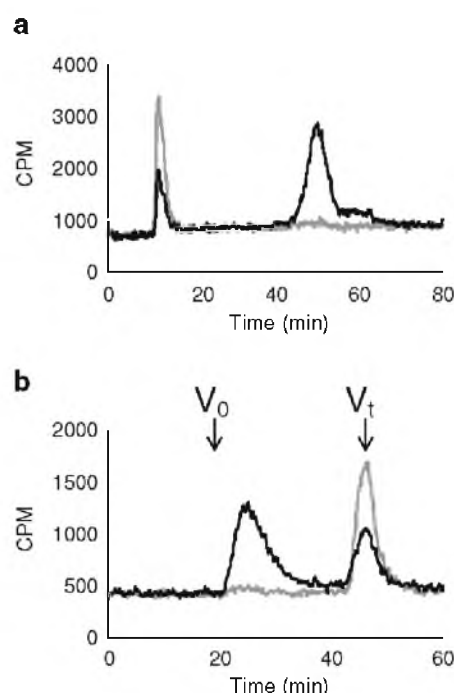


Fig. 3 a Anion exchange chromatography analysis of GAG chains produced by xyloside 9 in pgsA-745 cell lines: Purified GAG chains (grey trace for control cells and black trace for cells treated with 100 μ M xyloside 9) were analyzed using HPLC-DEAE anion exchange chromatography using a linear gradient of 0.2 M to 1 M NaCl as an eluant over 80 min at a flow rate of 1 ml/min. b Size exclusion profiles of GAG chains produced by xyloside 9 in pgsA-745 cell line: GAG chains were fractionated using two 3000 SW_L^X SEC columns that were connected in tandem using an isocratic gradient of phosphate buffer for 90 min at a flow rate of 0.5 ml/min as described in the experimental section (grey trace for control cells and black trace for cells treated with 100 μ M xyloside 9). V_0 and V_t represent void and total volume, respectively. These elution profiles are representative of two independent experiments

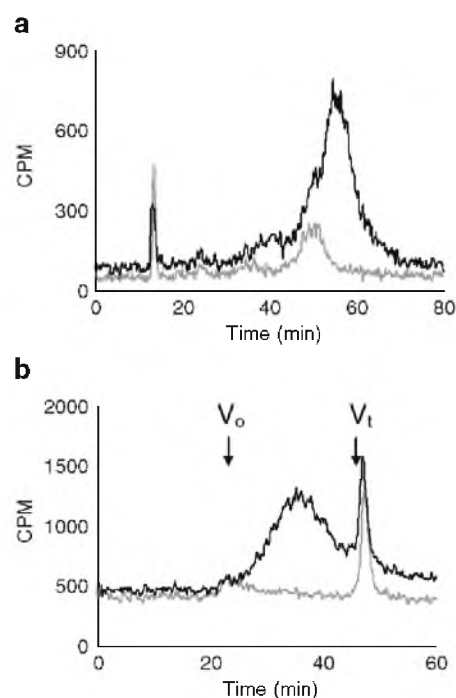


Fig. 4 a GAG chains, primed by xyloside 5 in endothelial cell line, were analyzed using anion exchange HPLC. The bound GAG chains were eluted with a linear gradient of 0.2 M to 1 M NaCl over 80 min at a flow rate of 1 ml/min. The radiodetector trace of the GAG chains isolated from control cells (grey trace) and cells treated with 100 μ M xyloside (black trace) are shown. b GAG chains, primed by xyloside 5 in endothelial cell line, were analyzed using two SEC (3000 SW_L^X) that were connected in tandem and were eluted with an isocratic gradient of phosphate buffer for 90 min at a flow rate of 0.5 ml/min as described in the experimental section. The elution profile of the GAG chains, primed by xyloside 5 at 100 μ M (black trace; control as grey trace), is shown. V_0 and V_t represent void and total volume, respectively. These elution profiles are representative of two independent experiments

ditions, the generation of regioselective molecules with high efficiency in water and compatibility with most functional groups in biological systems [35–37]. This bioconjugation approach relies on the Cu(I)-catalyzed orthogonal reaction of azide containing xylosyl scaffold with terminal alkyne containing RGD motifs in the presence of other reactive functional groups. Furthermore, this approach offers two advantages: a) the 1, 2, 3-triazole ring generated during the click-chemistry is a metabolically stable linker between xylose residue and RGD peptide; b) the triazole ring can facilitate hydrogen-bonding interactions resulting in favorable and productive biological effects.

Xylosyl azide 1 was converted into 3 by first converting the azide group into the chloroacetamide followed by the replacement of the chloride group with an azide as shown

in Scheme 1. These two xylosyl derivatives, 1 & 3, contain reactive azide group for orthogonal coupling with RGD peptides containing terminal alkyne group in the subsequent steps. RGD peptides, 4 and 7, were purchased from commercial sources. These RGD peptides were coupled with propargyl amine using well established coupling procedure. In a similar manner, cyclic RGD peptide 7 containing side chain amine group was reacted with propargylic acid under similar conditions to obtain propargylated cyclic RGD peptide 8 in high yield as shown in Scheme 3. After preparing appropriate orthogonally functionalized RGD peptides and xylosides, we turned to assembling RGD-conjugated xylosides, 5, 6 and 9, using click-chemistry as described in Schemes 2 and 3. The final products were purified on reverse phase C18 column using HPLC as described in the experimental section.

Priming activity of RGD-xylosides in CHO cells

The very first step in the biosynthesis of proteoglycans is the xylosylation of certain serine residues of the core protein [38]. Following xylosylation of the core protein, a tetrasaccharide linkage region, which serves as an acceptor site for elongation of GAG chains, is assembled [39–42]. It has been known for over three decades that GAG chains can also be assembled on xylosides without a core protein provided xylosides carry hydrophobic aglycone [20, 22]. We have synthesized various click-xylosides with hydrophobic moiety and demonstrated their ability to induce GAG chains in a cellular system [23]. A mutant Chinese hamster ovary [CHO] cell line, pgsA-745, is a convenient cellular system for determining the priming activity of exogenously supplied RGD-conjugated xylosides, because this cell line lacks active xylosyltransferase enzyme and therefore does not make endogenous GAG chains [43]. Thus, it is easier to determine whether RGD-conjugated xylosides induce GAG chains using this cell line. RGD-conjugated xylosides were screened in cell culture at various concentrations (10, 30, 100 and 300 μM). We found that the nature of linkage between xylose and RGD can affect the priming activity (Fig. 1). The results from priming activity analysis suggest that RGD-xyloside **5** is a better GAG primer than RGD-xyloside **6** at 100 μM and 300 μM . Therefore, the GAG chains primed by xyloside **5** were further analyzed for their sulfation pattern by DEAE-anion exchange HPLC column and for their molecular weights using size exclusion columns as outlined in the experimental section. It is interesting to note that the extent of sulfation of GAG chains primed by xylosides at 100 μM and 300 μM are nearly identical suggesting that these concentrations are optimal for GAG induction without challenging the Golgi machinery (Fig. 2). Nevertheless, Xyloside **5** primed nearly three times more GAG chains at 300 μM compare to 100 μM in CHO cells. The chain length of GAG chains primed by xyloside **5** in CHO cells was determined by measuring migration time of GAG chains in comparison to those of polystyrene sulfonate standards performed under similar conditions on size exclusion analyses and suggests that GAG chains, primed by xyloside **5** in CHO cells, have an average molecular weight of 45 KDa at 100 μM and 19 KDa at 300 μM concentration.

Cyclic RGD peptides are shown to bind more selectively than their linear motifs to $\alpha_v\beta_3$ integrin expressing activated endothelial cells and cancer cell lines [28, 44, 45]. Therefore, we synthesized xyloside conjugated to cyclic-RGD peptide motif (**8**) using click-chemistry (Scheme 3). It is interesting to note that xyloside **9** primed GAG chains whose average molecular weight is higher than those primed by xyloside **5** in CHO cells. Xyloside **9**

primed GAG chains migrated between 20–28 min in size exclusion column with average molecular weight of 67 KDa in comparison to those of polystyrene sulfonate standard (Fig. 3). GAG chains primed by xylosides **5** and **9** were digested with heparin lyases I, II and III to determine HS/CS composition. It is interesting to note that xyloside **5** primed about 50% HS chains, whereas Xyloside **9** primed about 25% HS chains. Xyloside **6**, on the other hand, primed about 80% HS chains even though this scaffold has lower priming activity than Xyloside **5**.

Priming activity of xylosides in endothelial cells (BLMVEC) and cancer cell line (4T1)

$\alpha_v\beta_3$ integrin receptors are elevated in activated endothelial cells, angiogenic cardiomyocytes and highly vascularized

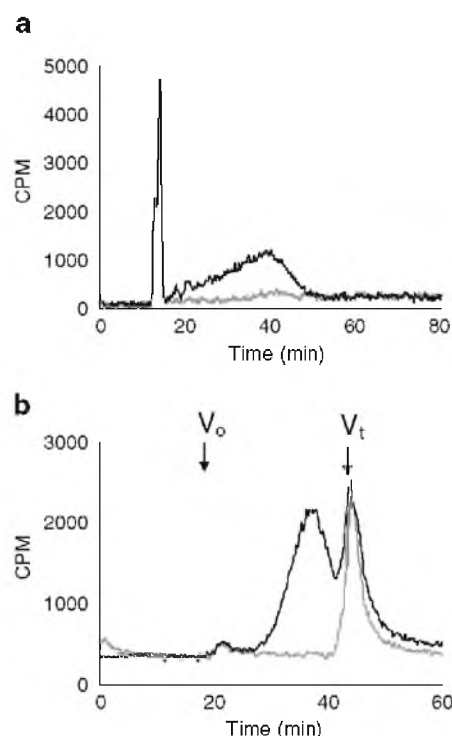


Fig. 5 **a** GAG chains primed by xyloside **5** in cancer cell line were analyzed using anion exchange HPLC. The bound GAG chains were eluted with a linear salt gradient for 80 min as described in the experimental section. The radiodetector trace of the eluted GAG chains from control cells (*grey trace*) and cells treated with 100 μM xyloside (*black trace*) are shown. **b** GAG chains primed by xyloside **5** in 4T1 cell line were analyzed using SEC column as described in the experimental section, were eluted with an isocratic gradient of phosphate buffer for 90 min at a flow rate of 0.5 ml/min. The radiodetector traces of the eluted GAG chains, primed by xyloside **5** at 100 μM (*black trace*) and control cells (*grey trace*), are shown. These elution profiles shown here are representative of two independent experiments

cancer cells, and therefore, RGD-conjugated xylosides are expected to be up taken by these cells. For these reasons, we chose to determine the priming activity of RGD-conjugated xylosides in endothelial cells (BLMVEC) and mouse breast cancer cell line (4T1). The priming activity of RGD xylosides in endothelial cells and cancer cells are determined as described earlier for CHO cells. The xyloside **5** did prime on both endothelial cells and cancer cells (Figs. 4 and 5). Xyloside **5** was able to induce GAG chains by 6-fold in endothelial cells and 3-fold in cancer cell line. Molecular weight of GAG chains primed by xyloside **5** was found to be ~10 kDa in the endothelial cell and cancer cell line. It was disappointing to note that cyclic-RGD conjugated xyloside **9** was unable to prime GAG chains in either the endothelial cells or cancer cell line. It is possible that the cyclic-RGD motif may prevent the selective transport of xyloside to the Golgi machinery, where they prime GAG chains. Alternatively, cyclic motif may sterically interfere with biosynthetic enzymes preventing the priming of GAG chains by xyloside **9**. For these reasons, we plan to make a library of cyclic-RGD motifs with variable distance between the xylose and the peptide with an aim to discover new scaffolds that prime GAG chains.

In summary, we have successfully synthesized RGD-conjugated xylosides that target cells displaying the $\alpha_v\beta_3$ integrin using click chemistry. These RGD-conjugated homing xylosides are able to prime GAG chains in various cellular systems indicating their likely applications in tackling MI, thrombosis and cancer associated vascular complications, where GAG chains are known to modulate various pathological processes. Future studies will focus on the synthesis of additional homing xylosides and evaluation of their pharmacokinetics and pharmacodynamics in various animal models.

Acknowledgment This work was supported by NIH (GM075168) and Human Frontier Science Program grants to BK.

References

- Cummings, R.D.: The repertoire of glycan determinants in the human glycome. *Mol. Biosyst.* **5**, 1087–1104 (2009)
- Damus, P.S., Hicks, M., Rosenberg, R.D.: Anticoagulant action of heparin. *Nature*. **246**, 355–357 (1973)
- Hopwood, J., Hook, M., Linker, A., Lindahl, U.: Anticoagulant activity of heparin: isolation of antithrombin-binding sites. *FEBS Lett.* **69**, 51–54 (1976)
- Kuberan, B., Lech, M.Z., Beeler, D.L., Wu, Z.L., Rosenberg, R. D.: Enzymatic synthesis of antithrombin III-binding heparan sulfate pentasaccharide. *Nat. Biotechnol.* **21**, 1343–1346 (2003)
- Sasisekharan, R., Shriver, Z., Venkataraman, G., Narayanasami, U.: Roles of heparan-sulphate glycosaminoglycans in cancer. *Nat. Rev. Cancer.* **2**, 521–528 (2002)
- Raman, K., Kuberan, B.: Chemical tumor biology of heparan sulfate proteoglycans. *Curr. Chem. Biol.* **4**, 20–31 (2010)
- Purushothaman, A., Chen, L., Yang, Y., Sanderson, R.D.: Heparanase stimulation of protease expression implicates it as a master regulator of the aggressive tumor phenotype in myeloma. *J. Biol. Chem.* **283**, 32628–32636 (2008)
- Fux, L., Ilan, N., Sanderson, R.D., Vlodavsky, I.: Heparanase: busy at the cell surface. *Trends Biochem. Sci.* **34**, 511–519 (2009)
- Vlodavsky, I., Ilan, N., Nadir, Y., Brenner, B., Katz, B.Z., Naggi, A., Torri, G., Casu, B., Sasisekharan, R.: Heparanase, heparin and the coagulation system in cancer progression. *Thromb. Res.* **120** (Suppl. 2), S112–120 (2007)
- Yang, J., Price, M.A., Neudauer, C.L., Wilson, C., Ferrone, S., Xia, H., Iida, J., Simpson, M.A., McCarthy, J.B.: Melanoma chondroitin sulfate proteoglycan enhances FAK and ERK activation by distinct mechanisms. *J. Cell Biol.* **165**, 881–891 (2004)
- Yip, G.W., Smollich, M., Gotte, M.: Therapeutic value of glycosaminoglycans in cancer. *Mol. Cancer Ther.* **5**, 2139–2148 (2006)
- Varki, N.M., Varki, A.: Heparin inhibition of selectin-mediated interactions during the hematogenous phase of carcinoma metastasis: rationale for clinical studies in humans. *Semin. Thromb. Hemost.* **28**, 53–66 (2002)
- Borsig, L., Wong, R., Feramisco, J., Nadeau, D.R., Varki, N.M., Varki, A.: Heparin and cancer revisited: mechanistic connections involving platelets, P-selectin, carcinoma mucins, and tumor metastasis. *Proc. Natl. Acad. Sci. U. S. A.* **98**, 3352–3357 (2001)
- Kishimoto, T.K., Viswanathan, K., Ganguly, T., Elankumaran, S., Smith, S., Pelzer, K., Lansing, J.C., Sriranganathan, N., Zhao, G., Galcheva-Gargova, Z., Al-Hakim, A., Bailey, G.S., Fraser, B., Roy, S., Rogers-Cotrone, T., Buhse, L., Whary, M., Fox, J., Nasr, M., Dal Pan, G.J., Shriver, Z., Langer, R.S., Venkataraman, G., Austen, K.F., Woodcock, J., Sasisekharan, R.: Contaminated heparin associated with adverse clinical events and activation of the contact system. *N. Engl. J. Med.* **358**, 2457–2467 (2008)
- Blossom, D.B., Kallen, A.J., Patel, P.R., Elward, A., Robinson, L., Gao, G., Langer, R., Perkins, K.M., Jaeger, J.L., Kurkjian, K.M., Jones, M., Schillie, S.F., Shehab, N., Ketterer, D., Venkataraman, G., Kishimoto, T.K., Shriver, Z., McMahon, A.W., Austen, K.F., Kozlowski, S., Srinivasan, A., Turabelidze, G., Gould, C.V., Arduino, M.J., Sasisekharan, R.: Outbreak of adverse reactions associated with contaminated heparin. *N. Engl. J. Med.* **359**, 2674–2684 (2008)
- Gibson, K.D., Segen, B.J., Audhya, T.K.: The effect of beta-D-xylosides on chondroitin sulphate biosynthesis in embryonic chicken cartilage in the absence of protein synthesis inhibitors. *Biochem. J.* **162**, 217–233 (1977)
- Schwartz, N.B., Ho, P.L., Dorfman, A.: Effect of beta-xylosides on synthesis of cartilage-specific proteoglycan in chondrocyte cultures. *Biochem. Biophys. Res. Commun.* **71**, 851–856 (1976)
- Robinson, H.C., Brett, M.J., Tralagan, P.J., Lowther, D.A., Okayama, M.: The effect of D-xylose, beta-D-xylosides and beta-D-galactosides on chondroitin sulphate biosynthesis in embryonic chicken cartilage. *Biochem. J.* **148**, 25–34 (1975)
- Galligani, L., Hopwood, J., Schwartz, N.B., Dorfman, A.: Stimulation of synthesis of free chondroitin sulfate chains by beta-D-xylosides in cultured cells. *J. Biol. Chem.* **250**, 5400–5406 (1975)
- Schwartz, N.B., Galligani, L., Ho, P.L., Dorfman, A.: Stimulation of synthesis of free chondroitin sulfate chains by beta-D-xylosides in cultured cells. *Proc. Natl. Acad. Sci. U. S. A.* **71**, 4047–4051 (1974)
- Abrahamsson, C.O., Ellervik, U., Eriksson-Bajtner, J., Jacobsson, M., Mani, K.: Xylosylated naphthoic acid-amino acid conjugates for investigation of glycosaminoglycan priming. *Carbohydr. Res.* **343**, 1473–1477 (2008)
- Okayama, M., Kimata, K., Suzuki, S.: The influence of p-nitrophenyl beta-d-xyloside on the synthesis of proteochondroitin sulfate by slices of embryonic chick cartilage. *J. Biochem.* **74**, 1069–1073 (1973)

23. Kuberan, B., Ethirajan, M., Victor, X.V., Tran, V., Nguyen, K., Do, A.: “Click” xylosides initiate glycosaminoglycan biosynthesis in a mammalian cell line. *ChemBiochem*. **9**, 198–200 (2008)
24. Fritz, T.A., Lugenwa, F.N., Sarkar, A.K., Esko, J.D.: Biosynthesis of heparan sulfate on beta-D-xylosides depends on aglycone structure. *J. Biol. Chem.* **269**, 300–307 (1994)
25. Victor, X.V., Nguyen, T.K., Ethirajan, M., Tran, V.M., Nguyen, K.V., Kuberan, B.: Investigating the elusive mechanism of glycosaminoglycan biosynthesis. *J. Biol. Chem.* **284**, 25842–25853 (2009)
26. DeNardo, S.J., Burke, P.A., Leigh, B.R., O'Donnell, R.T., Miers, L.A., Kroger, L.A., Goodman, S.L., Matzku, S., Jonczyk, A., Lamborn, K.R., DeNardo, G.L.: Neovascular targeting with cyclic RGD peptide (cRGDF-ACHA) to enhance delivery of radioimmunotherapy. *Cancer Biother. Radiopharm.* **15**, 71–79 (2000)
27. Meyer, A., Auerheimer, J., Modlinger, A., Kessler, H.: Targeting RGD recognizing integrins: drug development, biomaterial research, tumor imaging and targeting. *Curr. Pharm. Des.* **12**, 2723–2747 (2006)
28. Park, K., Kim, Y.S., Lee, G.Y., Park, R.W., Kim, I.S., Kim, S.Y., Byun, Y.: Tumor endothelial cell targeted cyclic RGD-modified heparin derivative: inhibition of angiogenesis and tumor growth. *Pharm. Res.* **25**, 2786–2798 (2008)
29. Carlson, C.B., Mowery, P., Owen, R.M., Dykhuizen, E.C., Kiessling, L.L.: Selective tumor cell targeting using low-affinity, multivalent interactions. *ACS Chem. Biol.* **2**, 119–127 (2007)
30. Owen, R.M., Carlson, C.B., Xu, J., Mowery, P., Fasella, E., Kiessling, L.L.: Bifunctional ligands that target cells displaying the alpha v beta3 integrin. *ChemBiochem*. **8**, 68–82 (2007)
31. Wang, W., Borchardt, R.T., Wang, B.: Orally active peptidomimetic RGD analogs that are glycoprotein IIb/IIIa antagonists. *Curr. Med. Chem.* **7**, 437–453 (2000)
32. Gyorgydeak, Z., Szilagyí, L., Paulsen, H.: Synthesis, structure, and reactions of glycosyl azide. *J. Carbohydr. Chem.* **12**, 139–163 (1993)
33. Inazu, T., Kobayashi, K.: A new method for the synthesis of N^ε-Fmoc-N⁶-glycosylated-L-asparagine derivatives. *Synlett*. 869–870 (1993)
34. Aich, U., Loganathan, D.: Synthesis of N-(beta-glycopyranosyl) azidoacetamides. *J. Carbohydr. Chem.* **24**, 1–12 (2005)
35. Tornøe, C.W., Christensen, C., Meldal, M.: Peptidotriazoles on solid phase: [1, 2, 3]-triazoles by regioselective copper(I)-catalyzed 1, 3-dipolar cycloadditions of terminal alkynes to azides. *J. Org. Chem.* **67**, 3057–3064 (2002)
36. Meldal, M., Tornøe, C.W.: Cu-catalyzed azide-alkyne cycloaddition. *Chem. Rev.* **108**, 2952–3015 (2008)
37. Bertozzi, C.R., Kiessling, L.L.: Chemical glycobiology. *Science*. **291**, 2357–2364 (2001)
38. Lindahl, U., Roden, L.: The role of galactose and xylose in the linkage of heparin to protein. *J. Biol. Chem.* **240**, 2821–2826 (1965)
39. Sugahara, K.: The carbohydrate-protein linkage region of proteoglycans and glycosaminoglycan biosynthesis. *Seikagaku*. **61**, 496–500 (1989)
40. Kitagawa, H., Oyama, M., Masayama, K., Yamaguchi, Y., Sugahara, K.: Structural variations in the glycosaminoglycan-protein linkage region of recombinant decorin expressed in Chinese hamster ovary cells. *Glycobiology*. **7**, 1175–1180 (1997)
41. Kitagawa, H., Tone, Y., Tamura, J., Neumann, K.W., Ogawa, T., Oka, S., Kawasaki, T., Sugahara, K.: Molecular cloning and expression of glucuronyltransferase I involved in the biosynthesis of the glycosaminoglycan-protein linkage region of proteoglycans. *J. Biol. Chem.* **273**, 6615–6618 (1998)
42. Gulberti, S., Lattard, V., Fondeur, M., Jacquinet, J.C., Mulliert, G., Netter, P., Magdalou, J., Ouzzine, M., Fournel-Gigleux, S.: Phosphorylation and sulfation of oligosaccharide substrates critically influence the activity of human beta1, 4-galactosyltransferase 7 (GalT-7) and beta1, 3-glucuronosyltransferase I (GlcAT-I) involved in the biosynthesis of the glycosaminoglycan-protein linkage region of proteoglycans. *J. Biol. Chem.* **280**, 1417–1425 (2005)
43. Esko, J.D., Stewart, T.E., Taylor, W.H.: Animal cell mutants defective in glycosaminoglycan biosynthesis. *Proc. Natl. Acad. Sci. U. S. A.* **82**, 3197–3201 (1985)
44. Pfaff, M., Tangemann, K., Müller, B., Gurrath, M., Müller, G., Kessler, H., Timpl, R., Engel, J.: Selective recognition of cyclic RGD peptides of NMR defined conformation by alpha IIb beta 3, alpha V beta 3, and alpha 5 beta 1 integrins. *J. Biol. Chem.* **269**, 20233–20238 (1994)
45. Kaufmann, D., Fiedler, A., Junger, A., Auerheimer, J., Kessler, H., Weberskirch, R.: Chemical conjugation of linear and cyclic RGD moieties to a recombinant elastin-mimetic polypeptide—a versatile approach towards bioactive protein hydrogels. *Macromol. Biosci.* **8**, 577–588 (2008)

CHAPTER 5

SYNTHESIS AND BIOLOGICAL EVALUATION OF CLUSTER-XYLOSIDES AS POTENTIAL PROTEOGLYCAN MIMETICS

5.1. Introduction

PGs are the most ubiquitous glycoconjugates found on cell surfaces and in the extra cellular matrix (1). These highly charged, complex PGs regulate various molecular, cellular, pathological, and physiological events through binding to a wide array of proteins (2, 3). The distinct structural feature of all PGs, with the exception of decorin, is the substitution of a core protein with multiple GAG chains such as HS, CS, and/or DS (Figure 5.1) (1).

GAG attachment sites are highly conserved among various PGs in several mammals (4, 5). This implies that multiple GAG chains are required for optimal biological functionality of PGs in various species. Single GAG chains can perhaps not provide the same functionality that multiple GAG chains can. Only a few studies have examined the biological significance of GAG multivalency (4, 6). The cell surface PGs

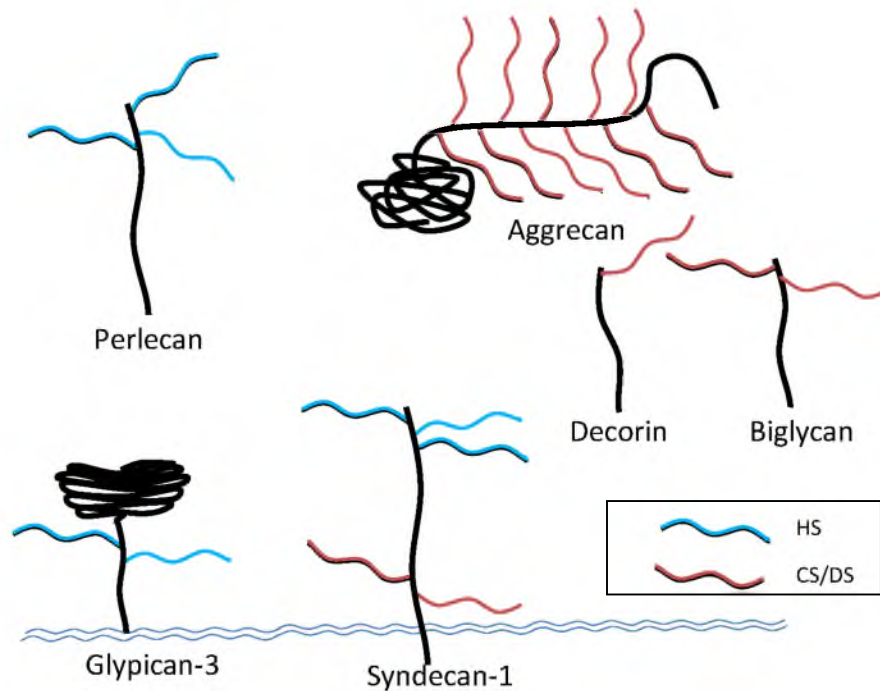


Figure 5.1. Schematic representation of various cell surface and ECM-bound PGs

from simple and stratified epithelium are shown to be polymorphic due mostly to variability in both the number of GAG chains attached to the core protein and GAG size (7). The variable chain valency is suggested to facilitate the distinct adhesive requirements of these two epithelial cell types.

Xylosylation of certain serine residues of the core proteins, a rate limiting first step in the assembly of PGs, is catalyzed by xylosyltransferases (8-10). It is known that xylosides can function as GAG chain initiators without a core protein provided that xylosides carry a hydrophobic group (11-15). We have earlier shown that click-xylosides prime a diverse array of GAG chains and suggested the presence of GAGOSOMES, distinct macromolecular enzyme complexes that regulate the combinatorial biosynthesis of complex GAG chains (16, 17). Several earlier studies have rigorously utilized synthetic mono-xylosides to further our understanding of the role of endogenous PGs in model organisms and also to elucidate the elusive biosynthetic mechanism. Only one study has examined synthetic bis-xylosides, which carry two xylose residues per molecular scaffold, for their priming activity (18). These synthetic bis-xylosides carry very labile *O*-glycosidic linkage. Given the importance of multiple GAG chains for cooperative interactions with protein ligands and for optimal biological functions, there is a great deal of interest in synthesizing stable, small molecular scaffolds carrying a variable number of xylose residues for biological studies. Thus, synthetic cluster-xylosides should afford molecular scaffolds with multiple GAG chains mimicking endogenous PGs to define the role of GAG glycome and GAG multivalency in various developmental and physiological processes.

In the present study, “click chemistry” is utilized to assemble cluster-xylosides carrying one, two, three, or four xylose residues. The priming activity of these cluster-

xylosides was investigated in a model cellular system, pgsA-745 cell line, lacking active xylosyltransferase (19). Furthermore, the distance between two xylose residues in a group of bis-xylosides and the number of xylose units in cluster-xylosides were examined to affect the priming activity, the type of GAG chains primed, their sulfation pattern, and chain length. The results obtained in the present study provide further insights into the nature of assembly of multiple GAG chains on the synthetic scaffolds and suggest that these potential PG mimetics can be utilized to study the functional role of GAG chain valency in biological systems.

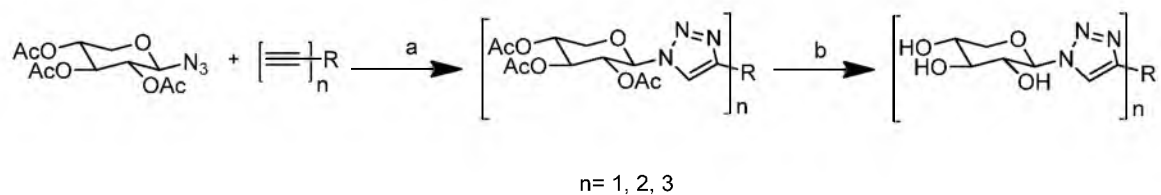
5.2. Results

5.2.1. Synthesis of Cluster-xylosides

Cluster-xylosides were hypothesized to carry multiple GAG chains per scaffold and mimic PGs. Therefore, these scaffolds can be utilized to define the biological significance of GAG multivalency. Towards this goal, a library of cluster-xylosides was designed that can prime multiple GAG chains per scaffold and mimic naturally occurring PGs. A library of mono-xylosides synthesized by “click chemistry” has been found to be stable under *in vitro* conditions and furthermore possesses good GAG priming activity (16). Therefore, mono-xylosides, bis-xylosides, and tris-xylosides, were synthesized, as shown in Table 5.1. Tetrakis-xylosides were received from Prof. Loganathan (IIT Madras, India). Fully acetylated xylosyl azide was conjugated to various hydrophobic molecules containing triple bonds by click chemical methodology and the resulting library of xylosides was deprotected under Zemplén condition to obtain the final products, as outlined in Scheme 5.1. The overall reaction yields of this two-step process, click chemistry and deprotection, range from 50% to 70%.

Table 5.1. Structures of cluster-xylosides

Number	Structure
1	
2	
3	
4	
5	
6	
7	
8	
9	
10	Tetrakis-xylosides
11	Tetrakis-xylosides



Scheme 5.1. Synthesis of cluster-xylosides. a: acetone, deionized water, copper (II) sulfate, and sodium ascorbate. b: methanol and sodium methoxide

The final products **1-18** were purified on a reverse phase C18 column using HPLC as described in the “Experimental Methods” section [5.5] followed by structural analysis using NMR spectroscopy and mass spectrometry.

5.2.2. Priming Activity of Cluster-xylosides

A mutant CHO cell line, pgsA-745, is a convenient cellular system for determining the priming activity of cluster-xylosides because this cell line lacks an active xylosyltransferase enzyme and therefore does not make endogenous GAG chains. Thus, it is straightforward to determine the priming activity of cluster-xylosides using this cell line. The cluster-xylosides were screened at two concentrations, 100 μ M and 1 mM. The primed GAGs were purified using mini DEAE-sepharose columns. It is interesting to note that deprotected bis-xylosides were able to prime at these concentrations with a tendency to prime better at the higher concentration. However, deprotected tris- and tetrakis-xylosides were unable to prime at both the concentrations, suggesting that these highly water soluble, polar molecular scaffolds experience difficulties in crossing the intracellular and/or outer membranes. For these reasons, fully acetylated tris- and tetrakis-xylosides were studied for their priming activity. Fully protected xylosides, **8-11**, precipitated at 1 mM concentration in the cell culture

medium whereas these scaffolds were found to prime GAG chains without getting precipitated at the 100 μ M concentration in the cell culture medium. However, tris- and tetrakis-xylosides, **8-11** did not prime a significant amount of GAG chains.

Next, the effect of spacer length between xylose units was examined on the priming activity. The obtained data show that the distance between the xylose units located on a single scaffold affects the priming activity at 100 μ M concentration, as shown in Figure 5.2. At the 100 μ M concentration, as the spacer distance increases, the priming activity tends to decrease for all cluster-xylosides, suggesting that longer alkyl linkers may prohibit effective transport of cluster-xylosides across the membrane. At 1 mM concentration, however, the spacer distance between the two xylose units did not have any effect on the priming activity of bis-xyloside due to overloading the bis-xyloside into cells.

5.2.3. Structural Analysis of Primed GAG Chains

In order to verify the multidirectional priming ability of cluster-xylosides, we analyzed the molecular weights of GAG chains induced by cluster-xylosides in pgsA-745 cells using size exclusion chromatography. The chain length of the GAG chains was determined by measuring the migration time of GAG chains in comparison to that of polystyrene sulfonate standards under similar conditions. The average molecular weights were found to be 16 kDa for GAG chains primed by mono-xyloside **1**, 55 kDa for GAG chains primed by bis-xyloside **3**, 32 kDa for GAG chains primed by tris-xyloside **8**, and 40 kDa for GAG chains primed by tetrakis-xyloside **10**. The tris-xyloside produced GAG chains with a higher average molecular weight than the mono-xylosides but lower molecular weight than the bis-xylosides, possibly due to

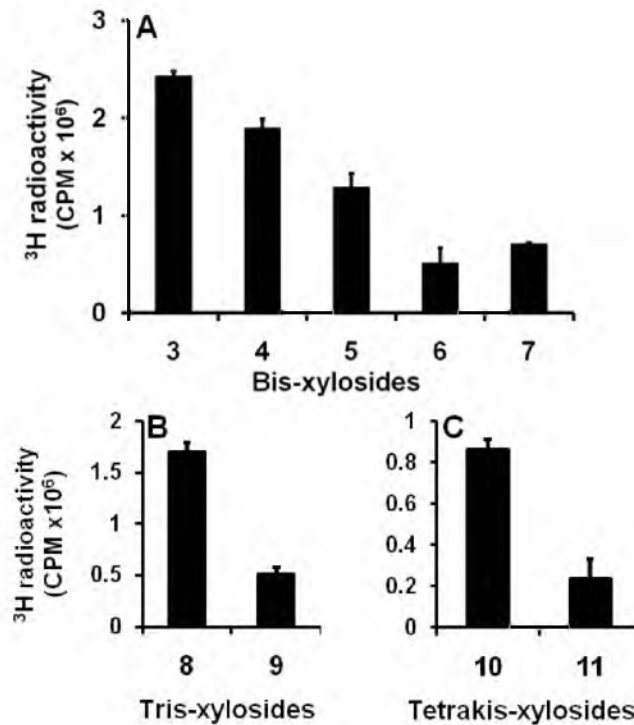


Figure 5.2. Priming activity of cluster-xylosides. CHO cells were treated with cluster-xylosides at 100 μM in the presence of ^3H -GlcNH₂ (100 μCi) as described in the “Experimental Methods” section [5.5]. The GAG chains were purified by anion exchange chromatography and quantitated using a liquid scintillation counter. A: Priming activity of bis-xylosides, B: Priming activity of tris-xylosides and C: Priming activity of tetrakis-xylosides. The results were the average of two independent experiments that were carried out in duplicate.

molecular steric hindrance that decreased enzyme efficiency during GAG biosynthesis (Figure 5.3). Therefore, the structures of induced GAG chains were analyzed by bis-xylosides in pgsA-745 cells in detail. Though these xylosides prime better at 1 mM concentration compared to 100 μM concentration, the primed GAG chains have significantly lower molecular weights (Figure 5.4A). It is possible that at such a high concentration, the GAG biosynthetic machinery is overloaded and unable to produce large GAG chains. Interestingly, the spacer distance between the two residues in bis-

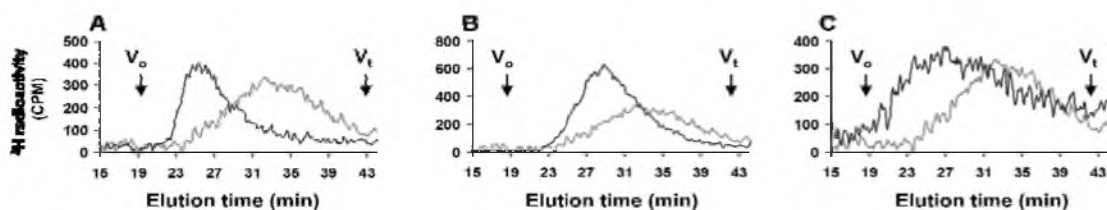


Figure 5.3. Molecular weight profiles of GAG chains primed by cluster-xylosides. GAG chains primed by cluster-xylosides at 100 μ M concentration in pgsA-745 cells for 24 h. The purified GAG chains were analyzed by size exclusion chromatography, fractionated on two tandem 3000 SW_{XL} columns, and were eluted with an isocratic gradient of phosphate buffer for 90 minutes at a flow rate of 0.5 ml/min as described in the experimental section. A: The elution profiles of GAG chains primed by mono-xyloside **1** (gray trace, control) and bis-xyloside **3** (black trace). B: The elution profiles of GAG chains primed by mono-xyloside **1** (gray trace, control) and tris-xyloside **8** (black trace). C: The elution profiles of GAG chains primed by mono-xyloside **1** (gray trace, control) and tetrakis-xyloside **10** (black trace).

xylosides did not affect the average MWs of primed GAG chains even though the spacer distance affected their priming activity at 100 μ M concentration.

To analyze the sulfation patterns of primed GAGs, we utilized high-pressure DEAE anion-exchange chromatography. The sulfate density of GAG chains primed by bis-xylosides was largely unaffected by alkyl linkers. Notably, GAG chains primed at lower concentrations contained more sulfate groups than GAGs primed at higher concentrations. Additionally, the sulfation pattern of GAGs primed at 100 μ M was less polydisperse and more homogenous than at the 1 mM concentration (Figure 5.4B). The HS/CS composition of primed GAG chains was determined by treating them with heparitinases I/II/III. It was found that these bis-xylosides in this study prime CS predominantly and relatively smaller quantities of HS (see the “Supporting Information” [5.6]). Earlier studies, including our own, have shown that aglycone structures dramatically influence the GAG composition and that aglycones carrying the

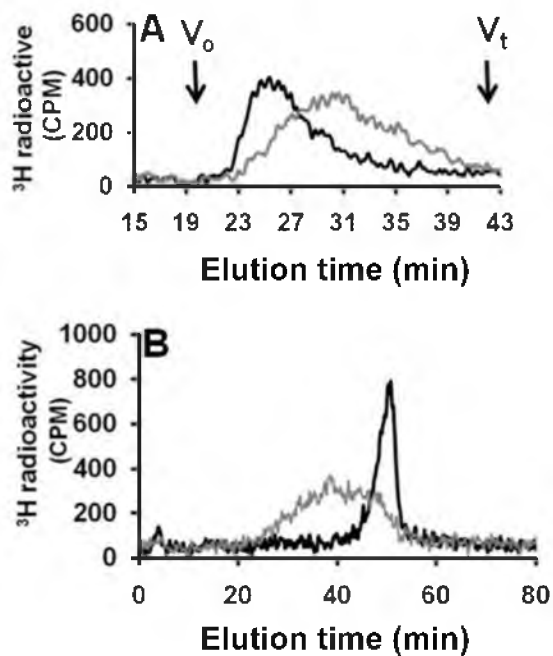


Figure 5.4. Structural analysis of primed GAG chains. A. Size exclusion profiles of GAG chains primed by bis-xyloside **3** at 100 μ M and 1 mM concentrations in pgsA-745 cells for 24 h. The primed GAG chains were analyzed by size exclusion chromatography and were eluted with an isocratic gradient of phosphate buffer for 90 minutes at a flow rate of 0.5 ml/min as described in the “Experimental Method” section [5.5]. The elution profiles of bis-xyloside **3** at 1 mM (gray trace) and at 100 μ M (black trace). B. Sulfate density profile of GAG chains primed by bis-xyloside **3** in pgsA-745 cell lines at 1 mM (gray trace) and at 100 μ M (black trace) were analyzed using anion exchange HPLC: the bound GAG chains were eluted with a linear gradient of 0.2 M to 1 M NaCl over 80 minutes at a flow rate of 1ml/min. These elution profiles are representative of two independent experiments.

naphthyl or aryl group tend to prime more HS chains. For these reasons, additional bis-xyloside scaffolds were synthesized in which phenyl- or naphthyl- group containing linkers were used to bridge two xylose residues, as shown in Table 5.2.

In our later efforts, we primarily focused on synthesizing additional bis-xylosides only as they tend to prime GAG chains with higher molecular weights and less polydispersity than tris- and tetrakis- xylosides. The additional scaffolds, **12-17**, primed mostly CS chains and very few HS chains, even though they carry phenyl or

Table 5.2. Structures of bis-xylosides carrying an aryl group in the aglycone

Number	Structure
12	
13	
14	
15	
16	
17	
18	

naphthyl groups. Nevertheless, bis-xylosides should mimic PGs such as biglycan that carry two CS chains and therefore can be used as potential PG mimetics to define the GAG multivalency in the biological systems. Furthermore, it is possible that these scaffolds prime different GAG types in other cellular systems.

To determine the disaccharide composition, the purified GAG chains were digested with chondroitinase ABC, which digests CS chains into disaccharides. The radiolabeled disaccharides were then identified by comparison of their elution positions relative to those of disaccharide standards. Disaccharide analysis revealed that primed CS chains composed of two major disaccharides, Δ UA-GalNAc and Δ UA-GalNAc(4S). GAG chains primed by the bis-xylosides, at 100 μ M concentration, were composed mostly of 4-*O*-sulfated disaccharide (Figure 5.5).

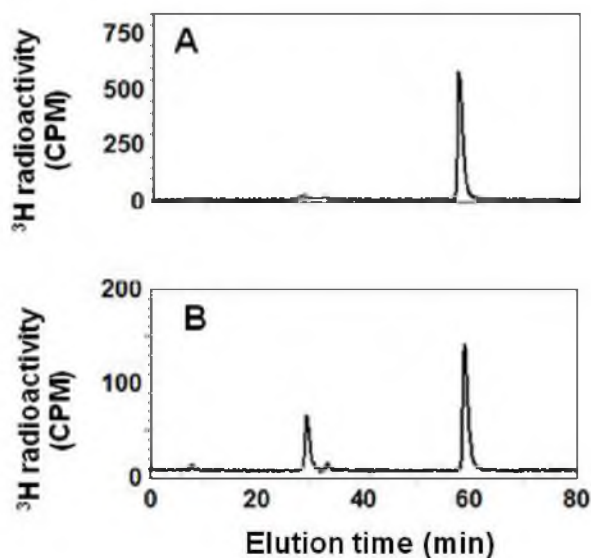


Figure 5.5. Disaccharide profiles of bis-xyloside primed CS chains. GAG chains, which were primed by bis-xylosides **3** at 100 μ M and 1 mM, were treated with chondroitinase ABC. The enzyme treated GAG chains were analyzed using SAX-HPLC with inline flow scintillation analyzer along with CS disaccharide standards “ Δ UA-GalNAc, Δ UA-GalNAc2S, Δ UA-GalNAc4S, Δ UA-GalNAc6S.” The resulting disaccharides were “I: Δ UA-GalNAc; and II: Δ UA-GalNAc4S.”

5.2.4. Evidence of Bidirectional Priming by Bis-xylosides

In order to verify bidirectional priming by bis-xyloside, the primed GAG chains by mono-xylosides and bis-xylosides were cleaved by periodate oxidation-alkaline elimination. GAG chains primed by mono-xylosides was not cleaved under periodate oxidation-alkaline elimination condition (Figure 5.6A) but GAG chains primed by bis-xylosides were cleaved from 55 kDa to 20 kDa (Figure 5.6B). It suggested that bis-xylosides primed bidirectional GAG chains, which mimic the natural PGs. Bidirectional priming by bis-xylosides was verified again by ozonolysis reaction. GAG chains that were primed by bis-xyloside **18**, containing a double bond, cleaved selectively under an ozone condition. (see “Supporting Information” [5.6]).

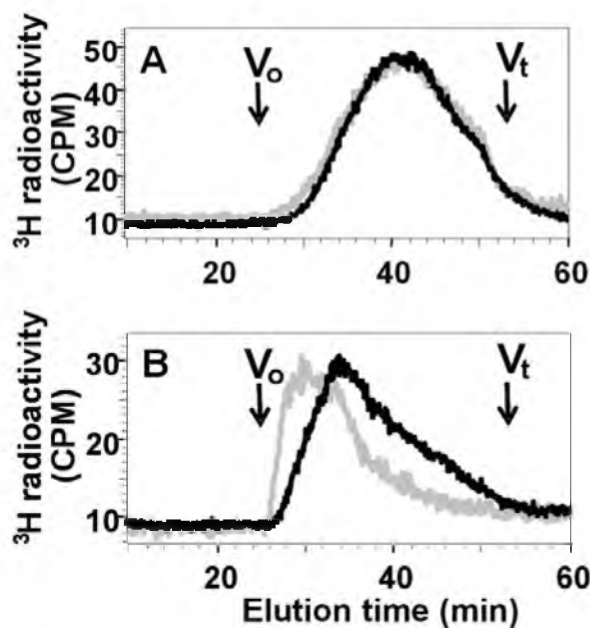


Figure 5.6. Periodate oxidation-alkaline elimination of GAG chains. GAG chains, which were primed by mono-xyloside **2** and bis-xyloside **7** at 100 μ M, were subjected to periodate oxidation-alkaline elimination. A: The elution profiles of GAG chains primed by mono-xyloside **2** (gray trace) and periodate oxidation-alkaline elimination of GAG chains primed by mono-xyloside **2** (black trace). B: The elution profiles of GAG chains primed by bis-xyloside **7** (gray trace) and periodate oxidation-alkaline elimination of GAG chains primed by bis-xyloside **7** (black trace).

5.3. Discussion

A distinct structural feature of all PGs, with the exception of decorin, is that the core protein is substituted with two or more GAG chains. In addition, PGs exhibit a molecular polymorphism attributed to differences in their GAG chain valency and size (7). The multivalent nature of PGs has been suggested to be important in regulating a wide variety of cellular processes, including optimal function of syndecans in cell invasion, migration, and adhesion (20). A recent study has exemplified the cooperative interaction of fibroblast growth factor (FGF) 2 with heparin oligosaccharides attached to the dendrimer in potentiating FGF2 activity (21).

Click-xylosides carrying different aglycone moiety were demonstrated that prime diverse GAG chains and suggested the presence of GAGOSOMEs that can regulate the production of cell-specific combinatorial GAG structures with distinct sulfation pattern, size, and type (17, 22-24). In this report, we examined a method to assess the effect of the distance between two GAG initiation sites on priming activity, the type of GAG produced, GAG sulfate density and chain length. Available data suggest that bis-xylosides prime GAG chains that have higher molecular weights and less polydispersity in comparison to those that are primed by tris- or tetrakis-xylosides. Although bis-xylosides prime better at 1 mM concentration compare to 100 μ M concentration, primed GAG chains are lower in their molecular weights. This could be due to the overloading of GAG biosynthetic machinery with xylosides. We have also found that the spacer distance between the two residues in bis-xylosides did not affect average MWs of primed GAG chains even though the spacer distance affected their priming activity at 100 μ M concentration.

Cluster-xylosides primed mostly CS chains and very few HS chains, even though they carry phenyl or naphthyl groups. Nevertheless, bis-xylosides should mimic PGs such as biglycan that carry two CS chains and therefore can be used as potential PG mimetics to define the GAG multivalency in the biological systems. Furthermore, it is possible that these scaffolds prime different GAG types in other cellular systems (Figure 5.7).

Lander et al. proposed a two-step biosynthetic model in which the decisions to attach CS or HS to a core protein are made sequentially (25). If this were true, one would expect to observe distinct GAG types at two different GAG initiation sites that are in close proximity within the same scaffold. It is therefore tempting to propose an alternative model in which scaffolds reach specific GAGOSOMES through their selective trafficking into the Golgi where they are committed for assembling either HS or CS/DS at multiple initiation sites as long as the initiation sites are in close proximity. However, the model proposed by Lander may very well be true if there are additional unknown factors that can recognize protein sequences and thereby facilitate the assembly mechanism in a two-step process that eventually leads to the production of PGs carrying both HS and CS/DS on the same core protein. Thus, the biosynthetic machinery cannot impose these molecular restrictions on cluster-xylosides as these scaffolds lack such elaborative structural features to facilitate the two-step process.

5.4. Conclusions

In summary, a wide variety of cluster-xylosides carrying single, two, three, or four xylose residues per scaffold were synthesized using click chemistry and

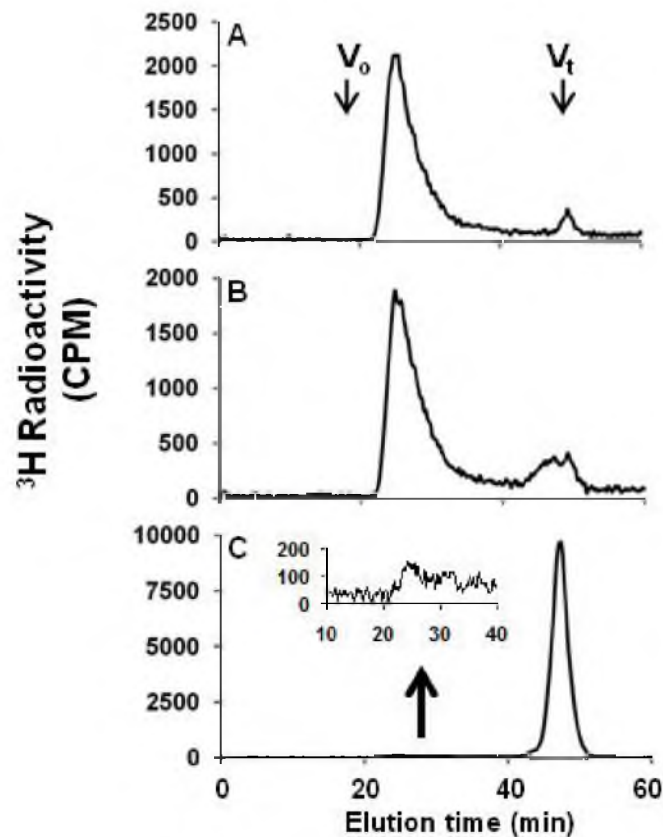


Figure 5.7. Structural analysis of GAG chains primed by bis-xyloside. PgsA-745 cells were incubated with the bis-xyloside **3** at 100 μ M for 24 h. The HS/CS composition of the primed GAG chains was determined by digesting the GAG chains with heparitinase I/ II/ III and chondroitinase ABC enzymes. The reaction mixture was loaded on to two tandem G3000 SWXL columns (7.8 mm x 30 cm) and analyzed with the aid of an inline radiometric detector using phosphate buffer (100 mM KH_2PO_4 , 100 mM NaCl, pH 6) as an eluent. A: The elution profile of GAG chains without enzymes treatment. B: The elution profile of GAG chains with heparitinase I/ II/ III. C: The elution profile of GAG chains after treatment with chondroitinase ABC enzyme.

systematically studied for their ability to stimulate GAG biosynthesis. Cluster-xylosides primed multiple GAG chains per scaffold mimicking endogenous PGs. However, most of these cluster-xylosides primed predominantly CS chains and very few HS chains. Future studies will involve the synthesis of additional scaffolds to delineate the PG biosynthetic pathways, determine priming of HS chains, and examine the biological significance of GAG multivalency in a systematic manner.

5.5. Experimental Methods

Anhydrous solvents were purchased and used directly or dried over standard drying agents and freshly distilled prior to use. Reactions were monitored by TLC on silica gel 60 F-254 with detection by Von's reagent. Intermediate compounds were purified by flash chromatography columns using silica gel 60 (230–400 mesh) and were run under medium pressure at 5–7 psi. Final products were purified by high performance liquid chromatography (HPLC) on a reverse phase C18 column (VYDAC 2.2 cm×25 cm) with solvent A (25 mM formic acid in water) and solvent B (95% acetonitrile) at a flow rate of 5 ml/min in a linear gradient over 120 minutes starting with 0% B. All synthetic compounds were characterized by NMR using a Varian Mercury 400 MHz spectrometer. The compounds were also confirmed for their final structures by electrospray ionization mass spectrometry (ESI-MS) using a Finnigan LCQ mass spectrometer or a Bruker Q-ToF mass spectrometer in either positive or negative ion mode .

The mutant Chinese hamster ovary (CHO) cell line, pgsA-745, was obtained from American Type Culture Collection. The cell culture reagents for the CHO cell line were obtained from HyClone. Tritium glucosamine (^3H) and Ultima-FloAP flow scintillation mixture for flow radiometric analysis were obtained from Perkin Elmer Life Sciences. All other chemicals and biochemicals were obtained from Sigma Aldrich. DEAE-Sepharose gel was purchased from Amersham Biosciences. The anion-exchange column, TSKgel DEAE-3SW (7.4 mm x 7.5 cm), and the size exclusion column, G3000SWXL (7.8 mm x 30 cm), were obtained from Tosoh Bioscience. Anhydrous solvents were purchased and used directly or dried over standard drying agents and freshly distilled prior to use.

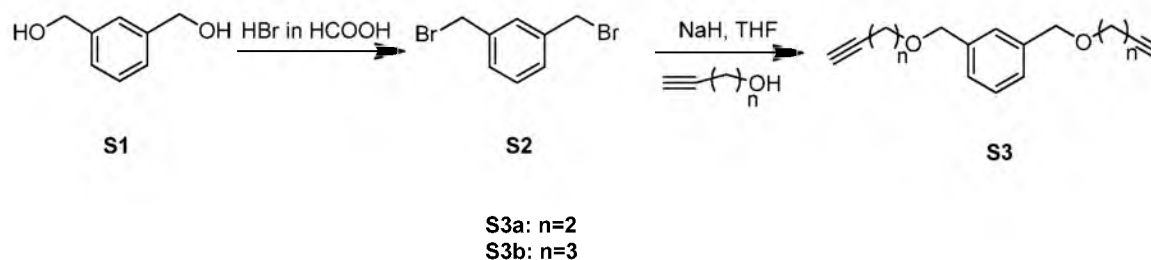
5.5.1. Synthesis of Cluster-xylosides

Compound **S2**: 1, 3-Benzenedimethanol (3.618 mmol, 500 mg) was treated with 31 % HBr in acetic acid (5 ml). The reaction was stirred at room temperature for 2 h. After addition of dichloromethane (10 ml), the organic solvent was washed with water, saturated bicarbonate solution, dried over Na₂SO₄, and evaporated. The crude material was purified by flash chromatography on silica gel to give the compound (**S2**) (900mg, 90% yield). ¹H NMR (CDCl₃): δ 7.42 (1H, s), 7.33 (3H, d, *J* = 1.2 Hz), 4.48 (4H, s) (Scheme S5.1 and Table S5.1).

Compound **S3**: To an anhydrous THF solution (10 ml) of alcohol carrying an alkyne group (2 mmol) was added sodium hydride (3 mmol). The reaction mixture was stirred for 30 minutes at room temperature under argon atmosphere followed by the addition of (**S2**) (1 mmol). The mixture was stirred overnight at room temperature. THF solvent was evaporated. The crude material was dissolved in ethyl acetate, washed with water and then saturated sodium chloride solution, dried over Na₂SO₄, and evaporated. The residue was purified by column chromatography to give the compound (**S3**) (Scheme S5.1 and Table S5.1).

Compound **S3a**: ¹H NMR (CDCl₃) δ 7.34-7.25 (4H, m), 4.51 (4H, s), 3.58 (4H, t, *J* = 6.6 Hz), 2.51 (4H, dt, *J* = 6.8, 2.7 Hz), 2.00 (2H, t, *J* = 2.7 Hz).

Compound **S3b**: ¹H NMR (CDCl₃) δ 7.34-7.25 (4H, m), 4.51 (4H, s), 3.58 (4H, t, *J* = 6.3 Hz), 2.32 (4H, dt, *J* = 7.0, 2.7 Hz), 1.94 (2H, t, *J* = 2.7 Hz), 1.84 (4H, p, *J* = 6.3 Hz).



Scheme S5.1. Preparation of precursors carrying alkyne group for click chemistry

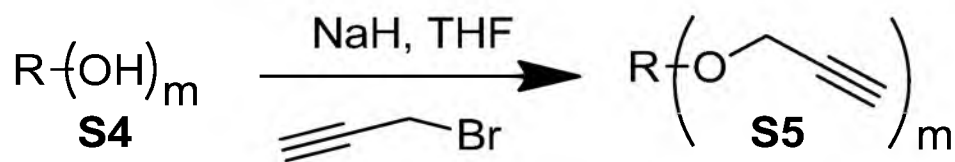
Table S5.1. Yields of reactions

n	S3	Yield (%)
2	S3a	84%
3	S3b	97%

Compound **S5**: To an anhydrous THF solution (10 ml) of compound (**S4**) (1 mmol) was added sodium hydride ($[m+1]$ mmol). The reaction mixture was stirred for 30 minutes at room temperature under argon atmosphere followed by addition of propargyl bromide ($[m+1]$ mmol). The mixture was stirred overnight at room temperature. Solvent was evaporated. The crude material was dissolved in ethyl acetate and washed with water and saturated sodium chloride solution, dried over Na_2SO_4 and evaporated. The residue was purified by column chromatography to give the compound (**S5**) (Scheme S5.2 and Table S5.2).

Compound **S5a**: ^1H NMR (CDCl_3) δ 7.39-7.30 (4H, m), 4.61 (4H, s), 4.18 (4H, d, $J = 2.3$ Hz), 2.47 (2H, t, $J = 2.3$ Hz)

Compound **S5b**: ^1H NMR (CDCl_3) δ 7.35 (4H, s), 4.61 (4H, s), 4.17 (4H, d, $J = 2.3$ Hz), 2.45 (2H, t, $J = 2.3$ Hz)



Scheme S5.2. Preparation of propargylated precursors for the synthesis of bis- and tris-xylosides

Table S5.2. Yields of reactions

S4	m	S5	Yield (%)	Reference*
	2	S5a	48%	N/A
	2	S5b	65%	(26)
	2	S5c	54%	(27)
	3	S5d	27%	N/A

* the procedure was slightly modified from the published reports

Compound **S5c**: $^1\text{H NMR}$ (CDCl_3) δ 4.12 (4H, d, $J = 2.4$ Hz), 3.61-3.58 (12H, m), 2.38 (2H, s)

Compound **S5d**: $^1\text{H NMR}$ (CDCl_3) δ 4.12 (6H, d, $J = 2.4$ Hz), 3.51 (6H, t, $J = 5.9$ Hz), 2.42 (3H, t, $J = 2.4$ Hz), 2.03-1.99 (6H, m), 1.55-1.48 (6H, m)

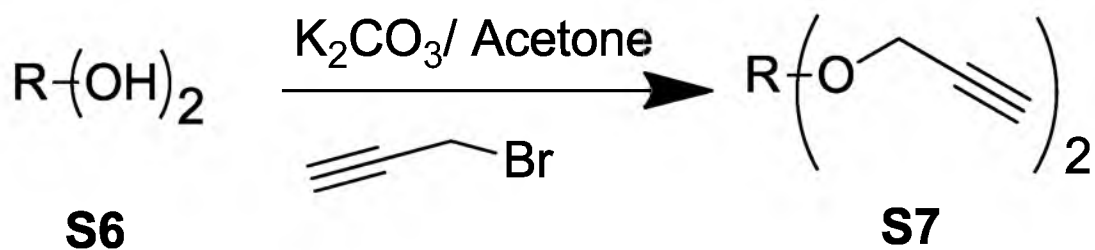
Compound **S7**: To the solution (10 ml) of compound (**S6**) (1 mmol) in acetone, was added potassium carbonate (3 mmol). The reaction mixture was stirred for 30 minutes at room temperature. Propargyl bromide (3 mmol) was then added and the

mixture was stirred overnight. The reaction mixture was concentrated. The resulting crude material was dissolved in ethyl acetate, washed with water and saturated sodium chloride solution, dried over Na₂SO₄, and rotary evaporated under reduced pressure. The residue was purified by column chromatography to give the compound (S7) (Scheme S5.3 and Table S5.3).

Compound S7a: ¹H NMR (CDCl₃) δ 7.89 (2H, d, *J* = 7.8), 7.38 (2H, t, *J* = 7.8), 6.97 (2H, d, *J* = 7.0), 4.88 (4H, s), 2.53 (2H, s)

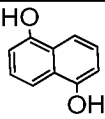
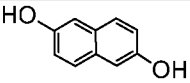
Compound S7b: ¹H NMR (CDCl₃) δ 7.68 (2H, d, *J* = 8.6 Hz), 7.19 (4H, d, *J* = 12.1 Hz), 4.78 (4H, s), 2.54 (2H, s).

Compound S8: Nitromethanetrispropanol (2.127 mmol) was dissolved in SOCl₂ (42.54 mmol). The reaction mixture was refluxed at 60 °C. After the completion of reaction, the reaction mixture was dissolved in ethyl acetate and washed with water, brine, and then dried over Na₂SO₄. The final mass is 380 mg (62 %) and the crude product was used in the next step without any further purification (Scheme S5.4).. ¹H NMR (CDCl₃): δ 3.54 (6H, t, *J* = 6.4 Hz), 2.10-2.06 (6H, m), 1.74-1.67 (6H, m).



Scheme S5.3. Preparation of additional propargylated precursors

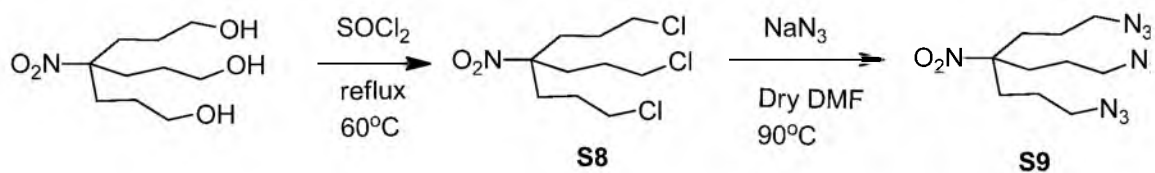
Table S5.3. Yields of reactions

S6	S7	Yield (%)	Reference
	S7a	20%	(28)
	S7b	56%	(29)

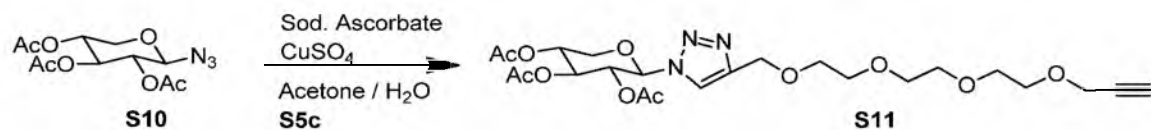
* The procedures were modified from the published reports

Compound **S9**: The compound (**S8**) (1.275 mmol) was dissolved in dry DMF (10 ml) followed by addition of sodium azide (6.38 mmol). The reaction was heated to 90 °C under stirring. After completion of the reaction as indicated by TLC, the reaction mixture was dissolved in ethyl acetate, washed with water and brine, and then dried over Na₂SO₄ (Scheme S5.4). The final mass is (270mg, 66%). ¹H NMR (CDCl₃): δ 3.28 (2H, t, *J* = 6.6 Hz), 1.95-1.91 (2H, m), 1.47-1.39 (2H, m).

Compound **S11**: To a solution of alkyne (**S5c**) (4.98 mmol) and xylosyl azide (**S10**) (1.66 mmol) in 8 ml of acetone and water (1:1) solvent mixture, sodium ascorbate (0.66 mmol) was added, followed by Cu₂SO₄ · 5H₂O (1.33 mmol) at room temperature, and the mixture was stirred until disappearance of compound (**S10**) (as indicated by TLC). At the end of the reaction, the reaction mixture was evaporated using rotary evaporator under reduced pressure to obtain the final product (360 mg, 41%) (Scheme S5.5).^(30, 31) ¹H NMR (CD₃OD): δ 8.24 (1H, s), 6.02 (1H, d, *J* = 8.6 Hz), 5.58-5.47 (2H, m), 5.23-5.17 (1H, m), 4.64 (2H, s), 4.25 (1H, dd, *J* = 5.9, 11.3 Hz), 4.18 (2H, d, *J* = 2.3 Hz), 3.77 (1H, t, *J* = 10.9 Hz), 3.66-3.62 (12H, m), 2.83 (1H, t, *J* = 2.3 Hz), 2.04 (3H, s), 2.02 (3H, s), 1.83 (3H, s)



Scheme S5.4. Preparation of the precursor for the synthesis of tris-xyloside 9



Scheme S5.5. Synthesis of mono-xylosides using click chemistry

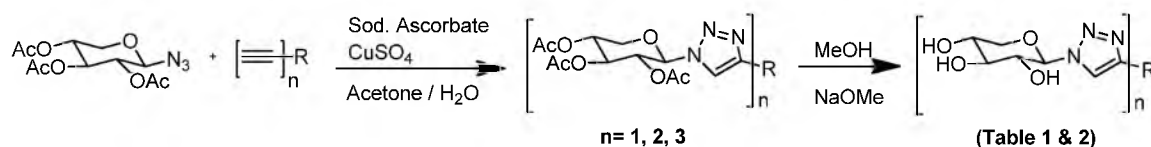
To a solution of propargylated precursors (1 mmol) and xylosyl azide (1, 2 or 3 mmol for the synthesis of mono-, bis- or tris-xylosides, respectively) in acetone (8 ml) and water (2.6 ml) mixture, excess sodium ascorbate was added, followed by $\text{CuSO}_4 \cdot 5\text{H}_2\text{O}$ (0.4 mmol) at room temperature and the mixture was stirred until the disappearance of the starting materials, as indicated by TLC. At the end of the reaction, the reaction mixture was concentrated using a rotary evaporator under reduced pressure and the syrup obtained was dissolved in ethyl acetate and washed with water. Finally, the organic layers were washed with saturated sodium chloride and the crude products were purified by silica flash column to give the desired protected xylosides. Deprotection procedure: Fully acetylated xyloside (1 mmol) was taken in dry methanol (10 ml) and treated with freshly prepared 1 M solution of sodium methoxide in dry methanol until the solution reaches pH ~9, as indicated by pH paper. After the deacetylation was complete, as indicated by TLC, H^+ resins were added to bring the pH to 7. The reaction mixture was then filtered, concentrated under reduced pressure to the crude product, and was further purified on HPLC-reverse phase C18 column with

solvent A (25 mM formic acid in water) and solvent B (95% acetonitrile) to give the deprotected-xylosides (**1-9** and **12-18**) (Scheme S5.6).

Xyloside **1**: ^1H NMR (CD_3OD): δ 7.98 (1H, s, triazolyl H), 5.47 (1H, d, $J = 9.4$ Hz, H-1), 4.00 (1H, dd, $J = 5.1, 11.3$ Hz, H-5a), 3.87 (1H, t, $J = 9.4$ Hz, H-2), 3.67-3.63 (1H, m, H-4), 3.49 (1H, t, $J = 9.0$ Hz, H-3), 3.45 (1H, t, $J = 10.9$ Hz, H-5b), 2.92 (2H, t, $J = 7.4$ Hz), 2.54 (2H, dt, $J = 2.3$ Hz, 7.4 Hz), 2.27 (1H, t, $J = 2.7$ Hz); ^{13}C NMR (CD_3OD): δ 147.4, 122.7, 90.2, 83.8, 78.6, 73.9, 70.7, 70.5, 69.8, 25.9, 19.3; ESI-MS: Calcd for $\text{C}_{11}\text{H}_{15}\text{N}_3\text{O}_4\text{Na}$: 276.0960 $[\text{M}+\text{Na}]^+$, Found 275.9333.

Xyloside **2**: ^1H NMR (CD_3OD): δ 7.89 (1H, s, triazolyl H), 5.45 (1H, d, $J = 9.4$ Hz, H-1), 4.00 (1H, dd, $J = 5.1, 11.1$ Hz, H-5a), 3.87 (1H, t, $J = 9.4$ Hz, H-2), 3.69-3.63 (1H, m, H-4), 3.48 (1H, t, $J = 9.4$ Hz, H-3), 3.45 (1H, t, $J = 10.9$ Hz, H-5b), 2.71 (2H, t, $J = 7.8$ Hz), 2.17-2.14 (3H, m), 1.72-1.65 (2H, m), 1.52-1.36 (6H, m); ^{13}C NMR (CD_3OD): δ 149.2, 122.2, 90.1, 85.0, 78.7, 73.8, 70.7, 69.8, 69.5, 30.4, 29.7, 29.6, 29.5, 26.2, 19.0; ESI-MS: Calcd for $\text{C}_{30}\text{H}_{46}\text{N}_6\text{O}_8\text{Na}$: 641.3275 $[2\text{M}+\text{Na}]^+$, Found 640.7333.

Xyloside **3**: ^1H NMR (CD_3OD): δ 7.84 (2H, s, triazolyl H), 5.45 (2H, d, $J = 9.4$ Hz, H-1), 3.99 (2H, dd, $J = 5.5, 11.3$ Hz, H-5a), 3.83 (2H, t, $J = 9.4$ Hz, H-2), 3.69-3.63 (2H, m, H-4), 3.48 (2H, t, $J = 9.0$ Hz, H-3), 3.44 (2H, t, $J = 10.9$ Hz, H-5b), 3.09 (4H, s); ^{13}C NMR (CD_3OD): δ 169.0, 122.7, 90.2, 78.6, 74.0, 70.7, 69.8, 26.2; ESI-MS: Calcd for $\text{C}_{16}\text{H}_{24}\text{N}_6\text{O}_8\text{Na}$: 451.1553 $[\text{M}+\text{Na}]^+$, Found 451.1333.



Scheme S5.6. Synthesis of cluster-xylosides using click chemistry(30, 31)

Xyloside 4: ^1H NMR (CD_3OD): δ 7.94 (2H, s, triazolyl H), 5.46 (2H, d, $J = 9.4$ Hz, H-1), 3.99 (2H, dd, $J = 5.5, 11.3$ Hz, H-5a), 3.87 (2H, t, $J = 9.4$ Hz, H-2), 3.70-3.64 (2H, m, H-4), 3.49 (2H, t, $J = 9.0$ Hz, H-3), 3.45 (2H, t, $J = 10.9$ Hz, H-5b), 2.76 (4H, t, $J = 7.4$ Hz), 2.05 (2H, p, $J = 7.4$ Hz); ^{13}C NMR (CD_3OD): δ 148.4, 122.5, 90.2, 78.6, 73.9, 70.7, 69.8, 29.9, 25.5; ESI-MS: Calcd for $\text{C}_{17}\text{H}_{27}\text{N}_6\text{O}_8$: 443.1890 $[\text{M}+\text{H}]^+$, Found 442.8667.

Xyloside 5: ^1H NMR (CD_3OD): δ 7.89 (2H, s, triazolyl H), 5.45 (2H, d, $J = 9.4$ Hz, H-1), 3.99 (2H, dd, $J = 5.1, 11.1$ Hz, H-5a), 3.86 (2H, t, $J = 9.4$ Hz, H-2), 3.69-3.63 (2H, m, H-4), 3.48 (2H, t, $J = 9.0$ Hz, H-3), 3.45 (2H, t, $J = 11.3$ Hz, H-5b), 2.74 (4H, t, $J = 6.6$ Hz), 1.75-1.72 (4H, m); ^{13}C NMR (CD_3OD): δ 148.9, 122.3, 90.2, 78.7, 73.9, 70.7, 69.8, 29.7, 25.9; ESI-MS: Calcd for $\text{C}_{18}\text{H}_{29}\text{N}_6\text{O}_8$: 457.2047 $[\text{M}+\text{H}]^+$, Found 456.9333.

Xyloside 6: ^1H NMR (CD_3OD): δ 7.89 (2H, s, triazolyl H), 5.46 (2H, d, $J = 9.4$ Hz, H-1), 4.00 (2H, dd, $J = 5.5, 11.3$ Hz, H-5a), 3.87 (2H, t, $J = 9.4$ Hz, H-2), 3.70-3.64 (2H, m, H-4), 3.49 (2H, t, $J = 9.0$ Hz, H-3), 3.45 (2H, t, $J = 11.3$ Hz, H-5b), 2.71 (4H, t, $J = 7.8$ Hz), 1.75-1.68 (4H, m), 1.42 (2H, p, $J = 7.8$ Hz); ^{13}C NMR (CD_3OD): δ 149.1, 122.3, 90.1, 78.7, 73.9, 70.7, 69.8, 30.0, 29.5, 26.1; ESI-MS: Calcd for $\text{C}_{19}\text{H}_{31}\text{N}_6\text{O}_8$: 471.2203 $[\text{M}+\text{H}]^+$, Found 471.0000.

Xyloside 7: ^1H NMR (CD_3OD): δ 7.89 (2H, s, triazolyl H), 5.45 (2H, d, $J = 9.4$ Hz, H-1), 3.99 (2H, dd, $J = 5.1, 11.3$ Hz, H-5a), 3.87 (2H, t, $J = 9.0$ Hz, H-2), 3.70-3.63 (2H, m, H-4), 3.48 (2H, t, $J = 9.0$ Hz, H-3), 3.45 (2H, t, $J = 11.3$ Hz, H-5b), 2.69 (4H, t, $J = 7.4$ Hz), 1.70-1.66 (4H, m), 1.41-1.38 (4H, m); ^{13}C NMR (CD_3OD): δ 149.2, 122.3, 90.1, 78.7, 73.9, 70.7, 69.8, 30.2, 29.8, 26.1; ESI-MS: Calcd for $\text{C}_{20}\text{H}_{32}\text{N}_6\text{O}_8\text{Na}$: 507.2179 $[\text{M}+\text{Na}]^+$, Found 507.1333.

Xyloside **8**: ^1H NMR (CDCl_3): δ 7.78 (3H, s, triazolyl H), 5.80 (3H, d, $J = 9.0$ Hz, H-1), 5.44-5.38 (6H, m, H-2, H-3), 5.20-5.14 (3H, m, H-4), 4.59 (6H, s), 4.29 (3H, dd, $J = 5.5, 11.5$ Hz, H5-a), 3.60 (3H, t, $J = 11.3$ Hz, H-5b); 3.45 (6H, t, $J = 5.9$ Hz), 2.07 (9H, s, Ac-H), 2.05 (9H, s, Ac-H), 1.98-1.94 (6H, m), 1.86 (9H, s, Ac-H), 1.51-1.44 (6H, m); ESI-MS: Calcd for $\text{C}_{53}\text{H}_{76}\text{N}_{10}\text{O}_{26}\text{Na}$: 1275.4517 $[\text{M}+\text{Na}]^+$, Found 1275.2039.

Xyloside **9**: ^1H NMR (MeOD): δ 8.23 (3H, s, triazolyl H), 7.97 (3H, s, triazolyl H), 6.02 (3H, d, $J = 9.0$ Hz, H-1), 5.57 (3H, t, $J = 9.4$ Hz, H-2), 5.49 (3H, t, $J = 9.4$ Hz, H-3), 5.23-5.163 (3H, m, H-4), 4.64 (6H, s), 4.62 (6H, s), 4.37 (6H, t, $J = 6.6$ Hz), 4.23 (3H, dd, $J = 5.5$ Hz, 11.5 Hz, H-5a), 3.76 (3H, t, $J = 10.9$ Hz, H-5b), 3.64-3.59 (36H, m), 2.04 (9H, s, Ac-H), 2.01 (9H, s, Ac-H), 1.89-1.84 (6H, m), 1.82 (9H, s, Ac-H), 1.65 (6H, m); ^{13}C NMR (CD_3OD): δ 171.5, 171.5, 170.5, 146.7, 125.4, 124.2, 94.4, 87.2, 73.8, 72.0, 71.5, 71.5, 70.8, 70.7, 69.8, 66.2, 65.0, 64.8, 50.7, 33.0, 25.4, 20.6, 20.6, 20.2. ESI-MS: Calcd for $\text{C}_{79}\text{H}_{117}\text{N}_{19}\text{O}_{35}\text{Na}$: 1914.7857 $[\text{M}+\text{Na}]^+$, Found 1914.4667.

Xyloside **12**: ^1H NMR (CD_3OD): δ 8.16 (2H, s, triazolyl H), 7.37 (1H, s, Ar-H), 7.33-7.28 (3H, m, Ar-H), 5.52 (2H, d, $J = 9.4$ Hz, H-1), 4.65 (4H, s), 4.58 (4H, s), 4.01 (2H, dd, $J = 5.5, 11.3$ Hz, H-5a), 3.90 (2H, t, $J = 9.0$ Hz, H-2), 3.709-3.647 (2H, m, H-4), 3.50 (2H, t, $J = 9.4$ Hz, H-3), 3.47 (2H, t, $J = 10.9$ Hz, H-5b); ^{13}C NMR (CD_3OD): 144.8, 138.3, 128.4, 127.4, 127.3, 123.1, 89.0, 77.4, 72.7, 72.0, 69.5, 68.7, 62.8; ESI-MS: Calcd for $\text{C}_{24}\text{H}_{33}\text{N}_6\text{O}_{10}$: 565.2258 $[\text{M}+\text{H}]^+$, found 565.1189.

Xyloside **13**: ^1H NMR (CD_3OD): δ 8.14 (2H, s, triazolyl H), 7.34 (4H, s), 5.51 (2, d, $J = 9.4$ Hz, H-1), 4.65 (4H, s), 4.58 (4H, s), 4.01 (2H, dd, $J = 5.1, 11.1$ Hz, H-5a), 3.88 (2H, t, $J = 9.4$ Hz, H-2), 3.71-3.64 (2H, m, H-4), 3.49 (2H, t, $J = 9.4$ Hz, H-3), 3.46

(2H, t, $J = 10.9$ Hz, H-5b); ESI-MS: Calcd for $C_{24}H_{32}N_6O_{10}Na$: 587.2078 $[M+Na]^+$, found 587.2000.

Xyloside **14**: 1H NMR (CD_3OD): δ 7.91 (2H, s, triazolyl H), 7.22 (1H, s, Ar-H), 7.21 (2H, d, $J = 7.0$ Hz, Ar-H), 7.29 (1H, t, $J = 7.0$ Hz, Ar-H), 5.46 (2H, d, $J = 9.0$ Hz, H-1), 4.51 (4H, s), 3.99 (2H, dd, $J = 5.5, 11.3$ Hz, H-5a), 3.86 (2H, t, $J = 9.0$ Hz, H-2), 3.74 (4H, t, $J = 6.6$ Hz), 3.67-3.63 (2H, m), 3.49 (2H, t, $J = 9.0$ Hz, H-3), 3.45 (4H, t, $J = 10.9$ Hz, H-5b), 3.00 (4H, t, $J = 6.6$ Hz); ESI-MS: Calcd for $C_{26}H_{36}N_6O_{10}Na$: 615.2391 $[M+Na]^+$, found 615.1550.

Xyloside **15**: 1H NMR (CD_3OD): δ 7.83 (2H, s, triazolyl H), 7.34-7.25 (4H, m), 5.44 (2H, d, $J = 9.0$ Hz, H-1), 4.51 (4H, s), 3.99 (2H, dd, $J = 5.5, 11.3$ Hz, H-5a), 3.83 (2H, t, $J = 9.0$ Hz, H-2), 3.70-3.64 (2H, m), 3.54-3.42 (8H, m), 2.81 (4H, t, $J = 7.8$ Hz), 1.99-1.92 (4H, m); ESI-MS: Calcd for $C_{28}H_{46}N_6O_{10}Na$: 643.2704 $[M+Na]^+$, found 643.2667.

Xyloside **16**: 1H NMR (CD_3OD): δ 8.33 (2H, s, triazolyl H), 7.81 (2H, d, $J = 8.6$ Hz, Ar-H), 7.35 (2H, t, $J = 7.8$ Hz, Ar-H), 7.10 (2H, d, $J = 7.8$ Hz, Ar-H), 5.55 (2H, d, $J = 9.0$ Hz, H-1), 5.35 (4H, s), 4.02 (2H, dd, $J = 5.5, 11.3$ Hz, H-5a), 3.93 (2H, t, $J = 9.0$ Hz, H-2), 3.74-3.65 (2H, m, H-4), 3.50 (2H, t, $J = 9.0$ Hz, H-3), 3.48 (2H, t, $J = 11.3$ Hz, H-5b); ^{13}C NMR (CD_3OD): δ 155.2, 145.1, 128.1, 126.3, 124.6, 115.9, 107.2, 90.3, 78.6, 73.9, 70.7, 69.9, 62.7; ESI-MS: Calcd for $C_{26}H_{29}N_6O_{10}$: 585.1945 $[M-H]^-$, found 585.0000.

Xyloside **17**: 1H NMR (CD_3OD): δ 8.32 (2H, s, triazolyl H), 7.73 (2H, d, $J = 9.0$ Hz, Ar-H), 7.39 (2H, s, Ar-H), 7.18 (2H, d, $J = 9.0$ Hz, Ar-H), 5.55 (2H, d, $J = 9.0$ Hz, H-1), 5.29 (4H, s), 4.01 (2H, dd, $J = 5.5, 11.3$ Hz, H-5a), 3.91 (2H, t, $J = 9.4$ Hz, H-2), 3.70-3.64 (2H, m, H-4), 3.49 (2H, t, $J = 9.4$ Hz, H-3), 3.48 (2H, t, $J = 10.94$ Hz, H-5b);

^{13}C NMR (CD_3OD): δ 156.4, 145.1, 131.4, 129.6, 124.7, 120.2, 108.6, 90.2, 78.7, 73.9, 70.7, 69.9, 62.4; ESI-MS: Calcd for $\text{C}_{26}\text{H}_{29}\text{N}_6\text{O}_{10}$: 585.1945 [M-H], found 585.0667.

Xyloside **18**: ^1H NMR (CD_3OD): δ 8.22 (2H, s, triazolyl H), 5.73 (2H, s), 5.55 (2H, d, $J = 9.4$ Hz, H-1), 4.60 (4H, s), 4.12 (4H, s), 4.01 (2H, dd, $J = 5.5, 11.3$ Hz, H-5a), 3.91 (2H, t, $J = 9.4$ Hz, H-2), 3.67-3.53 (2H, m, H-4), 3.51-3.44 (4H, m, H-3, H-5b); Calcd $\text{C}_{20}\text{H}_{30}\text{N}_6\text{O}_{10}\text{Na}$: 537.202 [M+Na] $^+$, found 537.151

5.5.2. Screening of Cluster-xylosides in CHO Cells

To determine whether cluster-xylosides were able to prime GAG chains, the cells were treated with cluster-xylosides at 100 μM or 1 mM concentration in the presence of ^3H -glucosamine. Primed GAGs were purified and analyzed as described below. 4×10^5 cells were seeded per well in complete growth medium in a 6-well plate. The cells were incubated at 37 $^\circ\text{C}$ in a humidified incubator for 24 h to 50% confluency. The cells were then washed with sterile PBS and replaced with 990 μL DMEM containing 10% dialyzed FBS and 1mM of glucose. A solution containing a specific primer at 100x the final concentration was prepared. 10 μL of appropriate 100X primer stock were added to various wells to achieve an appropriate concentration. 100 μCi of ^3H -glucosamine was also added to each well as tracer. The 6-well plates were incubated at 37 $^\circ\text{C}$ in a humidified incubator (5% CO_2) for 24 h.

5.5.3. Purification and Quantitation of GAG Chains

The entire content of each well was transferred to a microcentrifuge tube and subjected to centrifugation at 16000xg for 5 minutes. The supernatant was transferred to a fresh tube and 0.016% Triton X-100 (1.5 volumes) was added. The diluted

supernatant was loaded on 0.2 ml DEAE-sepharose column pre-equilibrated with 2ml of wash buffer (20mM NaOAc, 0.1 M NaCl and 0.01% Triton X-100, pH 6.0) and the column was washed with 6 ml of wash buffer. The bound HS/CS was eluted with 1.2 ml of elution buffer (20mM NaOAc and 1M NaCl, pH 6.0). The priming activity of cluster-xylosides was evaluated by measuring the 3H-radioactivity incorporated into the purified GAG chains using liquid scintillation counter.

5.5.4. Analysis of Primed GAG Chains

Anion-exchange HPLC analysis: The purified GAG chains were analyzed by HPLC with an inline radiometric detector. Xyloside primed GAG chains of equal quantity were diluted five-fold with HPLC solvent A (10 mM KH_2PO_4 , pH 6.0, 0.2% CHAPS) for anion-exchange chromatography analysis. The sample was loaded on a HPLC-DEAE column and eluted from the column with a linear gradient of 0.2 M - 1 M NaCl over 80 minutes at a flow rate of 1ml/min. The radiolabeled GAG chains were detected by a radiometric flow-one A505A detector. The HPLC effluent was mixed with Ultima-Flo AP scintillation cocktail at 1:2 ratio and detected in the flow scintillation analyzer.

Size exclusion HPLC analysis: The chain length of the GAG chains synthesized by various cluster-xylosides was determined by measuring the migration time on two tandem G3000SWXL (Tosoh, 7.8 mm x 30 cm) size exclusion columns using the HPLC Hitachi system with an inline radiodetector. The solvent containing phosphate (100 mM KH_2PO_4 , 100 mM NaCl, pH 6) was used as an eluent. The average molecular weight was determined by measuring the migration time of GAG chains in comparison to those of polystyrene sulfonate standards examined under similar conditions.

Compositional analysis: The HS/CS composition of the primed GAG chains was determined by digesting the GAG chains with heparitinase I/II/III or chondroitinase ABC enzymes. The solution containing GAGs was diluted to 0.2 M NaCl, followed by the addition of heparitinase or chondroitinase ABC buffer and 5 mU of heparitinase I/II/III or chondroitinase ABC enzyme. The reaction mixture was incubated at 37 °C for 2 h, the solution was then loaded onto two tandem G3000 SWXL columns (7.8 mm x 30 cm) and analyzed with the aid of an inline radiometric detector using phosphate buffer (100 mM KH₂PO₄, 100 mM NaCl, pH 6) as an eluent. The percentage of HS/CS was determined based on the percentage area of undigested and digested GAG peaks.

Disaccharide analysis: the disaccharide composition of CS chains was determined by digesting the GAG chains with chondroitinase ABC enzymes. The enzyme treated GAG chains were loaded to SAX-HPLC with inline flow scintillation analyzer along with CS disaccharide standards “ Δ UA-GalNAc, Δ UA-GalNAc2S, Δ UA-GalNAc4S, Δ UA-GalNAc6S”. The sample was eluted from the column with a linear gradient of 0 M – 0.18 M NaCl over 100 minutes at a flow rate of 0.5 ml/min. The radiolabeled GAG chains were detected by a radiometric flow-one A505A detector. The HPLC effluent was mixed with Ultima-Flo AP scintillation cocktail at 1:2 ratio and detected in the flow scintillation analyzer.

Periodate oxidation-alkaline elimination reactions: Mono- and bis-primed GAG chains were subjected to periodate oxidation using 0.02 M NaIO₄, 0.1 M sodium formate, pH 4.0 at 4 °C for 30 minutes. The reaction was stopped by addition of 0.04 M mannitol. The samples were desalted using 3000 cutoff membrane columns and subjected to alkali treatment with 0.1 M NaOH at pH 12 at 4 °C for 5 minutes (18).

Ozonolysis of GAG chains: bis-xyloside **18** primed GAG chains were subjected to ozonolysis using ozone solution in dichloromethane. The reaction mixture was stirred for 30 minutes. The chain length of the GAG layer in water that was separated from the dichloromethane layer was determined by measuring the migration time on two tandem G3000SWXL (Tosoh, 7.8 mm x 30 cm) size exclusion columns using the HPLC Hitachi system with an inline radiodetector.

5.6. Supporting Information

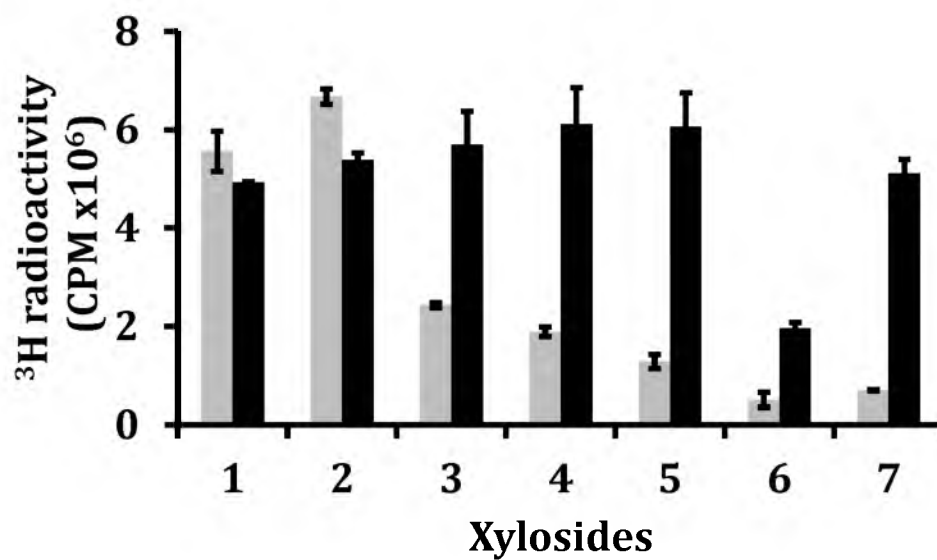


Figure S5.1. Comparison of priming activity of mono-xylosides and bis-xylosides. PgsA-745 cells were incubated with the mono-xylosides (**1** and **2**) and bis-xylosides (**3**, **4**, **5**, **6** and **7**) at 100 μ M for 24 h. The primed GAG chains were then purified and quantitated using a liquid scintillation counter

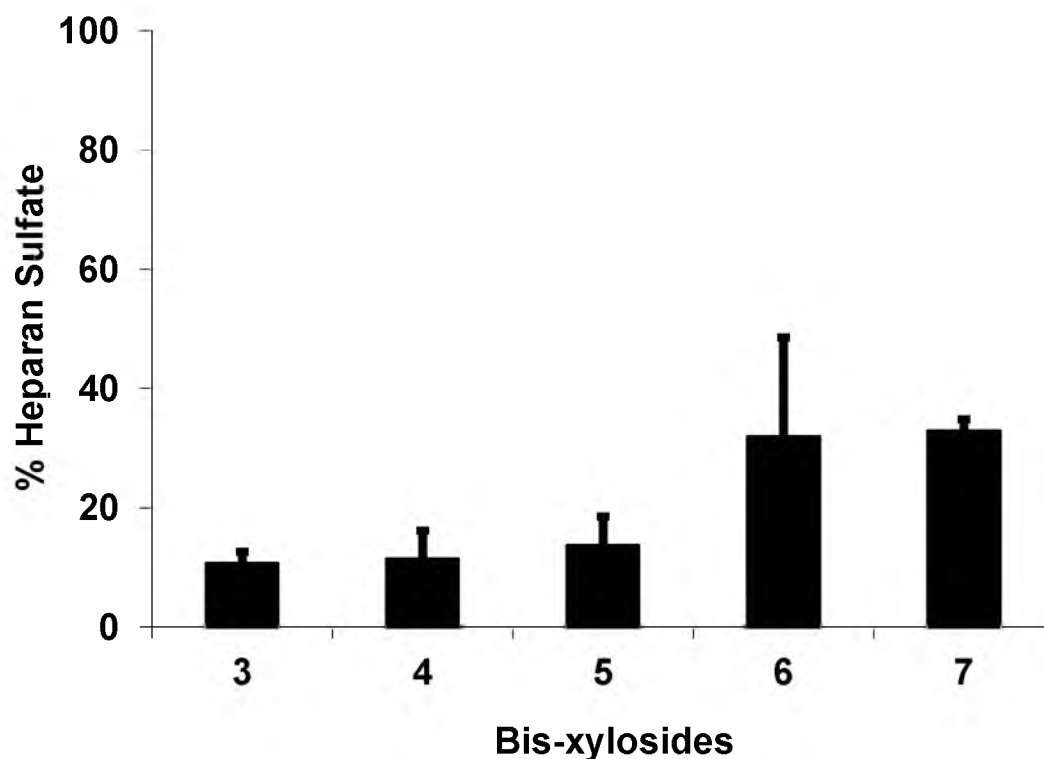


Figure S5.2. HS and CS compositions of GAG chains primed by bis-xyloside. PgsA-745 cells were incubated with the bis-xyloside (3, 4, 5, 6 and 7) at 100 μ M for 24 h. The primed GAG chains were then purified as described in the experimental section. The HS/CS composition of the primed GAG chains was determined by digesting the GAG chains with heparitinase I, II, III and chondroitinase ABC enzymes. The reaction mixture was incubated at 37 $^{\circ}$ C for 2 h, the solution was then loaded onto two tandem G3000 SWXL columns (7.8 mm x 30 cm) and analyzed with the aid of an inline radiometric detector using phosphate buffer (100 mM KH_2PO_4 , 100 mM NaCl, pH 6) as an eluent. The HS/CS composition was determined based on the percentage area of undigested and digested GAG peak.

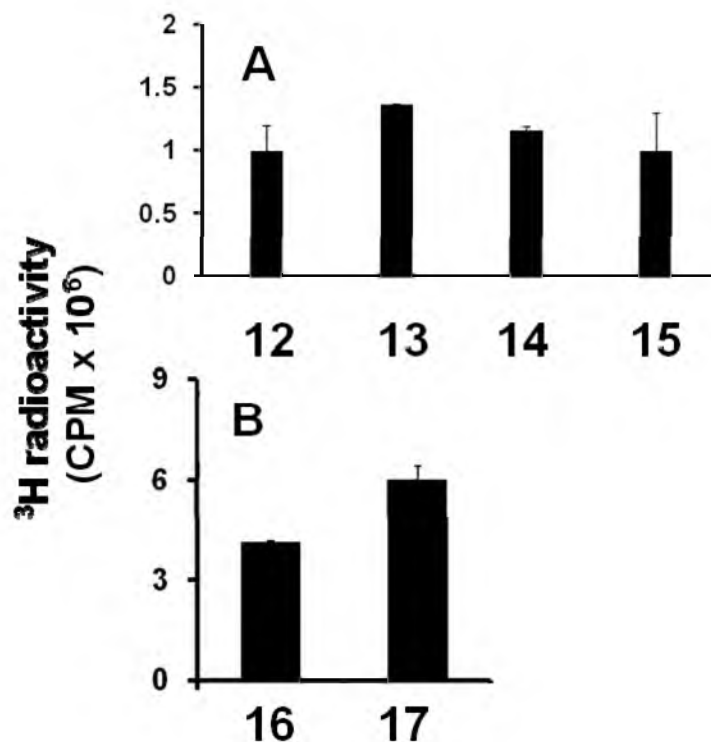


Figure S5.3. GAG priming activity was determined at 100 μM concentration by bis-xylosides. A: Priming activity of bis-xylosides (12 and 13). B: priming analysis of bis-xylosides (14, 15, 16 and 17). C: Priming activity of bis-xylosides (18 and 19). The priming ability of bis-xylosides were examined using xylosyl transferase deficient CHO cells (pgsA-745). 400,000 cells were seeded in wells of 6-well plates and treated with bis-xylosides at 100 μM in the presence of 100 μCi of D -[6- ^3H]-glucosamine. The medium was removed from the well at 24 h, GAG chains were purified and quantified as described in the experimental section.

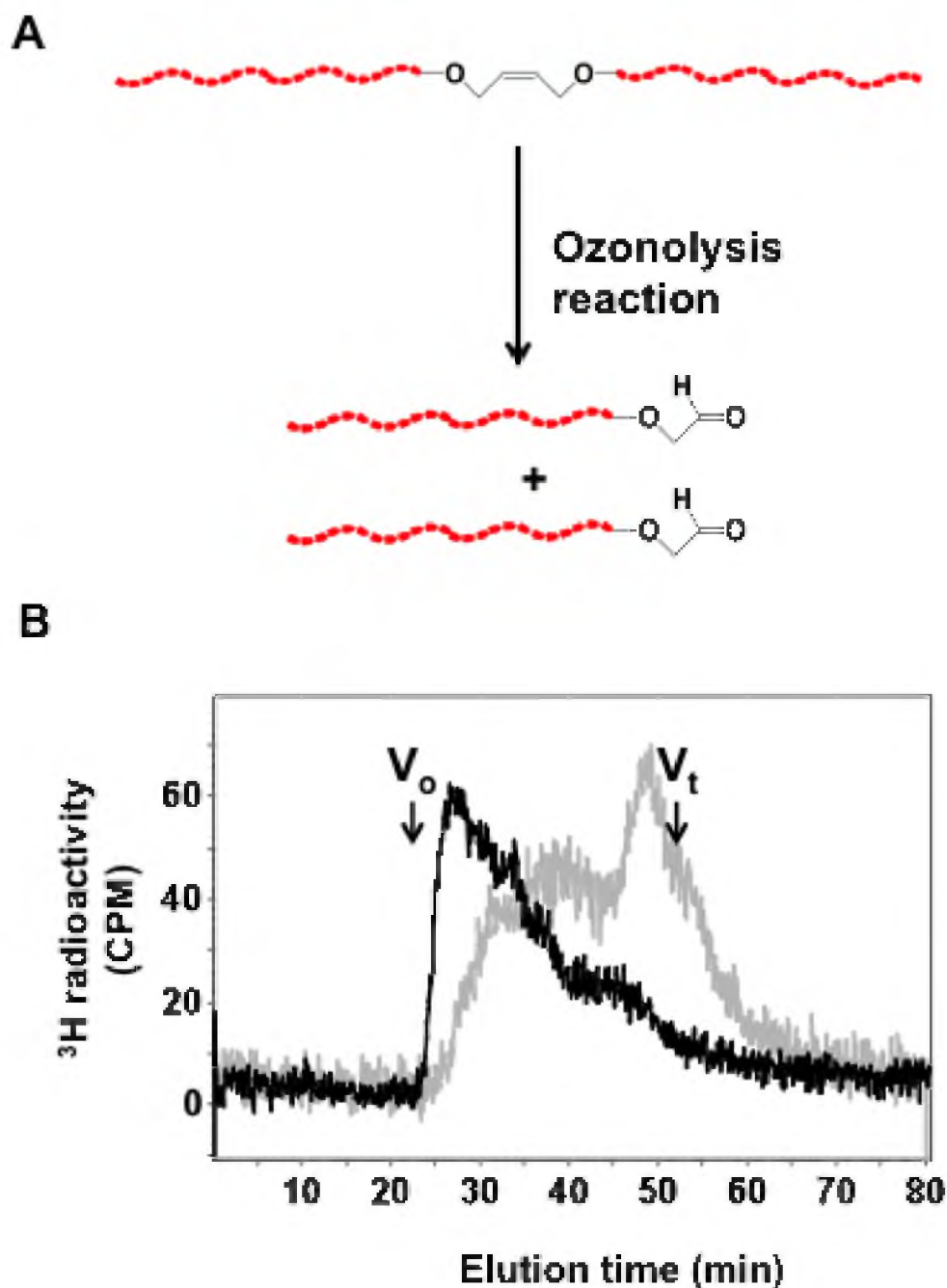


Figure S5.4. Ozonolysis of GAG chains. GAG chains, which were primed by bis-xyloside **19** at 100 μM , were subjected to ozonolysis reactions. **A:** two GAG chains per scaffold were primed by bis-xylosides **19** cleaved by ozone solution. **B:** The elution profiles of GAG chains primed by bis-xyloside **19** (black trace) and ozonolysis of GAG chains primed by bis-xyloside **19** (gray trace).

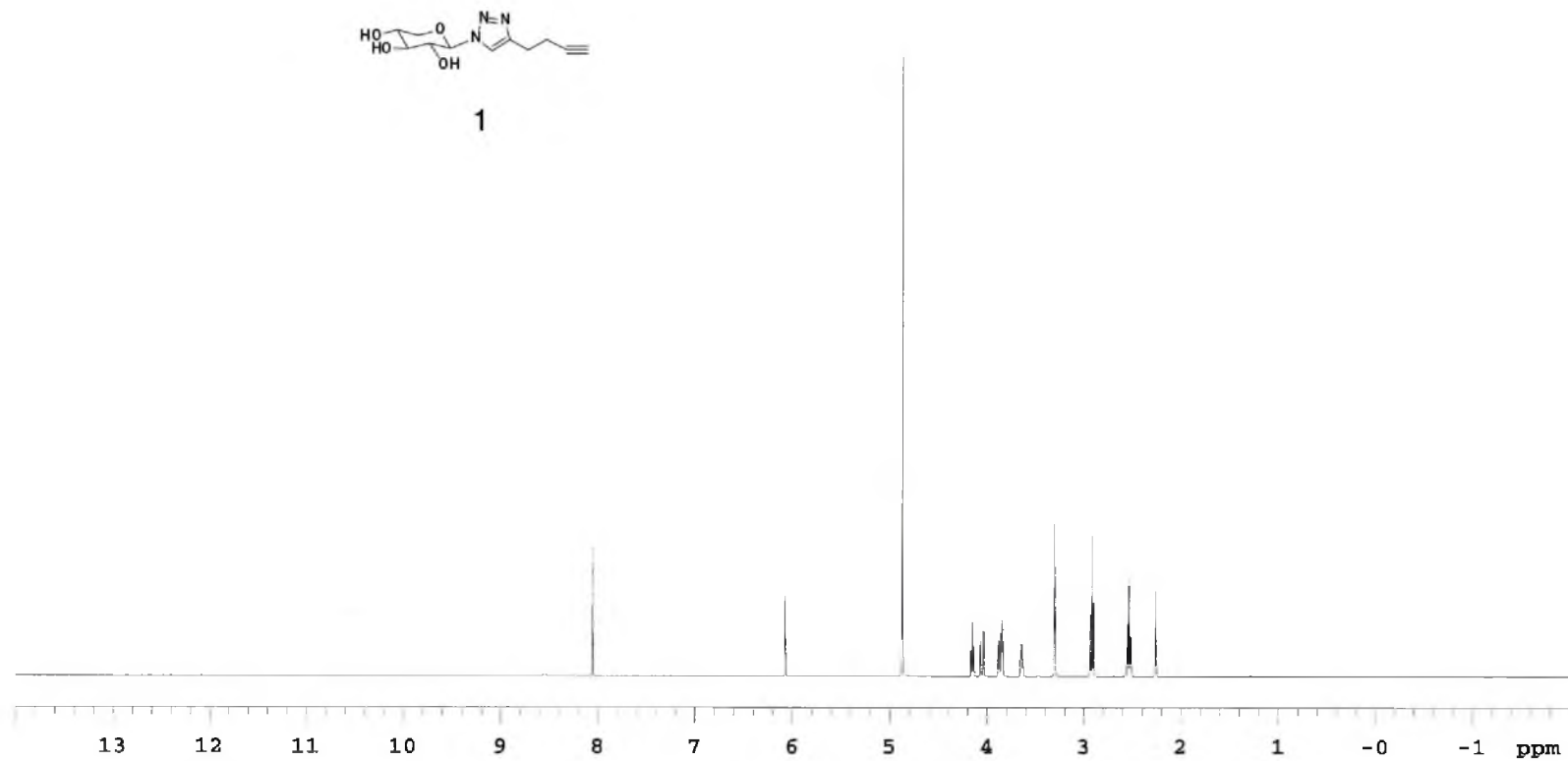


Figure S5.5. NMR spectra of cluster-xyloside 1

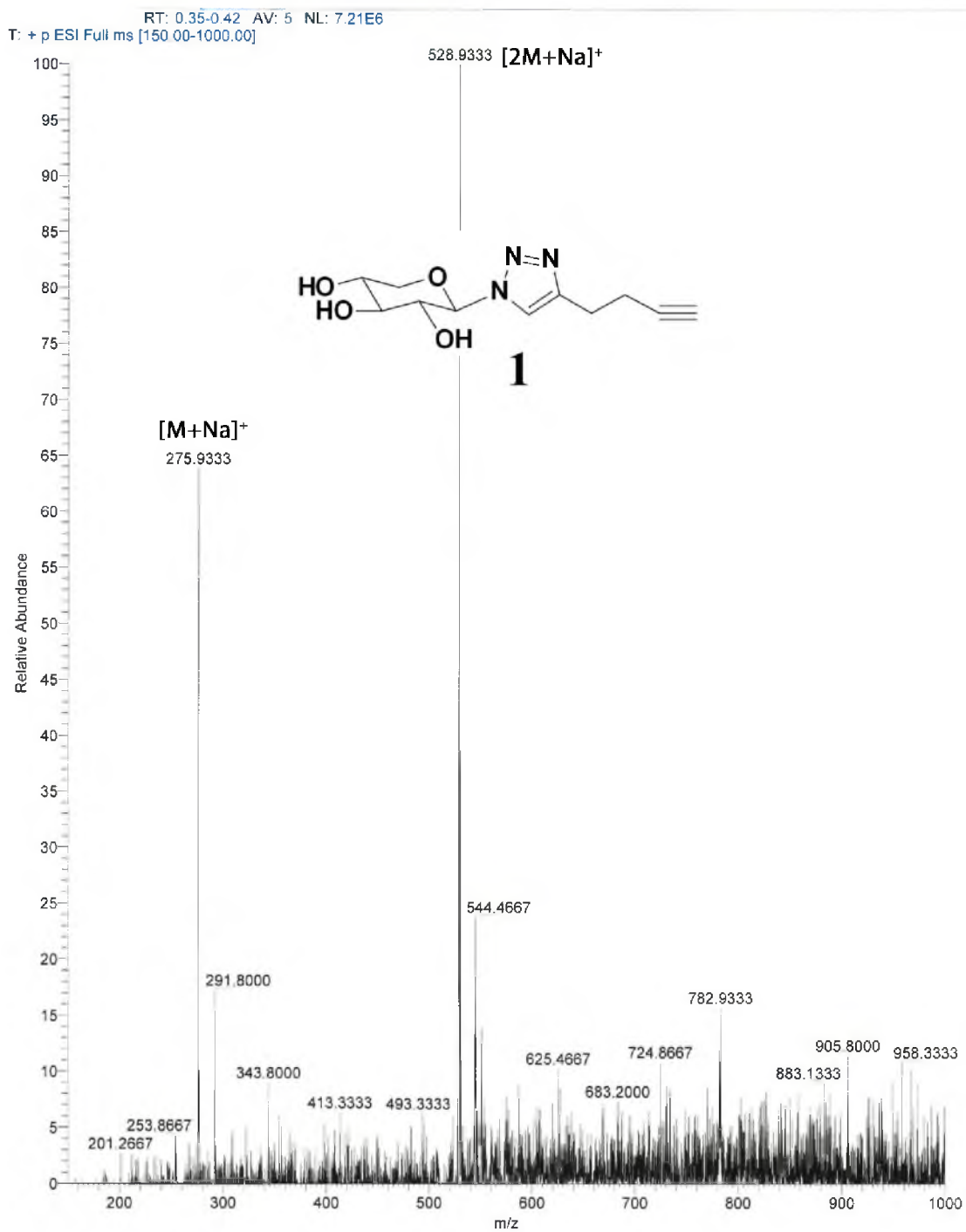


Figure S5.6. Mass spectra of cluster-xyloside 1

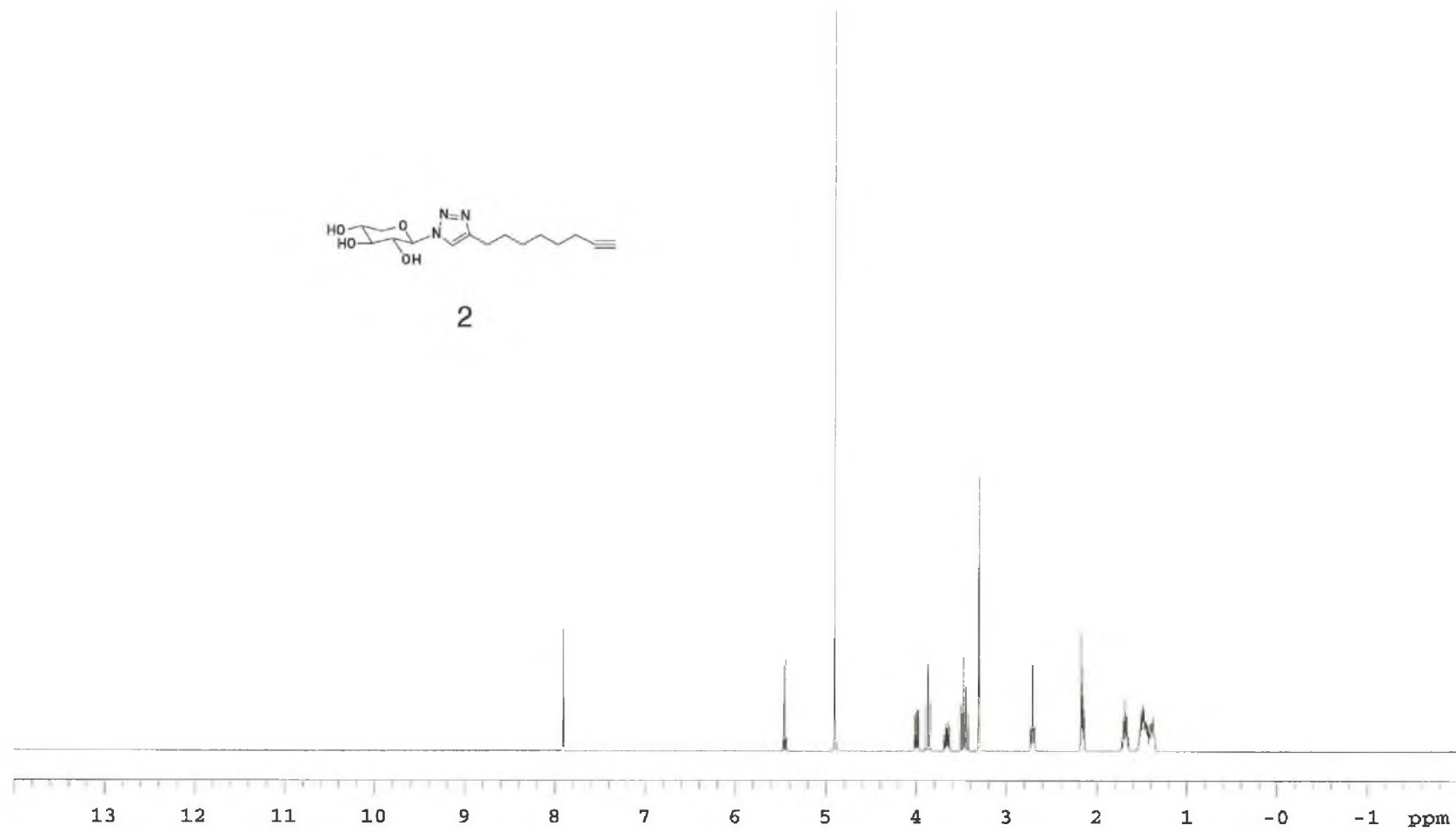


Figure S5.7. NMR spectra of cluster-xyloside 2

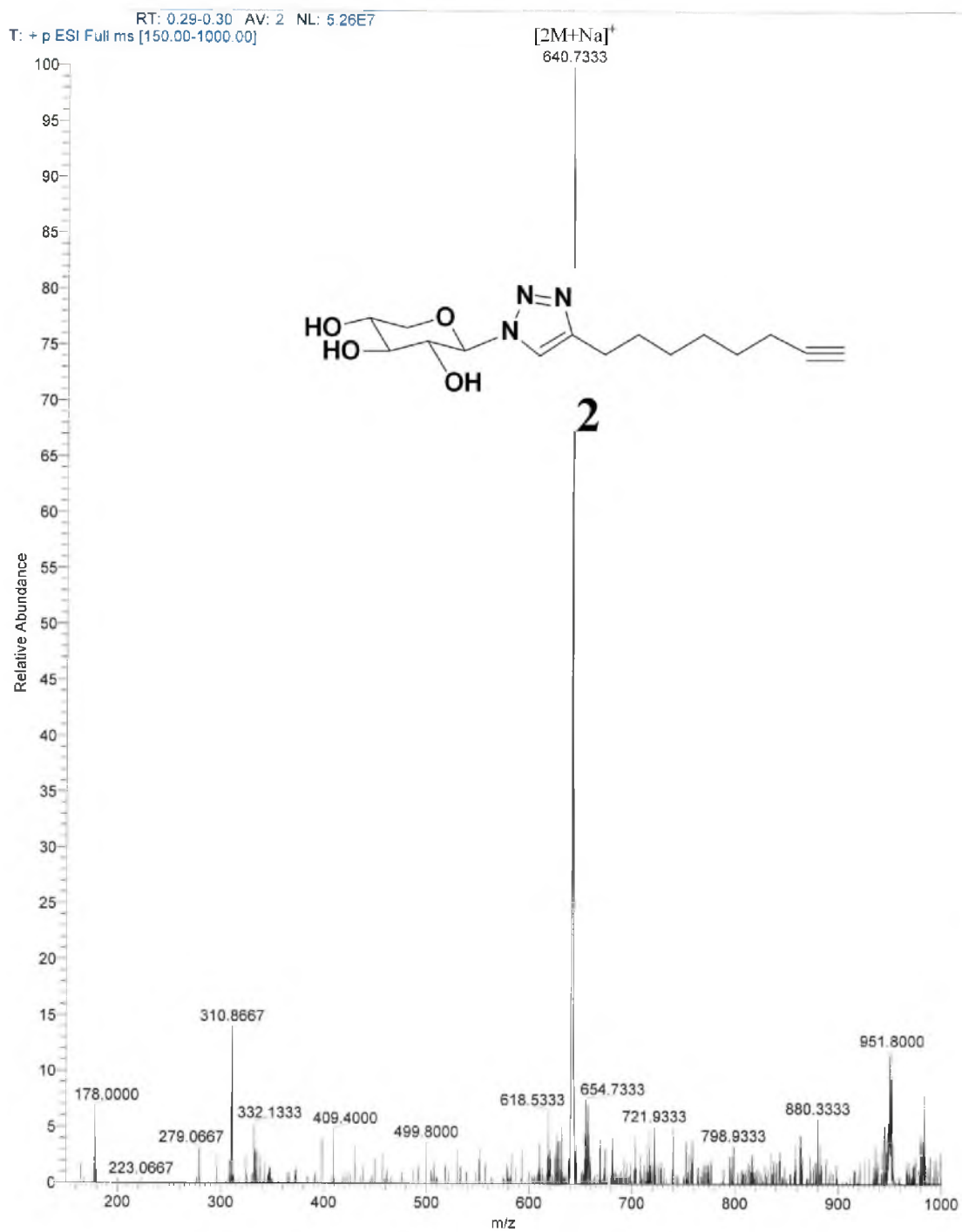
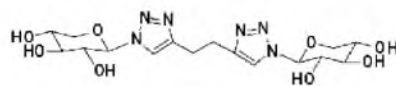


Figure S5.8. Mass spectra of cluster-xyloside 2



3

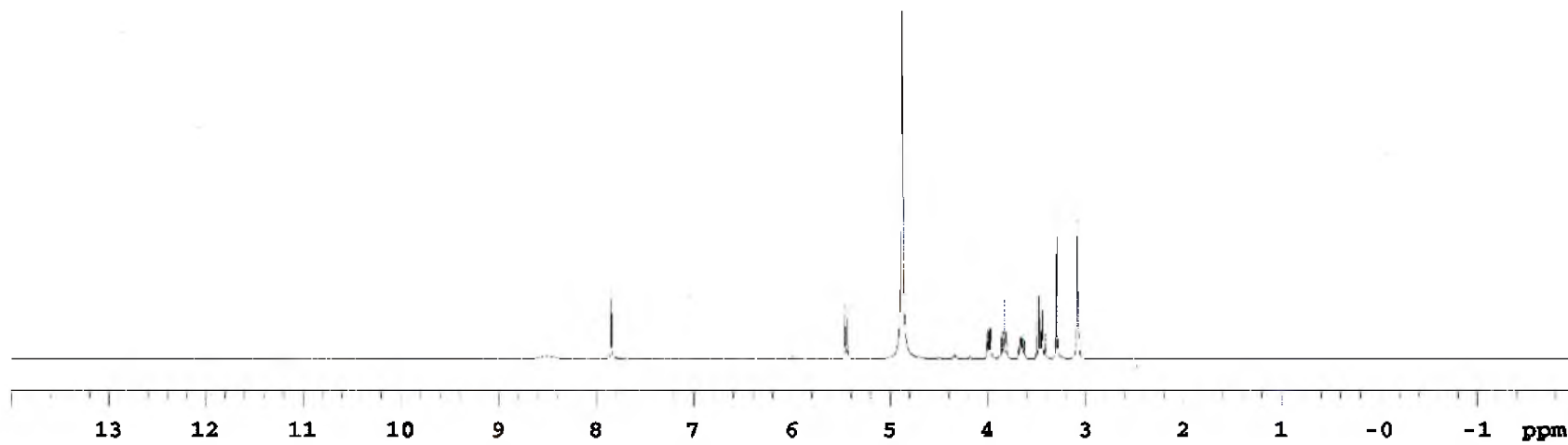


Figure S5.9. NMR spectra of cluster-xyloside 3

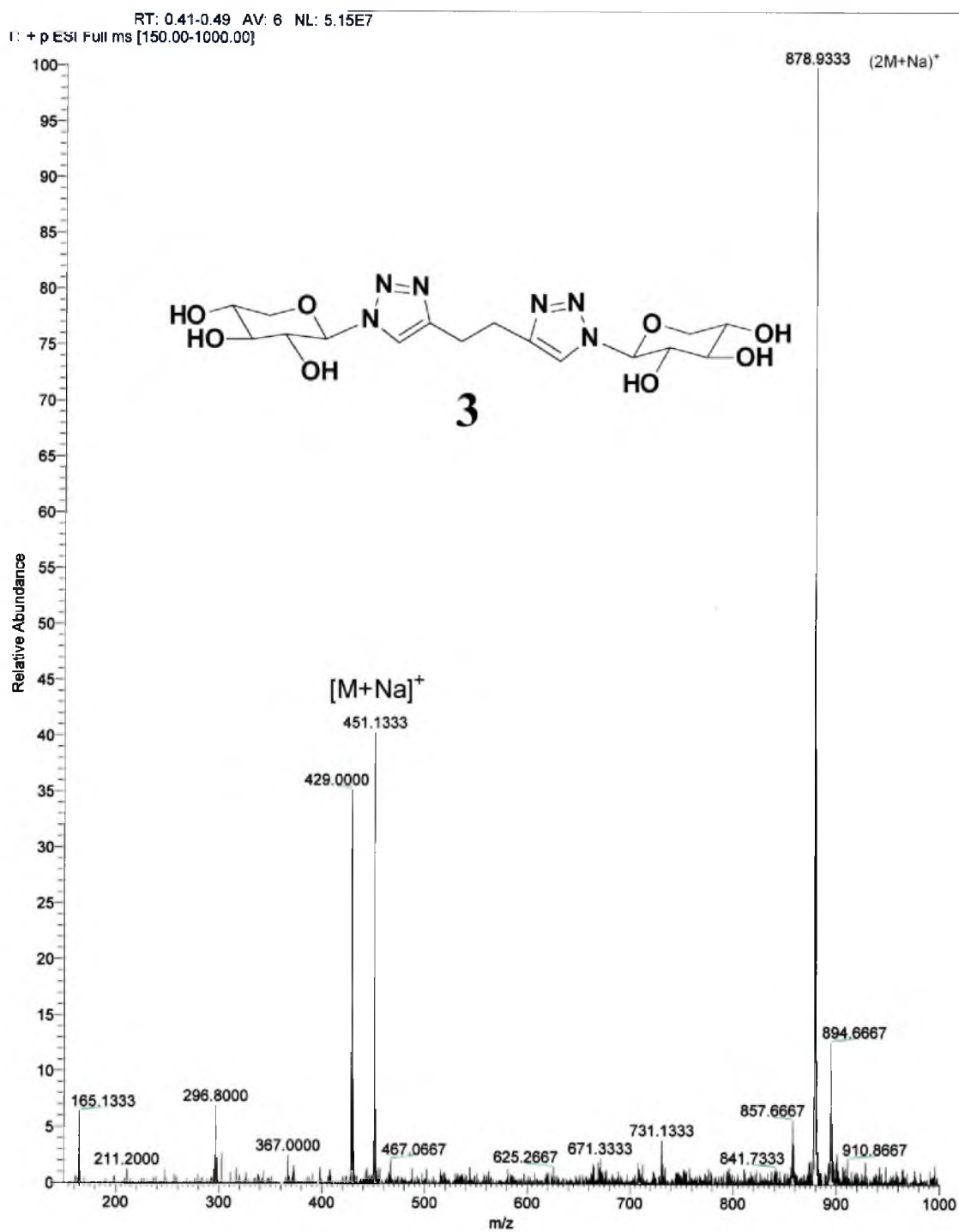


Figure S5.10. Mass spectra of cluster-xyloside 3

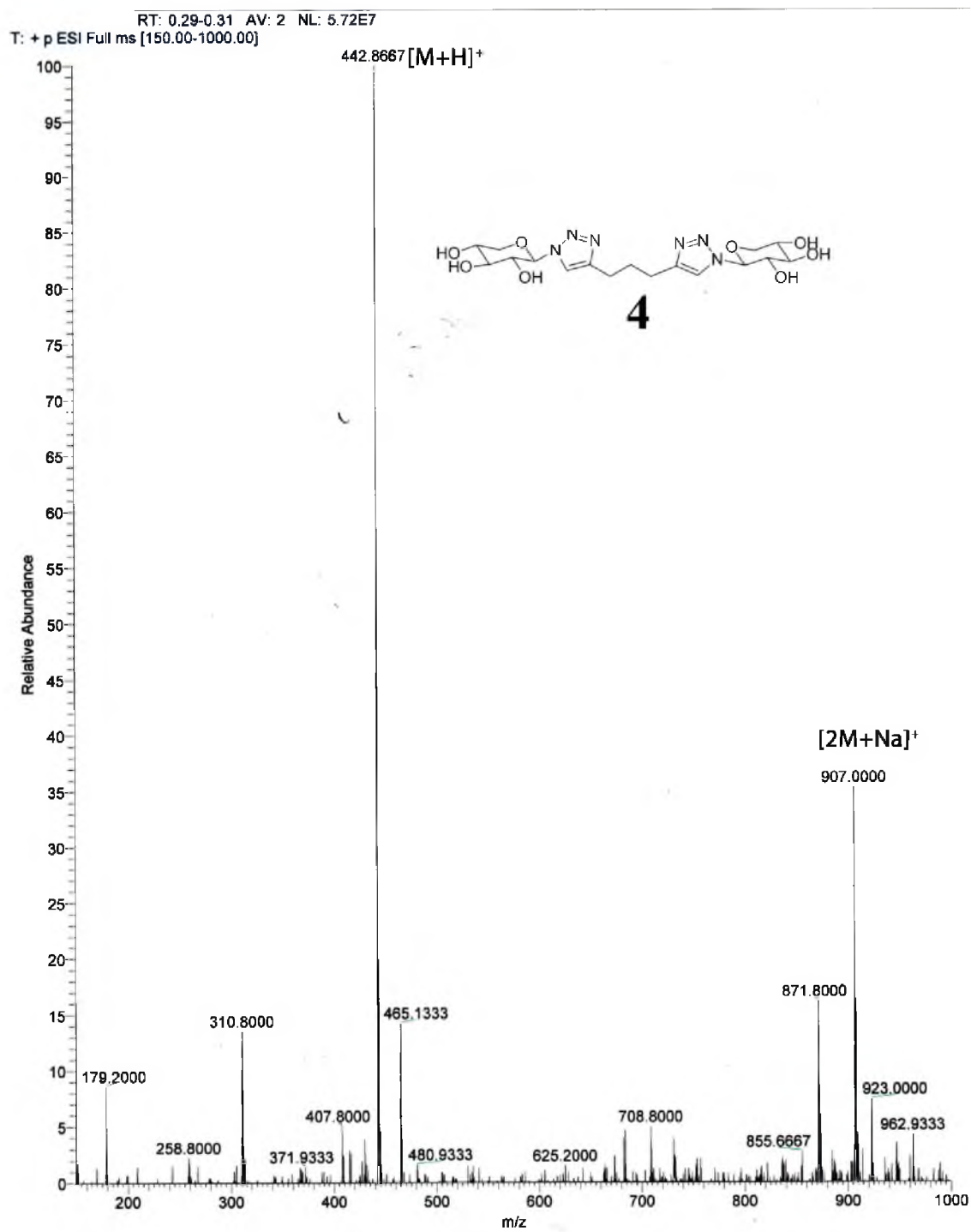
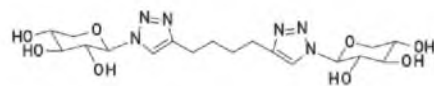


Figure S5.12. Mass spectra of cluster-xyloside 4



5

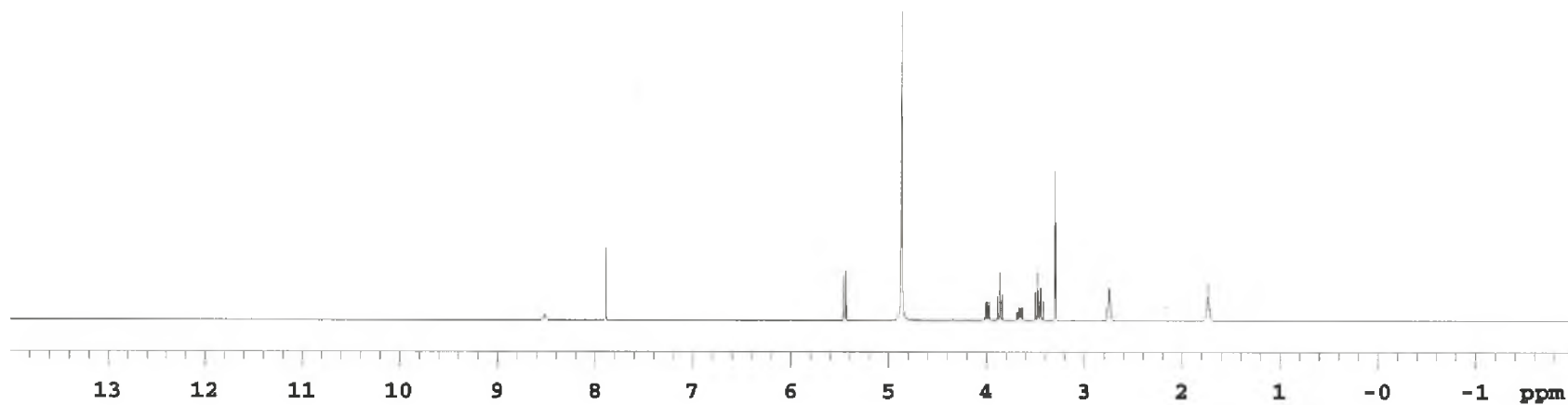


Figure S5.13. NMR spectra of cluster-xyloside 5

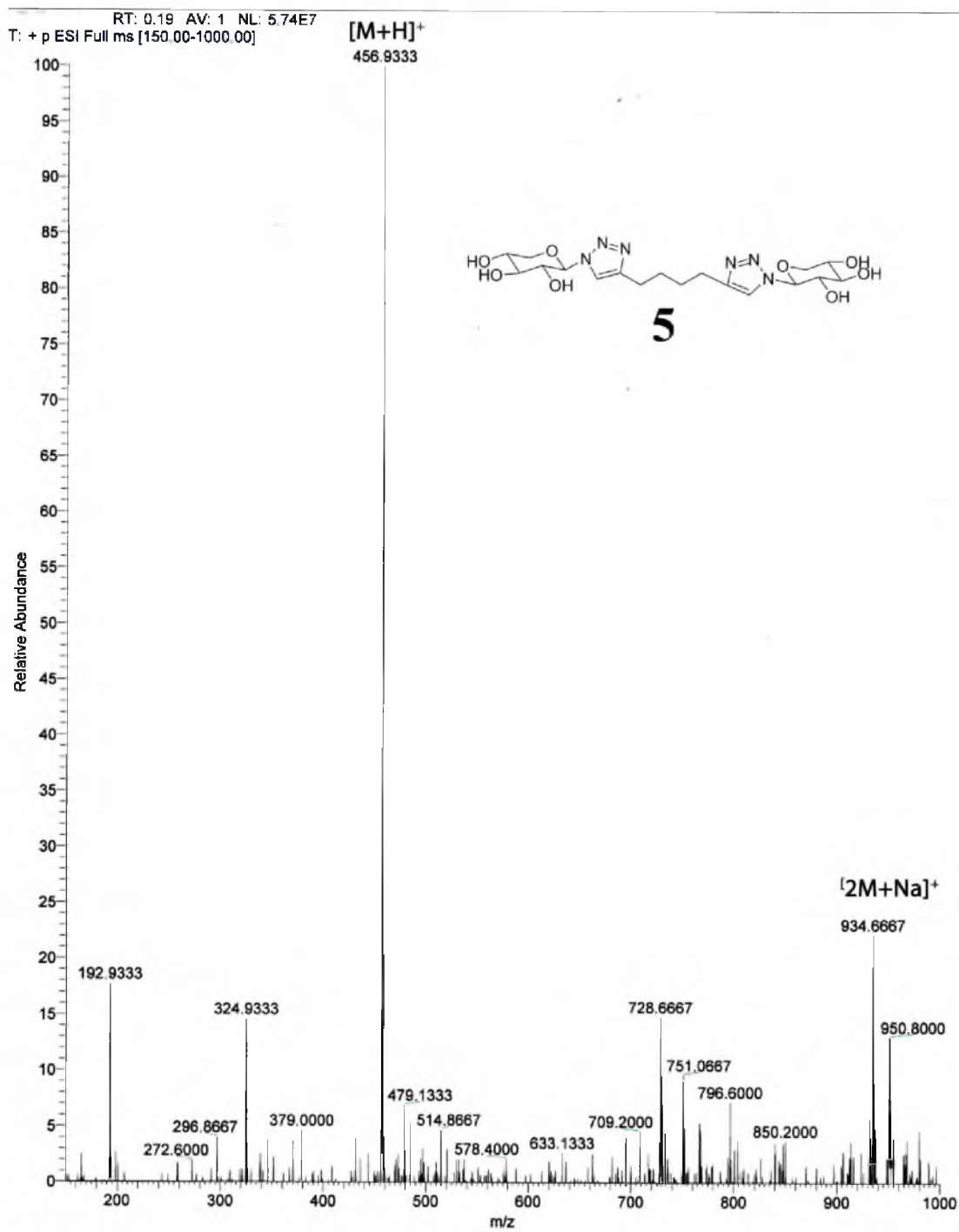
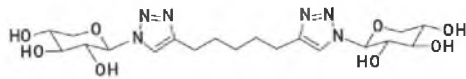


Figure S5.14. Mass spectra of cluster-xyloside 5



6

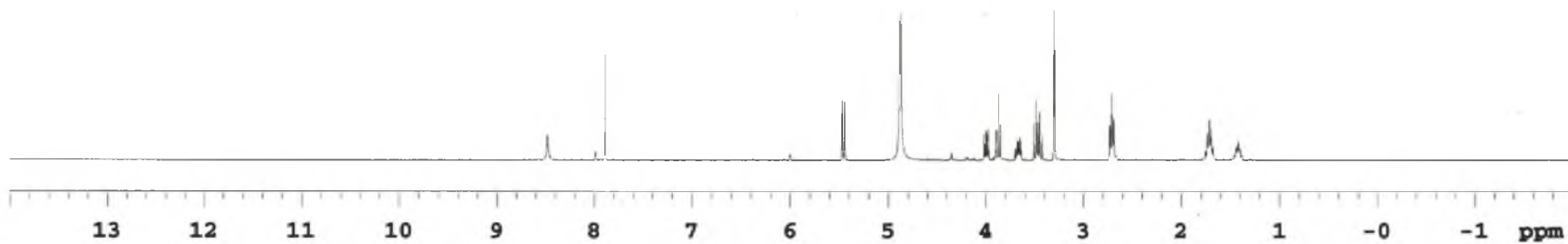


Figure S5.15. NMR spectra of cluster-xyloside 6

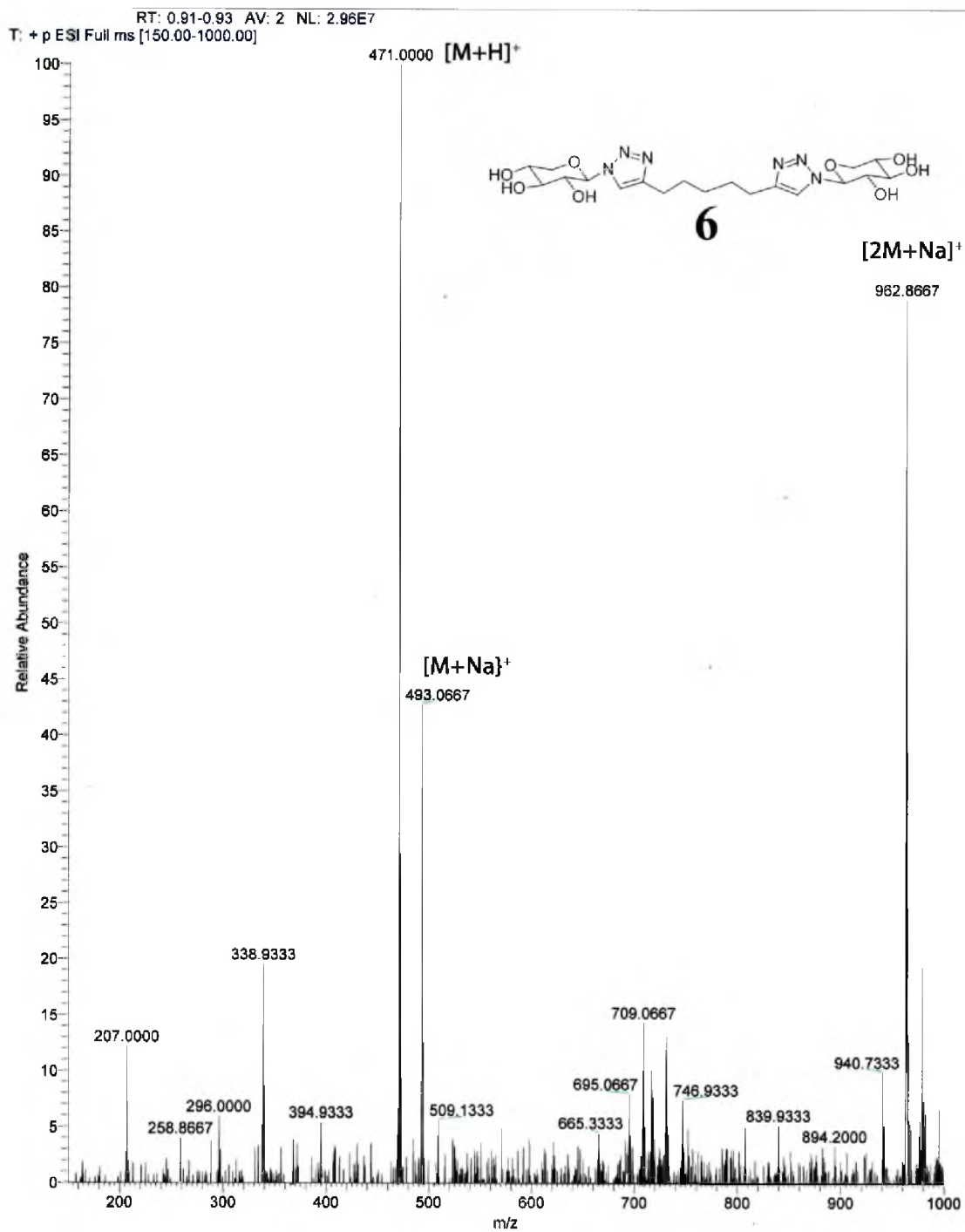
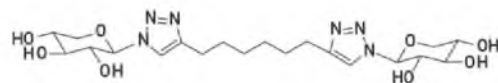


Figure S5.16. Mass spectra of cluster-xyloside 6



7

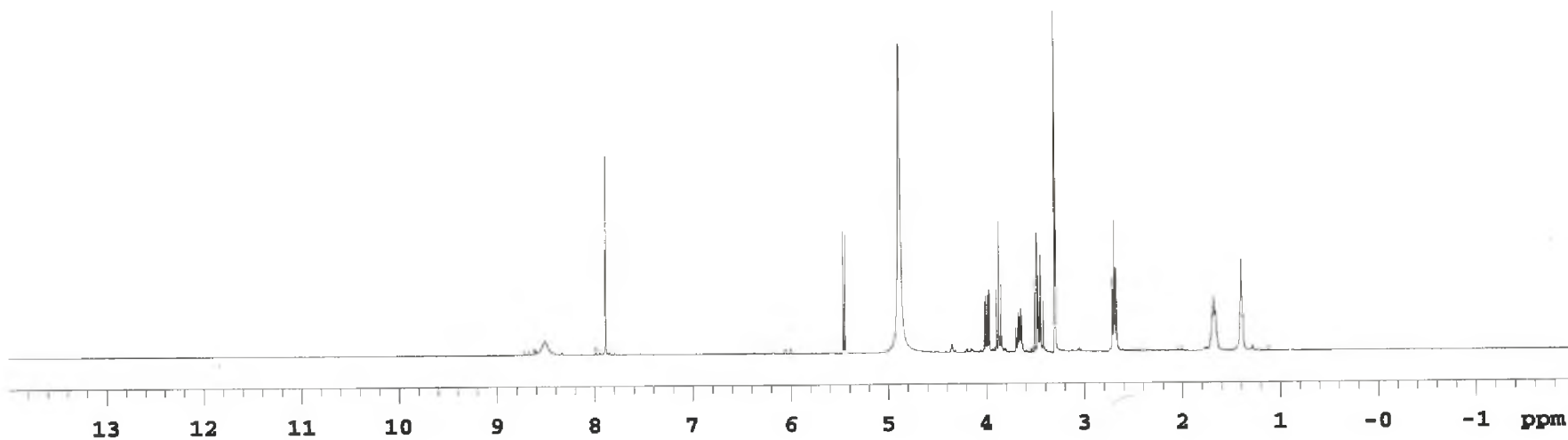


Figure S5.17. NMR spectra of cluster-xyloside 7

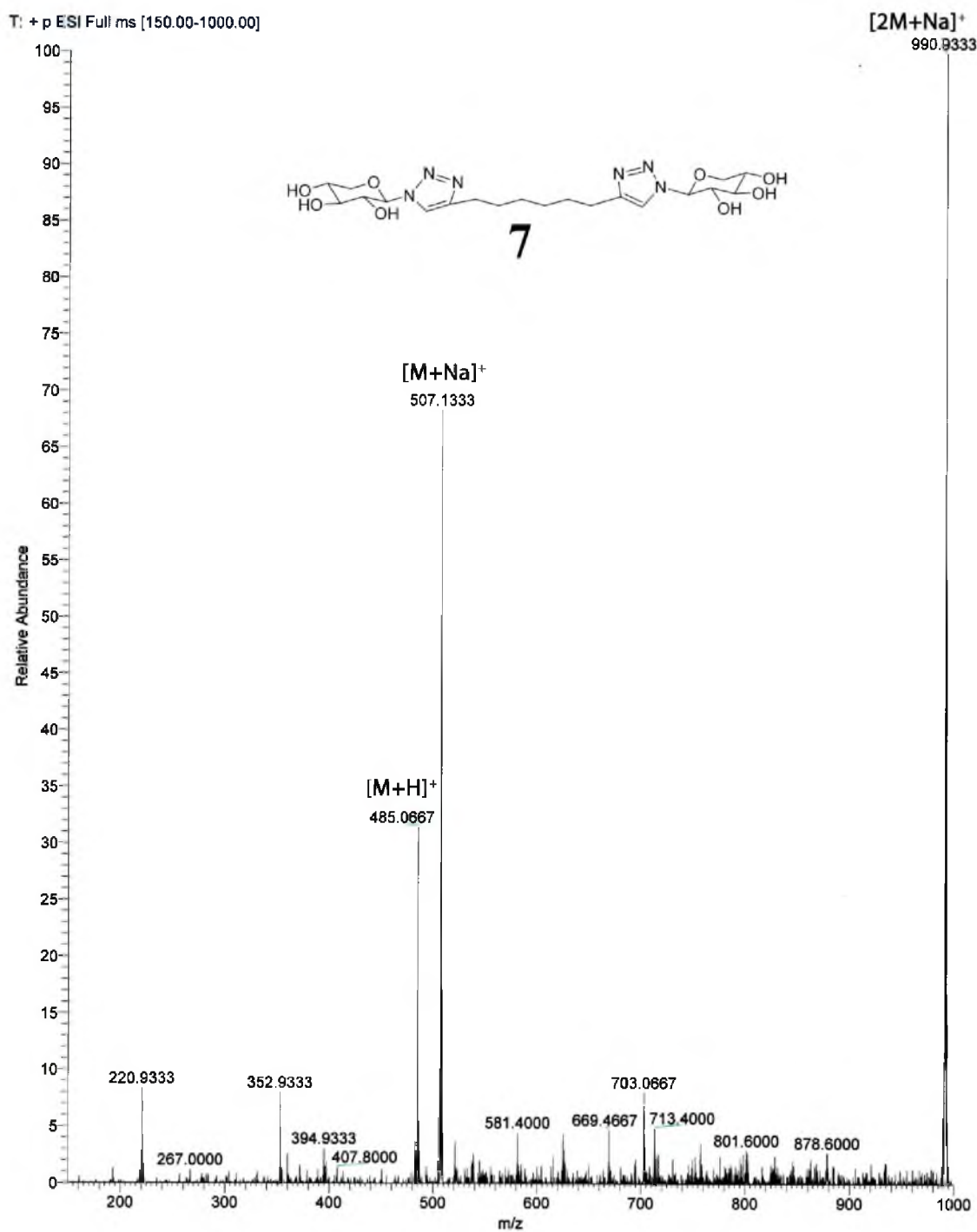


Figure S5.18. Mass spectra of cluster-xyloside 7

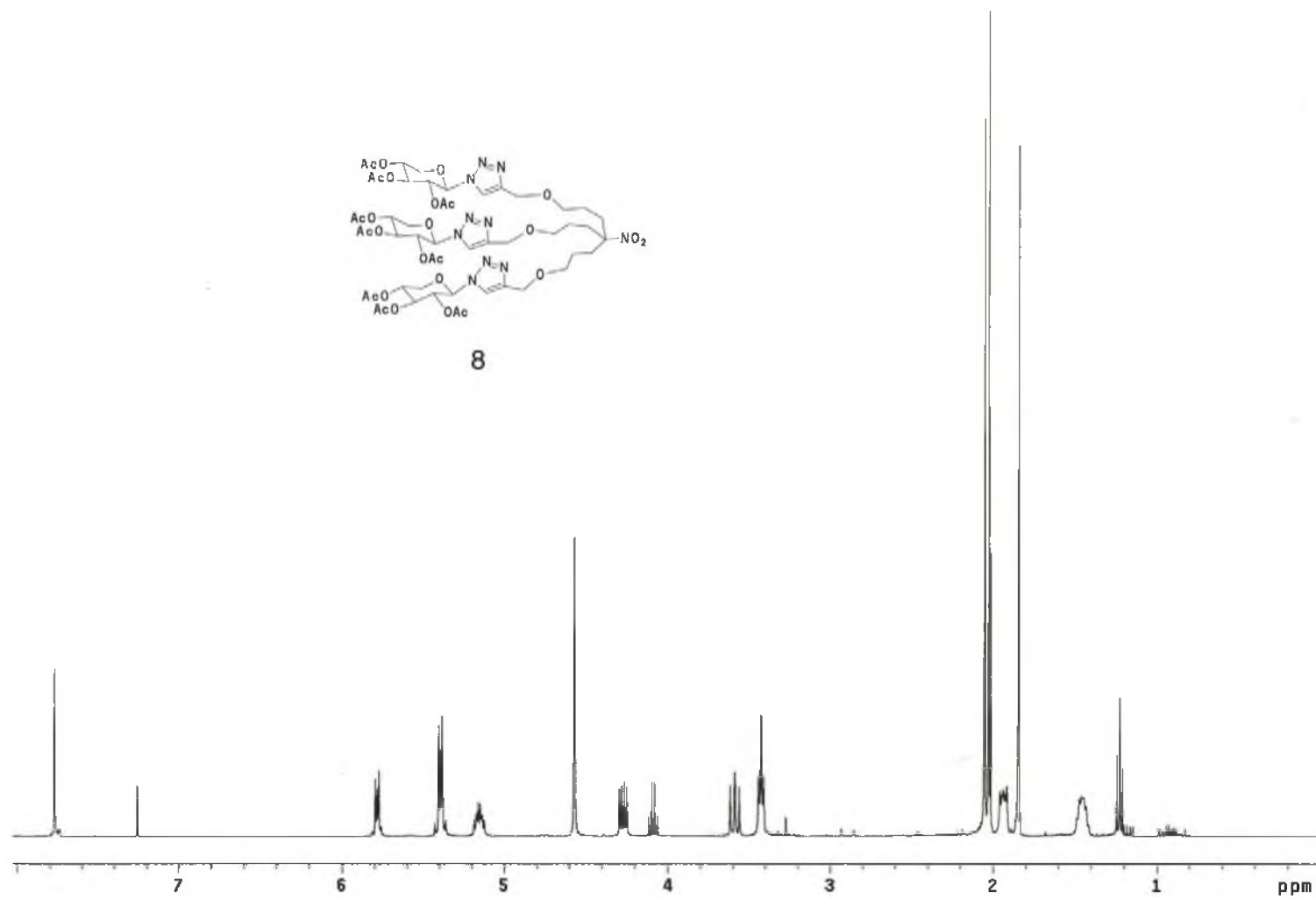


Figure S5.19. NMR spectra of cluster-xyloside 8

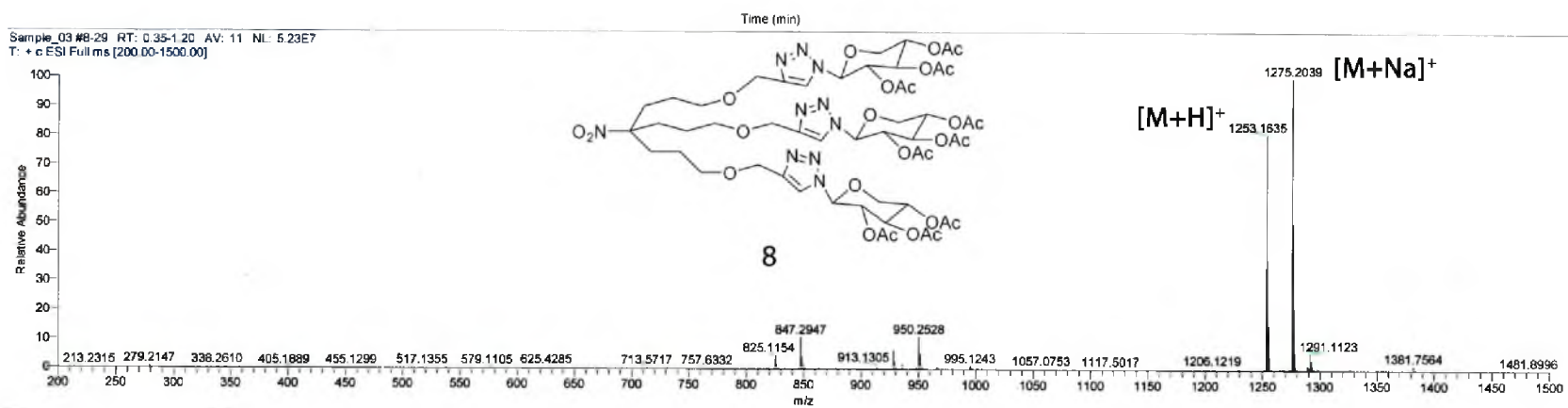
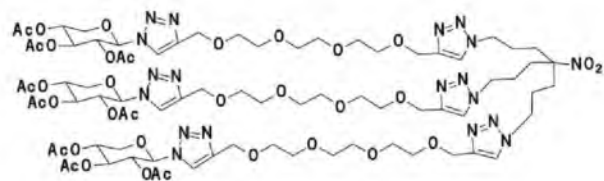


Figure S5.20. Mass spectra of cluster-xyloside 8



9

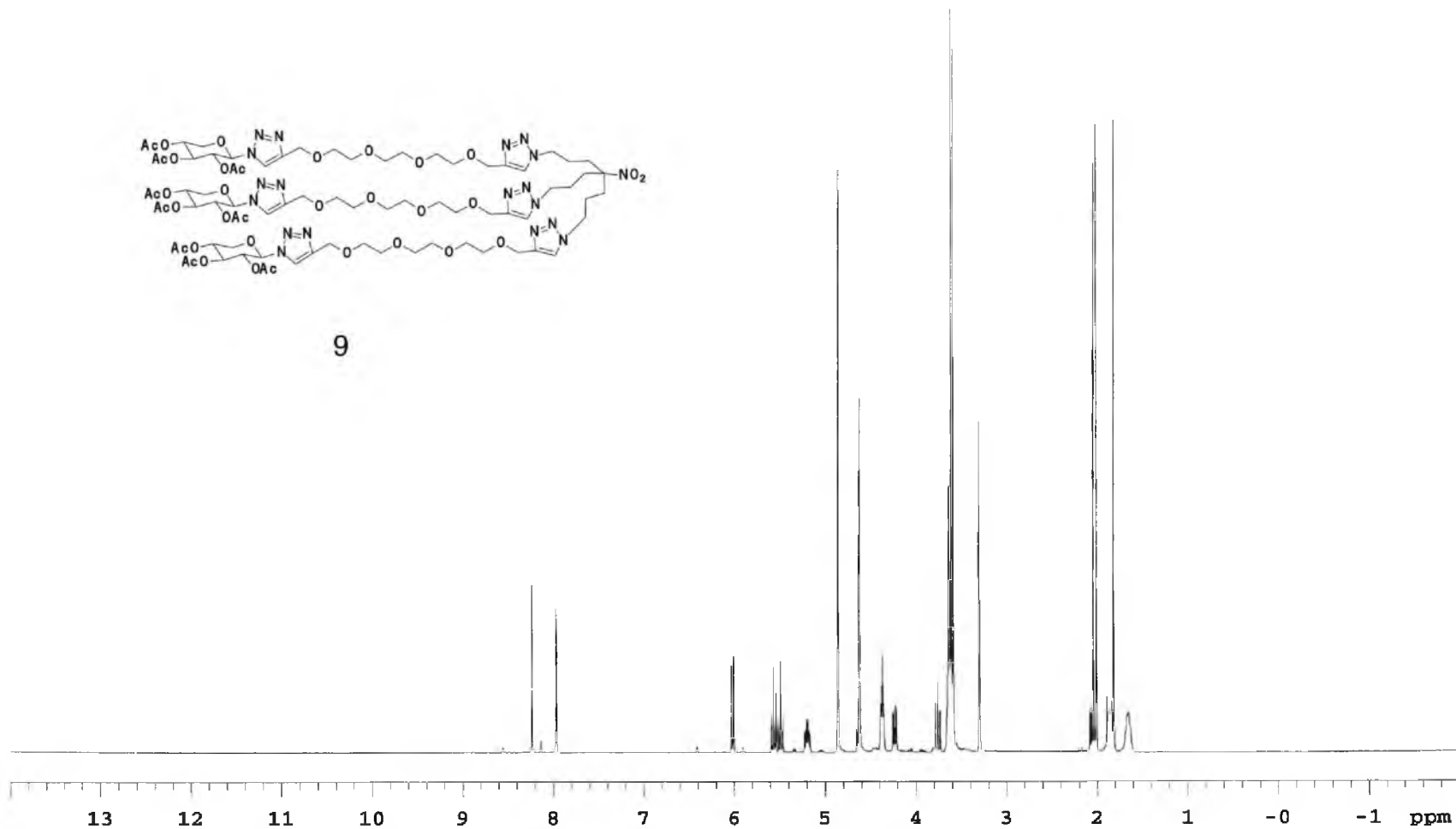


Figure S5.21. NMR spectra of cluster-xyloside 9

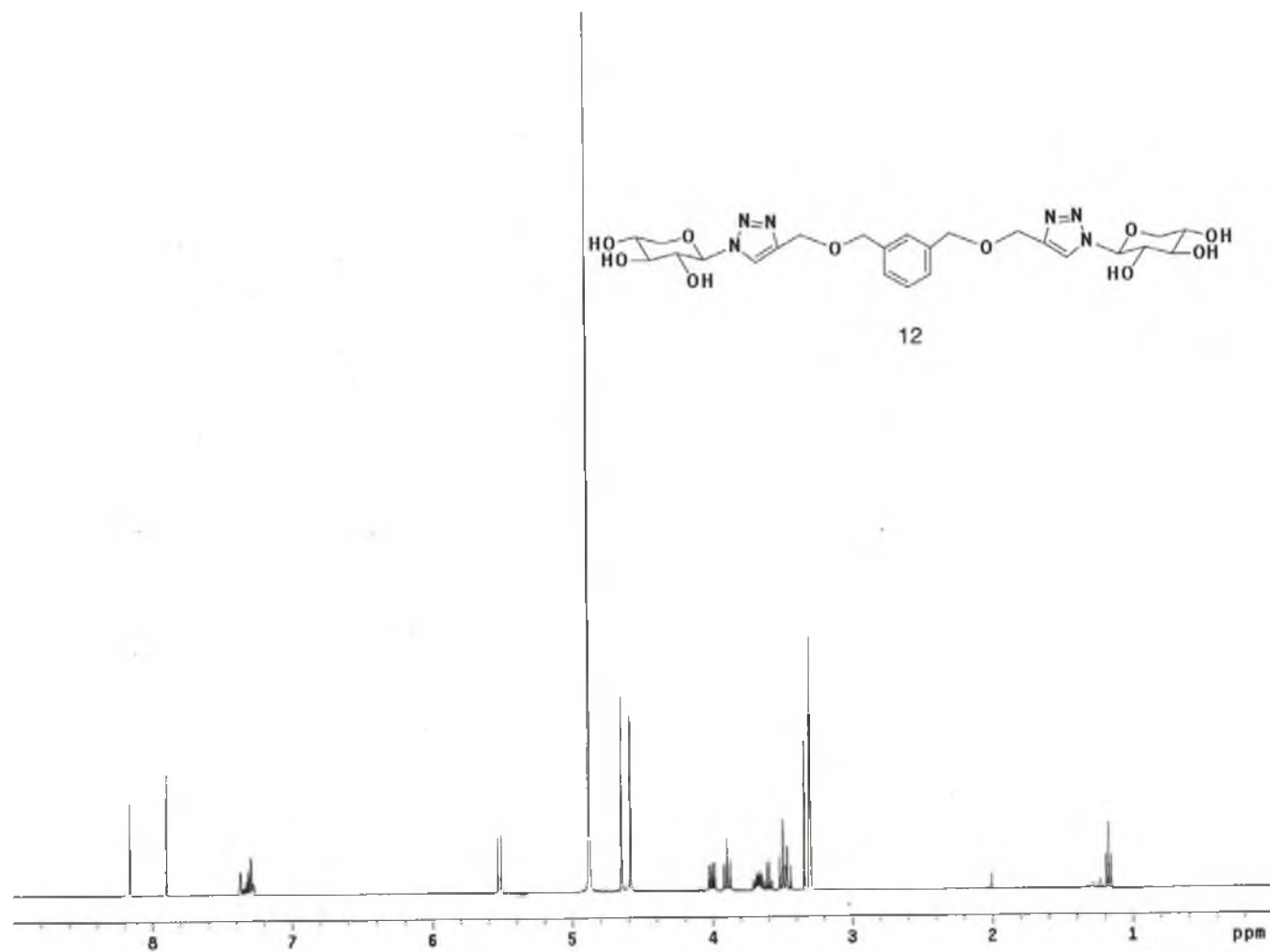


Figure S5.22. NMR spectra of cluster-xyloside 12

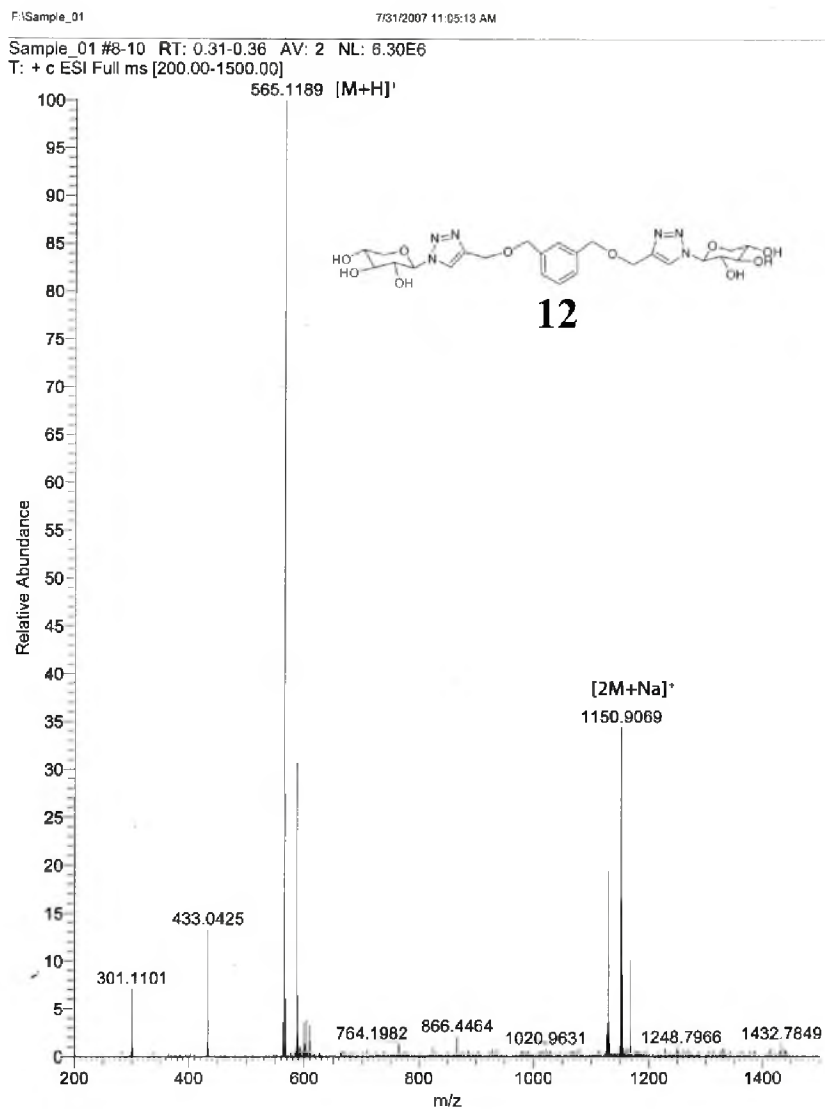


Figure S5.23. Mass spectra of cluster-xyloside 12

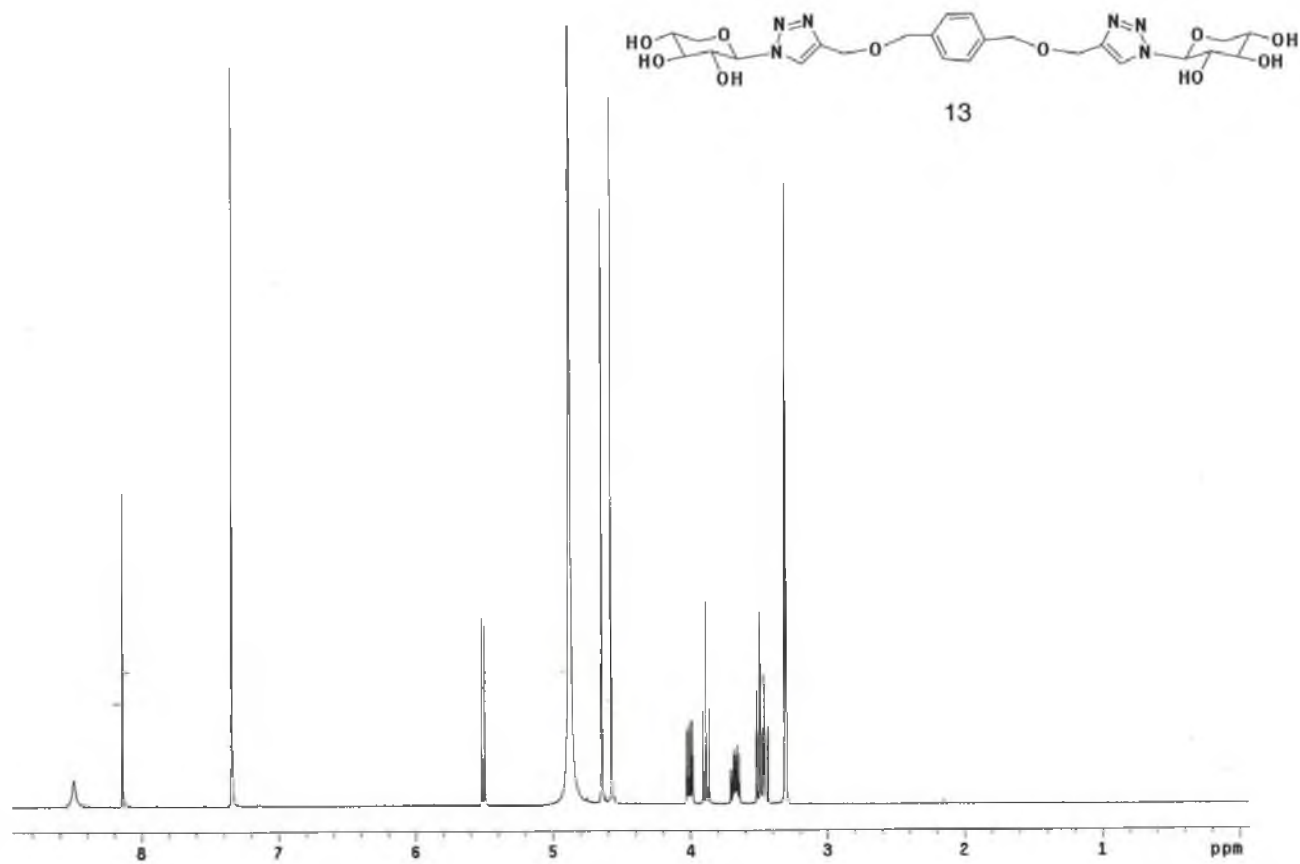


Figure S5.24. NMR spectra of cluster-xyloside 13

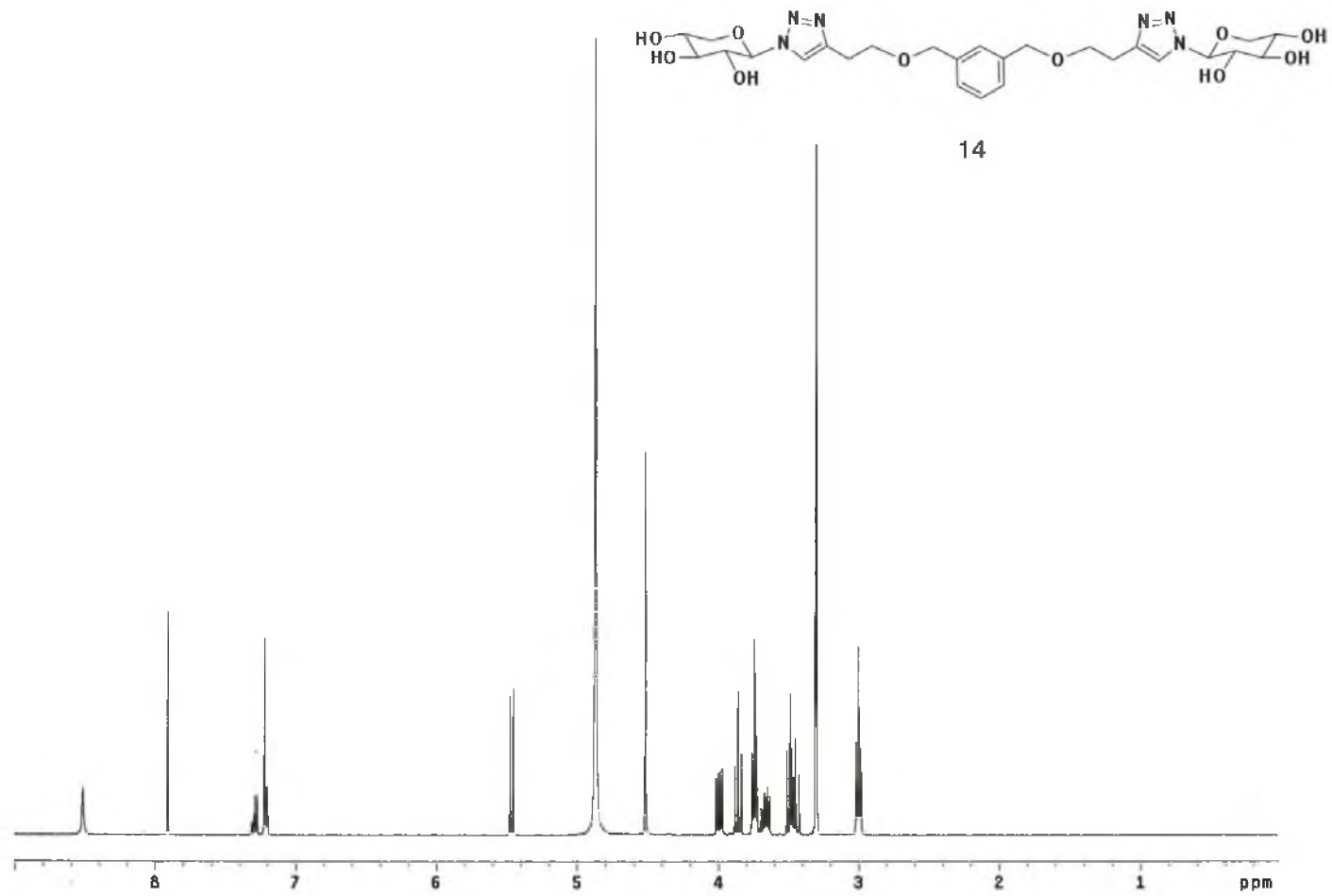


Figure S5.25. NMR spectra of cluster-xyloside 14

C:\Xcalibur\...Kuby Lab\y\VT-IA-273di

6/18/2007 1:19:41 PM

0.000000

VT-IA-273di #1-30 RT: 0.02-0.70 AV: 30 NL: 4.60E6

T: + p ESI Full ms [200.00-1000.00]

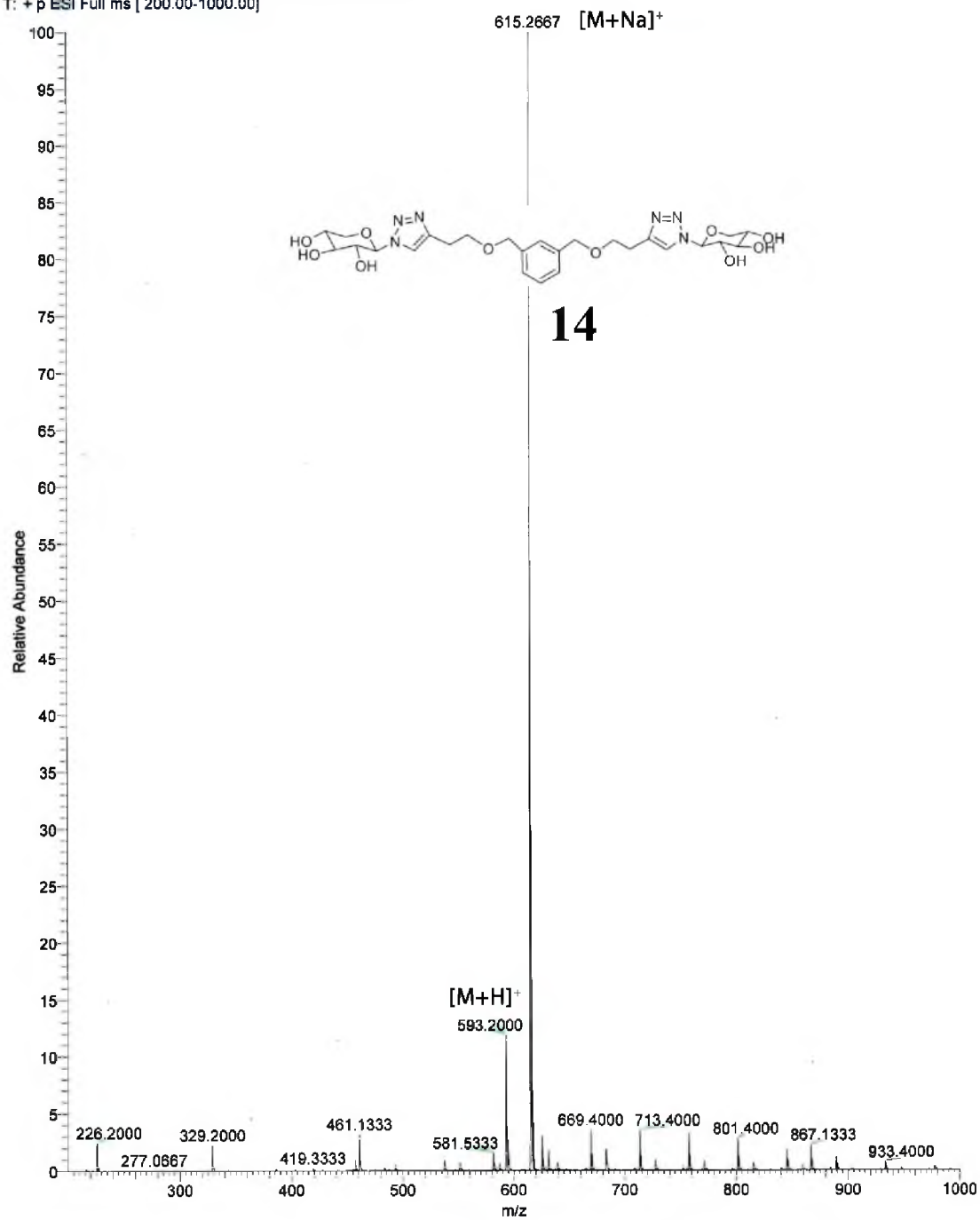


Figure S5.26. Mass spectra of cluster-xyloside 14

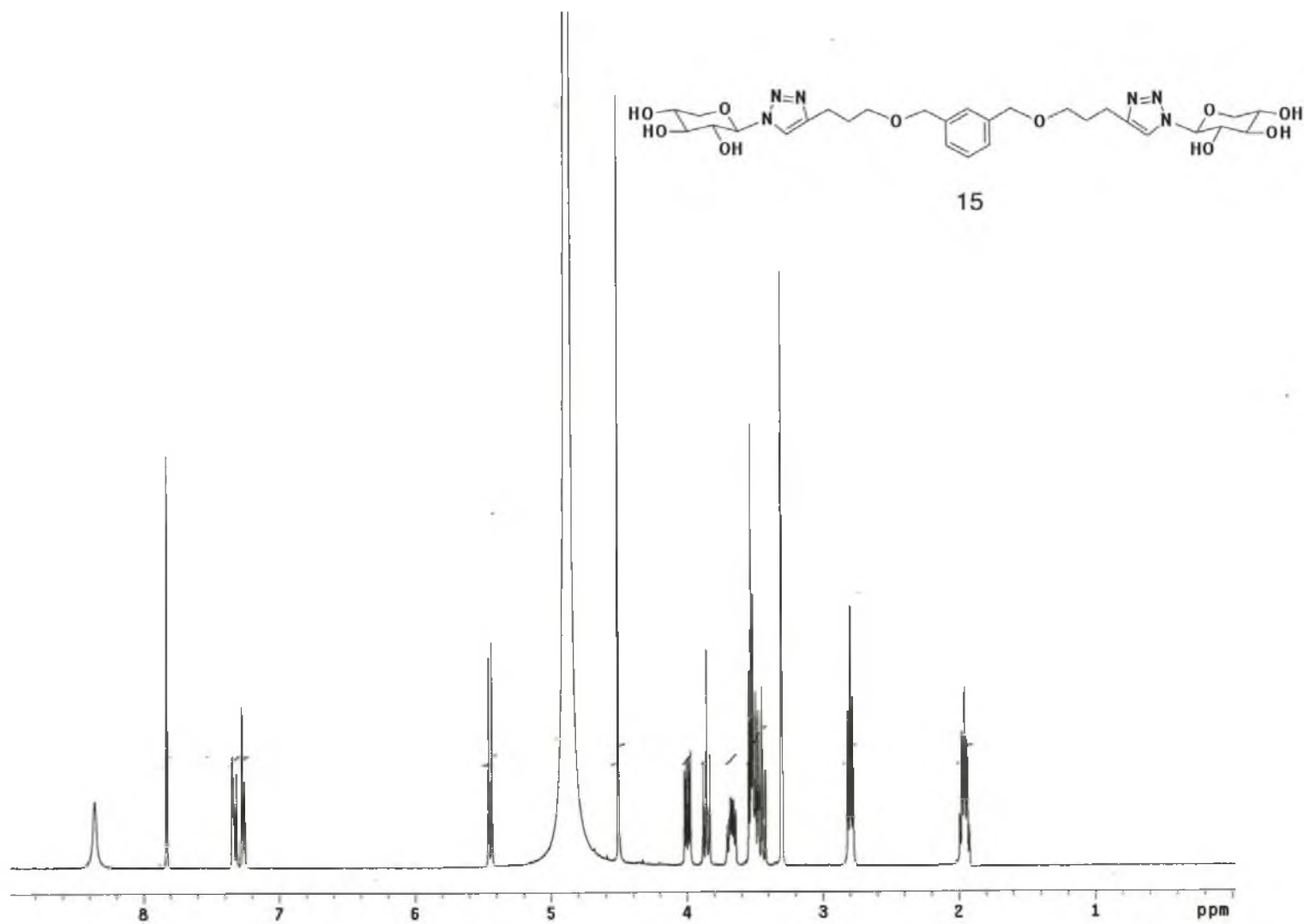


Figure S5.27. NMR spectra of cluster-xyloside 15

C:\Calibur\...WyVT-IA-275-56-57di

6/18/2007 1:37:04 PM

0.000000

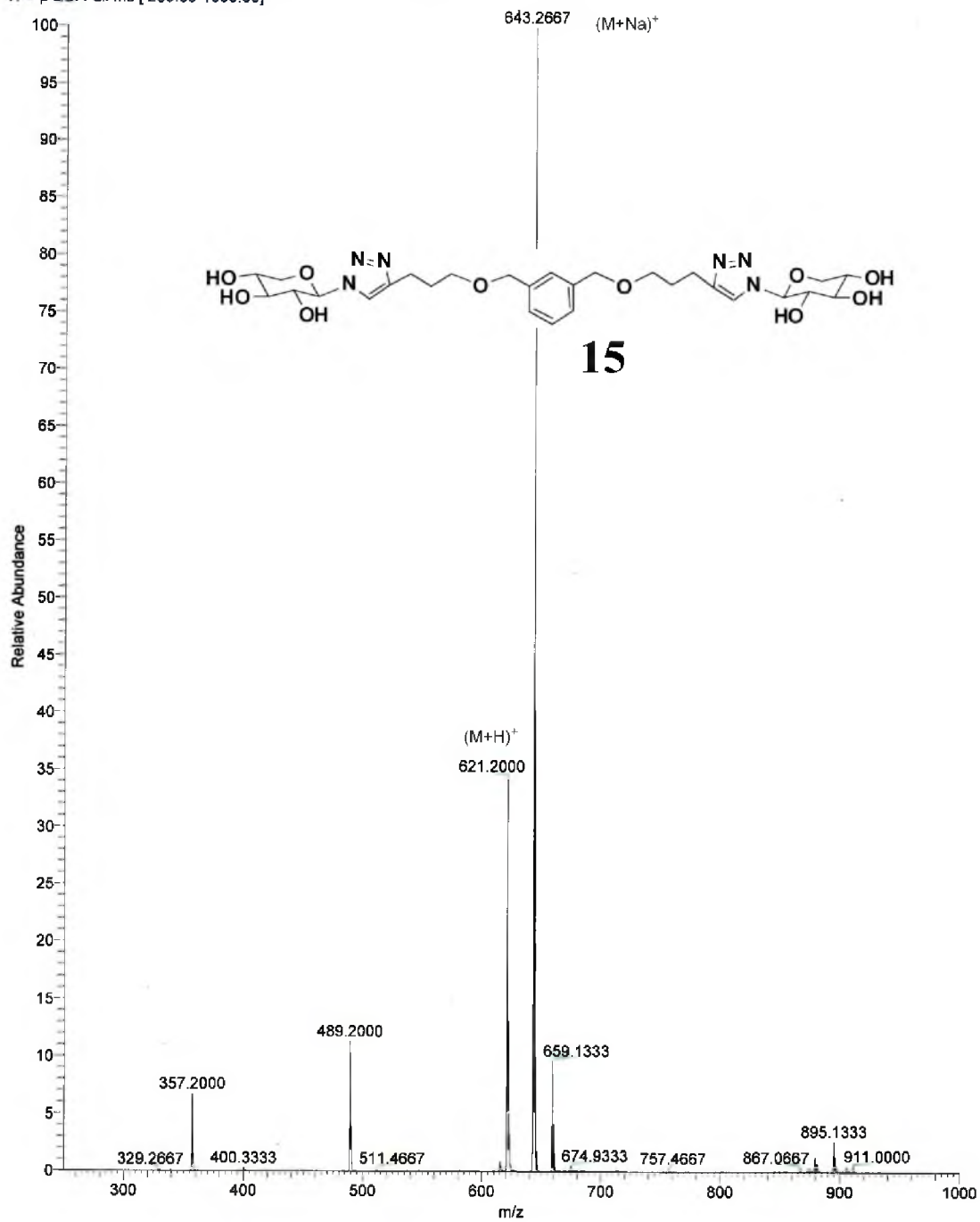
VT-IA-275-56-57di #1-29 RT: 0.01-0.65 AV: 29 NL: 2.91E6
T: + p ESI Full ms [250.00-1000.00]

Figure S5.28. Mass spectra of cluster-xyloside 15

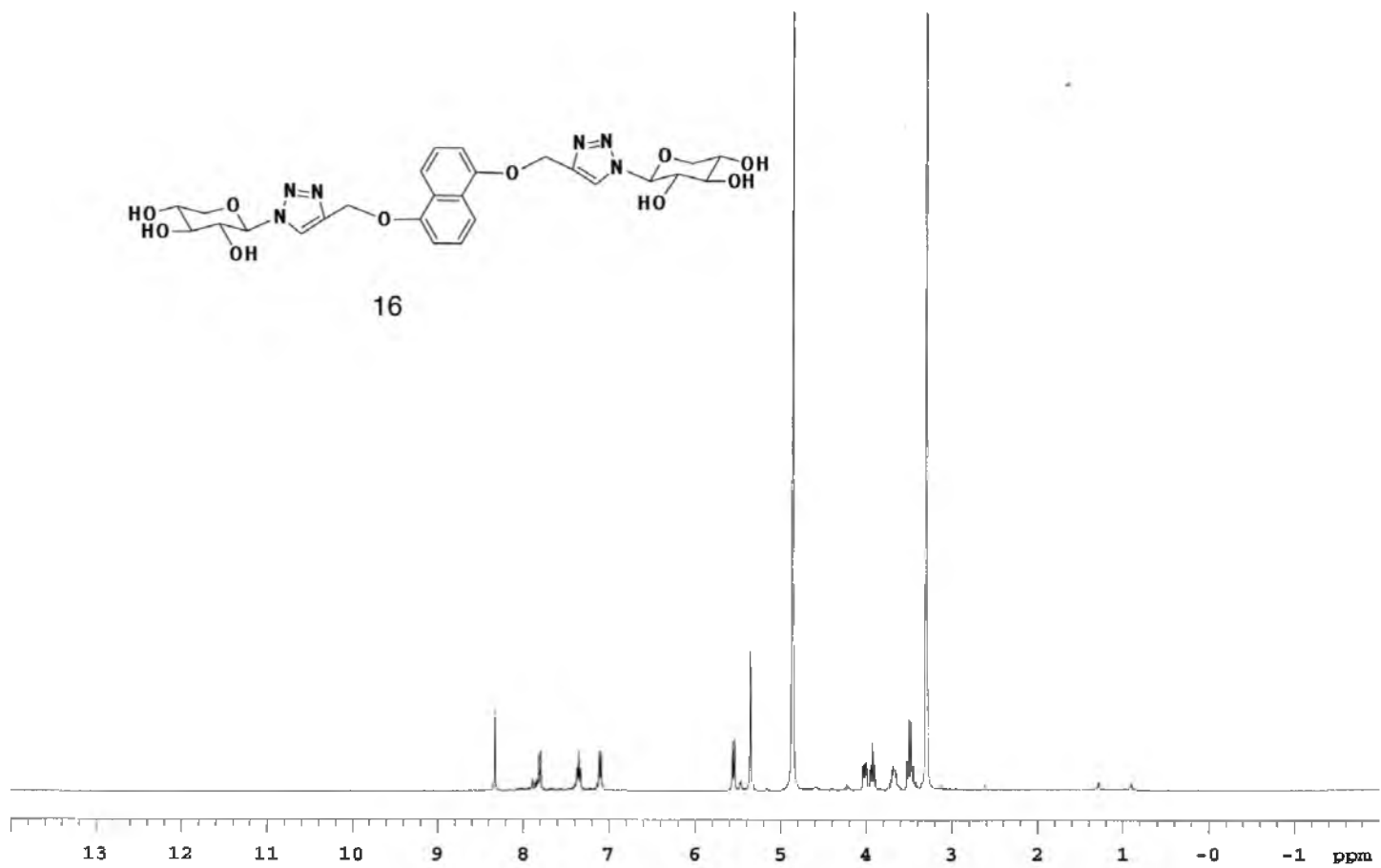


Figure S5.29. NMR spectra of cluster-xyloside 16

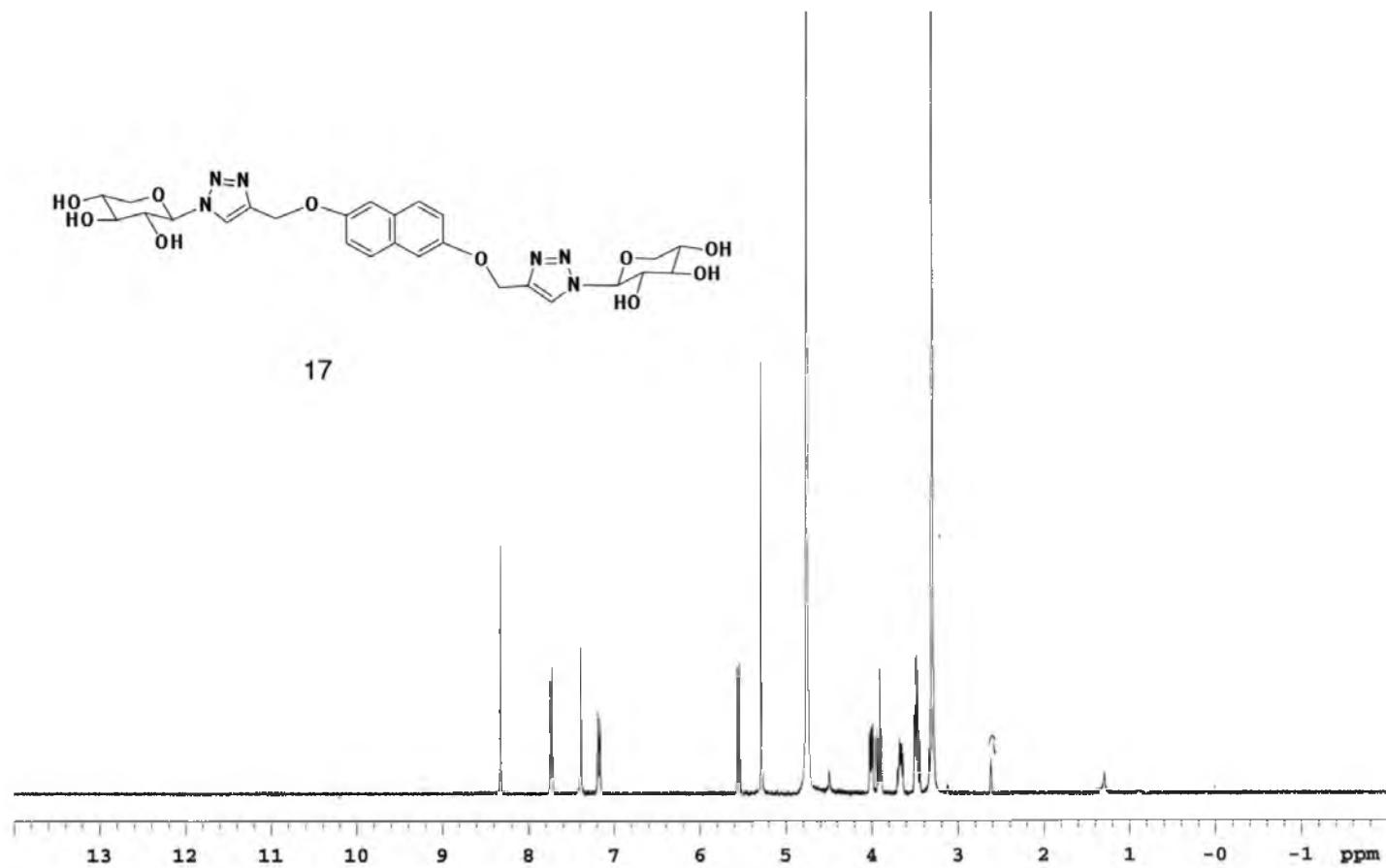


Figure S5.30. NMR spectra of cluster-xyloside 17

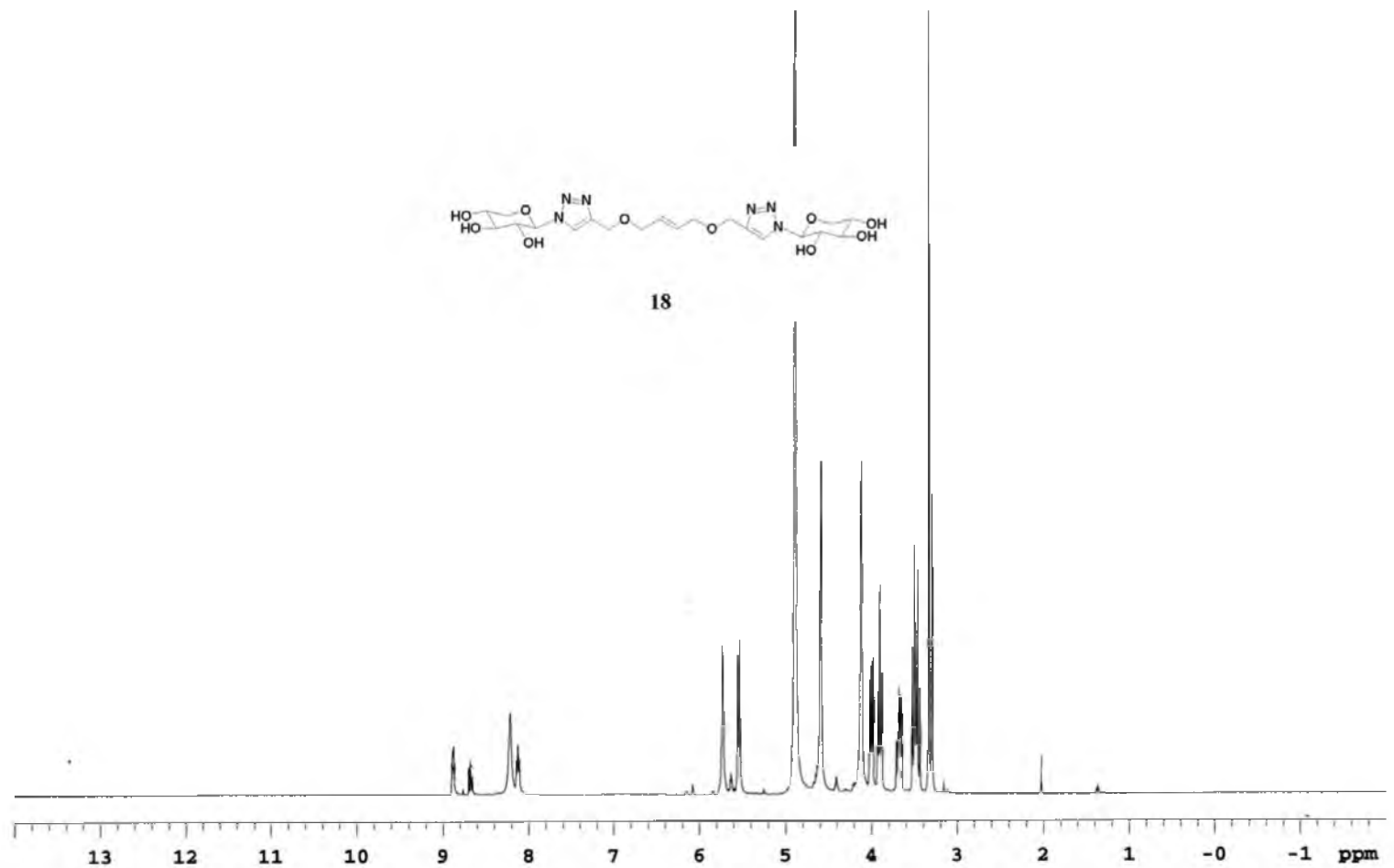


Figure S5.31. NMR spectra of cluster-xyloside 18

5.7. References

1. Perrimon, N., and Bernfield, M. (2000) Specificities of heparan sulphate proteoglycans in developmental processes, *Nature* 404, 725-728.
2. Bernfield, M., Gotte, M., Park, P. W., Reizes, O., Fitzgerald, M. L., Lincecum, J., and Zako, M. (1999) Functions of cell surface heparan sulfate proteoglycans, *Annu Rev Biochem* 68, 729-777.
3. Raman, K., and Kuberan, B. (2010) Chemical tumor biology of heparan sulfate proteoglycans, *Current Chemical Biology* 4, 20-31.
4. Langford, J. K., Stanley, M. J., Cao, D., and Sanderson, R. D. (1998) Multiple heparan sulfate chains are required for optimal syndecan-1 function, *J Biol Chem* 273, 29965-29971.
5. Zhang, L., and Esko, J. D. (1994) Amino acid determinants that drive heparan sulfate assembly in a proteoglycan, *J Biol Chem* 269, 19295-19299.
6. Gopal, S., Bober, A., Whiteford, J. R., Multhaupt, H. A., Yoneda, A., and Couchman, J. R. (2010) Heparan sulfate chain valency controls syndecan-4 function in cell adhesion, *J Biol Chem* 285, 14247-14258.
7. Sanderson, R. D., and Bernfield, M. (1988) Molecular polymorphism of a cell surface proteoglycan: distinct structures on simple and stratified epithelia, *Proc Natl Acad Sci U S A* 85, 9562-9566.
8. Gotting, C., Kuhn, J., and Kleesiek, K. (2007) Human xylosyltransferases in health and disease, *Cell Mol Life Sci* 64, 1498-1517.
9. Gotting, C., Muller, S., Schottler, M., Schon, S., Prante, C., Brinkmann, T., Kuhn, J., and Kleesiek, K. (2004) Analysis of the DXD motifs in human xylosyltransferase I required for enzyme activity, *J Biol Chem* 279, 42566-42573.
10. Schon, S., Prante, C., Bahr, C., Kuhn, J., Kleesiek, K., and Gotting, C. (2006) Cloning and recombinant expression of active full-length xylosyltransferase I (XT-I) and characterization of subcellular localization of XT-I and XT-II, *J Biol Chem* 281, 14224-14231.
11. Okayama, M., Kimata, K., and Suzuki, S. (1973) The influence of p-nitrophenyl beta-d-xyloside on the synthesis of proteochondroitin sulfate by slices of embryonic chick cartilage, *J Biochem* 74, 1069-1073.
12. Galligani, L., Hopwood, J., Schwartz, N. B., and Dorfman, A. (1975) Stimulation of synthesis of free chondroitin sulfate chains by beta-D-xylosides in cultured cells, *J Biol Chem* 250, 5400-5406.

13. Schwartz, N. B. (1977) Regulation of chondroitin sulfate synthesis. Effect of beta-xylosides on synthesis of chondroitin sulfate proteoglycan, chondroitin sulfate chains, and core protein, *J Biol Chem* 252, 6316-6321.
14. Lugenwa, F. N., and Esko, J. D. (1991) Estradiol beta-D-xyloside, an efficient primer for heparan sulfate biosynthesis, *J Biol Chem* 266, 6674-6677.
15. Mani, K., Belting, M., Ellervik, U., Falk, N., Svensson, G., Sandgren, S., Cheng, F., and Fransson, L. A. (2004) Tumor attenuation by 2(6-hydroxynaphthyl)-beta-D-xylopyranoside requires priming of heparan sulfate and nuclear targeting of the products, *Glycobiology* 14, 387-397.
16. Kuberan, B., Ethirajan, M., Victor, X. V., Tran, V., Nguyen, K., and Do, A. (2008) "Click" xylosides initiate glycosaminoglycan biosynthesis in a mammalian cell line, *Chembiochem* 9, 198-200.
17. Victor, X. V., Nguyen, T. K., Ethirajan, M., Tran, V. M., Nguyen, K. V., and Kuberan, B. (2009) Investigating the elusive mechanism of glycosaminoglycan biosynthesis, *J Biol Chem* 284, 25842-25853.
18. Johnsson, R., Mani, K., and Ellervik, U. (2007) Synthesis and biology of bis-xylosylated dihydroxynaphthalenes, *Bioorg Med Chem* 15, 2868-2877.
19. Esko, J. D., Stewart, T. E., and Taylor, W. H. (1985) Animal cell mutants defective in glycosaminoglycan biosynthesis, *Proc Natl Acad Sci U S A* 82, 3197-3201.
20. Kirn-Safran, C., Farach-Carson, M. C., and Carson, D. D. (2009) Multifunctionality of extracellular and cell surface heparan sulfate proteoglycans, *Cell Mol Life Sci* 66, 3421-3434.
21. de Paz, J. L., Noti, C., Bohm, F., Werner, S., and Seeberger, P. H. (2007) Potentiation of fibroblast growth factor activity by synthetic heparin oligosaccharide glycodendrimers, *Chem Biol* 14, 879-887.
22. Sasisekharan, R., and Venkataraman, G. (2000) Heparin and heparan sulfate: biosynthesis, structure and function, *Curr Opin Chem Biol* 4, 626-631.
23. Esko, J. D., and Selleck, S. B. (2002) Order out of chaos: assembly of ligand binding sites in heparan sulfate, *Annu Rev Biochem* 71, 435-471.
24. Presto, J., Thuveson, M., Carlsson, P., Busse, M., Wilen, M., Eriksson, I., Kusche-Gullberg, M., and Kjellen, L. (2008) Heparan sulfate biosynthesis enzymes EXT1 and EXT2 affect NDST1 expression and heparan sulfate sulfation, *Proc Natl Acad Sci U S A* 105, 4751-4756.

25. Chen, R. L., and Lander, A. D. (2001) Mechanisms underlying preferential assembly of heparan sulfate on glypican-1, *J Biol Chem* 276, 7507-7517.
26. Lemercier, G., Gendreizig, S., Kindermann, M., and Johnsson, K. (2007) Inducing and sensing protein--protein interactions in living cells by selective cross-linking, *Angew Chem Int Ed Engl* 46, 4281-4284.
27. McPhee, M. M., and Kerwin, S. M. (2001) Synthesis, DNA cleavage, and cytotoxicity of a series of bis(propargylic) sulfone crown ethers, *Bioorg Med Chem* 9, 2809-2818.
28. Venugopalan, B., and Balasubramanian, K. K. (1985) Studies of Claisen rearrangement of bispropargyl ethers. Synthesis of naphthodipyrans, naphthodifurans and naphthofuopyrans, *Heterocycles* 23, 81-92.
29. Whitlock, B. J., Jarvi, E. T., and Whitlock, H. W. (1981) Preparation and characterization of 1,8,19,26-tetraoxa[8.8](2,6)naphthalenophane-3,5,21,23-tetrayne and related donut-shaped cyclophanes, *J Org Chem* 46, 1832-1835.
30. Tornøe Christian, W., Christensen, C., and Meldal, M. (2002) Peptidotriazoles on solid phase: [1,2,3]-triazoles by regiospecific copper(i)-catalyzed 1,3-dipolar cycloadditions of terminal alkynes to azides, *J Org Chem* 67, 3057-3064.
31. Meldal, M., and Tornøe Christian, W. (2008) Cu-catalyzed azide-alkyne cycloaddition, *Chem Rev* 108, 2952-3015.

CHAPTER 6

CONCLUSIONS

GAGs play important roles in wound healing, cell signaling, cell proliferation, cell migration, cell differentiation, tumor metastasis, blood clotting, various infections, and numerous other biological processes (*1-10*). For example, HS and heparin contain a specific pentasaccharide sequence that binds with high affinity and activates anti-thrombin III to inhibit blood clotting (*11-13*). However, direct administration of these animal derived heparins is wrought with problems of molecular heterogeneity, possible contamination with pathogens, and intentional chemical adulteration. Recently, an adulterated batch of heparin killed several hundred people in US, Germany, and other parts of the world (*14*). Moreover, the structure-function relationships of GAG chains are difficult to establish because of their structural complexity arising from their highly variable length and composition. An attractive alternative approach is to use xylosides to induce specific GAG chain biosynthesis without a core protein. Xylosides can act as acceptors for initiation of linkage region and production of GAG chains. It was demonstrated that the xylosides induced GAG chains secreted into the medium bearing the xyloside residues at the reducing end. In general, cells secrete PGs directly from Golgi into the extracellular environment by secretory pathway and some are shed from the cell surface through proteolytic cleavage of the core protein. Therefore, the primed GAG chains are also considered to be packaged in secretory vesicles in the Golgi apparatus and are secreted through exocytosis.

The quantity and type of GAG chains depends on the system where it was tested and also on the structure of aglycone moiety of xylosides. For example, β -xylosides produced low levels of CS in 1-day limb bud cells; however, they stimulated GAG biosynthesis 2 to 10 folds in glial cells, neuroblastoma, and two strains of hepatoma cells.

Another example, β -*D*-xylosides carrying two aromatic rings efficiently primed more HS chains than β -*D*-xyloside carrying one aromatic ring.

The xylosides were also found to regulate many important biological processes such as the elongation of zebrafish embryos, angiogenesis, and invasion. The library of xylosides carrying various aglycone groups was synthesized using “click chemistry.” This approach introduces a diverse set of aglycones very quickly and allows one to examine the effect of aglycone moieties on the stimulation or inhibition of GAG chain biosynthesis in a variety of cellular systems rapidly. Moreover, these click-xylosides are stable up to 5 days in cells whereas traditional *O*-xylosides are hydrolytically unstable and degrade quickly within the cellular environment. Therefore, in this thesis, a library of click-xylosides was synthesized to address several questions related to GAG chain biosynthesis. In the future, these xylosides will be important tools to study structure-function relationship of GAG chains *in vitro* and *in vivo* and can potentially be used as drugs to treat cancers, cardiovascular diseases and CNS injury.

In the prior chapters, the extensive design and characterization of a number of xylosides that are important in studying the structures and functions of PGs have been shown. The primed chains are varied in terms of their sulfate density, average molecular weight, number of GAG chains per scaffold, and composition of GAG chains. The average molecular weight of primed GAG chains was calculated based on the migration time of polystyrene sulfonate standard. Then, this approach only provides apparent/relative molecular weight rather than exact molecular weight since the structure of polystyrene sulfonate polymer is different from the structure of GAG chains. Therefore,

in the future, it is necessary to synthesize the GAG standard for determination of chain length of GAG chains.

6.1. Modulation of GAG Biosynthesis by Click-xylosides

Xylosides with hydrophobic aglycone groups can pass through cell membranes and compete with endogenous core protein acceptors for the assembly of GAG chains in the Golgi apparatus *in vitro* and *in vivo*. In our studies, the priming of these xylosides is concentration dependant and most of the xylosides generate a significant quantity of GAG chains at 100 μ M or higher concentrations. One possible explanation for this concentration dependence and the variety of priming activity is that the diffusion rates of the primers depend on the aglycones and lead to differential biosynthesis of the GAG chains. However, several xylosides primed more effectively at 100 μ M than at 1 mM. The inhibition of GAG priming at higher concentration of xylosides might be due to substrate level inhibition of the enzymes involved in assembly of the linkage region.

The aglycone group of xylosides affected not only the priming activity but also the sulfate density of primed GAG chains. Some xylosides produced homogeneously sulfated GAG chains, whereas other xylosides produced a heterogeneous population of variably sulfated GAG chains. The factors that regulate the appearance of cell-specific GAG chains with diverse sulfate patterns remain largely unknown. It has been proposed the GAG chains are synthesized in the Golgi by two different mechanisms (11, 15-17). In one mechanism, enzymes are anchored to the Golgi membrane at different locations and randomly modify and create diverse structures of GAG chains. In another mechanism, the diversity of GAG chains may be attributed to the presence of discrete

enzyme complexes, named GAGOSOME, which are located in different Golgi sub-compartments (11). Since a wide variation in the sulfate patterns of GAG chains primed by various xylosides were observed, these variations in the sulfate patterns should be attributed to the presence of discrete enzyme complexes in different Golgi compartments that may differentially regulate the biosynthesis of GAG chains. Selective compartmentalization of certain xylosides would likely result in the synthesis of homogenous and distinct populations of the GAG chains. However, other xylosides may be targeted to more than one GAGOSOME, resulting in the production of heterogenous GAG chains. Therefore, our study support the GAGOSOME mechanism that different xylosides can enter different GAGOSOME and that different GAGOSOME can make different GAG chains (15).

With regard to the chain composition, most xylosides that were studied made mostly CS. This observation supports the theory that the aglycone is not the only factor that affects the composition of GAG chains. Future studies will determine the effect of changing the glycosidic linkage of xylosides on the chain composition of GAGs produced. Utilizing xylosides with various types of glycosidic linkages may help elucidate the mechanism behind xyloside-stimulated GAG biosynthesis and may affect the percentage of HS chains in xyloside-stimulated GAGs.

Based on earlier studies, the aglycone group of xylosides is important in determining the amount of GAG produced and the specific structure of GAG chains produced. A library of 4-deoxy-4-fluoro-xylosides was designed based on the aglycones that primed effectively. These fluoro-xylosides were examined for their ability to inhibit endogenous GAG production. Surprisingly, a number of 4-deoxy-4-fluoro-xylosides

selectively inhibited GAG biosynthesis without having any toxicity. Future studies will utilize the library to decipher the functions of HS and CS *in vitro* and *in vivo* by blocking the production of endogenous GAG chains.

6.2. Design of Fluorescent Xylosides to Profile Cell-specific GAG Chains

Deciphering dynamic changes in GAG structures will provide new avenues to diagnose disease states and to improve our understanding of the spatio-temporal roles of GAGs in development. Typically, radiolabels are utilized to track GAG chains in most cellular studies. However, these radiolabeled GAG chains are usually toxic for living organisms. Fluorescent xylosides may serve as excellent chemical probes to profile cell-specific GAG structures and to define the role of GAG chains in biological processes. Several groups have used the well-known scaffold, 4-methyl umbelliferyl- β -D-xyloside, for over 4 decades but it primes small CS chains and therefore has limited utility (18-20). To overcome this major impediment, novel fluorescent xylosides were designed and synthesized to prime larger GAG chains for potential use as chemical probes to understand GAG biosynthesis.

Pyrene xylosides and UMB-click-xylosides were able to prime GAG chains at various concentrations. The average MW of GAG chains induced by these fluorescent xylosides was much larger than the average MW of GAG chains induced by commercial 4-methyl umbelliferyl- β -D-xyloside. Therefore, these fluorescent xylosides will provide novel avenues to profile and elucidate cellular GAG signatures in a robust manner, and assist in establishing cell-specific GAG-protein interactions. In future, additional fluorescent xylosides should be synthesized and screened for their ability to prime

specific HS or CS. These additional fluorescent xylosides will help to understand other factors that regulate the GAG biosynthesis and also be used to visualize Golgi compartments in order to prove the GAGOSOME concept.

6.3. RGD-xyloside Conjugates Prime GAGs

GAG chains play important roles in various cardiovascular functions and in various cancer processes (21-23). Heparin/HS activates ATIII, which eventually prevents the clot formation (24, 25). Moreover, HSPGs allow cancer cells to proliferate, escape from immune response and invade neighboring tissues (26, 27). RGD peptides can be targeted to activated endothelial cells and cancer cells which over express $\alpha_v\beta_3$ integrins (28). Furthermore, RGD peptides can also prevent platelet aggregation by preventing binding of glycoprotein to the GPIIb/IIIa receptors (29). Given the important roles of GAG chains and RGD peptides in vascular and tumor biology, linear and cyclic RGD peptides were conjugated to xylose residues by utilizing “click chemistry.” These RGD-conjugated xylosides can be selectively targeted to activated endothelial cells and cancer cells. Our results have shown that linear-RGD conjugated xylosides were able to prime GAG chains in an endothelial cell and many cancer cells. However, cyclic RGD-conjugated xylosides were not able to prime GAG chains in endothelial cells or cancer cells. Many studies suggest that formation of HS on core proteins depends on the presence of hydrophobic amino acids next to xylosylation sites (30-32). For these reasons, in the future, a library of hydrophobically modified linear and cyclic RGD conjugated xylosides containing a hydrophobic amino acid including Ala, Leu, Ile, Phe, and Val should be designed to stimulate HS biosynthesis. Long-term future prospects for

these molecules include their use in anticancer therapy and the treatment of myocardial infarcts as non-RGD-containing xylosides have been utilized to treat these diseases previously.

6.4. Synthesis and Biological Evaluation of Cluster-xylosides as PG Mimetics

Natural PGs normally contain more than two GAG side chains. In order to study the functions of PGs, cluster-xylosides carrying one, two, three, or four xylose residues per scaffold and various hydrophobic aglycones were synthesized using click chemistry. Based on the average MW analysis, “oxidation and elimination” reactions, and ozonolysis reactions, these synthetic cluster-xylosides induced multiple GAG chains per scaffold and mimicked naturally occurring PGs. Linker distances between xylose residues affected the priming activity but not the average MW of primed GAG chains. The average MW of GAG chains, however, was found to depend on the concentration of cluster-xylosides. The cluster-xylosides made significant CS/DS and less HS in CHO cells. Moreover, the effect of cluster-xylosides was also studied on zebrafish development. Only cluster-xylosides caused hyper-elongation of zebrafish embryos. It suggested that GAG multivalency in nature is important for their biological functions. Since these cluster-xylosides made significant quantities of CS and very few HS, future studies will examine the effect of different aglycone or glycosidic linkages on the amount of HS produced and the structure of primed GAGs (i.e. the effect of having one HS chain and one CS chain per scaffold).

In conclusion, understanding the structure-function relationship of GAGs will provide novel therapeutic targets to treat diseases such as cancers. However, the

chemical heterogeneity and polydispersity of GAGs pose challenges for research and design of drugs. A library of xylosides, synthesized using click chemistry, has a potential to overcome this problem in the field since structures of PGs could be controlled by changing aglycones of xylosides. These stable click-xylosides stimulated various GAG structures. In the case of 4-fluoro-xylosides, they selectively inhibited PGs. In addition, these xylosides were easily conjugated to RGD peptides so that RGD-xylosides can function as blood thinner by priming anticoagulant GAG chains selectively at target sites such as activated endothelial cells and cancer cells. Cluster-xylosides primed multiple CS chains per scaffold and should be used as potential PG mimetics to define the GAG multivalency in the biological systems. In summary, click-xylosides will serve as a great tool to study the structure-function relationship of GAG chains *in vitro* and *in vivo* and have a great potential as glycomedicines in the near future.

6.5. References

1. Dhoot, G. K., Gustafsson, M. K., Ai, X., Sun, W., Standiford, D. M., and Emerson, C. P., Jr. (2001) Regulation of Wnt signaling and embryo patterning by an extracellular sulfatase, *Science* 293, 1663-1666.
2. Hacker, U., Nybakken, K., and Perrimon, N. (2005) Heparan sulphate proteoglycans: the sweet side of development, *Nat Rev Mol Cell Biol* 6, 530-541.
3. Hwang, H. Y., Olson, S. K., Esko, J. D., and Horvitz, H. R. (2003) *Caenorhabditis elegans* early embryogenesis and vulval morphogenesis require chondroitin biosynthesis, *Nature* 423, 439-443.
4. Perrimon, N., and Bernfield, M. (2000) Specificities of heparan sulphate proteoglycans in developmental processes, *Nature* 404, 725-728.
5. Casu, B., Guerrini, M., Naggi, A., Perez, M., Torri, G., Ribatti, D., Carminati, P., Giannini, G., Penco, S., Pisano, C., Belleri, M., Rusnati, M., and Presta, M. (2002) Short heparin sequences spaced by glycol-split uronate residues are antagonists of fibroblast growth factor 2 and angiogenesis inhibitors, *Biochemistry* 41, 10519-10528.
6. Iozzo, R. V., and San Antonio, J. D. (2001) Heparan sulfate proteoglycans: heavy hitters in the angiogenesis arena, *J Clin Invest* 108, 349-355.
7. Vlodavsky, I., Goldshmidt, O., Zcharia, E., Atzmon, R., Rangini-Guatta, Z., Elkin, M., Peretz, T., and Friedmann, Y. (2002) Mammalian heparanase: involvement in cancer metastasis, angiogenesis and normal development, *Semin Cancer Biol* 12, 121-129.
8. Benowitz, L. I., Goldberg, D. E., and Irwin, N. (2002) Inosine stimulates axon growth in vitro and in the adult CNS, *Prog Brain Res* 137, 389-399.
9. Liu, J., Shriver, Z., Pope, R. M., Thorp, S. C., Duncan, M. B., Copeland, R. J., Raska, C. S., Yoshida, K., Eisenberg, R. J., Cohen, G., Linhardt, R. J., and Sasisekharan, R. (2002) Characterization of a heparan sulfate octasaccharide that binds to herpes simplex virus type 1 glycoprotein D, *J Biol Chem* 277, 33456-33467.
10. Casu, B., Guerrini, M., and Torri, G. (2004) Structural and conformational aspects of the anticoagulant and anti-thrombotic activity of heparin and dermatan sulfate, *Curr Pharm Des* 10, 939-949.
11. Esko, J. D., and Selleck, S. B. (2002) Order out of chaos: assembly of ligand binding sites in heparan sulfate, *Annu Rev Biochem* 71, 435-471.

12. Choay, J., Petitou, M., Lormeau, J. C., Sinay, P., Casu, B., and Gatti, G. (1983) Structure-activity relationship in heparin: a synthetic pentasaccharide with high affinity for antithrombin III and eliciting high anti-factor Xa activity, *Biochem Biophys Res Commun* 116, 492-499.
13. Petitou, M., Herault, J. P., Bernat, A., Driguez, P. A., Duchaussoy, P., Lormeau, J. C., and Herbert, J. M. (1999) Synthesis of thrombin-inhibiting heparin mimetics without side effects, *Nature* 398, 417-422.
14. Simasathien, S., Thomas, S. J., Watanaveeradej, V., Nisalak, A., Barberousse, C., Innis, B. L., Sun, W., Putnak, J. R., Eckels, K. H., Hutagalung, Y., Gibbons, R. V., Zhang, C., De La Barrera, R., Jarman, R. G., Chawachalasai, W., and Mammen, M. P., Jr. (2008) Safety and immunogenicity of a tetravalent live-attenuated dengue vaccine in flavivirus naive children, *Am J Trop Med Hyg* 78, 426-433.
15. Victor, X. V., Nguyen, T. K., Ethirajan, M., Tran, V. M., Nguyen, K. V., and Kuberan, B. (2009) Investigating the elusive mechanism of glycosaminoglycan biosynthesis, *J Biol Chem* 284, 25842-25853.
16. Sasisekharan, R., and Venkataraman, G. (2000) Heparin and heparan sulfate: biosynthesis, structure and function, *Curr Opin Chem Biol* 4, 626-631.
17. Ledin, J., Ringvall, M., Thuveson, M., Eriksson, I., Wilen, M., Kusche-Gullberg, M., Forsberg, E., and Kjellen, L. (2006) Enzymatically active N-deacetylase/N-sulfotransferase-2 is present in liver but does not contribute to heparan sulfate N-sulfation, *J Biol Chem* 281, 35727-35734.
18. Salimath, P. V., Spiro, R. C., and Freeze, H. H. (1995) Identification of a novel glycosaminoglycan core-like molecule. II. Alpha-GalNAc-capped xylosides can be made by many cell types, *J Biol Chem* 270, 9164-9168.
19. Freeze, H. H., Sampath, D., and Varki, A. (1993) Alpha- and beta-xylosides alter glycolipid synthesis in human melanoma and Chinese hamster ovary cells, *J Biol Chem* 268, 1618-1627.
20. Shibata, S., Takagaki, K., Ishido, K., Konn, M., Sasaki, M., and Endo, M. (2003) HNK-1-Reactive oligosaccharide, sulfate-O-3GlcAbeta1-4Xylbeta1-MU, synthesized by cultured human colorectal cancer cells, *Tohoku J Exp Med* 199, 13-23.
21. Powell, A. K., Yates, E. A., Fernig, D. G., and Turnbull, J. E. (2004) Interactions of heparin/heparan sulfate with proteins: appraisal of structural factors and experimental approaches, *Glycobiology* 14, 17R-30R.

22. Sasisekharan, R., Shriver, Z., Venkataraman, G., and Narayanasami, U. (2002) Roles of heparan-sulphate glycosaminoglycans in cancer, *Nat Rev Cancer* 2, 521-528.
23. Murrey, H. E., and Hsieh-Wilson, L. C. (2008) The chemical neurobiology of carbohydrates, *Chem Rev* 108, 1708-1731.
24. Princivalle, M., Hasan, S., Hosseini, G., and de Agostini, A. I. (2001) Anticoagulant heparan sulfate proteoglycans expression in the rat ovary peaks in preovulatory granulosa cells, *Glycobiology* 11, 183-194.
25. Carrell, R., Skinner, R., Jin, L., and Abrahams, J. P. (1997) Structural mobility of antithrombin and its modulation by heparin, *Thromb Haemost* 78, 516-519.
26. Sugahara, K., Mikami, T., Uyama, T., Mizuguchi, S., Nomura, K., and Kitagawa, H. (2003) Recent advances in the structural biology of chondroitin sulfate and dermatan sulfate, *Curr Opin Struct Biol* 13, 612-620.
27. Eswarakumar, V. P., Lax, I., and Schlessinger, J. (2005) Cellular signaling by fibroblast growth factor receptors, *Cytokine Growth Factor Rev* 16, 139-149.
28. Temming, K., Schiffelers, R. M., Molema, G., and Kok, R. J. (2005) RGD-based strategies for selective delivery of therapeutics and imaging agents to the tumour vasculature, *Drug Resist Updat* 8, 381-402.
29. Wang, W., Borchardt, R. T., and Wang, B. (2000) Orally active peptidomimetic RGD analogs that are glycoprotein IIb/IIIa antagonists, *Curr Med Chem* 7, 437-453.
30. Esko, J. D., and Zhang, L. (1996) Influence of core protein sequence on glycosaminoglycan assembly, *Curr Opin Struct Biol* 6, 663-670.
31. Zhang, L., and Esko, J. D. (1994) Amino acid determinants that drive heparan sulfate assembly in a proteoglycan, *J Biol Chem* 269, 19295-19299.
32. Zhang, L., David, G., and Esko, J. D. (1995) Repetitive Ser-Gly sequences enhance heparan sulfate assembly in proteoglycans, *J Biol Chem* 270, 27127-27135.

APPENDIX

CURRICULUM VITAE

VY MY TRAN

EDUCATION

- Ph.D graduate student** **Fall 2006 – Summer 2012**
Department of Bioengineering, University of Utah, Utah
- Bachelor of Science** **Aug 2004 - May 2006**
Department of Chemistry, University of Utah, Utah
- Associate Degree** **Jan 2002 - May 2004**
General Study, University of Wisconsin-Marinette, Wisconsin

PUBLICATIONS

- “Synthesis and assessment of glycosaminoglycan priming activity of cluster-xylosides for potential use as proteoglycan mimetics”, Tran, V. M.; Nguyen, T. K.; Sorna, V.; Loganathan, D. and Kuberan, B. 2012 (manuscript under revision)
- “Multimerized glycosaminoglycan chains increase FGF signaling during zebrafish development”, Nguyen, T. K.; Tran, V. M.; Sorna, V.; Kjellén, L.; Dorsky, R.; Chien, C. and Kuberan, B. 2012 (manuscript under revision)
- “Design of fluorescent xylosides to profile cell-specific GAG chains”, Tran, V. M and Kuberan, B. 2012 (manuscript will be submitted)
- “Synthetic heparin sulfate oligosaccharide library reveals the novel enzymatic action of D-glucosaminyl 3-O-sulfotransferase-3a”, Nguyen, T.K.; Arungundram, S.; Tran, V. M.; Raman, K.; Al-Mafraji, K.; Venot, A.; Boons, G.; Kuberan, B. Mol Biosyst 2012, 8(2), 609-14
- “Investigating the mechanism of the assembly of FGF1-binding heparan sulfate motifs”, Nguyen, T.K.; Raman, K.; Tran, V. M.; Kuberan, B. FEBS Letter 2012, 585 (17), 2698-702

- “Applications of isotopes in advancing structural and functional heparanomics”, Tran, V. M.; Nguyen, T. K.; Raman, K.; Kuberan, B. *Anal Bioanal Chem* 2011, 399 (2), 559-70
- “RGD-xyloside conjugates prime glycosaminoglycans”, Tran, V. M.; Victor, X. V.; Yockman, J. W.; Kuberan, B. *Glycoconj J* 2010, 27 (6), 625-33
- “Characterization of uniformly and atom-specifically (13)C-labeled heparin and heparan sulfate polysaccharide precursors using ¹³C NMR spectroscopy and ESI mass spectrometry”, Nguyen, T. K.; Tran, V. M.; Victor, X. V.; Skalicky, J. J.; Kuberan, B. *Carbohydr Res* 2010, 345 (15), 2228-32
- “Investigating the elusive mechanism of glycosaminoglycan biosynthesis”, Victor, X. V.; Nguyen, T. K.; Ethirajan, M.; Tran, V. M.; Nguyen, K. V.; Kuberan, B. *J Biol Chem* 2009, 84 (38), 25842-53
- “Inhibition of heparan sulfate and chondroitin sulfate proteoglycan biosynthesis”, *Garud, D. R.; *Tran, V. M.; Victor, X. V.; Koketsu, M.; Kuberan, B. *J Biol Chem* 2008, 283 (43), 28881-7 (* equal contribution)
- “Click-xylosides initiate glycosaminoglycan biosynthesis in a mammalian cell line”, Kuberan, B.; Ethirajan, M.; Victor, X. V.; Tran, V.; Nguyen, K.; Do, A. *Chembiochem* 2008, 9 (2), 198-200

CONFERENCE PRESENTATIONS:

- “Modulating zebrafish GAG biosynthesis to decipher GAG-FGF interactions in vivo”, Thao, Nguyen; Vy Tran; Venkataswamy Sorna; Lena Kjällén; Richard Dorsky; Chi-Bin Chien; Balagurunathan Kuberan, Gordon Research Conference on Proteoglycans, Andover, July 2010
- “RGD-Xylosides initiate glycosaminoglycan biosynthesis”, Vy Tran; Xylophone Victor, James Yockman and Balagurunathan Kuberan, ACS National Meeting, San Francisco, March 2010 (poster presentation)
- “Synthetic proteoglycan mimetics”, Vy Tran; Venkataswamy Sorna, Duraikkannu Loganathan and Balagurunathan Kuberan, ACS National Meeting, San Francisco, March 2010 (oral presentation)
- “Multimeric heparan sulfate modulates FGF signaling in zebrafish development”, Thao Nguyen; Vy Tran; Eric Veien; Richard Dorsky; Chi-bin Chien; Balagurunathan Kuberan; The American Society for biochemistry and Molecular biology annual meeting, New Orleans, April 2009

- “Assembly of proteoglycans: A puzzle resolved?”, Vy Tran and Balagurunathan Kuberan, ACS National Meeting, Salt Lake city, March 2009 (poster presentation)
- “Cellular heparanomics: A robust approach to define HS-protein interactions”, Ponnusamy Babu, Vy Tran and Balagurunathan Kuberan, ACS National Meeting, Salt Lake city, March 2009
- “Mechanism of glycosaminoglycan biosynthesis”, Xylophone Victor, Manivannan Ethirajan, Thao Nguyen, Vy Tran and Balagurunathan Kuberan, ACS National Meeting, Salt Lake city, March 2009
- “A new paradigm to define the structural basis for HS-FGF interactions during zebrafish development”, Thao Nguyen; Vy Tran; Eric Veien; Richard Dorsky; Chi-Bin Chien; Balagurunathan Kuberan, Glycobiology annual meeting, Fort Worth, November 2008
- “Synthesis of cluster xylosides that prime heparan sulfate and chondroitin sulfate polysaccharides”, Vy Tran, Xylophone Victor, Thao Nguyen, Manivannan Ethirajan and Balagurunathan Kuberan, Glycobiology annual meeting, Boston, November 2007 (poster presentation)

PROFESSIONAL ACTIVITIES:

- Member, Society for Glycobiology 2007-current
- Member, American Society for Mass Spectrometry 2008-current
- Member, American Chemical Society 2009-current